THÈSE

UNIVERSITE DE PAU ET DES PAYS DE L'ADOUR

École doctorale des Sciences Exactes et de leurs Applications

Présentée et soutenue le 31 janvier 2019

par Emmanuelle MARIA

pour obtenir le grade de docteur
de l'Université de Pau et des Pays de l'Adour
Spécialité : Chimie Analytique et Environnement

MIGRATION AUGMENTEE DE L'URANIUM DANS LES EAUX SOUTERRAINES PAR VOIE COLLOÏDALE

DIRECTRICE DE THÈSE
Gaëtane LESPES, Professeur/Université de Pau et des Pays de l'Adour

CO-ENCADRANTS DE THÈSE
Pierre CRANÇON, Ingénieur de recherche/CEA-DAM Ile-de-France
Maxime BRIDOUX, Ingénieur de recherche/CEA-DAM Ile-de-France

RAPPORTEURS
Pascal REILLER, Directeur de recherche/CEA Saclay - DEN
Aline DIA, Directrice de recherche/Université de Rennes I

EXAMINATEURS
Dirk SCHAUMLÖFFEL, Directeur de recherche/CNRS, IPREM
Philippe LE COUSTUMER, Maître de conférence/Université de Bordeaux
Edith PARLANTI, Chargée de recherche/CNRS, Université de Bordeaux

« L'inspiration commence l'œuvre ; la volonté l'achève. »

Eugène Marbeau

A mes grands-parents.

REMERCIEMENTS

Ce manuscrit de thèse est le résultat d'un long travail de réflexion, d'expérimentation, de recherche et d'échange. Il n'aurait pas pu voir le jour sans l'aide et le soutien de nombreuses personnes, que je tiens ici à remercier.

Je voudrais tout d'abord adresser mes remerciements à Gaëtane LESPES, ma directrice de thèse et mon encadrante à l'IPREM de Pau. Merci pour la confiance et la liberté que tu m'as accordées dès les premiers jours, pour ta disponibilité (même en ayant la grippe) et pour ta capacité à trouver des métaphores pour expliquer n'importe quelle situation.

Merci à Pierre CRANÇON, mon encadrant au CEA de Bruyères-le-Châtel, pour m'avoir donné la chance de travailler sur ce sujet de thèse. Ton aide et ton implication, en particulier dans la dernière ligne droite, m'ont été précieuses. L'énergie dont tu fais preuve en toute circonstance est impressionnante, et communicative, malgré le peu d'échanges directs que nous avons pu avoir.

J'aimerais remercier Maxime, grand gourou de l'Orbitrap du laboratoire LEXAN du CEA de Bruyères-le-Châtel. Merci de m'avoir permis de découvrir la spectrométrie de masse moléculaire et une partie de ses nombreuses possibilités. Ça a été une collaboration très intéressante et j'espère avoir l'occasion de retravailler avec toi.

Mes remerciements vont aux membres de mon jury de thèse, et en particulier à mes rapporteurs Aline Dia et Pascal Reiller, pour avoir accepté d'évaluer mon travail mais aussi pour m'avoir apporté de quoi continuer à me poser des questions. J'aimerais également remercier les personnes qui, de près ou de loin, ont contribué scientifiquement à ce travail de thèse. Merci notamment à Stéphane Ducos (IPREM) et Gabriel Couchaux (CEA) pour les analyses COT, Philippe Le Coustumer pour le TEM (BIC), Sylvie Blanc pour la fluorescence (IPREM).

Une partie des expérimentations de ma thèse s'est déroulée au CEA, plus précisément au sein du laboratoire LEXAN et c'est pourquoi je tenais à adresser un grand merci à l'équipe de l'ER-B. Françoise, Frédéric, Sébastien, Gabriel, merci de m'avoir aussi bien accueillie. Les deux mois passés loin des montagnes m'ont paru beaucoup moins longs grâce à vous. Une mention spéciale pour toi, Françoise. Merci de m'avoir transmis les informations dont j'avais besoin, d'avoir transféré mon courrier, pour toutes nos conversations et surtout, merci pour ton soutien.

Une bonne ambiance est primordiale pour travailler efficacement et pour cela je dois remercier les doctorants et postdocs de l'IPREM :

Merci tout d'abord à Marine, ma première coloc de bureau. Superbe rencontre que j'ai faite là, et comme on dit : le hasard fait bien les choses… Merci pour bien des choses mais surtout pour m'avoir écoutée râler, meilleur remède contre la déprime.

Merci à tous mes colocs du bureau O120 qui se sont suivis mais ne se ressemblaient pas (Maxime, Dimitri, Stéphane, Paulina, Mathilde, Maroussia…). Maximus (ce sera toujours un plaisir de t'entendre débattre avec ferveur d'à peu près n'importe quel sujet), Dimdim (tes interludes musicaux m'ont beaucoup manqué pendant la période de rédaction (I will follow him…)), j'espère qu'on gardera le contact. Merci également à toi Stéphane pour ton aide durant ces trois années de thèse, et en particulier de m'avoir formé avec autant de rigueur sur l'ICP.

Je remercie toutes les autres personnes (collègues et/ou amis) que j'ai pu côtoyer, et qui ont contribué à faire de Pau, un endroit tellement agréable où vivre et travailler (Floflo, Elias, Marina, Sara, Laurent, Jesús, Andy, Javi, Bastien, Robin, Gelito, Alexandr, Isabella, Tony, Soëge, Élise, Cédric, Géraldine, Micka…).

Un grand merci à toi, Mathieu, ultime rescapé de la première année encore à Pau. La thèse, et en particulier la fin, se serait sans doute passée autrement sans ton soutien. Merci pour tout, et vivement ton tour !

Enfin, j'adresse tous mes remerciements à ma famille, à mes parents et à mes frère et sœurs. Sans votre aide, et surtout sans vos encouragements constants (clin d'œil à toi Papa), je ne serais sans doute pas là où j'en suis.

RESUME

La connaissance des processus de mobilisation et de migration de l'uranium dans les milieux souterrains est un enjeu majeur pour évaluer les risques environnementaux associés aux activités anciennes ou actuelles d'installations nucléaires en vue d'anticiper et gérer tout impact environnemental. La mobilisation et la migration sont habituellement décrites comme fortement contrôlées par les réactions d'adsorption, la présence de ligands, notamment sous forme colloïdale, étant susceptible de l'augmenter considérablement. La capacité des entités colloïdales à transporter l'uranium sur de longues distances va dépendre de leur origine, de leur composition, de leur structure, de leur stabilité et de leur réactivité, ainsi que de leur capacité à complexer l'uranium de manière forte et irréversible. Cependant, les faibles concentrations colloïdales dans les eaux souterraines s'avèrent parfois être un verrou analytique à la détection et à la caractérisation de la mobilisation et du transport colloïdaux de polluant(s) dans les eaux souterraines. Les protocoles d'extraction des phases colloïdales depuis les sols ou les méthodes destinées à concentrer les colloïdes depuis un échantillon d'eau souterraine ne sont pas toujours optimisés pour à la fois assurer un rendement d'extraction satisfaisant et respecter l'intégrité physique et chimique des entités colloïdales.

Dans ce contexte, deux axes de recherche ont été définis dans ce travail de thèse afin de : 1) appréhender l'impact de l'utilisation de méthodes de préconcentration sur la phase colloïdale et 2) améliorer notre compréhension de la dynamique de mobilisation de l'uranium au sein d'un sol podzolisé dans l'optique d'implémenter les modèles prédictifs du transport colloïdal de l'uranium dans les eaux souterraines.

Les méthodes de séparation membranaires permettent de préconcentrer la phase colloïdale des eaux souterraines tout en assurant un recouvrement supérieur à 80%. Elles engendrent néanmoins des modifications des paramètres intrinsèques des entités colloïdales avec en particulier un décalage vers les grandes tailles de la distribution en taille de ces entités ainsi qu'une modification de la distribution des espèces entre phases dissoute et colloïdale. Ces modifications peuvent mener à une mauvaise évaluation des concentrations colloïdales. Elles peuvent également engendrer des biais dans l'appréciation des mécanismes de complexation/sorption impliquant la surface des entités colloïdales ainsi que leur stabilité dans les eaux souterraines. La matière organique constitutive des eaux du sol d'étude a été identifiée comme étant le vecteur principal de la (re)mobilisation de l'uranium dans les eaux de sol, sans toutefois avoir un contrôle total de ce processus. Elle est constituée majoritairement d'acides fulviques et humiques de petite taille qui tendent à s'agglomérer au cours du temps, lors de la lixiviation du sol. La composition moléculaire de la matière organique varie de manière temporelle à la fois à l'échelle de l'horizon superficiel mais aussi le long du profil de sol. Divers processus, et en particulier des réactions de réduction et de dénitrification, interviennent durant la migration de la matière organique vers les horizons plus profonds et pourraient modifier ainsi sa nature. A l'échelle de l'horizon superficiel, les mécanismes de mobilisation diffèrent selon l'élément considéré. L'uranium en particulier est mobilisé rapidement mais de manière limitée (<2% du sol considéré), tandis que la matière organique est générée en continu, selon une cinétique du premier ordre. Les mécanismes de mobilisation similaires du fer, de l'aluminium et de la matière organique dans la fraction colloïdale témoignent de l'existence d'un processus de complexolyse prépondérant au sein de l'horizon superficiel d'un podzol.

ABSTRACT

Knowledge of the processes of mobilization and migration of uranium in underground environments is a major challenge to assess the environmental risks associated with ancient or current activities of nuclear facilities in order to anticipate and manage any environmental impact. Mobilization and migration are usually described as strongly controlled by adsorption reactions, the presence of ligands, especially in colloidal form, being able to increase considerably. The ability of colloidal entities to transport uranium over long distances will depend on their origin, composition, structure, stability and reactivity, as well as their ability to complex uranium in a significant and irreversible manner. However, low colloidal concentrations in groundwater sometimes prove to be an analytical lock on the detection and characterization of colloidal mobilization and transport of pollutant(s) in groundwater. Protocols for extracting colloidal phases from soils or methods for concentrating colloids from a groundwater sample are not always optimized to both ensure satisfactory extraction yield and respect physical and chemical integrity colloidal entities.

In this context, two lines of research have been defined in this thesis work in order to: 1) understand the impact of the use of preconcentration methods on the colloidal phase and 2) improve our understanding of uranium mobilization dynamics within a podzolized soil to implement predictive models of colloidal uranium transport in groundwater.

The membrane separation methods make it possible to preconcentrate the colloidal phase of the groundwater while ensuring a recovery greater than 80%. They nonetheless cause changes in the intrinsic parameters of the colloidal entities with a shift towards large sizes of the size distribution of these entities as well as a modification of the species distribution between dissolved and colloidal phases. These changes may lead to a poor assessment of colloidal concentrations. They can also cause bias in the assessment of complexation/sorption mechanisms involving the surface of colloidal entities and their stability in groundwater. The constituent organic matter of the soil waters has been identified as the main vector for the (re)mobilization of uranium in the groundwater, without however having a total control of this process. It consists mainly of small fulvic and humic acids that tend to agglomerate over time, during leaching of the soil. The molecular composition of organic matter varies temporally both at the level of the superficial horizon and along the soil profile. Various processes, such as reduction and denitrification reactions, occur during the migration of organic matter to deeper horizons and could thus change its nature. At the level of the superficial horizon, mobilization mechanisms differ according to the element considered. Uranium is mobilized quickly but in a limited way (<2% of the soil considered), while organic matter is generated continuously, with first-order kinetics. The similar mechanisms of iron, aluminium and organic matter mobilization in the colloidal fraction testify to the existence of a predominant complexolysis process within the superficial horizon of a podzol.

TABLE DES MATIERES

TABLE DES ILLUSTRATIONS

Figures

Tableaux

Tables

GLOSSAIRE

A

A1 · Horizon superficiel du sol d'étude (podzol des Landes)

A4F · Fractionnement par couplage Flux-Force Asymétrique

AF · Acides fulviques

AH · Acides humiques

AI · "Aromaticity Index" - Indice d'aromaticité

Al · Aluminium

B

BCR · "Community Bureau of Reference"

Bh · Horizon d'accumulation du sol d'étude

C

CAS · "Condensed Aromatic Structures"

CEA · Commissariat à l'Energie Atomique et aux Energies Alternatives

CEC · Capacité d'Echange Cationique

COD · Carbone organique dissous (<0.45µm)

COT · Carbone organique total

D

DBE · "Doucle Bond Equivalent" ou degré d'insaturation

DLS · "Dynamic Light Scattering" - Diffusion dynamique de la lumière

DOC · "Dissolved Organic Carbon" = Carbone organique < 0.45µm

DOM · "Dissolved Organic Matter"

E

EEM · "Emission-Excitation Matrix"

ESI · Source d'ionisation Electrospray

F

Fe · Fer

FI · "Fluorescence Index" - Indice de fluorescence

G

GW · Nappe superficielle du site d'étude

H

HRMS · Spectrométrie de masse haute-résolution

I

ICP-MS · Spectrométrie de masse élémentaire à plasma induit

K

kDa · kilodalton - 1 kDa = 1000 g/mol

KM · Masse de Kendrick

KMD · Défaut de masse de Kendrick

M

MALS · "Multi-Angle Light Scattering" - Diffusion de la lumière statique et multi-angle

MO · Matière Organique

MOD · Matière Organique Dissoute (<0.45µm)

MON · Matière Organique Naturelle

N

NIST · "National Institute of Standards and Technology"

O

OM · "Organic Matter"

P

PES · Polyéthersulfone"

PTFE · Polytétrafluoroéthylène (Téflon)

S

SEM · "Scanning Electronic Microscopy" - Microscopie électronique à balayage

SH · Substances Humiques

SPE · "Solid Phase Extraction"

SUVA · Absorbance UV Spécifique

T

TEM · "Transmission Electronic Microscopic" - Microscopie électronique à transmission

TOC · "Total Organic Carbon"

U

U · Uranium

UF · Ultrafiltration

UO_2^{2+} · Ion uranyle

INTRODUCTION GENERALE

L'uranium est naturellement présent à l'état de trace dans l'environnement, mais peut être introduit dans l'environnement par les activités humaines. La toxicité de l'uranium est fonction de sa spéciation. Etudier et prédire le devenir de l'uranium dans l'environnement est un enjeu majeur. Cependant, les processus de transport de l'uranium sont multiples et complexes. L'absence de prise en compte d'un processus spécifique, ou bien sa sous-estimation, peut mener à une large erreur sur la détermination de son impact environnemental.

Depuis une trentaine d'années, le rôle majeur de la phase colloïdale dans le transport de polluants a été établi (Kretzschmar et al. 1999; McCarthy and Zachara 1989; Seaman et al. 1995). En effet, les entités colloïdales sont capables de complexer fortement les polluants à l'état de trace, en particulier les actinides, et participent à augmenter leur mobilité dans l'environnement (Roberts et al. 2004). Kersting et al. (1999a) ont ainsi observé que le plutonium présent dans les eaux souterraines d'un site au Nevada était associé à la fraction colloïdale, soulignant l'importance d'intégrer dans les modèles de migration des polluants le transport colloïdal. La mobilité de l'uranium et son impact environnemental dépendent donc de sa distribution entre phase colloïdale et phase dissoute (Kretzschmar et al. 1999). Pour permettre le transport colloïdal d'un polluant dans le milieu souterrain, trois conditions doivent être réunies : les entités colloïdales doivent être générées dans l'eau interstitielle du sol (c'est-à-dire mobilisées), le polluant doit être associé à ces entités, et celles-ci doivent être transportées dans le milieu aqueux (interstitiel du sol, ou dans l'aquifère) (Ryan and Elimelech 1996). Les paramètres physico-chimiques du milieu aqueux, tels que le pH, le potentiel redox, la salinité ou encore la présence de carbone organique dissous, sont des facteurs clés qui peuvent affecter la structure et la stabilité des entités colloïdales, et favoriser ou non le transport de polluants (Degueldre et al. 2000). L'étude de la phase colloïdale est donc devenue un enjeu environnemental pour caractériser et prédire le comportement des polluants dans le milieu naturel. Il est cependant difficile d'étudier la phase colloïdale sans la perturber, d'autant plus qu'elle peut nécessiter une étape de préconcentration qui peut mener à la modification de la structure et/ou de la composition chimique des entités colloïdales.

Ce travail de recherche est la continuité de précédentes études sur la migration de l'uranium au sein d'un site d'intérêt, pour lequel la phase colloïdale, et en particulier les complexes organiques, a été identifiée comme étant le principal vecteur de mobilisation et transport (Crançon 2001; Crançon et al. 2010; Harguindeguy et al. 2018). Ces travaux avaient respectivement (1) montré l'existence d'un transport colloïdal de l'uranium dans le milieu souterrain (Crançon, 2001 ; Crançon, 2010), (2) précisé la structure des entités colloïdales et leur association avec l'uranium, et (3) étudié la mobilité de l'uranium (Harguindeguy, 2014 ; Harguindeguy et al., 2018). Le présent travail de recherche a pour but de caractériser la nature et de déterminer les propriétés des phases colloïdales porteuses de l'uranium, et d'acquérir des informations visant à préciser les mécanismes de mobilisation de l'uranium depuis le sol vers le milieu aqueux souterrain

de ce même site d'intérêt. Il n'a pas pour objet l'étude de la migration des phases colloïdales dans le milieu souterrain. Ainsi, la caractérisation des processus physiques spécifiques contrôlant le transport colloïdal dans les milieux poreux du sol et de l'aquifère ne rentrent pas dans le cadre de cette thèse.

Ce mémoire de thèse se compose des cinq chapitres suivants :

Le premier chapitre, rédigé en français, est une synthèse bibliographique posant le contexte de l'étude et faisant état des connaissances actuelles sur les propriétés physico-chimiques des entités colloïdales et leur capacité à transporter des polluants dans les milieux naturels en se focalisant plus particulièrement sur le cas de l'uranium. Les méthodes de préconcentration et d'extraction de la phase colloïdale ont été discutées. Ce chapitre présente également les différents objectifs du travail de thèse.

Les autres chapitres sont consacrés aux résultats obtenus en prenant comme support d'étude un sol du site d'intérêt. Ces chapitres sont rédigés en anglais sous forme d'articles :

- Le chapitre 2 est intitulé "*Comparison of preconcentration methods of the colloidal phase for the study of uranium transport in soils*". Les caractéristiques morphologiques et structurelles à l'échelle de la population colloïdale ainsi que la composition chimique d'un lixiviat du sol, préconcentré par différentes méthodes de séparation membranaire, ont été comparées. Les biais induits par ces méthodes sur la phase colloïdale ont ainsi pu être appréhendés.
- Le chapitre 3 est intitulé "*Spatial variations In the molecular composition of dissolved organic matter from the podzol soils of the wetlands In western France*". Les structures moléculaires de la matière organique constitutive du sol y ont été appréhendées de façon spatiale en les caractérisant le long du profil de sol par spectrométrie de masse moléculaire haute résolution.
- Le chapitre 4 est intitulé "*Dynamics of uranium mobilization from soil by natural humic colloids*". La mobilisation de l'uranium depuis un sol y a été appréhendée en fonction du temps de lixiviation, en portant une attention particulière à l'évolution de la distribution de l'uranium et des composants majeurs entre les phases dissoute et colloïdale. Plus spécifiquement, la phase colloïdale a été considérée dans son continuum de taille en utilisant une approche couplée multi-techniques.

Enfin, une conclusion est apportée à ce travail de recherche. Elle reprend, en les hiérarchisant, les principaux résultats obtenus dans cette étude, suite aux différentes problématiques qui ont été posées. Des perspectives proposent enfin d'approfondir certains points particuliers de la mobilisation colloïdale de l'uranium dans les milieux naturels.

1) CADRE SCIENTIFIQUE DE LA THESE

1.1 CONTEXTE, PROBLEMATIQUE ET OBJECTIFS DU TRAVAIL DE RECHERCHE

Les travaux présentés dans ce manuscrit s'intègrent dans la problématique générale liée à la mobilité de l'uranium dans l'environnement, et plus spécifiquement dans le cas d'application à un sol sableux podzolisé. Une attention particulière est portée au rôle des entités colloïdales naturelles dans la mobilisation de l'uranium depuis les horizons superficiels du sol vers les milieux aqueux. Ils s'inscrivent dans la continuité de précédentes études sur la migration de l'uranium au sein d'un site d'intérêt pour le CEA, dans lesquelles la fraction colloïdale, et en particulier les complexes organiques, avait été identifiée comme ayant un rôle majeur dans les processus de migration de l'uranium en subsurface (Crançon 2001; Crançon et al. 2010; Crançon and Van der Lee 2003; Harguindeguy et al. 2018). La nature des entités colloïdales et leur association avec l'uranium avaient été précisés, ainsi que les grandes lignes d'une migration facilitée de l'uranium par les vecteurs colloïdaux (Harguindeguy, 2014 ; Harguindeguy et al., 2018). Les principaux résultats de ces travaux portaient sur la distribution de l'uranium dans les différents compartiments de l'environnement, sur sa spéciation, sur sa rétention sur les matrices sableuses constituant les différents horizons du podzol, ainsi que sur la migration colloïdale de l'uranium. L'association entre uranium et entités colloïdales naturelles avait été évaluée sur le terrain et au laboratoire, à travers l'étude de la distribution de l'uranium entre les différentes fractions qui composent le milieu aqueux naturel. Les entités colloïdales organiques naturelles avaient été caractérisées à l'échelle de la population, notamment en termes de taille, dans différents compartiments de l'environnement du site d'étude. L'influence des entités colloïdales sur le transport de l'uranium en subsurface avait été démontrée, ainsi que la sensibilité de ce processus aux paramètres physico-chimiques du milieu, en particulier la force ionique. Le lecteur trouvera ainsi un détail complet des éléments contextuels sur le site d'étude, ainsi que les résultats obtenus sur la géochimie et la migration colloïdale de l'uranium dans ce contexte naturel, dans l'ensemble des publications se rapportant à ces travaux antérieurs (Crançon, 2001 ; Crançon et al., 2003 ; Crançon et al., 2010 ; Harguindeguy, 2014 ; Harguindeguy et al. 2018).

L'association entre l'uranium et les entités colloïdales n'a toutefois pas été entièrement caractérisée, et un certain nombre de zones d'ombre persistent :

- La thermodynamique de l'association entre l'uranium et les complexants organiques naturels (substances humiques), notamment par la détermination des constantes de complexation. Ce point particulier a fait l'objet de travaux spécifiques, hors du cadre du présent travail de recherche.
- La nature, la structure et la composition fine des substances humiques composant la fraction colloïdale. En effet, si la distribution de l'uranium entre les différentes fractions colloïdales a été étudiée, ces fractions demeurent une sorte de « boite noire » insuffisamment caractérisées à ce jour. En particulier, aucune connaissance n'émerge sur les propriétés chimiques, ni sur la structure

moléculaire ou supramoléculaire des substances humiques colloïdales. De même, aucune information n'apparait sur l'évolution des propriétés physicochimiques de ces substances lors de leur transfert entre les différents horizons du sol et les eaux souterraines. Ce sont sur ces différents points que s'est concentré le présent travail de recherche.

Le présent travail a donc pour but principal de caractériser la nature et les propriétés des phases colloïdales porteuses de l'uranium, et de préciser les mécanismes de mobilisation de l'uranium depuis le sol vers le milieu aqueux souterrain, dans lesquels sont impliqués les entités colloïdales naturelles.

Il apparait toutefois plusieurs contraintes à la réalisation de cet objectif général :

- Les entités colloïdales, en particulier les substances humiques, sont présentes dans les eaux naturelles du site étudié à des concentrations trop faibles pour utiliser ces matrices brutes dans les différents protocoles analytiques envisagés, sans passer par une étape de préconcentration. Cette étape de préconcentration doit donc être définie et testée sur le plan méthodologique ;
- Le passage par une étape de préconcentration de type séparation membranaire est susceptible d'introduire des biais expérimentaux en altérant la structure et les propriétés physico-chimiques de la phase colloïdale initiale. Il est donc nécessaire de caractériser ces biais et leur portée méthodologique.

Ces deux points particuliers constituent à eux seuls un premier objectif de ce travail de recherche. Ce premier objectif atteint, on s'attachera alors à atteindre les deux objectifs suivants de ce travail de recherche :

- La caractérisation de la structure et de la composition des phases colloïdales, ainsi que l'évolution spatiale de la structure moléculaire de la matière organique (MO) au sein d'un sol podzolisé et différencié,
- Le rôle des fractions colloïdales dans la mobilisation de l'uranium depuis le sol vers le milieu aquatique du site étudié, notamment en termes de cinétique de lessivage de l'uranium depuis l'horizon supérieur du sol par les ligands organiques colloïdaux.

Chacun de ces objectifs formera donc un chapitre particulier de cette thèse.

Le fil rouge de ce travail de recherche demeure son application à la problématique du site d'étude, au travers notamment du contexte spécifique lié à la présence d'uranium dans le sol, et également en tenant compte des spécificités de fonctionnement hydrogéochimiques des différents compartiments du milieu naturel (sol, aquifère superficiel et milieux aquatiques aériens). En effet, un sol est très souvent sujet à des perturbations physico-chimiques liées aux infiltrations d'eau de pluie, aux remontées de la nappe, ou encore aux variations saisonnières de l'activité microbienne. Ces perturbations peuvent à chaque fois entraîner une

modification des propriétés et de l'abondance de la phase colloïdale de l'eau interstitielle du sol, qui peut à son tour favoriser ou non le transport colloïdal de l'uranium.

1.2 L'ETAT COLLOÏDAL

L'état colloïdal est défini comme un état de dispersion d'entités de taille comprise entre 1 nm et 1 µm, soumises majoritairement au mouvement brownien dans une phase dispersante (Nič et al. 2009). Ubiquistes dans l'environnement, ces entités colloïdales sont de natures très différentes. Dans les eaux, elles peuvent être :

- Des solides cristallisés et/ou amorphes de nature inorganique,
- Des structures macromoléculaires et/ou supramoléculaires, de la matière organique condensée et/ou des structures intermédiaires dans l'état de condensation de la MO,
- Des structures mixtes inorganiques/organiques.

Ces différentes formes sont décrites plus en détails dans ce qui suit.

1.2.1 Structure et propriétés physiques des entités colloïdales

Les entités colloïdales sont caractérisées en premier lieu par leur taille, qui leur confère des propriétés spécifiques, dont une grande réactivité et une grande mobilité (Jones and Bryan 1998). Les systèmes colloïdaux dans un sol sont généralement polydisperses, et en raison de leur nature agglomérante, ils présentent une distribution de taille asymétrique relativement bien ajustée par une distribution de type Poisson (Shaw 1992) (voir Figure 1.2-1). Leur surface spécifique, définie comme étant le rapport entre la surface réelle et le volume apparent, est également importante : elle varie entre 10 et 800 $m^2.g^{-1}$ (Kretzschmar and Schafer 2005). Cette propriété est à l'origine de leur grande réactivité : la forte densité de sites qu'elle implique favorise les processus de complexation et de sorption d'éléments à leur surface. Les phases colloïdales sont très souvent porteuses d'une charge de surface. Elles peuvent acquérir une charge variable (dépendante du pH) par l'adsorption à leur surface de sels entièrement dissociés, ou bien d'acides faibles tels que les acides carboxyliques, ou bien être elles-mêmes constituées de composés/groupements fonctionnels chargés (typiquement, les groupements hydroxyles et carboxyles). Elles peuvent également avoir une charge constante qui résulte de substitutions isomorphes. Celles-ci sont principalement observées dans les minéraux silicatés et engendrent généralement une charge négative. Dans les sols, les surfaces des particules minérales sont souvent recouvertes de matière organique, et notamment de substances humiques (Akbour et al. 2008). Il est donc possible pour une phase colloïdale d'avoir à la fois une charge variable et une charge constante.

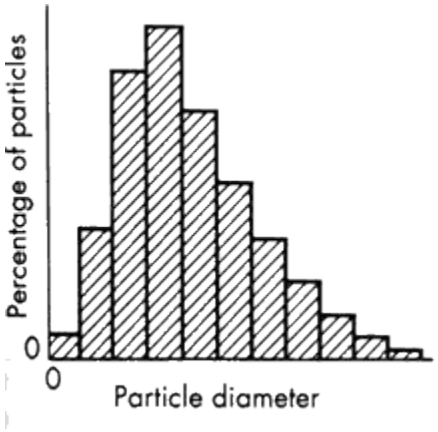

Figure 1.2-1: Distribution en taille des entités (particules) colloïdales pour un système colloïdal polydisperse représentée en histogrammes (Shaw 1992).

Ce sont toutes ces propriétés qui font de l'ensemble des entités colloïdales un vecteur important dans le transport de polluants et en particulier des radionucléides tels que l'uranium (McCarthy 1998; Moulin and Ouzounian 1992).

Du fait du mouvement Brownien, les collisions entre phases colloïdales sont fréquentes et peuvent mener à des phénomènes d'agrégation, qui sont également favorisés par des forces attractives de surface de type Van der Waals. La stabilité du système colloïdal est assurée lorsque ces forces attractives sont compensées par des forces répulsives intervenant entre les charges électriques au sein des entités colloïdales. Les répulsions électrostatiques diminuent lorsque la force ionique augmente du fait de la double couche de surface qui devient plus fine. Quand les forces répulsives deviennent trop faibles, il y a agrégation des phases colloïdales entre elles, menant éventuellement à leur sédimentation. Dans le cas de la MO, les conditions physico-chimiques du milieu impactent fortement sa structure. Sa forme tend à suivre un modèle de bobine aléatoire dont la taille est majoritairement inférieure à 100 kDa (Hayes and Clapp 2001). Les entités colloïdales organiques de plus grandes tailles sont généralement attribuées à un processus de ramification et d'agrégation. En effet, les propriétés amphiphiles de la MO lui donnent la possibilité de former des micelles, plus ou moins condensés en fonction de paramètres tels que la concentration en MO et/ou le pH (voir Figure 1.2-2). En faibles concentrations, les molécules organiques amphiphiles existent en tant qu'entités individuelles, mais passé une certaine concentration (appelée concentration micellaire critique : CMC), elles vont s'associer et former des agrégats de type micelles plus ou moins condensés, via des liaisons hydrophobes (Wershaw 1999). Les groupements hydrophiles (tels que les acides carboxyliques ou les groupements cétones, alcools ou aldéhydes) seront ainsi concentrés à l'extérieur de l'agrégat.

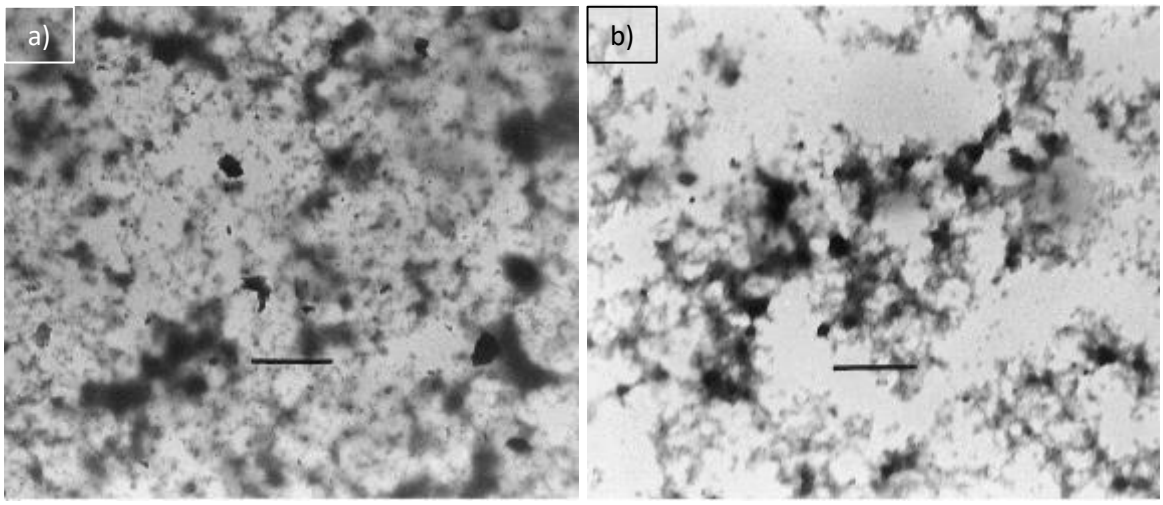

Figure 1.2-2 : Images de Microscopie électronique à Transmission d'acides fulviques de sol. Force ionique = 5 mM, (a) pH = 5,9 ; (b) pH = 3,4. Echelle = 1 µm. Wilkinson et al. (1999). Les acides fulviques sont plus agrégés et condensés en conditions plus acides.

Ainsi, la structure des entités colloïdales est susceptible de varier très rapidement en fonction des modifications des conditions du milieu et donc peut modifier fortement leur réactivité vis-à-vis des éléments en solution en fonction de leur localisation à l'échelle du milieu et dans le temps.

1.2.2 Composition et propriétés chimiques des entités colloïdales

Particules colloïdales minérales et inorganiques

Les particules colloïdales inorganiques naturelles proviennent des minéraux constitutifs du sol et regroupent les aluminosilicates, les carbonates, les oxydes métalliques… Leur capacité à complexer des éléments va dépendre de leur degré de cristallisation, de leur taille et des paramètres physico-chimiques du milieu (Warren and Haack 2001). Dans les sols, on les retrouve principalement sous forme de composés siliceux et argileux provenant de l'altération des minéraux primaires et/ou néoformés et sous forme d'(oxy)hydroxydes de fer (Lead and Wilkinson 2006).

Les oxydes de fer (et d'aluminium) peuvent être cristallisés ou amorphes, et présentent une grande surface spécifique. Ils sont en général chargés positivement (dans les milieux où le pH est inférieur à leur pH_{ZPC}, c'est-à-dire inférieur à 8-9 (Kretzschmar and Schafer 2005)). C'est pourquoi on les retrouve généralement associés aux argiles et/ou à la matière organique dans les milieux naturels (Girard et al. 2011). Ils sont potentiellement en compétition avec d'autres cations pour la complexation avec la MO.

Les argiles peuvent avoir une grande surface spécifique, en fonction du type de leur structure en feuillets. Ils sont sujets aux substitutions isomorphes et ont à ce titre une charge permanente. La présence de groupements fonctionnels de type silanol sur certains d'entre eux peur également leur conférer une charge

variable, notamment en fonction du pH. Ils sont susceptibles d'adsorber les cations métalliques par échange d'ions (Maes and Cremers 1987).

Entités colloïdales organiques

Les entités colloïdales organiques dans les milieux souterrains sont issues de la dégradation de la matière organique naturelle (MON) provenant de la flore et de la faune.

La MON peut être qualifiée de dissoute (MOD) ou de particulaire (MOP), selon qu'elle soit respectivement inférieure ou supérieure à une taille standard fixée à 0,45µm (Frimmel 1998; Thurman 1985). Certains auteurs ont défini de manière plus spécifique la matière organique colloïdale (MOC) suivant les mêmes critères de taille que ceux définis pour l'état colloïdal (Nič et al. 2009). La MON joue un rôle particulièrement important dans le cycle du carbone ainsi que dans le transport des métaux. En effet, elle est généralement chargée négativement et peut donc se complexer avec les cations (dont les métaux) et faciliter ainsi leur mobilisation. Elle représente ainsi un acteur important dans la migration de certains polluants (métaux, actinides…) (Fotovat and Naidu 1998; Kanti Sen and Khilar 2006). Le rôle des complexants organiques naturels dans le processus de migration de l'uranium depuis un sol vers la nappe a été mis en évidence (Doi et al. 1975; Erikson et al. 1990; Mibus et al. 2007; Oliver et al. 2008; Ragnarsdottir and Charlet 2000; Singhal et al. 2005).

Dans les sols, et en particulier dans les sols de zones humides, la matière organique se retrouve majoritairement sous formes soluble et colloïdale (à hauteur de 80%), appelées substances humiques (Thurman 1985). Ubiquistes dans les sols et les eaux naturelles, les substances humiques (SH) sont définies selon les procédures d'extraction utilisées pour les isoler (MacCarthy et al. 1990b). On distingue trois fractions : l'humine (fraction insoluble quel que soit le pH), les acides fulviques (AF, fraction la plus soluble quelle que soit la valeur du pH) et les acides humiques (AH, fraction insoluble à pH acide), les deux dernières étant en moyenne réparties de telle sorte qu'il y ait environ 20% d'AF et 80% d'AH. Ces trois fractions sont constituées de molécules organiques très diverses, tant par leur structure que par leur composition, qui dépendent de l'origine et de la nature de la matière organique ainsi que des conditions environnementales accompagnant sa dégradation (Barančíková et al. 1997). Les SH sont un mélange complexe de composés supramoléculaires hétérogènes, réactifs mais cependant de nature très réfractaire à la dégradation. Elles sont produites lors du processus d'humification qui permet à la matière organique résistante (issue de la lignine) de se dégrader. Cependant, le processus de formation des substances humiques aussi bien que leur structure moléculaire restent encore peu connus (MacCarthy et al. 1990b). Une théorie sur la structure supramoléculaire des substances humiques a été proposée ; elle a défini les SH comme un assemblage de macromolécules relativement petites et hétérogènes, stabilisé par des interactions faibles de type Van der Waals ou hydrogène plutôt que par des liaisons covalentes (Piccolo 2001).

Contrairement aux autres composants de la matière organique, les SH présentent donc une structure de type polymère polydisperse de grande variabilité (Nebbioso and Piccolo 2012; Wagner et al. 2016). Les SH sont considérées comme un mélange de composés organiques dont il est n'est pas possible d'isoler un composant moléculaire caractéristique de la structure de la MO (MacCarthy 2001). Ainsi, si les molécules humiques sont composées de différents maillons structuraux assemblés de manière aléatoire, il est peu probable qu'il puisse exister deux molécules identiques au-delà d'une certaine masse molaire (Hayes and Swift 1990). Cependant, la dégradation de la MO en laboratoire (que ce soit par pyrolyse, hydrolyse…) laisse apparaître des produits (composés) organiques principalement de type acide, et en particulier des acides aromatiques tels que des benzènes et des benzènes carboxyliques, ainsi que des cycles aromatiques fortement substitués par des groupements méthoxy et hydrocarbonés. Cette dégradation donne également lieu à l'apparition de molécules solubles comme les sucres, les acides aminés ou des substances phénoliques (Hayes and Clapp 2001). Il est admis que ces composés représentent des maillons structuraux majoritaires de la MO (Hayes and Clapp 2001).

Un exemple des gammes de masses molaires rencontrées pour les AH et AF dans différents environnements naturels tels que des sols ou des eaux de surface est présenté dans le Tableau 1-1.

Tableau 1-1 : Gamme de Masses molaires de substances humiques dans différents environnements, d'après Malcolm (1990).

Masses molaires (en g/mol)	**Acides humiques**	**Acides fulviques**
Sols	50 000 – 500 000	1 000 – 5 000
Eaux de surface	1 500 – 5 000	600 – 1 000

Les SH présentent une grande diversité de groupements fonctionnels acides ou neutres, tels que les groupements carboxyliques, phénoliques ou encore alcooliques. Les abondances relatives de chaque type de groupement fonctionnel varient selon la nature des SH (acides fulviques ou humiques) et selon leur origine (McDonald et al. 2004; Nebbioso and Piccolo 2012; Thurman 1985). Les acides fulviques ont une plus grande abondance relative en groupements fonctionnels carboxyliques (-COOH), ce qui leur confère une solubilité et donc une mobilité plus importantes dans les eaux (Chung et al. 2005). Les acides humiques possèdent plus de groupements aromatiques et phénoliques donnant lieu à un rapport C/O plus élevé (Muscolo et al. 2007).

Dans le Tableau 1-2 sont présentés des exemples de concentrations relatives typiques de SH dans différents milieux aquatiques, ainsi que les concentrations relatives en carbone organique dissous (COD, qui correspond au COT inférieur à 0.45µm) correspondantes (Thurman 1985).

Tableau 1-2 : Exemples de concentrations typiques de COD et SH dans différents systèmes aquatiques, d'après Thurman, (1985).

Type de milieu	**Substances humiques (SH)**		**Carbone organique dissous (COD)**
	($mg.L^{-1}$)	%COD	($mg.L^{-1}$)
Eau de mer	0,06 - 0,6	≈ 30	0,2 - 2,0
Eaux souterraines	0,03 - 0,6	≈ 30	0,1 - 2,0
Rivière	0,5 - 4,0	≈ 40-50	1 - 10

De manière générale, les AH sont majoritaires dans les milieux aquatiques et les sols, mais cela peut varier d'un milieu à un autre. Par exemple, dans les sols acides podzolisés, on retrouve principalement des AF (ratio AH/AF = 0,8) (Kononova and Alexandrova 1973).

Ainsi, la MO naturelle est constituée majoritairement de composés très réactifs et chargés négativement (SH) qui peuvent potentiellement complexer des espèces positivement chargées en solution, telles que les composés d'uranium, et augmenter ainsi leur migration dans les sols et les eaux souterraines. Cependant, la structure et la composition de ces composés restent très dépendantes des conditions physico-chimiques du milieu, ces conditions contrôlant également les processus de complexation et de sorption des éléments par la MO.

Entités colloïdales naturelles

Dans les milieux naturels, les entités colloïdales sont ubiquistes et se présentent essentiellement comme des mélanges de constituants organiques et inorganiques, générés de manière continue depuis les horizons superficiels du sol (Degueldre et al. 1989). Dans les eaux interstitielles du sol, les concentrations colloïdales varient entre un et plusieurs centaines de mg/L (Grolimund et al. 1998). Plus généralement dans les eaux naturelles, de surface, interstitielles, souterraines ou océaniques, il peut arriver que les entités colloïdales soient relativement concentrées (Gounaris et al. 1993; McCarthy and Zachara 1989; Moulin and Ouzounian 1992; Ryan and Elimelech 1996). Les constituants colloïdaux naturels majoritaires sont de manière générale des acides humiques et fulviques et des nanoparticules de fer et/ou de minéraux argileux (Lead and Wilkinson 2006). Les oxydes d'aluminium sont également souvent constitutifs de phases colloïdales. La composition complexe et variable des entités colloïdales résulte souvent d'une association de macromolécules organiques, de nanoparticules minérales et de débris biologiques pouvant être recouverts de MO (Stumm and Morgan 1996). Les particules inorganiques (en particulier les argiles) sont plus stables à l'état naturel que sous forme de suspension inorganique pure générée au laboratoire. En effet, dans le milieu naturel, les particules colloïdales inorganiques sont généralement recouvertes de composés

organiques, compensant ainsi leur charge positive et évitant leur agrégation et/ou leur adsorption sur les phases solides composant la matrice.

1.2.3 Genèse et mobilité des entités colloïdales naturelles

Bien que les entités colloïdales soient reconnues pour être ubiquistes dans l'environnement, leurs mécanismes de genèse sont multiples et encore peu documentés. Certains processus, qu'ils soient physiques, chimiques et/ou biologiques, ont été identifiés comme générateur d'entités colloïdales. On peut citer en particulier la dégradation des matières végétales, l'altération physico-chimique des minéraux de la roche mère, la lixiviation des sols, ou encore la néoformation de phases minérales lors de modifications des conditions physico-chimiques du milieu (Degueldre et al. 2000; Ryan and Elimelech 1996). Les principales perturbations chimiques à l'origine de la mobilisation d'entités colloïdales sont les modifications de la force ionique dues à l'infiltration d'eau météorique (Bunn et al. 2002), ou bien du pH. Les variations de concentrations en MO dans le milieu aqueux peuvent également avoir un impact sur la mobilisation de particules colloïdales. Les particules et entités colloïdales ainsi formées sont alors disponibles pour migrer dans le milieu aqueux naturel (Lead and Wilkinson 2006; McDowell-Boyer et al. 1986). Cette migration est en général réalisée à la vitesse du fluide porteur, c'est-à-dire l'eau dans la plupart des milieux naturels. La migration des phases colloïdales dépendra ensuite de plusieurs paramètres, tels leur quantité, leur taille, ou leur charge électrique (Ryan and Elimelech 1996), et également le pH et la force ionique du milieu (Harmand 1996; Kretzschmar et al. 1997), ou encore les interactions avec les constituants du milieu et les processus d'adsorption/désorption ayant lieu au sein de la matrice géologique, au niveau des interfaces solide/liquide (Canseco Ruiz 2009). Les substances humiques, dont la charge est négative, peuvent ainsi être facilement adsorbées à la surface des grains de la matrice en conditions acides. La taille des entités colloïdales peut avoir plusieurs impacts sur le transport colloïdal, aussi bien positifs que négatifs. En effet, une taille plus grande va diminuer leur mobilité mais en même temps favoriser leur exclusion stérique, ce qui pourrait avoir pour effet *in fine* d'augmenter leur mobilité dans un sol poreux. Leur taille inférieure au micromètre ne les rendent pas sujettes à des phénomènes tels que la constriction ou la sédimentation (McDowell-Boyer et al. 1986), mais elles peuvent en revanche être retenues via des processus d'accumulation dans les zones stagnantes et/ou de fixation électrostatique (Van der Lee 1997). Ainsi, le transport de polluants via les eaux souterraines n'est possible que si les conditions permettant à la fois la genèse des entités colloïdales, leur stabilité et leur mobilité dans le milieu sont toutes réunies (voir Figure 1.2-3).

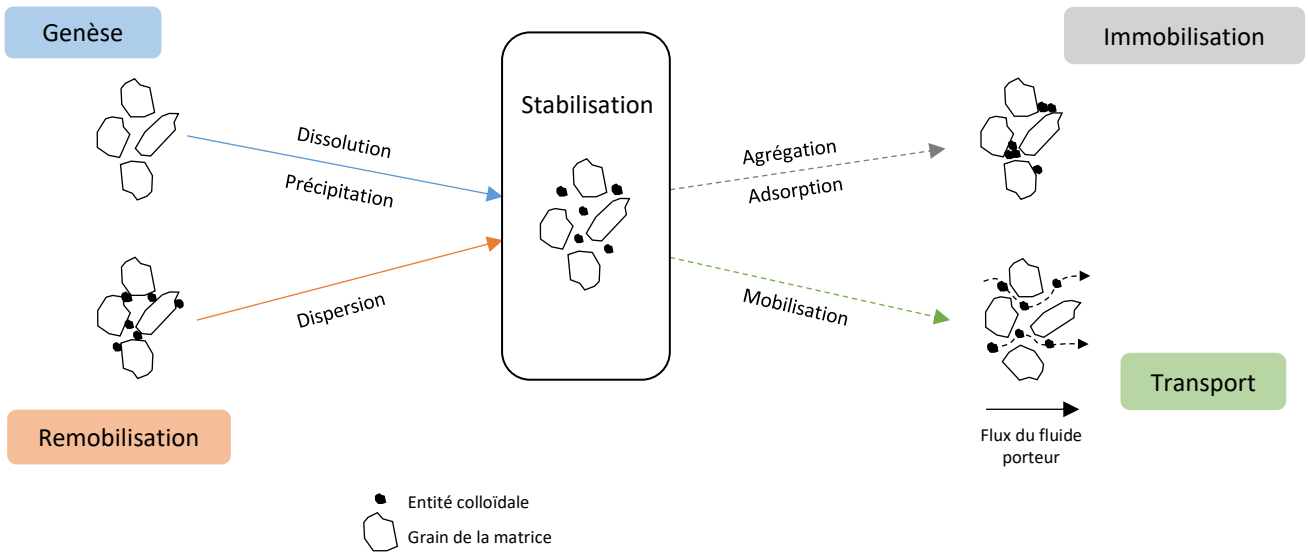

Figure 1.2-3: Comportement des entités colloïdales dans les sols. D'après MacCarthy et Zachara, (1989)

1.2.4 Association entre entités colloïdales et uranium

L'association d'éléments traces (sous leur forme ionique soluble) avec des entités colloïdales peut modifier non seulement leur état physique mais également leur forme chimique. Par conséquent ces associations peuvent modifier globalement les propriétés des éléments trace via les propriétés des complexes auxquels ils sont associés (typiquement labilité, solubilité, état d'agrégation/agglomération, mobilité, bioaccessibilité, biodisponibilité, toxicité). C'est particulièrement le cas pour les cations métalliques, tels que ceux impliquant par exemple les actinides (Kersting et al. 1999a; Ragnarsdottir and Charlet 2000; Van der Lee 1997).

Dans le cas spécifique de l'uranium, dans les milieux naturels, on le retrouve sous deux états d'oxydation : U(IV) et U(VI), ce dernier étant l'état le plus stable. Lorsque le pH est acide, U(VI) est présent principalement sous forme d'ion uranyle (UO_2^{2+}) ; il peut se complexer facilement à divers ligands, organiques et/ou inorganiques en fonction d'éventuels changements du pH et de la composition du milieu environnant (Crançon 2001; Ragnarsdottir and Charlet 2000; Ranville et al. 2007). Lorsque le pH tend à la neutralité, les ions uranyle peuvent former des complexes stables avec les phosphates et les carbonates (Zavodska et al. 2008). Le rôle prédominant que peut jouer la MO sur le comportement notamment de l'uranium a été démontré dans de nombreux travaux (Crançon and Van der Lee 2003; Moulin et al. 2004; Moulin and Moulin 1995; Moulin and Ouzounian 1992). En particulier la spéciation de l'uranium peut être impactée par la présence de substances humiques, en décalant les zones de prédominance des ions uranyle vers les pH plus acides (inférieurs à 4)(Cumberland et al. 2016). En présence de substances humiques, la formation de complexes UO_2-humate chargés négativement et présents majoritairement pour des pH compris entre 4 et 6 aurait alors des conséquences sur la dynamique de mobilisation/immobilisation de l'uranium (voir Figure 1.2-4). L'abondance de ces complexes est déterminée par la concentration en substances humiques, mais

aussi par le rapport des concentrations en U et en SH ; leur mobilité est également dépendante de ce rapport [U]/[HS] puisqu'avec l'augmentation de la concentration en uranium (dont les espèces sont principalement de charge positive), la charge négative des substances humiques auxquelles U est complexé est progressivement saturée, diminuant ainsi les forces répulsives entre le complexe et la matrice du sol (Benes et al. 1999). Les interactions entre l'uranium et la MO, et plus particulièrement les substances humiques, ont déjà été largement étudiées (Lubal et al. 2000; Montavon et al. 2000; Murphy et al. 1999; Reiller et al. 2012, 2008).

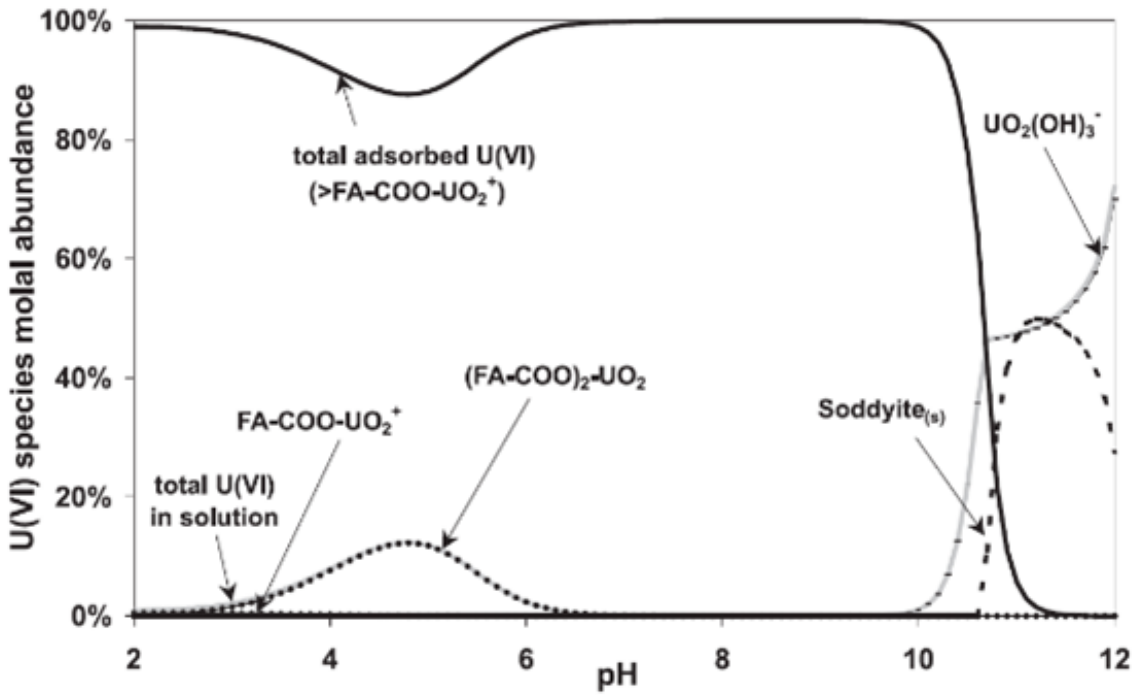

Figure 1.2-4: Courbes de spéciation et d'absorption de l'ion uranyle dans l'eau interstitielle d'un sol sableux podzolisé en fonction du pH et pour le système suivant : 0,035% de pression partielle de carbonate, 100 µg/L d'U(VI) aqueux total, 0,5 g/L de matière organique fixée (> FA) et 1 mg/L d'acides fulviques (FA). D'après Crançon et Van der Lee (2003).

Cependant, ces études ont été réalisées dans des conditions expérimentales contrôlées, avec une composition de la phase aqueuse, des concentrations en U et/ou en SH et un pH qui sont fixés. Elles ne peuvent donc entièrement refléter les mécanismes ayant lieu dans des milieux naturels, car elles ne prennent pas en compte la gamme très large de conditions géochimiques rencontrées dans ces milieux, ainsi que l'hétérogénéité du milieu et les variations physico-chimiques pouvant survenir dans le compartiment aqueux en réponse à une perturbation extérieure. Pour illustrer ce propos, on notera que plusieurs études menées sur les associations U-phases colloïdales dans des milieux naturels montrent que les proportions d'uranium colloïdal sont très variables, mais mettent toutes en évidence l'importance primordiale de l'association entre uranium et substances humiques (Crançon et al. 2010; Geckeis et al. 2003; Ranville et al. 2007; Stolpe et al. 2010).

Dans le cas de notre étude, la présence d'entités colloïdales organiques dans l'eau de sol conduirait donc à la formation d'associations uranium-MO colloïdales, dont le devenir, notamment en termes de stabilité, et de mobilité restent à estimer.

En présence d'autres ligands, tels que les oxyhydroxydes de fer ou d'aluminium, peut avoir lieu une compétition entre les différents équilibres de complexation qui peut induire des mécanismes d'adsorption/désorption de l'uranium à la surface des principaux complexants (Gabriel et al. 1998; Lenhart and Honeyman 1999; Morrison et al. 1995).

1.2.5 Mobilisation et transport colloïdal de l'uranium

Il est maintenant établi que le transport de polluants via la fraction colloïdale représente parfois une grande part de la mobilité de ces polluants (Kersting et al. 1999a; Kretzschmar et al. 1999; McCarthy and Zachara 1989; Seaman et al. 1995). Les processus d'adsorption/désorption des entités colloïdales influencent directement tout d'abord la mobilisation puis le transport des polluants. La nature des phases colloïdales intervenant dans la mobilisation et le transport dépend des conditions physico-chimiques du milieu et du polluant.

En pH acide, la matière organique intervient principalement dans la mobilisation et le transport colloïdal de l'uranium. Dans ce cas, la mobilité de U dépendra donc principalement de la capacité de la MO à le complexer et de la stabilité du complexe formé, ainsi que de différents facteurs liés aux conditions du milieu, tels que le pH, la force ionique ou la composition des phases colloïdales, qui favoriseront ou inhiberont la désorption de la MO de la phase solide vers l'eau de sol. Cependant, en présence d'autres adsorbants, tels que les oxyhydroxydes de fer ou d'aluminium, peut avoir lieu une compétition entre les différents équilibres de complexation qui entraîne des mécanismes d'adsorption/désorption de l'uranium à la surface des principaux constituants (Gabriel et al. 1998; Lenhart and Honeyman 1999; Morrison et al. 1995). D'autre part, la concentration de la phase colloïdale en milieu aqueux contrôlant fortement le transport colloïdal de polluants et au vu de la gamme de concentrations colloïdales existant dans les milieux naturels, il est important de déterminer la nature et la quantité de la phase colloïdale présente dans le système étudié.

1.3 MATIERE ORGANIQUE ET SOLS PODZOLISES

1.3.1 Les podzols

Les podzols sont des sols très différenciés dont la dynamique géochimique est très particulière. Plusieurs théories quant à leur processus de formation ont été proposées (Courchesne and Hendershot 1997). Dans la plupart des cas, la mobilisation des composés organiques et des sesquioxydes (c'est-à-dire des composés comportant 3 liaisons oxygène, typiquement Fe_2O_3 ou Al_2O_3) depuis les horizons supérieurs de sols très

acides, et leur précipitation dans un horizon profond dit d'accumulation est reconnu comme étant le principal mécanisme qui conduit à la différentiation du sol (Abakumov et al. 2010; Bonifacio et al. 2013). La matière organique joue le rôle de chélatant principal, participe à la complexolyse des minéraux et de leurs constituants (plus particulièrement Fe et Al) et génère ainsi un processus d'éluviation (Abakumov et al. 2010; Harguindéguy 2013). L'illuviation est ensuite possible via l'augmentation progressive du pH. La fraction colloïdale joue encore un rôle important dans le processus de podzolisation. Ainsi, Riise et al. (2000) ont observé que le fer était présent sous forme colloïdale dans tous les horizons du podzol.

L'une des caractéristiques du podzol est son appauvrissement progressif en matière organique avec la profondeur, résultant du processus d'éluviation décrit précédemment. Cependant, il est important de noter que cette éluviation n'est pas égale pour tous les composés organiques et les particules qui y sont adsorbées, et dépend de la solubilité et de la taille des molécules organiques. Ainsi, les humines ainsi que les acides humiques ont tendance à précipiter et/ou interagir avec la matrice plus rapidement que les acides fulviques et donc à migrer moins profondément. Les acides fulviques ainsi que les oxydes de fer et d'aluminium, plus mobiles, précipitent plus profondément au sein de l'horizon d'accumulation.

1.3.2 **Le site d'étude**

Le sol du site d'intérêt est un podzol des Landes de Gascogne de type humo-ferrugineux (Casenave 1970). Il se développe sur la formation quaternaire dite des Sables des Landes et est à ce titre constitué d'un matériau riche en quartz et très filtrant (Jolivet et al. 2007). La nappe superficielle est très peu profonde (< 1 m en période d'étiage) et affleure parfois à la surface (Righi and Wilbert 1984). La végétation typique de la lande humide est constituée principalement de plantes acidophiles de type Molinie, et d'Ericacées, généralement ligneuses et riches en tannins. La faible teneur en argiles dans le sol résulte en un complexe organo-argileux quasi-inexistant et en une capacité d'échange cationique (CEC) faible, essentiellement due à la matière organique (Crançon 2001). Les différents processus de migration de la MO et des oxydes métalliques sont résumés dans la Figure 1.3-1.

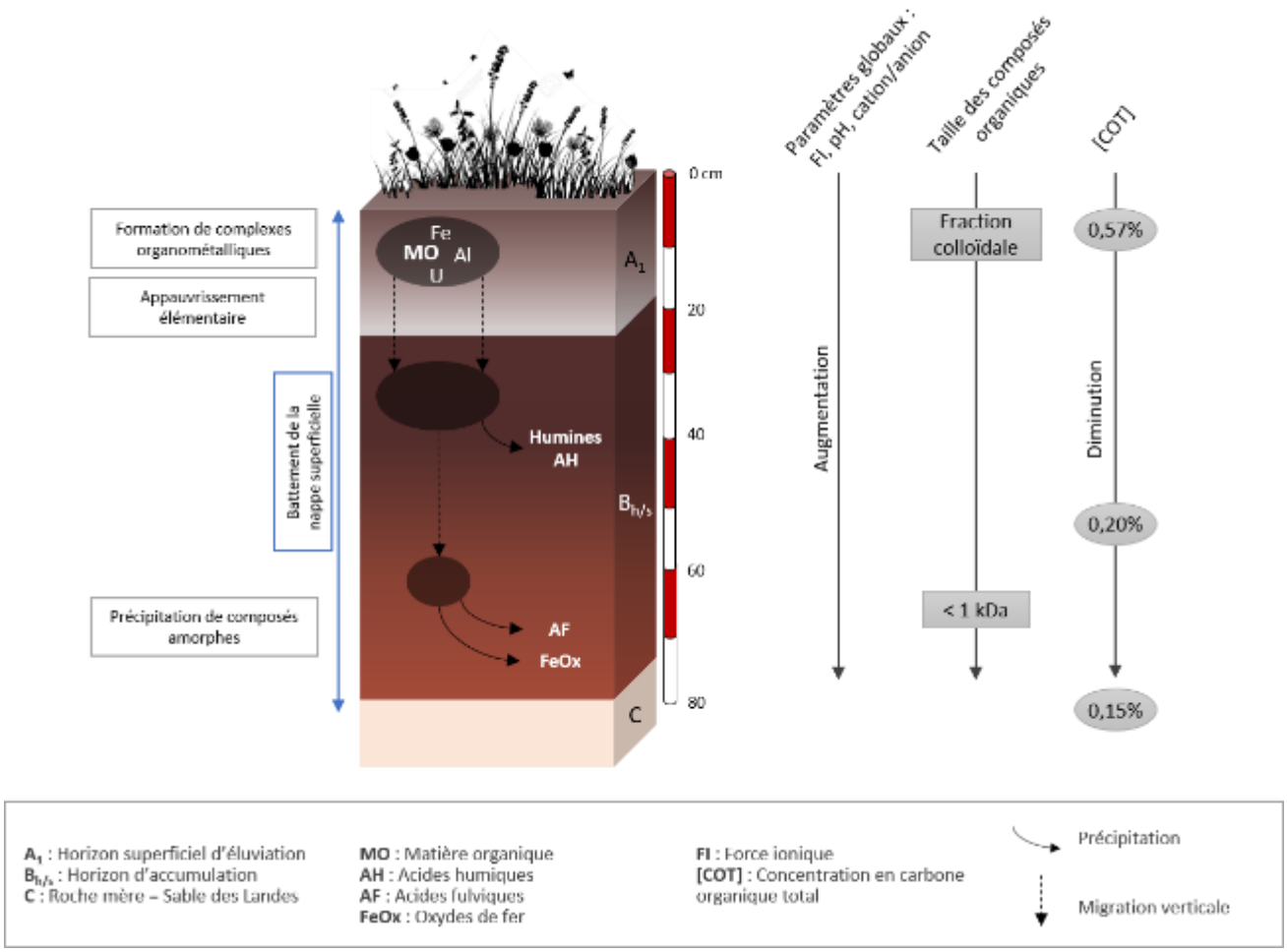

Figure 1.3-1: Schéma de fonctionnement du sol du site d'intérêt. Adapté d'après travaux de Crançon (2001), Casenave (1970) et Jolivet (2007)

1.4 DEFIS LIES A L'ETUDE DE LA PHASE COLLOÏDALE NATURELLE

Trois stratégies d'étude de la phase colloïdale peuvent être envisagées. La première, dans l'idéal, est de pouvoir caractériser la phase colloïdale d'eaux de sol prélevées sur site, de façon à obtenir des résultats représentatifs du milieu. Cependant, il s'avère parfois délicat de prélever un échantillon aqueux sans entraîner une perturbation des conditions du milieu. D'autre part, la phase colloïdale peut s'avérer être en très faible concentration. La seconde stratégie d'investigation consiste à prélever du sol, puis à le lixivier en laboratoire, par lixiviation en réacteur fermé par exemple. Ceci permet d'obtenir des échantillons aqueux dans des conditions physico-chimiques maîtrisées. Bien qu'une telle méthode ne reproduise pas fidèlement les conditions naturelles, elle a l'avantage d'être répétable ; elle permet de produire *in fine* des données comparables, à partir desquelles il est plus aisé de déterminer les liens entre conditions du milieu et caractéristiques observées. Elle permet également d'ajuster les conditions opératoires en fonction de l'objectif d'étude. La troisième stratégie d'investigation est la combinaison des deux premières, qui cherche

à en allier les avantages respectifs (notamment la représentativité du milieu et le contrôle des conditions expérimentales) et en minimiser leurs inconvénients.

Parmi les contraintes citées ci-avant, celle qui s'avère être le principal verrou à la mise en œuvre d'une stratégie d'investigation est la très faible concentration des phases colloïdales dans les eaux naturelles (Saito et al. 2015; Stolpe et al. 2005). Or ceci est une des caractéristiques des eaux collectées sur le site étudié. Pour lever ce verrou, une solution est d'introduire dans le processus analytique une étape de préconcentration des eaux, en préalable à la caractérisation de la phase colloïdale. Les conditions de mise en œuvre de cette étape dépendent de la nature des entités colloïdales à concentrer et des objectifs de l'étude. Quatre méthodes de préconcentration des phases colloïdales peuvent être envisagées (Lead et al. 1997; Majedi and Lee 2016) :

- La séparation membranaire,
- La centrifugation,
- La lyophilisation, particulièrement utilisée pour la récupération de la matière organique,
- L'extraction, qui permet d'isoler des espèces chimiques, en particulier les ions métalliques ou encore la matière organique.

Chacune de ces méthodes a ses propres avantages et inconvénients que nous discuterons plus loin. Lead et Wilkinson (2006) indiquent que différentes approches conceptuelles de caractérisation des entités colloïdales doivent être envisagées selon que l'on cherche à étudier la phase colloïdale sur tout son continuum ou bien seulement une de ses fractions, que ce soit en termes de tailles ou de phases homologues (substances humiques, oxydes métalliques…) (Lead and Wilkinson 2006). Dans l'optique d'une attention particulière donnée à la caractérisation de la matière organique, la séparation membranaire par ultrafiltration et l'extraction sur phase solide (SPE) sont les méthodes les plus utilisées sur des échantillons d'eaux naturelles (Sandron et al. 2015) : la première permet une caractérisation dans le continuum de taille ; la seconde permet une caractérisation ciblée de la matière organique. Les facteurs de concentration appliqués avec chacune de ces deux méthodes dépendent essentiellement de la concentration initiale en phase colloïdale et de la composition générale de l'eau à concentrer. Elles sont toutes les deux présentées et discutées dans les parties suivantes.

1.4.1 Séparation membranaire

La méthode de séparation membranaire regroupe plusieurs sous-techniques qui diffèrent selon la force motrice impliquée dans le processus de séparation. L'utilisation de ces techniques spécifiques dépend également de la taille des analytes à concentrer (voir Figure 1.4-1). Dans le cas de la caractérisation d'une phase colloïdale provenant d'une eau naturelle, l'intérêt de la filtration comme méthode de

préconcentration réside dans la récupération du rétentat après avoir éliminé une partie plus ou moins importante de la phase dissoute (en fonction du facteur de concentration désiré). Les techniques impliquant un gradient de pression (filtration) sont largement utilisées pour la concentration des entités colloïdales naturelles, sous plusieurs formes selon le support choisi pour fixer la membrane et selon la direction du flux d'écoulement à travers celle-ci (voir Figure 1.4-2).

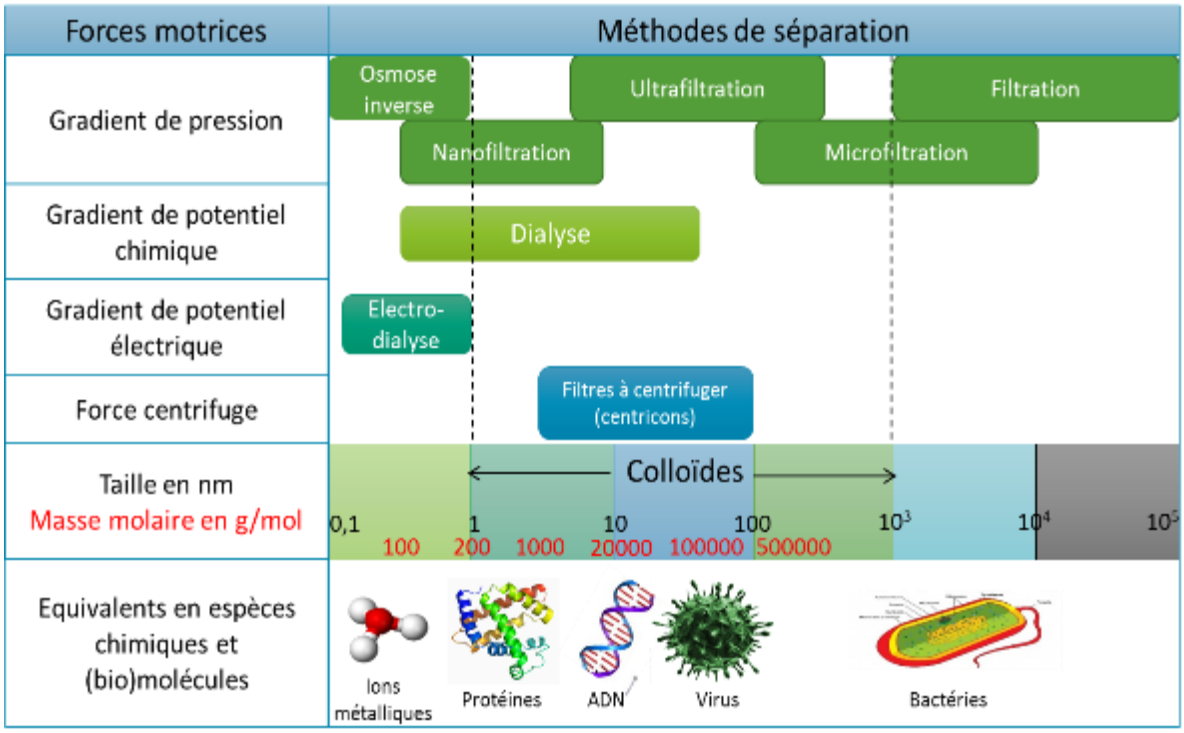

Figure 1.4-1 : Techniques de séparations membranaires, Forces motrices impliquées, tailles de particules.

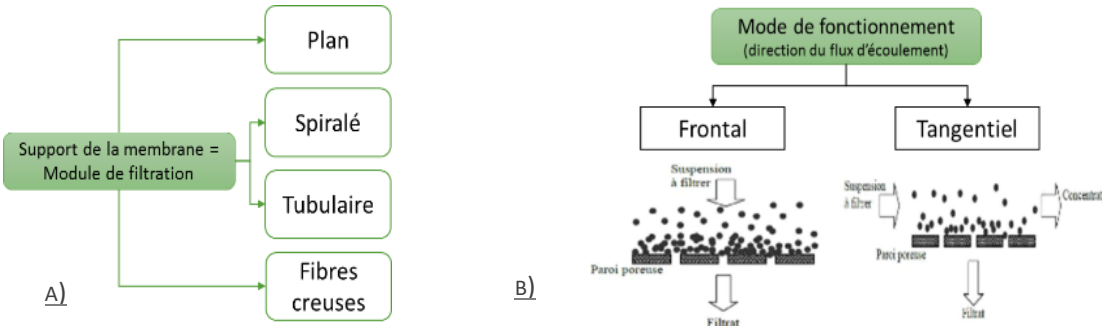

Figure 1.4-2 : Différents types de filtration selon a) le support de la membrane, et b) la direction du flux d'écoulement

Parmi les différents modules (supports de membrane), le support plan est le plus répandu lors d'une séparation membranaire, mais sa surface de filtration est souvent limitée. Quel que soit le mode d'écoulement appliqué, les mêmes difficultés sont notées. Aiken (1984) et Cornel et al. (1986) rapportent plusieurs problèmes et artefacts provenant de l'utilisation de modules de filtration plans, avec une tendance

au colmatage des pores de la membrane et un phénomène de polarisation de sa surface. On peut voir apparaitre également une couche solide qui, en s'épaississant petit à petit, diminue le débit de la filtration ainsi que son efficacité (Marley et al. 1991). Cependant, des solutions techniques ont été proposées pour minimiser ces inconvénients. De plus, la filtration par module plan reste une méthode rapide et simple (Eyrolle and Charmasson 2000), qui peut être utilisée sur le terrain si besoin (Baalousha et al. 2005a). Dans le cas de la filtration frontale, la solution à filtrer circule de manière perpendiculaire à la membrane, alors que la filtration tangentielle laisse circuler le fluide, ce qui limite le dépôt de plus grosses entités colloïdales sur le filtre, favorisant ainsi la percolation des plus petites, mais diminue le rendement de préconcentration.

Le colmatage des membranes est l'un des inconvénients majeurs de la séparation/concentration par filtration et a fait l'objet de nombreuses études (Choi et al. 2005; Espinasse 2003; Knutsen and Davis 2006; Morrison and Benoit 2001; Zirkler et al. 2012). La filtration peut être biaisée par le colmatage progressif des pores de la membrane, ou par sa polarisation (Culfaz et al. 2011), c'est à dire l'apparition de gradients de concentration à l'interface membrane/solution, avec transfert sélectif de certaines espèces à travers la membrane. On peut également observer l'apparition d'une couche solide à sa surface (Zirkler et al. 2012).

Plusieurs techniques ont été testées afin d'améliorer l'efficacité des filtrations frontale et tangentielle en limitant la formation de la couche solide et l'agrégation des particules entre elles. C'est le cas de l'application d'ultrasons, utilisée pour la première fois dans les années 80 (Okahata and Noguchi, 1983) et dont l'efficacité dans la limitation du colmatage a été démontrée de nombreuses fois (Ahmad et al., 2012; Mirzaie and Mohammadi, 2012; Muthukumaran et al., 2007). Il a été également reporté que les ultrasons étaient parfois à l'origine de perturbations physiques, voire de perte d'intégrité de la membrane (augmentation de la taille des pores, de leur densité ainsi qu'apparition de fissures) ainsi que de la dénaturation des phases colloïdales (en particulier modification de leurs tailles) (Masselin et al., 2001; Villamiel and de Jong, 2000). De la même façon, l'apparition de la couche solide a lieu plus fréquemment dans le cas d'une filtration en mode frontal mais il est possible de limiter son développement en agitant la solution au niveau du filtre (Baalousha et al. 2005a). Ceci permet de ralentir le colmatage de la membrane mais favorise en revanche la formation d'entités particulaires plus grosses par agglomération ainsi que la croissance microbienne (Lead et al. 1997). De nombreuses études ont également permis de mieux appréhender les conditions de formation de cette couche solide ainsi que sa structure, sa porosité, et sa résistance mécanique spécifique dans des conditions données. Il est possible de compenser les effets du colmatage par l'application de modèles de filtration (Daniel et al. 2011; Hwang et al. 1998; Mackley and Sherman 1994; Raha et al. 2009; Vigneswaran and Kwon 2015). Par exemple, un modèle a été établi pour caractériser la baisse du débit d'écoulement en fonction du colmatage irréversible des pores et de la formation réversible d'une couche solide. Ce modèle a ensuite été utilisé pour prévoir la fréquence optimale de flux inversé à appliquer pour éviter un colmatage trop rapide de la membrane (Daniel et al. 2011). Un autre inconvénient à l'utilisation de membranes est leur sélectivité,

aussi bien électrochimique que géométrique, et leur dépendance aux conditions physico-chimiques. En effet, les caractéristiques propres aux différents constituants de la solution à filtrer comme la charge, la forme chimique, le pH, la force ionique, mais aussi la pression exercée lors de la filtration ou encore le facteur de concentration appliqué, peuvent avoir une influence sur la capacité de la membrane à séparer les différentes espèces (Cornel et al. 1986). De plus, les membranes sont souvent chargées négativement, entraînant un effet sélectif (par répulsion) envers les formes anioniques de certaines espèces dissoutes, et la surestimation de leurs formes colloïdales (Guo et al. 2007; Zirkler et al. 2012). Guo et al. (2007) estiment que le pourcentage de molécules de faible masse molaire (<1000 g/mol) retenues par une membrane dont le seuil de coupure est de 1kDa peut atteindre les 30 à 60%. Il est également prouvé que les seuils de coupure des membranes disponibles actuellement sont imprécis et que la séparation d'espèces moléculaires s'effectue suivant leur taille et non suivant leur masse molaire (Hassellov et al. 1999). Malgré tous ses inconvénients, la filtration reste un outil de séparation/concentration relativement performant avec par exemple des valeurs de rétention des analytes d'une masse molaire supérieure à 1000 g/mol allant jusqu'à 80% (Guo et al. 2007). De plus, d'après Wilding et al. (2004) (Wilding et al. 2004), le recouvrement des différentes espèces présentes dans la solution est élevé. C'est pourquoi la filtration est une méthode largement utilisée, aussi bien en laboratoire que dans des unités de production (pharmaceutiques, agro-alimentaires, d'épuration, etc).

Parmi les différentes solutions techniques de filtration existantes, la séparation membranaire avec force centrifuge a également été proposée. Elle peut mettre en œuvre la force centrifuge en micro- ou ultrafiltration. Les modules de microfiltration centrifuge sont surtout utilisés pour la purification d'huiles ou d'eaux et on les retrouve principalement dans les applications industrielles. En laboratoire, il existe des tubes de centrifugation pour ultrafiltration destinés à la purification de composés macromoléculaires ou encore à la préconcentration d'échantillons (Menguy et al. 1998). Dans ces tubes, la membrane est placée de manière sub-verticale (ce qui limite sa polarisation et s'apparente au flux tangentiel appliqué par gradient de pression) et permet de séparer efficacement et rapidement des échantillons en obtenant des facteurs de concentration élevés (c'est-à-dire > 100, pour des eaux de mer)(Kim et al. 2015). Les seuils de coupure peuvent varier de 1 à 100 kDa et il est possible de récupérer en fin de filtration aussi bien le rétentat que le filtrat. L'ultrafiltration centrifuge, bien qu'elle soit largement utilisée comme méthode de préconcentration, est peu décrite dans la littérature scientifique, mais elle semble réunir les avantages de la séparation membranaire en limitant son inconvénient majeur qui est le colmatage de la membrane.

Plusieurs filtrations successives peuvent être mises en œuvre. Par exemple, dans le cas de la purification des eaux usées, les différents processus (de la microfiltration jusqu'à l'osmose inverse) sont appliqués les uns après les autres avant que l'eau ne puisse être consommée (Matin et al. 2016; Mondal and Wickramasinghe 2008; Van der Bruggen and Vandecasteele 2002). Kim et al. (2015) (Kim et al. 2015) ont utilisé

successivement deux méthodes d'ultrafiltration tangentielle (fibres creuses et filtres à centrifuger) avec un même seuil de coupure de 100kDa, afin d'affiner la préconcentration de virus présents dans des échantillons d'eaux marines. La première étape d'ultrafiltration permettant de passer de quelques litres d'eau de mer à 150mL et la deuxième étape de filtration par filtration centrifuge afin d'obtenir des volumes de 0.6 à 1mL (soit une préconcentration totale de 1000 à 10000 fois) tout en conservant l'intégrité des analytes au cours de ces deux étapes. Dans le cas des phases colloïdales une première filtration à 0.45µm a souvent lieu, réalisée sur le terrain juste après l'échantillonnage. Cela permet d'éviter une éventuelle agrégation des phases entre elles (Lapworth et al. 2013) et/ou une adsorption des entités chargées sur les surfaces du matériel d'échantillonnage ("Echantillonnage des eaux souterraines - Office fédéral de l'environnement OFEV" n.d.). Pour pouvoir récupérer ensuite l'ensemble du matériel colloïdal et le concentrer, une méthode de filtration permettant de séparer les analytes d'une taille inférieure à 1nm devrait être utilisée, dans les faits il s'agit souvent d'une membrane ayant un seuil de coupure entre 1 et 10kDa.

1.4.2 Extraction d'un constituant de la phase colloïdale

L'extraction permet d'isoler de manière sélective un ou plusieurs composés d'un mélange initial grâce à ses/ leurs propriétés chimiques ou physiques. Elle peut être effectuée via une phase solide ou une phase liquide mais repose dans les deux cas sur l'affinité plus forte du (des) composé(s) à extraire pour cette phase que pour la matrice dans laquelle il(s) se trouve(nt). Encore aujourd'hui, le type d'extraction le plus couramment utilisé est l'extraction liquide-liquide. Cependant, dans le cas de la préconcentration d'entités colloïdales, elle ne parait pas appropriée, d'autant plus qu'elle présente comme inconvénients de générer beaucoup de déchets et d'utiliser des solvants organiques qui peuvent être des sources de contamination.

L'extraction en phase solide est une méthode de préparation d'échantillons (purification) et/ou de préconcentration de plus en plus utilisée en toxicologie analytique et environnementale. Par le développement de nombreuses phases stationnaires, elle permet une extraction de plus en plus ciblée mais aussi l'extraction d'un grand nombre de substances de différentes natures chimiques (Humbert 2010). L'une de ses principales applications est l'extraction de la matière organique qualifiée de dissoute (c'est-à-dire inférieure à 0.45µm) en amont d'analyses HPLC-MS ou de spectrométrie de masse (Swenson et al. 2014). Son principe repose sur la séparation de composés entre la phase liquide (l'échantillon) et la phase solide ou stationnaire (l'adsorbant). Elle se compose de 3 à 4 étapes. La première étape est le conditionnement de la phase stationnaire qui permet d'activer les sites de rétention, la deuxième est le passage de l'échantillon dans la phase stationnaire avec rétention des analytes d'intérêt et l'élimination de la plupart des espèces interférentes (sels inorganiques par exemple). La troisième étape, facultative, est le lavage de l'échantillon permettant d'éliminer les espèces interférentes restantes. Enfin, l'élution, pour laquelle le solvant utilisé doit être facilement évaporable tout en étant le plus efficace possible pour réduire son volume et obtenir ainsi un

facteur de concentration important. Le choix de l'adsorbant dépend des analytes d'intérêt dont les caractéristiques intrinsèques (polarité relative, présence de groupements fonctionnels chargés, solubilité…) font varier l'efficacité et la sélectivité. La méthode SPE permettant une extraction ciblée, il est donc d'abord nécessaire de déterminer les espèces à isoler et préconcentrer. Si la gamme de polarité des composés à extraire est grande, il peut être nécessaire d'appliquer deux extractions successives.

Dans le cas de l'extraction ciblée de la MO provenant d'eaux naturelles, les phases stationnaires ont généralement des propriétés hydrophobes car la matrice étant une phase aqueuse, c'est le support le plus adapté. L'eau est en effet, sur ce type de phase, la phase mobile la moins éluante (Chapuis et al. 2005). Ces phases sont donc conditionnées via des solvants organiques polaires comme le méthanol et/ou l'acétonitrile. La MO est ensuite récupérée en utilisant le même solvant comme éluant. Cette méthode nécessite souvent de larges volumes d'échantillon, induisant des procédures d'extraction longues et augmentant les risques de contamination et/ou de dégradation de l'échantillon. En effet, il a été reporté qu'en dépit des étapes de conditionnement et de rinçage durant la procédure, il arrive que la MO extraite soit contaminée par des composés organiques provenant de la phase stationnaire. De la même manière, une partie de la MO est susceptible d'être adsorbée de façon irréversible sur le sorbant (Little and Jacobus 1985). Parce que les SH sont de nature polyélectrolytique, avec de nombreux groupements aromatiques, les principales phases stationnaires utilisées aujourd'hui sont les phases échangeuses d'ions et/ou les sorbants poreux (Zherebker et al. 2016). La société internationale des substances humiques (IHSS) préconise l'usage de cartouche SPE de type XAD-8 qui est constituée d'un polymère réticulé hydrophile dont l'efficacité d'extraction des SH a été évaluée à 65% (Aiken et al. 1979). Cependant, cette phase extrait de manière préférentielle les composés organiques de type fulvique (plus hydrophiles) et ne rend pas compte de la réelle contribution des acides humiques au sein des substances humiques. Une utilisation combinée des deux méthodes (échange d'ions et phase inverse) semble être un bon compromis pour une meilleure estimation de la composition des SH du milieu naturel.

1.4.3 Bilan

Dans l'optique d'une étude focalisée sur la phase colloïdale à différentes échelles d'investigation, la séparation membranaire et la SPE apparaissent être deux méthodes complémentaires. En particulier, l'application de ces deux types de méthodes aux échantillons d'eaux naturelles prélevés sur le site est intéressante compte tenu de la problématique, des objectifs de l'étude, connaissant le rôle de la phase colloïdale et de la matière organique dans la mobilisation et le transport de l'uranium, et donc connaissant la nature des constituants d'intérêt. Ainsi, séparation membranaire et SPE ont été considérées comme devant permettre respectivement (1) de préconcentrer la phase colloïdale des eaux afin de la caractériser physico-chimiquement dans sa globalité en tentant de la perturber la moins possible, et (2) de caractériser

chimiquement à l'échelle moléculaire la matière organique, acteur majeur du devenir de l'uranium dans ce site.

Compte tenu du bilan de l'état de l'art, plusieurs méthodes de séparation membranaire peuvent être envisagées pour la préconcentration de la phase colloïdale. Cependant, peu d'études comparatives ont été réalisées. Du fait du besoin analytique de préconcentration, il nous a donc semblé important dans un premier temps de se pencher sur les performances des méthodes d'ultrafiltration frontale, tangentielle et centrifuge, afin de pouvoir déterminer la stratégie d'investigation la mieux appropriée aux eaux du site d'intérêt, avec pour objectif un réinvestissement méthodologique pour l'étude des mécanismes de mobilisation colloïdale de l'uranium. La SPE apparaissant être une méthode bien maitrisée pour l'extraction de la matière organique, elle a dans un deuxième temps été utilisée dans la partie dédiée à la caractérisation de la MO.

REFERENCES BIBLIOGRAPHIQUES

Abakumov, E., Trubetskoj, O., Demin, D., Celi, L., Cerli, C., Trubetskaya, O., 2010. Humic acid characteristics in podzol soil chronosequence. Chem. Ecol. 26, 59–66. https://doi.org/10.1080/02757540.2010.497758

Abbt-Braun, G., Lankes, U., Frimmel, F.H., 2004. Structural characterization of aquatic humic substances – The need for a multiple method approach. Aquat. Sci. 66, 151–170. https://doi.org/10.1007/s00027-004-0711-z

Aeschbacher, M., Sander, M., Schwarzenbach, R.P., 2010. Novel Electrochemical Approach to Assess the Redox Properties of Humic Substances. Environ. Sci. Technol. 44, 87–93. https://doi.org/10.1021/es902627p

Aiken, G., 1984. Evaluation of Ultrafiltration for Determining Molecular-Weight of Fulvic-Acid. Environ. Sci. Technol. 18, 978–981. https://doi.org/10.1021/es00130a016

Aiken, G.R., 1985. Humic Substances in Soil, Sediment, and Water: Geochemistry, Isolation, and Characterization. John Wiley and Sons.

Aiken, G.R., Thurman, E.M., Malcolm, R.L., Walton, H.F., 1979. Comparison of XAD macroporous resins for the concentration of fulvic acid from aqueous solution. Anal. Chem. 51, 1799–1803. https://doi.org/10.1021/ac50047a044

Akbour, R.A., Douch, J., Hamdani, M., Schmitz, P., 2008. Effet de l'agrégation sur le transport de la kaolinite recouverte d'acide humique à travers un sable de quartz d'origine naturelle. /data/revues/16310713/03340013/02018400/.

Altieri, K.E., Hastings, M.G., Peters, A.J., Sigman, D.M., 2012. Molecular characterization of water soluble organic nitrogen in marine rainwater by ultra-high resolution electrospray ionization mass spectrometry. Atmos. Chem. Phys. 12, 3557–3571. https://doi.org/10.5194/acp-12-3557-2012

Artinger, R., Rabung, T., Kim, J.I., Sachs, S., Schmeide, K., Heise, K.H., Bernhard, G., Nitsche, H., 2002. Humic colloid-borne migration of uranium in sand columns. J Contam Hydrol 58, 1–12. https://doi.org/10.1016/S0169-7722(02)00032-3

Augusto, S., Máguas, C., Matos, J., Pereira, M.J., Branquinho, C., 2010. Lichens as an integrating tool for monitoring PAH atmospheric deposition: A comparison with soil, air and pine needles. Environmental Pollution 158, 483–489. https://doi.org/10.1016/j.envpol.2009.08.016

Baalousha, M., Kammer, F.V.D., Motelica-Heino, M., Le Coustumer, P., 2005a. Natural sample fractionation by FlFFF–MALLS–TEM: Sample stabilization, preparation, pre-concentration and fractionation. Journal of Chromatography A 1093, 156–166. https://doi.org/10.1016/j.chroma.2005.07.103

Baalousha, M., Kammer, F.V.D., Motelica-Heino, M., Le Coustumer, P., 2005b. 3D characterization of natural colloids by FlFFF-MALLS-TEM. Analytical and Bioanalytical Chemistry 383, 549–556. https://doi.org/10.1007/s00216-005-0006-9

Baalousha, M., Motelica-Heino, M., Galaup, S., Le Coustumer, P., 2005c. Supramolecular structure of humic acids by TEM with improved sample preparation and staining. Microscopy Research and Technique 66, 299–306. https://doi.org/10.1002/jemt.20173

Bae, E., Yeo, I.J., Jeong, B., Shin, Y., Shin, K.-H., Kim, S., 2011. Study of Double Bond Equivalents and the Numbers of Carbon and Oxygen Atom Distribution of Dissolved Organic Matter with Negative-Mode FT-ICR MS. Anal. Chem. 83, 4193–4199. https://doi.org/10.1021/ac200464q

Baker, W.E., 1973. The role of humic acids from Tasmanian podzolic soils in mineral degradation and metal mobilization. Geochimica et Cosmochimica Acta 37, 269–281. https://doi.org/10.1016/0016-7037(73)90134-8

Barančíková, G., Senesi, N., Brunetti, G., 1997. Chemical and spectroscopic characterization of humic acids isolated from different Slovak soil types. Geoderma 78, 251–266. https://doi.org/10.1016/S0016-7061(97)00033-5

Basabara, J., Starkey, R.L., 1966. Effect of plant tannins on decomposition of organic substances. Soil Science 101, 17–23.

Benes, P., Czerwinski, K.R., Dolansky, J., 1999. Effect of humic acid on the electrophoretic mobility of uranium (VI) in aqueous solutions. Radiochim. Acta 84, 95–100.

Benoit, R.E., Starkey, R.L., 1968. Enzyme inactivation as a factor in the inhibition of decomposition of organic matter by tannins. Soil Science 105, 203–208.

Benoit, R.E., Starkey, R.L., Basabara, J., 1968. Effect of purified plant tannin on decomposition of some organic compounds and plant materials. Soil Science 105, 153–158.

Bonifacio, E., Catoni, M., Falsone, G., Said-Pullicino, D., Celi, L., 2013. Evolution of surface properties and organic matter stabilisation in podzolic B horizons as assessed by nitrogen and phosphate sorption. Biol. Fertil. Soils 49, 505–516. https://doi.org/10.1007/s00374-013-0788-4

Buckau, G., Artinger, R., Geyer, S., Wolf, M., Fritz, P., Kim, J.I., 2000. Groundwater in-situ generation of aquatic humic and fulvic acids and the mineralization of sedimentary organic carbon. Appl. Geochem. 15, 819–832. https://doi.org/10.1016/S0883-2927(99)00078-5

Buffle, J., Leppard, G.G., 1995. Characterization of Aquatic Colloids and Macromolecules. 1. Structure and Behavior of Colloidal Material. Environ. Sci. Technol. 29, 2169–2175. https://doi.org/10.1021/es00009a004

Bunn, R.A., Magelky, R.D., Ryan, J.N., Elimelech, M., 2002. Mobilization of Natural Colloids from an Iron Oxide-Coated Sand Aquifer: Effect of pH and Ionic Strength. Environ. Sci. Technol. 36, 314–322. https://doi.org/10.1021/es0109141

Bussotti, F., Gravano, E., Grossoni, P., Tani, C., 1998. Occurrence of tannins in leaves of beech trees (Fagus sylvatica) along an ecological gradient, detected by histochemical and ultrastructural analyses. New Phytologist 138, 469–479. https://doi.org/10.1046/j.1469-8137.1998.00121.x

Campo, J., Nierop, K.G.J., Cammeraat, E., Andreu, V., Rubio, J.L., 2011. Application of pyrolysis-gas chromatography/mass spectrometry to study changes in the organic matter of macro- and microaggregates of a Mediterranean soil upon heating. J Chromatogr A 1218, 4817–4827. https://doi.org/10.1016/j.chroma.2011.03.038

Canseco Ruiz, V., 2009. Transport de colloïdes en milieu poreux: étude expérimentale (Thèse de doctorat). École doctorale des Sciences physiques et de l'Ingénieur, Bordeaux, France.

Casenave, A., 1970. Contribution à l'étude de l'alios. Universite de Bordeaux;Faculte des Sciences, Bordeaux (FRA).

Chapuis, F., Pichon, V., Hennion, M.-C., 2005. Méthode de préconcentration par extraction en phase solide: principe et application aux industries environnementales et pétrolières. Oil & gas science and technology 60, 899–912.

Chen, C.-L., Chang, H.-M., Kirk, T.K., 1983. Carboxylic Acids Produced Through Oxidative Cleavage of Aromatic Rings During Degradation of Lignin in Spruce Wood by Phanerochaete Chrysosporium. Journal of Wood Chemistry and Technology 3, 35–57. https://doi.org/10.1080/02773818308085150

Chen, W., Westerhoff, P., Leenheer, J.A., Booksh, K., 2003. Fluorescence Excitation−Emission Matrix Regional Integration to Quantify Spectra for Dissolved Organic Matter. Environ. Sci. Technol. 37, 5701–5710. https://doi.org/10.1021/es034354c

Choi, H., Zhang, K., Dionysiou, D.D., Oerther, D.B., Sorial, G.A., 2005. Effect of permeate flux and tangential flow on membrane fouling for wastewater treatment. Separation and Purification Technology 45, 68–78. https://doi.org/10.1016/j.seppur.2005.02.010

Chung, K.H., Choi, G.S., Shin, H.S., Lee, C.W., 2005. Vertical distribution and characteristics of soil humic substances affecting radionuclide distribution. J Environ Radioact 79, 369–379. https://doi.org/10.1016/j.jenvrad.2004.09.004

Coble, P.G., 1996. Characterization of marine and terrestrial DOM in seawater using excitation emission matrix spectroscopy. Mar. Chem. 51, 325–346. https://doi.org/10.1016/0304-4203(95)00062-3

Cornel, P.K., Summers, R.S., Roberts, P.V., 1986. Diffusion of humic acid in dilute aqueous solution. Journal of Colloid and Interface Science 110, 149–164. https://doi.org/10.1016/0021-9797(86)90364-4

Courchesne, F., Hendershot, W.H., 1997. La genèse des podzols. Géographie physique et Quaternaire 51, 235. https://doi.org/10.7202/033121ar

Crançon, P., 2001. Migration de l'uranium dans un podzol : le rôle des colloïdes dans la zone non saturée et la nappe ; application aux landes de Gascogne (phdthesis). Université Joseph-Fourier - Grenoble I.

Crançon, P., Pili, E., Charlet, L., 2010. Uranium facilitated transport by water-dispersible colloids in field and soil columns. Science of The Total Environment 408, 2118–2128. https://doi.org/10.1016/j.scitotenv.2010.01.061

Crançon, P., Van der Lee, J., 2003. Speciation and mobility of uranium(VI) in humic-containing soils. Radiochimica Acta 91, 673–679. https://doi.org/10.1524/ract.91.11.673.23470

Crawford, D., 1981. Microbial Conversions of Lignin to Useful Chemicals Using a Lignin-Degrading Streptomyces. Biotechnol. Bioeng. 275–291.

Cronan, C., 1985. Chemistry and Movement of Dissolved Humic Substances in 3 Forested Adirondack Watersheds. Org. Geochem. 8, 105–105. https://doi.org/10.1016/0146-6380(85)90058-0

Culfaz, P.Z., Buetehorn, S., Utiu, L., Kueppers, M., Bluemich, B., Melin, T., Wessling, M., Lammertink, R.G.H., 2011. Fouling Behavior of Microstructured Hollow Fiber Membranes in Dead-End Filtrations: Critical Flux Determination and NMR Imaging of Particle Deposition. Langmuir 27, 1643–1652. https://doi.org/10.1021/la1037734

Cumberland, S.A., Douglas, G., Grice, K., Moreau, J.W., 2016. Uranium mobility in organic matter-rich sediments: A review of geological and geochemical processes. Earth-Science Reviews 159, 160–185. https://doi.org/10.1016/j.earscirev.2016.05.010

D'Andrilli, J., Foreman, C.M., Marshall, A.G., McKnight, D.M., 2013. Characterization of IHSS Pony Lake fulvic acid dissolved organic matter by electrospray ionization Fourier transform ion cyclotron resonance mass spectrometry and fluorescence spectroscopy. Org. Geochem. 65, 19–28. https://doi.org/10.1016/j.orggeochem.2013.09.013

Daniel, R.C., Billing, J.M., Russell, R.L., Shimskey, R.W., Smith, H.D., Peterson, R.A., 2011. Integrated pore blockage-cake filtration model for crossflow filtration. Chemical Engineering Research and Design 89, 1094–1103. https://doi.org/10.1016/j.cherd.2010.09.006

David L. Finnegan, Joseph L. Thompson, 2001. Laboratory and Field Studies Related to Radionuclide Migration at the Nevada Test Site in Support of the Underground Test Area Program and Hydrologic Resources Management Project October 1, 1999-September 30, 2000 (No. LA-13787-PR, 775922). https://doi.org/10.2172/775922

Davis, W.M., Erickson, C.L., Johnston, C.T., Delfino, J.J., Porter, J.E., 1999. Quantitative Fourier Transform Infrared spectroscopic investigation humic substance functional group composition. Chemosphere 38, 2913–2928. https://doi.org/10.1016/S0045-6535(98)00486-X

Dawson, H., Ugolini, F., Hrutfiord, B., Zachara, J., 1978. Role of Soluble Organics in Soil Processes of a Podzol, Central Cascades, Washington. Soil Sci. 126, 290–296. https://doi.org/10.1097/00010694-197811000-00006

Degueldre, C., Baeyens, B., Goerlich, W., Riga, J., Verbist, J., Stadelmann, P., 1989. Colloids in water from a subsurface fracture in granitic rock, Grimsel Test Site, Switzerland. Geochimica et Cosmochimica Acta 53, 603–610. https://doi.org/10.1016/0016-7037(89)90003-3

Degueldre, C., Triay, I., Kim, J.I., Vilks, P., Laaksoharju, M., Miekeley, N., 2000. Groundwater colloid properties: a global approach. Appl. Geochem. 15, 1043–1051. https://doi.org/10.1016/S0883-2927(99)00102-X

Dittmar, T., Koch, B., 2006. Thermogenic organic matter dissolved in the abyssal ocean. Marine Chemistry 102, 208–217. https://doi.org/10.1016/j.marchem.2006.04.003

Doi, K., Hirono, S., Sakamaki, Y., 1975. Uranium Mineralization by Ground-Water in Sedimentary-Rocks, Japan. Economic Geology 70, 628–646. https://doi.org/10.2113/gsecongeo.70.4.628

Don, A., Kalbitz, K., 2005. Amounts and degradability of dissolved organic carbon from foliar litter at different decomposition stages. Soil Biology and Biochemistry 37, 2171–2179.

Echantillonnage des eaux souterraines - Office fédéral de l'environnement OFEV [WWW Document], n.d. URL http://www.bafu.admin.ch/publikationen/publikation/00376/index.html?lang=fr (accessed 12.16.15).

Erikson, R., Hostetler, C., Divine, J., Price, K., 1990. A review of the environmental behavior of uranium derived from depleted uranium alloy penetrators (No. PNL-7213, 5105913). https://doi.org/10.2172/5105913

Espinasse, B., 2003. Approche théorique et expérimentale de la filtration tangentielle de colloïdes: flux critique et colmatage. Université Paul Sabatier-Toulouse III.

Eyrolle, F., Charmasson, S., 2000. Ultrafiltration of large volumes for the determination of colloidally bound artificial radionuclides in natural waters. Appl. Radiat. Isot. 52, 927–936. https://doi.org/10.1016/S0969-8043(99)00149-9

Faucher, S., Le Coustumer, P., Lespes, G., 2018. Nanoanalytics: history, concepts, and specificities. Environ Sci Pollut Res Int. https://doi.org/10.1007/s11356-018-1646-6

Feng, X., Simpson, A.J., Wilson, K.P., Dudley Williams, D., Simpson, M.J., 2008. Increased cuticular carbon sequestration and lignin oxidation in response to soil warming. Nature Geoscience 1, 836–839. https://doi.org/10.1038/ngeo361

Fotovat, A., Naidu, R., 1998. Changes in composition of soil aqueous phase influence chemistry of indigenous heavy metals in alkaline sodic and acidic soils. Geoderma 84, 213–234. https://doi.org/10.1016/S0016-7061(97)00130-4

Franke, K., Rössler, D., Gottschalch, U., Kupsch, H., 2000. Mobilization and Retardation of Uranium DOC Species at Three Mine Piles in Schlema/Alberoda, Saxony, Germany. Isotopes in Environmental and Health Studies 36, 223–239. https://doi.org/10.1080/10256010008036383

Frimmel, F.H., 1998. Characterization of natural organic matter as major constituents in aquatic systems. Journal of Contaminant Hydrology 35, 201–216. https://doi.org/10.1016/S0169-7722(98)00133-8

Gabriel, U., Gaudet, J.P., Spadini, L., Charlet, L., 1998. Reactive transport of uranyl in a goethite column: an experimental and modelling study. Chem. Geol. 151, 107–128. https://doi.org/10.1016/S0009-2541(98)00074-6

Geckeis, H., Ngo Manh, T., Bouby, M., Kim, J.I., 2003. Aquatic colloids relevant to radionuclide migration: characterization by size fractionation and ICP-mass spectrometric detection. Colloids and Surfaces A: Physicochemical and Engineering Aspects, Symposium C of the E-MRS 2002 Spring Meeting in Strasbourg, France 217, 101–108. https://doi.org/10.1016/S0927-7757(02)00564-2

Ghabbour, E.A., Davies, G. (Eds.), 2002. Humic Substances: Structures, Models and Functions, 1 edition. ed. Royal Society of Chemistry, Cambridge.

Girard, M.-C., Schvartz, C., Jabiol, B., 2011. Etude des sols: Description, cartographie, utilisation. Dunod.

Godde, M., David, M.B., Christ, M.J., Kaupenjohann, M., Vance, G.F., 1996. Carbon mobilization from the forest floor under red spruce in the northeastern USA. Soil Biol. Biochem. 28, 1181–1189. https://doi.org/10.1016/0038-0717(96)00130-7

Goldberg, M., 1985. Aquatic Photolysis of Oxy-Organic Compounds Adsorbed on Goethite. Abstr. Pap. Am. Chem. Soc. 189, 18-GEOC.

Gounaris, V., Anderson, P.R., Holsen, T.M., 1993. Characteristics and environmental significance of colloids in landfill leachate. Environ. Sci. Technol. 27, 1381–1387. https://doi.org/10.1021/es00044a013

Graham, M.C., Oliver, I.W., MacKenzie, A.B., Ellam, R.M., Farmer, J.G., 2008. An integrated colloid fractionation approach applied to the characterisation of porewater uranium-humic interactions at a depleted uranium contaminated site. Sci. Total Environ. 404, 207–217. https://doi.org/10.1016/j.scitotenv.2008.05.042

Grannas, A.M., Hockaday, W.C., Hatcher, P.G., Thompson, L.G., Mosley-Thompson, E., 2006. New revelations on the nature of organic matter in ice cores. Journal of Geophysical Research: Atmospheres 111. https://doi.org/10.1029/2005JD006251

Grolimund, D., Elimelech, M., Borkovec, M., Barmettler, K., Kretzschmar, R., Sticher, H., 1998. Transport of in Situ Mobilized Colloidal Particles in Packed Soil Columns. Environ. Sci. Technol. 32, 3562–3569. https://doi.org/10.1021/es980356z

Guggenberger, G., Zech, W., 1994. Composition and dynamics of dissolved carbohydrates and lignin-degradation products in two coniferous forests, N.E. Bavaria, Germany. Soil Biology and Biochemistry 26, 19–27. https://doi.org/10.1016/0038-0717(94)90191-0

Guo, L., Warnken, K.W., Santschi, P.H., 2007. Retention behavior of dissolved uranium during ultrafiltration: Implications for colloidal U in surface waters. Mar. Chem. 107, 156–166. https://doi.org/10.1016/j.marchem.2007.06.017

Guo, X., Xi, B., Yu, H., Ma, W., He, X., 2011. The structure and origin of dissolved organic matter studied by UV-vis spectroscopy and fluorescence spectroscopy in lake in arid and semi-arid region. Water Sci. Technol. 63, 1010–1017. https://doi.org/10.2166/wst.2011.282

Hagerman, A.E., Riedl, K.M., Jones, G.A., Sovik, K.N., Ritchard, N.T., Hartzfeld, P.W., Riechel, T.L., 1998. High molecular weight plant polyphenolics (tannins) as biological antioxidants. J. Agric. Food Chem. 46, 1887–1892. https://doi.org/10.1021/jf970975b

Haider, K., 1992. Problems related to the humification processes in soils of temperate climates. In 'Soil Biochemistry, Vol 7'. Stotzky, G and J -M Bollag (Ed), New York, Usa; Basel, Switzerland, pp. 55–94.

Haitzer, M., Aiken, G.R., Ryan, J.N., 2002. Binding of Mercury(II) to Dissolved Organic Matter: The Role of the Mercury-to-DOM Concentration Ratio. Environ. Sci. Technol. 36, 3564–3570. https://doi.org/10.1021/es025699i

Harguindéguy, S., 2013. Transport de l'uranium dans les eaux et le sol : approche combinée colloïdale et isotopique. Pau.

Harguindeguy, S., Crançon, P., Potin Gautier, M., Pointurier, F., Lespes, G., 2018. Colloidal mobilization from soil and transport of uranium in (sub)-surface waters. Environ Sci Pollut Res. https://doi.org/10.1007/s11356-018-2732-5

Harmand, B., 1996. Contribution a la compréhension des processus de transport de colloïdes en milieu naturel poreux ou fracturé : application à la rétention de particules de latex dans un sable (thesis). Vandoeuvre-les-Nancy, INPL.

Hartland, A., Fairchild, I.J., Lead, J.R., Zhang, H., Baalousha, M., 2011. Size, speciation and lability of NOM–metal complexes in hyperalkaline cave dripwater. Geochimica et Cosmochimica Acta 75, 7533–7551. https://doi.org/10.1016/j.gca.2011.09.030

Haslam, E., 1993. Shikimic acid: metabolism and metabolites. Wiley, Chichester; New York.

Hassellov, M., Lyven, B., Haraldsson, C., Sirinawin, W., 1999. Determination of continuous size and trace element distribution of colloidal material in natural water by on-line coupling of flow field-flow fractionation with ICPMS. Anal. Chem. 71, 3497–3502. https://doi.org/10.1021/ac981455y

Hawkes, J.A., Dittmar, T., Patriarca, C., Tranvik, L., Bergquist, J., 2016. Evaluation of the Orbitrap Mass Spectrometer for the Molecular Fingerprinting Analysis of Natural Dissolved Organic Matter. Anal. Chem. 88, 7698–7704. https://doi.org/10.1021/acs.analchem.6b01624

Hayes, M.H.B., Clapp, C.E., 2001. HUMIC SUBSTANCES: CONSIDERATIONS OF COMPOSITIONS, ASPECTS OF STRUCTURE, AND ENVIRONMENTAL INFLUENCES. Soil Science 166, 723–737.

Hayes, M.H.B., Swift, R.S., 1990. Genesis, isolation, composition and structures of soil humic substances. In 'Soil Colloids and Their Associations in Aggregates.'. M.F. DeBoodt, M.H.B. Hayes, and A. Herbillon, New York, pp. 245–305.

Heald, C.L., Kroll, J.H., Jimenez, J.L., Docherty, K.S., DeCarlo, P.F., Aiken, A.C., Chen, Q., Martin, S.T., Farmer, D.K., Artaxo, P., 2010. A simplified description of the evolution of organic aerosol composition in the atmosphere: VAN KREVELEN DIAGRAM OF ORGANIC AEROSOL. Geophysical Research Letters 37. https://doi.org/10.1029/2010GL042737

Helms, J.R., Stubbins, A., Ritchie, J.D., Minor, E.C., Kieber, D.J., Mopper, K., 2008. Absorption spectral slopes and slope ratios as indicators of molecular weight, source, and photobleaching of chromophoric dissolved organic matter. Limnology and Oceanography 53, 955–969. https://doi.org/10.4319/lo.2008.53.3.0955

Hernes, P.J., Hedges, J.I., 2000. Determination of Condensed Tannin Monomers in Environmental Samples by Capillary Gas Chromatography of Acid Depolymerization Extracts. Analytical Chemistry 72, 5115–5124. https://doi.org/10.1021/ac991301y

Hertkorn, N., Frommberger, M., Witt, M., Koch, B.P., Schmitt-Kopplin, P., Perdue, E.M., 2008. Natural Organic Matter and the Event Horizon of Mass Spectrometry. Anal. Chem. 80, 8908–8919. https://doi.org/10.1021/ac800464g

Hockaday, W.C., Grannas, A.M., Kim, S., Hatcher, P.G., 2006. Direct molecular evidence for the degradation and mobility of black carbon in soils from ultrahigh-resolution mass spectral analysis of dissolved organic matter from a fire-impacted forest soil. Org. Geochem. 37, 501–510. https://doi.org/10.1016/j.orggeochem.2005.11.003

Hockaday, W.C., Purcell, J.M., Marshall, A.G., Baldock, J.A., Hatcher, P.G., 2009. Electrospray and photoionization mass spectrometry for the characterization of organic matter in natural waters: a qualitative assessment. Limnology and Oceanography: Methods 7, 81–95. https://doi.org/10.4319/lom.2009.7.81

Huc, A.Y., Durand, B.M., 1977. Occurrence and significance of humic acids in ancient sediments. Fuel 56, 73–80. https://doi.org/10.1016/0016-2361(77)90046-1

Humbert, L., 2010. Extraction en phase solide (SPE) : théorie et applications. Annales de Toxicologie Analytique 22, 61–68. https://doi.org/10.1051/ata/2010010

Hwang, K.J., Liu, H.C., Lu, W.M., 1998. Local properties of cake in cross-flow microfiltration of submicron particles. J. Membr. Sci. 138, 181–192. https://doi.org/10.1016/S0376-7388(97)00230-5

Ide, J., Ohashi, M., Takahashi, K., Sugiyama, Y., Piirainen, S., Kortelainen, P., Fujitake, N., Yamase, K., Ohte, N., Moritani, M., Hara, M., Finer, L., 2017. Spatial variations in the molecular diversity of dissolved organic matter in water moving through a boreal forest in eastern Finland. Sci Rep 7, 42102. https://doi.org/10.1038/srep42102

Ishiwatari, R., 1992. Macromolecular material (humic substance) in the water column and sediments. Marine Chemistry 39, 151–166. https://doi.org/10.1016/0304-4203(92)90099-V

Johnson, C.E., Driscoll, C.T., Siccama, T.G., Likens, G.E., 2000. Element fluxes and landscape position in a northern hardwood forest watershed ecosystem. Ecosystems 3, 159–184. https://doi.org/10.1007/s100210000017

Jolivet, C., Augusto, L., Trichet, P., Arrouays, D., 2007. Les sols du massif forestier des Landes de Gascogne : formation, histoire, propriétés et variabilité spatiale. Revue Forestière Française. https://doi.org/10.4267/2042/8480

Jones, M.N., Bryan, N.D., 1998. Colloidal properties of humic substances. Advances in Colloid and Interface Science 78, 1–48. https://doi.org/10.1016/S0001-8686(98)00058-X

Kaiser, K., Guggenberger, G., Haumaier, L., Zech, W., 2001. Seasonal variations in the chemical composition of dissolved organic matter in organic forest floor layer leachates of old-growth Scots pine (Pinus sylvestris L.) and European beech (Fagus sylvatica L.) stands in northeastern Bavaria, Germany. Biogeochemistry 55, 103–143. https://doi.org/10.1023/A:1010694032121

Kaiser, K., Kalbitz, K., 2012. Cycling downwards – dissolved organic matter in soils. Soil Biology and Biochemistry 52, 29–32. https://doi.org/10.1016/j.soilbio.2012.04.002

Kalbitz, K., Solinger, S., Park, J.-H., Michalzik, B., Matzner, E., 2000. Controls on the dynamics of dissolved organic matter in soils: A review. Soil Science 165, 277–304.

Kanti Sen, T., Khilar, K.C., 2006. Review on subsurface colloids and colloid-associated contaminant transport in saturated porous media. Advances in Colloid and Interface Science 119, 71–96. https://doi.org/10.1016/j.cis.2005.09.001

Kersting, A.B., Efurd, D.W., Finnegan, D.L., Rokop, D.J., Smith, D.K., Thompson, J.L., 1999a. Migration of plutonium in ground water at the Nevada Test Site. Nature 397, 56–59. https://doi.org/10.1038/16231

Kersting, A.B., Efurd, D.W., Finnegan, D.L., Rokop, D.J., Smith, D.K., Thompson, J.L., 1999b. Migration of plutonium in ground water at the Nevada Test Site. Nature 397, 56–59. https://doi.org/10.1038/16231

Kew, W., Blackburn, J.W.T., Clarke, D.J., Uhrín, D., 2017. Interactive van Krevelen diagrams – Advanced visualisation of mass spectrometry data of complex mixtures. Rapid Commun Mass Spectrom 31, 658–662. https://doi.org/10.1002/rcm.7823

Kim, S., Kramer, R.W., Hatcher, P.G., 2003. Graphical Method for Analysis of Ultrahigh-Resolution Broadband Mass Spectra of Natural Organic Matter, the Van Krevelen Diagram. Anal. Chem. 75, 5336–5344. https://doi.org/10.1021/ac034415p

Kim, S.-J., Kim, J.-O., Kim, W.-S., Oh, M.-J., 2015. Use of a two-step ultrafiltration procedure to concentrate viral hemorrhagic septicemia virus (VHSV) in seawater. Journal of Virological Methods 224, 30–34. https://doi.org/10.1016/j.jviromet.2015.08.006

Knicker, H., Ludemann, H.D., Haider, K. (Institut fur B. und physikalische B., 1997. Incorporation studies of NH4+ during incubation of organic residues by 15N-CPMAS-NMR-spectroscopy. European Journal of Soil Science (United Kingdom).

Knutsen, J.S., Davis, R.H., 2006. Deposition of foulant particles during tangential flow filtration. Journal of Membrane Science 271, 101–113. https://doi.org/10.1016/j.memsci.2005.06.060

Koch, B.P., Dittmar, T., 2006. From mass to structure: an aromaticity index for high-resolution mass data of natural organic matter. Rapid Communications in Mass Spectrometry 20, 926–932. https://doi.org/10.1002/rcm.2386

Koch, B.P., Dittmar, T., Witt, M., Kattner, G., 2007. Fundamentals of Molecular Formula Assignment to Ultrahigh Resolution Mass Data of Natural Organic Matter. Anal. Chem. 79, 1758–1763. https://doi.org/10.1021/ac061949s

Kononova, M.M., Alexandrova, I.V., 1973. Formation of humic acids during plant residue humification and their nature. Geoderma 9, 157–164. https://doi.org/10.1016/0016-7061(73)90056-6

Kraus, T.E.C., Dahlgren, R.A., Zasoski, R.J., 2003. Tannins in nutrient dynamics of forest ecosystems - a review. Plant and Soil 256, 41–66. https://doi.org/10.1023/A:1026206511084

Kretzschmar, R., Barmettler, K., Grolimund, D., Yan, Y., Borkovec, M., Sticher, H., 1997. Experimental determination of colloid deposition rates and collision efficiencies in natural porous media. Water Resources Research 33, 1129–1137. https://doi.org/10.1029/97WR00298

Kretzschmar, R., Borkovec, M., Grolimund, D., Elimelech, M., 1999. Mobile Subsurface Colloids and Their Role in Contaminant Transport. In 'Advances in Agronomy' (Ed. Sparks, D.L.). Academic Press, pp. 121–193.

Kretzschmar, R., Schafer, T., 2005. Metal Retention and Transport on Colloidal Particles in the Environment. Elements 1, 205–210. https://doi.org/10.2113/gselements.1.4.205

Lapworth, D.J., Stolpe, B., Williams, P.J., Gooddy, D.C., Lead, J.R., 2013. Characterization of Suboxic Groundwater Colloids Using a Multi-method Approach. Environ. Sci. Technol. 47, 2554–2561. https://doi.org/10.1021/es3045778

Lead, J.R., Davison, W., Hamilton-Taylor, J., Buffle, J., 1997. Characterizing colloidal material in natural waters. Aquatic Geochemistry 3, 213–232.

Lead, J.R., Wilkinson, K.J., 2006. Aquatic colloids and nanoparticles: Current knowledge and future trends. Environ. Chem. 3, 159–171. https://doi.org/10.1071/EN06025

Lenhart, J.J., Honeyman, B.D., 1999. Uranium(VI) sorption to hematite in the presence of humic acid. Geochim. Cosmochim. Acta 63, 2891–2901. https://doi.org/10.1016/S0016-7037(99)00269-0

Little, B., Jacobus, J., 1985. A comparison of two techniques for the isolation of adsorbed dissolved organic material from seawater. Organic Geochemistry 8, 27–33. https://doi.org/10.1016/0146-6380(85)90047-6

Liu, H., Amy, G., 1993. Modeling partitioning and transport interactions between natural organic matter and polynuclear aromatic hydrocarbons in groundwater. Environ. Sci. Technol. 27, 1553–1562. https://doi.org/10.1021/es00045a009

Lobodin, V.V., Rodgers, R.P., Marshall, A.G., 2012. Petroleomics and the analysis of complex organic mixtures with Fourier transform ion cyclotron resonance. In 'Comprehensive Environmental Mass Spectrometry (Advanced Topics in Environmental Science): 4'. ILM Publications, Glendale, AZ.

Lubal, P., Fetsch, D., Siroky, D., Lubalova, M., Senkyr, J., Havel, J., 2000. Potentiometric and spectroscopic study of uranyl complexation with humic acids. Talanta 51, 977–991. https://doi.org/10.1016/S0039-9140(00)00281-2

Lundstrom, U.S., van Breemen, N., Bain, D., 2000. The podzolization process. A review. Geoderma 94, 91–107. https://doi.org/10.1016/S0016-7061(99)00036-1

MacCarthy, P., 2001. THE PRINCIPLES OF HUMIC SUBSTANCES. Soil Science 166, 738–751.

MacCarthy, P., Bloom, P.R., Clapp, C.E., Malcolm, R.L., 1990a. Humic Substances in Soil and Crop Sciences: An Overview. Humic Substances in Soil and Crop Sciences: Selected Readings acsesspublicati, 261–271. https://doi.org/10.2136/1990.humicsubstances.c11

MacCarthy, P., Malcolm, R.L., Clapp, C.E., Bloom, P.R., 1990b. An introduction to soil humic substances. In 'Humic Substances in Soil and Crop Sciences: Selected Readings'. pp. 1–12.

Mackley, M., Sherman, N., 1994. Cross-Flow Filtration with and Without Cake Formation. Chem. Eng. Sci. 49, 171–178. https://doi.org/10.1016/0009-2509(94)80035-9

Maes, A., Cremers, A., 1987. Highly Selective Ion Exchange in Clay Minerals and Zeolites. In 'Geochemical Processes at Mineral Surfaces' 'ACS Symposium Series'. American Chemical Society, pp. 254–295. https://doi.org/10.1021/bk-1987-0323.ch013

Majedi, S.M., Lee, H.K., 2016. Recent advances in the separation and quantification of metallic nanoparticles and ions in the environment. Trac-Trends in Analytical Chemistry 75, 183–196. https://doi.org/10.1016/j.trac.2015.08.009

Malcolm, R., L., 1990. The uniqueness of humic substances in each of soil, stream and marine environments. Analytica Chimica Acta 232, 19–30. https://doi.org/10.1016/S0003-2670(00)81222-2

Marley, N., Gaffney, J., Orlandini, K., Dugue, C., 1991. An Evaluation of an Automated Hollow-Fiber Ultrafiltration Apparatus for the Isolation of Colloidal Materials in Natural-Waters. Hydrol. Process. 5, 291–299. https://doi.org/10.1002/hyp.3360050309

Martin, J.P., Haider, K., Kassim, G., 1980. Biodegradation and Stabilization after 2 Years of Specific Crop, Lignin, and Polysaccharide Carbons in Soils1. Soil Science Society of America Journal 44, 1250. https://doi.org/10.2136/sssaj1980.03615995004400060024x

Matin, A., Shafi, H., Wang, M., Khan, Z., Gleason, K., Rahman, F., 2016. Reverse osmosis membranes surface-modified using an initiated chemical vapor deposition technique show resistance to alginate fouling under cross-flow conditions: Filtration & subsequent characterization. Desalination 379, 108–117. https://doi.org/10.1016/j.desal.2015.11.003

Maurer, F., Christl, I., Kretzschmar, R., 2010. Reduction and Reoxidation of Humic Acid: Influence on Spectroscopic Properties and Proton Binding. Environ. Sci. Technol. 44, 5787–5792. https://doi.org/10.1021/es100594t

McCarthy, A.J., Paterson, A., Broda, P., 1986. Lignin solubilisation by Thermomonospora mesophila. Appl Microbiol Biotechnol 24, 347–352. https://doi.org/10.1007/BF00257062

McCarthy, J.F., 1998. Colloid-facilitated transport of contaminants in groundwater: mobilization of transuranic radionuclides from disposal trenches by natural organic matter. Physics and Chemistry of the Earth 23, 171–178. https://doi.org/10.1016/S0079-1946(98)00009-3

McCarthy, J.F., Zachara, J.M., 1989. Subsurface transport of contaminants. Environ. Sci. Technol. 23, 496–502. https://doi.org/10.1021/es00063a001

McDonald, S., Bishop, A.G., Prenzler, P.D., Robards, K., 2004. Analytical chemistry of freshwater humic substances. Analytica Chimica Acta 527, 105–124. https://doi.org/10.1016/j.aca.2004.10.011

McDowell, W.H., Likens, G.E., 1988. Origin, Composition, and Flux of Dissolved Organic Carbon in the Hubbard Brook Valley. Ecological Monographs 58, 177–195. https://doi.org/10.2307/2937024

McDowell-Boyer, L.M., Hunt, J.R., Sitar, N., 1986. Particle transport through porous media. Water Resources Research 22, 1901–1921. https://doi.org/10.1029/WR022i013p01901

McKnight, D.M., Boyer, E.W., Westerhoff, P.K., Doran, P.T., Kulbe, T., Andersen, D.T., 2001. Spectrofluorometric characterization of dissolved organic matter for indication of precursor organic material and aromaticity. Limnology and Oceanography 46, 38–48. https://doi.org/10.4319/lo.2001.46.1.0038

Mehrabanian, M., 2013. Molecular geochemistry of soil organic matter by pyrolysis gas chromatography/mass spectrometry (GC/MS) technique: A review. Journal of Soil Science and Environmental Management 4, 11–16. https://doi.org/10.5897/JSSEM12.033

Menguy, T., Chenevois, S., Guillain, F., le Maire, M., Falson, P., Champeil, P., 1998. Ligand binding to macromolecules or micelles: Use of centrifugal ultrafiltration to measure low-affinity binding. Anal. Biochem. 264, 141–148. https://doi.org/10.1006/abio.1998.2854

Mibus, J., Sachs, S., Pfingsten, W., Nebelung, C., Bernhard, G., 2007. Migration of uranium(IV)/(VI)in the presence of humic acids in quartz sand: A laboratory column study. J. Contam. Hydrol. 89, 199–217. https://doi.org/10.1016/j.jconhyd.2006.08.005

Michalzik, B., Matzner, E., 1999. Dynamics of dissolved organic nitrogen and carbon in a Central European Norway spruce ecosystem. European Journal of Soil Science 50, 579–590. https://doi.org/10.1046/j.1365-2389.1999.00267.x

Mokma, D.L., Yli-Halla, M., Lindqvist, K., 2004. Podzol formation in sandy soils of Finland. Geoderma 120, 259–272. https://doi.org/10.1016/j.geoderma.2003.09.008

Mondal, S., Wickramasinghe, S.R., 2008. Produced water treatment by nanofiltration and reverse osmosis membranes. J. Membr. Sci. 322, 162–170. https://doi.org/10.1016/j.memsci.2008.05.039

Montavon, G., Mansel, A., Seibert, A., Keller, H., Kratz, J.V., Trautmann, N., 2000. Complexation studies of UO22+ with humic acid at low metal ion concentrations by indirect speciation methods. Radiochim. Acta 88, 17–24. https://doi.org/10.1524/ract.2000.88.1.017

Morrison, M.A., Benoit, G., 2001. Filtration artifacts caused by overloading membrane filters. Environ. Sci. Technol. 35, 3774–3779. https://doi.org/10.1021/es010670k

Morrison, S., Spangler, R., Tripathi, V., 1995. Adsorption of Uranium(vi) on Amorphous Ferric Oxyhydroxide at High-Concentrations of Dissolved Carbon(iv) and Sulfur(vi). J. Contam. Hydrol. 17, 333–346. https://doi.org/10.1016/0169-7722(94)00039-K

Moulin, V., Amekraz, B., Barre, N., Planque, G., Mercier, F., Reiller, P., Moulin, C., 2004. The role of humic substances in trace element mobility in natural environments and applications to radionuclides. Taylor & Francis Ltd, London.

Moulin, V., Moulin, C., 1995. Fate of actinides in the presence of humic substances under conditions relevant to nuclear waste disposal. Applied Geochemistry 10, 573–580. https://doi.org/10.1016/0883-2927(95)00029-1

Moulin, V., Ouzounian, G., 1992. Role of colloids and humic substances in the transport of radio-elements through the geosphere. Applied Geochemistry 7, 179–186. https://doi.org/10.1016/S0883-2927(09)80074-7

Murphy, R.J., Lenhart, J.J., Honeyman, B.D., 1999. The sorption of thorium (IV) and uranium (VI) to hematite in the presence of natural organic matter. Colloid Surf. A-Physicochem. Eng. Asp. 157, 47–62. https://doi.org/10.1016/S0927-7757(99)00115-6

Muscolo, A., Sidari, M., Attinà, E., Francioso, O., Tugnoli, V., Nardi, S., 2007. Biological Activity of Humic Substances Is Related to Their Chemical Structure. Soil Science Society of America Journal 71, 75. https://doi.org/10.2136/sssaj2006.0055

Nebbioso, A., Piccolo, A., 2012. Molecular characterization of dissolved organic matter (DOM): a critical review. Anal Bioanal Chem 405, 109–124. https://doi.org/10.1007/s00216-012-6363-2

Nič, M., Jirát, J., Košata, B., Jenkins, A., McNaught, A. (Eds.), 2009. IUPAC Compendium of Chemical Terminology: Gold Book, 2.1.0. ed. IUPAC, Research Triagle Park, NC.

Oliver, I.W., Graham, M.C., Mackenzie, A.B., Ellam, R.M., Farmer, J.G., 2008. Depleted Uranium Mobility Across a Weapons Testing Site: Isotopic Investigation of Porewater, Earthworms, and Soils. Environ. Sci. Technol. 42, 9158–9164. https://doi.org/10.1021/es8013634

Opsahl, S., Benner, R., 1998. Photochemical reactivity of dissolved lignin in river and ocean waters. Limnol. Oceanogr. 43, 1297–1304. https://doi.org/10.4319/lo.1998.43.6.1297

Orrego-Ruiz, J.A., Gomez-Escudero, A., Rojas-Ruiz, F.A., 2016. Combination of Negative Electrospray Ionization and Positive Atmospheric Pressure Photoionization Fourier Transform Ion Cyclotron Resonance Mass Spectrometry as a Quantitative Approach of Acid Species in Crude Oils. Energy Fuels 30, 8209–8215. https://doi.org/10.1021/acs.energyfuels.6b01524

Otto, A., Simpson, M.J., 2006. Evaluation of CuO oxidation parameters for determining the source and stage of lignin degradation in soil. Biogeochemistry 80, 121–142. https://doi.org/10.1007/s10533-006-9014-x

Page, S.E., Sander, M., Arnold, W.A., McNeill, K., 2012. Hydroxyl radical formation upon oxidation of reduced humic acids by oxygen in the dark. Environ. Sci. Technol. 46, 1590–1597. https://doi.org/10.1021/es203836f

Paterson, A., Lundquist, K., 1985. Polymer biochemistry: Radical breakdown of lignin. Nature 316, 575–576. https://doi.org/10.1038/316575a0

Petersen, L., 1976. Podzols and podzolization. The Royal Veterinary and Agricultural University, Copenhagen, Denmark.

Piccolo, A., 2001. The supramolecular structure of humic substances. Soil science 166, 810–832.

Pracht, L.E., Tfaily, M.M., Ardissono, R.J., Neumann, R.B., 2018. Molecular characterization of organic matter mobilized from Bangladeshi aquifer sediment: tracking carbon compositional change during microbial utilization. Biogeosciences 15, 1733–1747. https://doi.org/10.5194/bg-15-1733-2018

Purcell, J.M., Juyal, P., Kim, D.-G., Rodgers, R.P., Hendrickson, C.L., Marshall, A.G., 2007. Sulfur speciation in petroleum: Atmospheric pressure photoionization or chemical derivatization and electrospray ionization fourier transform ion cyclotron resonance mass spectrometry. Energy Fuels 21, 2869–2874. https://doi.org/10.1021/ef700210q

Ragnarsdottir, K.V., Charlet, L., 2000. Uranium behaviour in natural environments. Mineralogical Society Great Britain & Ireland, London.

Raha, S., Pradip, Kapur, P.C., Khilar, K.C., 2009. Enhancement of Colloidal Filtration: A New Combined Approach Based on Cake and Suspension Destabilization. Ind. Eng. Chem. Res. 48, 7276–7282. https://doi.org/10.1021/ie801750w

Randall, E.W., Mahieu, N., Ivanova, G.I., 1997. NMR studies of soil, soil organic matter and nutrients: spectroscopy and imaging. Geoderma, NMR in Soil Science 80, 307–325. https://doi.org/10.1016/S0016-7061(97)00057-8

Ranville, J.F., Hendry, M.J., Reszat, T.N., Xie, Q., Honeyman, B.D., 2007. Quantifying uranium complexation by groundwater dissolved organic carbon using asymmetrical flow field-flow fractionation. Journal of Contaminant Hydrology 91, 233–246. https://doi.org/10.1016/j.jconhyd.2006.11.002

Reemtsma, T., These, A., Linscheid, M., Leenheer, J., Spitzy, A., 2008. Molecular and structural characterization of dissolved organic matter from the deep ocean by FTICR-MS, including hydrophilic nitrogenous organic molecules. Environ. Sci. Technol. 42, 1430–1437. https://doi.org/10.1021/es7021413

Reiller, P.E., Evans, N.D.M., Szabo, G., 2008. Complexation parameters for the actinides(IV)-humic acid system: a search for consistency and application to laboratory and field observations. Radiochim. Acta 96, 345–358. https://doi.org/10.1524/ract.2008.1500

Reiller, P.E., Marang, L., Jouvin, D., Benedetti, M.F., 2012. Uranium (VI) Binding to Humic Substances: Speciation, Estimation of Competition, and Application to Independent Data. In 'The New Uranium Mining Boom: Challenge and Lessons Learned' 'Springer Geology' (Eds. Merkel, B., Schipek, M.). Springer Berlin Heidelberg, Berlin, Heidelberg, pp. 565–572. https://doi.org/10.1007/978-3-642-22122-4_65

Remucal, C.K., Cory, R.M., Sander, M., McNeill, K., 2012. Low Molecular Weight Components in an Aquatic Humic Substance As Characterized by Membrane Dialysis and Orbitrap Mass Spectrometry. Environmental Science & Technology 46, 9350–9359. https://doi.org/10.1021/es302468q

Rice, J.A., MacCarthy, P., 1991. Statistical evaluation of the elemental composition of humic substances. Organic Geochemistry 17, 635–648. https://doi.org/10.1016/0146-6380(91)90006-6

Righi, D., Wilbert, J., 1984. Les sols sableux podzolisés des Landes de Gascogne (France) : répartition et caractères principaux. Science du sol 253–264.

Riise, G., Van Hees, P., Lundström, U., Tau Strand, L., 2000. Mobility of different size fractions of organic carbon, Al, Fe, Mn and Si in podzols. Geoderma 94, 237–247. https://doi.org/10.1016/S0016-7061(99)00044-0

Roberts, K.A., Santschi, P.H., Leppard, G.G., West, M.M., 2004. Characterization of organic-rich colloids from surface and ground waters at the actinide-contaminated Rocky Flats Environmental Technology Site (RFETS), Colorado, USA. Colloids and Surfaces A: Physicochemical and Engineering Aspects 244, 105–111. https://doi.org/10.1016/j.colsurfa.2004.06.009

Ryan, J.N., Elimelech, M., 1996. Colloid mobilization and transport in groundwater. Colloids and Surfaces A: Physicochemical and Engineering Aspects, A collection of papers presented at the Symposium on Colloidal and Interfacial Phenomena in Aquatic Environments 107, 1–56. https://doi.org/10.1016/0927-7757(95)03384-X

Saito, T., Hamamoto, T., Mizuno, T., Iwatsuki, T., Tanaka, S., 2015. Comparative study of granitic and sedimentary groundwater colloids by flow-field flow fractionation coupled with ICP-MS. Journal of Analytical Atomic Spectrometry 30, 1229–1236. https://doi.org/10.1039/c5ja00088b

Sandron, S., Rojas, A., Wilson, R., Davies, N.W., Haddad, P.R., Shellie, R.A., Nesterenko, P.N., Kelleher, B.P., Paull, B., 2015. Chromatographic methods for the isolation, separation and characterisation of dissolved organic matter. Environmental Science: Processes & Impacts 17, 1531–1567. https://doi.org/10.1039/C5EM00223K

Šantl-Temkiv, T., Finster, K., Dittmar, T., Hansen, B.M., Thyrhaug, R., Nielsen, N.W., Karlson, U.G., 2013. Hailstones: A Window into the Microbial and Chemical Inventory of a Storm Cloud. PLOS ONE 8, e53550. https://doi.org/10.1371/journal.pone.0053550

Sauer, D., Sponagel, H., Sommer, M., Giani, L., Jahn, R., Stahr, K., 2007. Review Article Podzol: Soil of the Year 2007 A review on its genesis, occurrence, and functions. J. Plant Nutr. Soil Sci. 170, 581–597. https://doi.org/10.1002/jpln.200700135

Schmitt-Kopplin, P., Harir, M., Tziotis, D., Zelimir, G., Hertkorn, N., 2012. Ultrahigh resolution Fourier transform ion cyclotron (FTICR) mass spectrometry for the analysis of natural organic matter from various environmental systems. In 'Comprehensive Environmental Mass Spectrometry'. ILM Publications, pp. 443–460.

Schulten, H.-R., Gleixner, G., 1999. Analytical pyrolysis of humic substances and dissolved organic matter in aquatic systems: structure and origin. Water Research 33, 2489–2498. https://doi.org/10.1016/S0043-1354(98)00493-X

Schwarzenbach, R.P., Gschwend, P.M., Imboden, D.M., 2002. Environmental Organic Chemistry, 2 edition. ed. Wiley-Interscience, New York.

Seaman, J.C., Bertsch, P.M., Miller, W.P., 1995. Chemical Controls on Colloid Generation and Transport in a Sandy Aquifer. Environ. Sci. Technol. 29, 1808–1815. https://doi.org/10.1021/es00007a018

Shaw, D.J., 1992. Introduction to colloid and surface chemistry, 4th ed. ed. Oxford ; Boston.

Singhal, R.K., Kumar, A., Karpe, P.J.R., Datta, M., Hegde, A.G., 2005. Association of uranium with colloids of natural organic matter in subsurface aquatic environment. J. Radioanal. Nucl. Chem. 265, 405–408. https://doi.org/10.1007/s10967-005-0841-3

Sleighter, R.L., Hatcher, P.G., 2008. Molecular characterization of dissolved organic matter (DOM) along a river to ocean transect of the lower Chesapeake Bay by ultrahigh resolution electrospray ionization Fourier transform ion cyclotron resonance mass spectrometry. Mar. Chem. 110, 140–152. https://doi.org/10.1016/j.marchem.2008.04.008

Spencer, R.G.M., Mann, P.J., Dittmar, T., Eglinton, T.I., McIntyre, C., Holmes, R.M., Zimov, N., Stubbins, A., 2015. Detecting the signature of permafrost thaw in Arctic rivers: SIGNATURE OF PERMAFROST THAW IN RIVERS. Geophysical Research Letters 42, 2830–2835. https://doi.org/10.1002/2015GL063498

Spencer, R.G.M., Stubbins, A., Hernes, P.J., Baker, A., Mopper, K., Aufdenkampe, A.K., Dyda, R.Y., Mwamba, V.L., Mangangu, A.M., Wabakanghanzi, J.N., Six, J., 2009. Photochemical degradation of dissolved organic matter and dissolved lignin phenols from the Congo River. Journal of Geophysical Research: Biogeosciences 114. https://doi.org/10.1029/2009JG000968

Steelink, C., 2002. Peer Reviewed: Investigating Humic Acids in Soils. Anal. Chem. 74, 326 A-333 A. https://doi.org/10.1021/ac022040m

Stenson, A.C., Landing, W.M., Marshall, A.G., Cooper, W.T., 2002. Ionization and fragmentation of humic substances in electrospray ionization Fourier transform-ion cyclotron resonance mass spectrometry. Anal. Chem. 74, 4397–4409. https://doi.org/10.1021/ac020019f

Stenson, A.C., Marshall, A.G., Cooper, W.T., 2003. Exact Masses and Chemical Formulas of Individual Suwannee River Fulvic Acids from Ultrahigh Resolution Electrospray Ionization Fourier Transform Ion Cyclotron Resonance Mass Spectra. Anal. Chem. 75, 1275–1284. https://doi.org/10.1021/ac026106p

Stevenson, F.J., 1994. Humus chemistry: genesis, composition, reactions. John Wiley & Sons, New York.

Stolpe, B., Guo, L., Shiller, A.M., Hassellöv, M., 2010. Size and composition of colloidal organic matter and trace elements in the Mississippi River, Pearl River and the northern Gulf of Mexico, as characterized by flow field-flow fractionation. Marine Chemistry 118, 119–128. https://doi.org/10.1016/j.marchem.2009.11.007

Stolpe, B., Hassellöv, M., Andersson, K., Turner, D.R., 2005. High resolution ICPMS as an on-line detector for flow field-flow fractionation; multi-element determination of colloidal size distributions in a natural water sample. Analytica Chimica Acta 535, 109–121. https://doi.org/10.1016/j.aca.2004.11.067

Stubbins, A., Hood, E., Raymond, P.A., Aiken, G.R., Sleighter, R.L., Hernes, P.J., Butman, D., Hatcher, P.G., Striegl, R.G., Schuster, P.F., Abdulla, H.A.N., Vermilyea, A.W., Scott, D.T., Spencer, R.G.M., 2012. Anthropogenic aerosols as a source of ancient dissolved organic matter in glaciers. Nature Geoscience 5, 198201. https://doi.org/10.1038/ngeo1403

Stubbins, A., Spencer, R.G.M., Chen, H., Hatcher, P.G., Mopper, K., Hernes, P.J., Mwamba, V.L., Mangangu, A.M., Wabakanghanzi, J.N., Six, J., 2010. Illuminated darkness: Molecular signatures of Congo River dissolved organic matter and its photochemical alteration as revealed by ultrahigh precision mass spectrometry. Limnology and Oceanography 55, 1467–1477. https://doi.org/10.4319/lo.2010.55.4.1467

Stubbins, A., Spencer, R.G.M., Mann, P.J., Holmes, R.M., McClelland, J.W., Niggemann, J., Dittmar, T., 2015. Utilizing colored dissolved organic matter to derive dissolved black carbon export by arctic rivers. Front. Earth Sci. 3. https://doi.org/10.3389/feart.2015.00063

Stumm, W., Morgan, J.J., 1996. Aquatic chemistry: chemical equilibria and rates in natural waters. Wiley.

Swenson, M.M., Oyler, A.R., Minor, E.C., 2014. Rapid solid phase extraction of dissolved organic matter. Limnol. Oceanogr. 12, 713–728. https://doi.org/10.4319/lom.2014.12.713

Świetlik, J., Sikorska, E., 2006. Characterization of Natural Organic Matter Fractions by High Pressure Size-Exclusion Chromatography, Specific UV Absorbance and Total Luminescence Spectroscopy 9.

Tfaily, M.M., Chu, R.K., Tolić, N., Roscioli, K.M., Anderton, C.R., Paša-Tolić, L., Robinson, E.W., Hess, N.J., 2015. Advanced solvent based methods for molecular characterization of soil organic matter by high-resolution mass spectrometry. Anal. Chem. 87, 5206–5215. https://doi.org/10.1021/acs.analchem.5b00116

Thevenot, M., Dignac, M.-F., Rumpel, C., 2010. Fate of lignins in soils: A review. Soil Biology and Biochemistry 42, 1200–1211. https://doi.org/10.1016/j.soilbio.2010.03.017

Thomas, J.D., 1997. The role of dissolved organic matter, particularly free amino acids and humic substances, in freshwater ecosystems. Freshwater Biology 38, 1–36. https://doi.org/10.1046/j.1365-2427.1997.00206.x

Thoss, V., Shevtsova, A., Nilsson, M.C., 2004. Environmental manipulation treatment effects on the reactivity of water-soluble phenolics in a subalpine tundra ecosystem. Plant Soil 259, 355–365. https://doi.org/10.1023/B:PLSO.0000020984.17403.82

Thurman, E.M., 1985. Aquatic Humic Substances. In 'Organic Geochemistry of Natural Waters' 'Developments in Biogeochemistry'. Springer Netherlands, pp. 273–361. https://doi.org/10.1007/978-94-009-5095-5_11

Trusiak, A., Treibergs, L.A., Kling, G.W., Cory, R.M., 2018. The role of iron and reactive oxygen species in the production of CO2 in arctic soil waters. Geochimica et Cosmochimica Acta 224, 80–95. https://doi.org/10.1016/j.gca.2017.12.022

Van der Bruggen, B., Vandecasteele, C., 2002. Distillation vs. membrane filtration: overview of process evolutions in seawater desalination. Desalination 143, 207–218. https://doi.org/10.1016/S0011-9164(02)00259-X

Van der Lee, J., 1997. Modélisation du comportement géochimique et du transport des radionucléides en présence de colloïdes (thesis). Paris, ENMP.

Van Krevelen, D.W., 1961. Graphical-statistical method for the study of structure and reaction processes of coal. Fuel 29, 269–283.

Vermilyea, A.W., Voelker, B.M., 2009. Photo-Fenton Reaction at Near Neutral pH. Environ. Sci. Technol. 43, 6927–6933. https://doi.org/10.1021/es900721x

Vigneswaran, S., Kwon, D.-Y., 2015. Effect of ionic strength and permeate flux on membrane fouling: Analysis of forces acting on particle deposit and cake formation. KSCE J. Civ. Eng. 19, 1604–1611. https://doi.org/10.1007/s12205-014-0079-0

Waggoner, D.C., Chen, H., Willoughby, A.S., Hatcher, P.G., 2015. Formation of black carbon-like and alicyclic aliphatic compounds by hydroxyl radical initiated degradation of lignin. Org. Geochem. 82, 69–76. https://doi.org/10.1016/j.orggeochem.2015.02.007

Waggoner, D.C., Wozniak, A.S., Cory, R.M., Hatcher, P.G., 2017. The role of reactive oxygen species in the degradation of lignin derived dissolved organic matter. Geochim. Cosmochim. Acta 208, 171–184. https://doi.org/10.1016/j.gca.2017.03.036

Wagner, M., Schmidt, W., Imhof, L., Grübel, A., Jähn, C., Georgi, D., Petzoldt, H., 2016. Characterization and quantification of humic substances 2D-Fluorescence by usage of extended size exclusion chromatography. Water Research 93, 98–109. https://doi.org/10.1016/j.watres.2016.01.050

Wagner, S., Cawley, K.M., Rosario-Ortiz, F.L., Jaffé, R., 2015. In-stream sources and links between particulate and dissolved black carbon following a wildfire. Biogeochemistry 124, 145–161. https://doi.org/10.1007/s10533-015-0088-1

Walters, C.C., 2006. The Origin of Petroleum. In 'Practical Advances in Petroleum Processing' (Eds. Hsu, C.S., Robinson, P.R.). Springer New York, New York, NY, pp. 79–101. https://doi.org/10.1007/978-0-387-25789-1_2

Warren, L.A., Haack, E.A., 2001. Biogeochemical controls on metal behaviour in freshwater environments. Earth Science Reviews 54, 261–320. https://doi.org/10.1016/S0012-8252(01)00032-0

Wershaw, R.L., 1999. Molecular aggregation of humic substances. Soil Sci. 164, 803–813. https://doi.org/10.1097/00010694-199911000-00004

Wilding, A., Liu, R.X., Zhou, J.L., 2004. Validation of cross-flow ultrafiltration for sampling of colloidal particles from aquatic systems. J. Colloid Interface Sci. 280, 102–112. https://doi.org/10.1016/j.jcis.2004.07.002

Wilkinson, K.J., Balnois, E., Leppard, G.G., Buffle, J., 1999. Characteristic features of the major components of freshwater colloidal organic matter revealed by transmission electron and atomic force microscopy. Colloids and Surfaces A: Physicochemical and Engineering Aspects 155, 287–310. https://doi.org/10.1016/S0927-7757(98)00874-7

Witt, M., Fuchser, J., Koch, B.P., 2009. Fragmentation Studies of Fulvic Acids Using Collision Induced Dissociation Fourier Transform Ion Cyclotron Resonance Mass Spectrometry. Anal. Chem. 81, 2688–2694. https://doi.org/10.1021/ac802624s

Wozniak, A.S., Bauer, J.E., Sleighter, R.L., Dickhut, R.M., Hatcher, P.G., 2008. Technical Note: Molecular characterization of aerosol-derived water soluble organic carbon using ultrahigh resolution electrospray ionization Fourier transform ion cyclotron resonance mass spectrometry. Atmospheric Chemistry and Physics 8, 5099–5111. https://doi.org/10.5194/acp-8-5099-2008

Wright, J., Schnitzer, M., 1959. Oxygen-Containing Functional Groups in the Organic Matter of a Podzol Soil. Nature 184, 1462–1462. https://doi.org/10.1038/1841462a0

Wu, Z., Rodgers, R.P., Marshall, A.G., 2004. Two- and three-dimensional van krevelen diagrams: a graphical analysis complementary to the kendrick mass plot for sorting elemental compositions of complex organic mixtures based on ultrahigh-resolution broadband fourier transform ion cyclotron resonance mass measurements. Anal. Chem. 76, 2511–2516. https://doi.org/10.1021/ac0355449

Yuan, Z., He, C., Shi, Q., Xu, C., Li, Z., Wang, C., Zhao, H., Ni, J., 2017. Molecular Insights into the Transformation of Dissolved Organic Matter in Landfill Leachate Concentrate during Biodegradation and Coagulation Processes Using ESI FT-ICR MS. Environ. Sci. Technol. 51, 8110–8118. https://doi.org/10.1021/acs.est.7b02194

Zavodska, L., Kosorinova, E., Scerbakova, L., Lesny, J., 2008. Environmental chemistry of uranium. HV ISSN 1418–7108.

Zeh, P., Czerwinski, K.R., Kim, J.I., 1997. Speciation of uranium in Gorleben groundwaters. Radiochimica Acta 76, 37–44.

Zhao, Y., Hallar, A.G., Mazzoleni, L.R., 2013. Atmospheric organic matter in clouds: exact masses and molecular formula identification using ultrahigh-resolution FT-ICR mass spectrometry. Atmos. Chem. Phys. 13, 12343–12362. https://doi.org/10.5194/acp-13-12343-2013

Zherebker, A.Y., Perminova, I.V., Konstantinov, A.I., Volikov, A.B., Kostyukevich, Y.I., Kononikhin, A.S., Nikolaev, E.N., 2016. Extraction of humic substances from fresh waters on solid-phase cartridges and their study by Fourier transform ion cyclotron resonance mass spectrometry. Journal of Analytical Chemistry 71, 372–378. https://doi.org/10.1134/S1061934816040109

Ziolkowski, L.A., Druffel, E.R.M., 2010. Aged black carbon identified in marine dissolved organic carbon. Geophysical Research Letters 37. https://doi.org/10.1029/2010GL043963

Zirkler, D., Lang, F., Kaupenjohann, M., 2012. “Lost in filtration”-The separation of soil colloids from larger particles. Colloid Surf. A-Physicochem. Eng. Asp. 399, 35–40. https://doi.org/10.1016/j.colsurfa.2012.02.021

2) "COMPARISON OF PRECONCENTRATION METHODS OF THE COLLOIDAL PHASE FOR THE STUDY OF URANIUM TRANSPORT IN SOILS"

RESUME

Quand il est question de caractériser un système naturel, un des impératifs est de pouvoir garantir que depuis le prélèvement jusqu'à l'analyse de l'échantillon, aucune perturbation ni modification n'a eu lieu, ou sinon d'en évaluer les impacts. L'étude de la phase colloïdale implique bien souvent une préparation de l'échantillon, du fait de sa faible concentration dans certaines eaux naturelles, typiquement les eaux souterraines. Ceci est d'autant plus crucial que les aquifères sont des vecteurs de contamination horizontale très importants. Dans ce cas, une étape de préconcentration est nécessaire avant l'utilisation d'outils analytiques ayant besoin d'une concentration colloïdale suffisante compte tenu de leur limite de détection.

Dans cette étude nous avons voulu évaluer et comparer trois méthodes de séparation membranaire par ultrafiltration pour la concentration de la phase colloïdale d'une eau naturelle. Il s'agit de l'ultrafiltration frontale, la technique de séparation membranaire la plus classique et la plus utilisée, l'ultrafiltration tangentielle, dont le flux perpendiculaire permettrait de limiter des biais de filtration et l'ultrafiltration centrifuge qui combine la centrifugation et la filtration. Dans le but de pouvoir comparer les caractéristiques colloïdales dans l'eau de sol avant et après l'étape de préconcentration, une eau de sol a été générée en laboratoire (batch). Ce choix d'investigation expérimentale permet en effet de fixer les conditions de lixiviation telles que la concentration de la phase colloïdale soit suffisante à sa caractérisation par les techniques analytiques disponibles au laboratoire. La méthodologie analytique utilisée repose sur une approche multitechnique impliquant la diffusion dynamique de la lumière (DLS), la microscopie électronique à transmission (TEM), la détermination du carbone organique total (COTmétrie) et la spectrométrie de masse (ICP-MS). D'un point de vue de l'analyse chimique en particulier, les quantités massiques des composants majeurs de la phase colloïdale, à savoir Al, Fe et le carbone organique total (COT), ainsi que la quantité massique d'uranium, ont été déterminées, à la fois dans les concentras et les filtrats. Cette méthodologie a été appliquée à l'eau de sol générée, prise comme référence, ainsi que sur chacun des trois échantillons concentrés de cette eau, obtenus via les méthodes de filtration étudiées. L'impact de ces méthodes sur la phase colloïdale a été évalué de façon comparative. Une évaluation qualitative de leur praticité a également été réalisée, en complément essentiel à l'évaluation analytique en vue de futures applications.

L'évaluation morphologique et structurelle des phases colloïdales met en évidence l'efficacité de ces trois méthodes pour préconcentrer la phase colloïdale. Cette préconcentration n'est cependant pas sans impact : en premier lieu elle entraîne une modification de la distribution de la phase colloïdale qui n'est pas identique selon la méthode utilisée. Avec l'ultrafiltration frontale en particulier apparaît une agrégation significative des entités colloïdales, et donc une modification de leur distribution en taille. D'autre part, l'ultrafiltration,

qu'elle soit frontale ou tangentielle, et la concentration de la phase colloïdale qu'elle induit provoquent un enrichissement notamment en matière organique des concentrats. Ceci mène à la formation, observée en TEM, de structures ramifiées de grandes tailles qui enrobent les particules qui étaient présentent de manière individuelle dans l'eau de référence. Des entités de taille équivalentes n'étant pas observées en analyse par diffusion de la lumière, elles pourraient être une conséquence de la préparation d'échantillon préalable à l'analyse en TEM (dépôt sur la grille et séchage). Les structures observées ne sont donc probablement pas représentatives de la phase colloïdale initiale. Elles ne sont sans doute pas également représentatives des phases colloïdales des concentrats ; elles révèlent plutôt l'existence d'associations (également à l'état colloïdal compte tenu des modifications de la distribution en taille) probables entre des particules colloïdales et la matière organique en plus grande concentration qu'à l'initial. Ces structures ne sont pas observées après ultrafiltration centrifuge, tout comme elles ne le sont pas dans l'eau du sol de référence. L'impact des méthodes ou plutôt la différence d'impact entre ces méthodes, en termes chimiques, semble a priori plus réduit(e). En effet, les taux de recouvrement de Al, Fe, U et COT (concentras + filtrats+ filtres) sont tous proches ou égaux à 100%, excepté pour l'ultrafiltration tangentielle où des pertes élémentaires sont observées, sans qu'elles ne soient dues à une sorption sur la membrane, mais plus probablement à une adsorption sur les parois du système. Les distributions des éléments déterminées entre les concentras et les filtrats restent du même ordre de grandeur. Cependant, les quantités massiques élémentaires ainsi que celles en carbone organique total s'avèrent être beaucoup plus importantes dans les concentras obtenus après ultrafiltrations frontale et tangentielle. Ceci suggère un phénomène d'enrichissement de la phase colloïdale par sorption d'espèces dissoutes durant le processus de concentration. Les quantités massiques élémentaires et organiques sont plus faibles dans le concentrat obtenu par ultrafiltration centrifuge, sans qu'il n'apparaisse de perte de matériel. Ces observations sont en accord avec celles réalisées en TEM. *In fine*, à la fois en termes d'impact sur la phase colloïdale et de praticité, la méthode d'ultrafiltration centrifuge paraît être le meilleur compromis pour la préconcentration de la phase colloïdale dans le respect de son intégrité physique et chimique.

2.1 INTRODUCTION

Colloidal particles are ubiquitous in the environment. Because of their size, from about 1 nm to 1 µm, they are mainly subjected to the Brownian motion (Mills et al. 1991). As a result, colloidal particles can remain in suspension for long periods of time and over long distances. They are therefore important components in waters, at the dissolved-particulate interface (Bin et al. 2011). Especially, the presence of ligands in colloidal form is likely to significantly affect the mobility of pollutants in natural environments. Therefore, the sorption/desorption processes of the colloidal particles from soil and their mobilization dynamics in (sub)surface waters have received a large attention the last few years (Bin et al. 2011; Novikov et al. 2009; Shein and Devin 2007). In particular, the ability of colloidal particles to increase pollutants transport depends on their size, structure, chemical composition, as well as their stability and reactivity with the pollutants according to the chemical characteristics of the surrounding environment (Ouyang et al. 1996; Ryan and Elimelech 1996).

The ubiquity of colloidal particles is due to the fact that they are continuously generated at the interface between a porous solid phase, typically soil, and an aqueous phase, for example groundwater (Kretzschmar et al. 1999; Ryan and Elimelech 1996). Therefore, even if colloidal particles are found in low concentration in a punctual water sample from an environment of interest, they can play a major role in contaminant transport in this environment. Thus, whatever the colloidal concentration, the determination of the physical and chemical characteristics of the colloidal phase is required to improve our understanding of the colloid transport mechanisms.

To decrease any change in both physical and chemical characteristics of the colloidal particles, and ensure the reliability of analytical results, a special attention has to be paid to the sample preparation step (Baalousha et al. 2005a; Degueldre et al. 1999; Lapworth et al. 2013; Powell and Puls 1993). Indeed, the preparation method can induce profound changes, in particular the size and structure (crystallinity) of the colloidal particles, and consequently also on the solubility of their constituent material(s), their dissolution and their sorption capability (Lead and Wilkinson 2006; Yousaf et al. 2015). This can be particularly the case of preconcentration methods of colloidal phases, where the concentration factor can range from about ten to several hundred times (Faucher and Lespes 2019). Two major preconcentration strategies can be used, based on centrifugation and membrane separation (filtration). Ultracentrifugation was used sequentially to prepare soil samples (Gimbert et al. 2005). However, because soil colloidal particles are extremely polydisperse and due to their wide density range, ultracentrifugation does not enable the colloidal phase to be completely recovered. In particular, the fraction of size less than a few nanometers up to a few tens of nanometers is difficult to recover because of the great gravitational force that must be applied. In addition, aggregation or shearing of colloidal particles may occur, leading to structural modifications of the colloidal

phase (Planken and Coelfen 2010; Salim and Cooksey 1981). Membrane separation is the most commonly used preconcentration methods. It can be implemented in different ways depending on the force applied to pass the water sample through the membrane (Aosai et al. 2014; Bacchin et al. 2006; Tsao et al. 2013; Wilding et al. 2004): either a pressure differential (by pressing, or vacuum suction) or a centrifugal force. The pressure gradient can be frontal (most often named dead-end in the literature, and also below) or tangential. Clogging of the membrane pores is one of the well-known major drawbacks of membrane separation processes (Knutsen and Davis 2006; Morrison and Benoit 2001; Smiles 1999). Formation of a filter cake or occurrence of membrane polarization are frequently mentioned in the literature (Chen et al. 1997; Zirkler et al. 2012). The characteristics of the colloidal phase may be affected by such phenomena. Thus, recent works have focused on these different phenomena, and/or on the possible enhancement of the filtration process (Choi et al. 2005; Iritani and Katagiri 2016; Vigneswaran and Kwon 2015) (Raha et al. 2009). For example, it was possible to limit the development of filter cake in dead-end mode by stirring the solution at the filter [8]. However, despite the common use of these methods and the interest in evaluating, understanding and solving of the problems inherent in filtration, the impact of the filtration process on a colloidal phase during preconcentration step is still poorly known.

This work is part of a general questioning concerning the role of the colloidal phase on the transport of trace elements of environmental interest, and more especially on the colloidal transport of uranium in soil waters. The aim of this investigation was to evaluate and compare various preconcentration methods based on membrane separation for the concentration of the colloidal phase. For that purpose, three different ultrafiltration methods (dead-end, tangential and centrifugal) were considered and used with the same concentration factor, on the same soil water sample taken as a reference sample. Physico-chemical characteristics of the colloidal phase of both the reference sample and the three concentrated samples were determined and compared. In addition, the practicality of these methods was evaluated. Indeed, this point is essential in view of the investigation strategy of water collected on site in future applications. Especially, the practicality evaluation aims to answer the following question: can preconcentration combined with field collection be considered, or should priority to be given to collection and then preconcentration at the laboratory? The response depends the preconcentration method selected according to its ability to preserve the characteristics of the colloidal phase.

2.2 EXPERIMENTAL SECTION

2.2.1 Soil

Samples of podzolised soil from the wetlands of Landes Gascony (France) were taken from a study site previously described (Crançon et al., 2003 ; Crançon et al. , 2010) and now well-documented with regard to the physico-chemistry of soils and waters, and uranium distribution. This soil, previously exhaustively characterized, was selected with the idea to obtain a reference soil colloids suspension that can be used as a test sample. Soil was sampled from the upper horizon E, where uranium is present as a result of ancient deposits of solid fragments on the soil surface (Crançon et al., 2010). Previous studies demonstrated the presence of uranium in dissolved and colloidal phases in the interstitial waters of this horizon especially (Crançon et al. 2010; Harguindeguy et al. 2014 and 2018). The soil collected was dried, homogenized, sieved to 1mm and stored at room temperature in the dark until use.

2.2.2 Chemicals

Ultra-high quality 69% nitric acid (GT Baker) was used for the preparation of the mass spectrometry analysis. Polystyrene standards (PSS) with hydrodynamic diameters ranging from 20 to 400 nm used for the size calibration process came from Duke Scientific Corp (Microgenics Corporation, Fremont, CA, USA). . The Total Organic Carbon (TOC) analyzer was calibrated using solutions of sodium hydrogen carbonate for the inorganic carbon measurements and using solutions of potassium hydrogen phthalate for the total carbon measurements (Nacalai Tesque, Kyoto, Japan).

2.2.3 Sample Preparation

Reference soil colloids suspension was obtained by using a static leaching method: A soil aliquot was mixed with milli-Q water using a rotary shaker with a solid/liquid ratio of 1/50. This ratio was chosen after preliminary tests (ratios tested between 1 and 100). These tests showed that the colloidal phase of the soil water obtained with this ratio had characteristics similar to those of the waters taken from the field (Harguindeguy et al 2014). After 48 hours shaking, the soil water sample was kept at 4.0(±0.5)°C and sheltered from the light for 48 hours in order to settle the largest suspended particles down. The supernatant was then recovered and passed through a PES filter of 0.45µm. This filter membrane was chosen because (i) the PES material did not generate an observable interaction with the sample, (ii) the 0.45 µm cut-off agreed with the dimensional characteristics of the colloidal fraction carrying the majority of the uranium (85 % of U was found over 1-450 nm). The soil colloids suspension obtained proved to be stable at least over a period of several months. Moreover, the process was repeatable (i.e. obtaining sample of similar physico-chemical characteristics). Therefore, the soil colloids suspension sample could serve as test sample

and its colloidal phase, after characterization, was taken as a reference sample for the preconcentration tests.

2.2.4 Membrane separation

Three different methods were applied on the test sample, based on dead-end, tangential, and centrifugal ultrafiltration (UF) respectively. The devices chosen for the preconcentration experiments were a polycarbonate filter holder (16510 serie, Sartorius), a Minimate™ TFF System (Pall Corporation) and a Pierce™ Protein Concentrator (Thermo Scientific) respectively. The membrane material was PES, according to the preliminary tests above-mentioned. A cut-off of 10kDa was chosen for both its convenience and its capacity to retain particles above approximately some nanometers (typically about 1-2nm). The methods were applied with a concentration factor of 10 and 500, within the range of preconcentrations usually used (Faucher and Lespes 2019). Both the concentrate (colloidal phase) and the filtrate (expected to represent the dissolved phase) of the test sample were collected and analyzed.

From the test sample, each preconcentration method was triplicated. All three methods need a rinse step of their membrane and their filtration module prior to use. For each UF method, the duration necessary to obtain the desired concentration factor was noted.

2.2.5 Colloidal phase characterization

The analytical investigation strategy was defined as described below preliminary to the characterization of the colloidal phase of the test sample and the three concentrated samples.

Investigation strategy. A set of physicochemical characteristics was defined to serve as comparison indicators between the concentrated samples (hereinafter referred to as concentrates) and the test sample whose colloidal phase was taken as a reference (soil suspension). The intrinsic parameters considered in this study for nano-objects are size, shape, structure, and chemical composition, because all the properties enabling the behavior and fate of the nano-objects to be known depend on these parameters (Faucher et al. 2018). The analytical strategy was constructed in order to be able to determine these parameters with sufficient precision for a comparison. Thus, the size distribution of the colloidal population was evaluated by dynamic light scattering (DLS); the shape and structure were visualized and determined by transmission electronic microscopy (TEM) imaging; the elemental chemical composition (major and trace) of the suspension where the colloidal population was concentrated was determined by atomic mass spectrometry (ICPMS) and the total organic carbon content (TOC) measured by TOCmeter. Such a multi-technique strategy enables all the analyses (or the preparation making it possible to fix the sample before analysis in the case of microscopy) to be carried out almost simultaneously for all the concentrates generated. Therefore, the possible biases induced by temporality can be limited.

Size distribution. Dynamic light scattering (DLS) analysis was performed using a DynaPro NanoStar (Wyatt) with a laser at 658 nm and a photodiode detector with a 90° detection angle. An external calibration with the polystyrene standards was carried out preliminary. This calibration was useful (i) to verify that the hydrodynamic radius values given by the instrument correspond to those of the analyzed size standards, (ii) to obtain a set of autocorrelation curves fitting the autocorrelation curve of each sample analyzed. It is thus possible to verify and validate the relevance of each size distribution estimated by the instrument. Each sample was analyzed for three times of 15 replicates. Mean hydrodynamic radii were obtained using a scattering intensity weighted autocorrelation function.

Shape and structure. Samples were examined with a transmission electronic microscope (TEM) Talos F200S device (ThermoFisher). For this TEM analysis, the samples were prepared as described by Baalousha et al. (Baalousha et al. 2005c): a drop of each sample solution was deposited onto a TEM grid covered by a copper membrane. After drying on filter paper, the grids were rinsed with milliQ water.

Elementary composition and total organic carbon content (TOC). Concentrations of major elements (aluminum and iron) and the trace element of interest (uranium) were obtained for all the samples by mass spectrometry analysis (ICP-MS). An ICPMS 7900ce model (Agilent Technology, Tokyo, Japan) was used, equipped with a concentric nebulizer (MicroMist), an ultra-high matrix introduction (UHMI) spray chamber model cooled to 2°C and a Collision Reaction Cell (CRC). The operating conditions were the following: nickel sample and skimmer cones; argon plasma and make up gas; plasma gas flow rate, 1 L min^{-1}; make up gas flow rate, 0.15 L min^{-1}. The different stable isotopes monitored were ^{27}Al, ^{57}Fe and ^{238}U. Prior to the analyses, a 5% nitric acid solution containing two internal standards (Yttrium and Bismuth) were added to compensate any instrumental sensitivity variation. A range of separate standards of known concentrations of Al, Fe and U was used for external calibration.

TOC concentrations for both the test sample and the concentrates were obtained from a total organic carbon analyzer (TOC-Vws, Shimadzu).

2.3 Results and Discussion

2.3.1 Size distribution of the colloidal phases

The colloidal phase of the reference suspension (Figure 2.3-1) showed a Gaussian-like distribution with hydrodynamic radii of approximately 65 to 155 nm, and a mean radius of 104±2 nm. These values are relevant to the values of gyration radius obtained complementarily (from 50 to 150 nm). They are also typical of a natural soil colloidal phase distribution, described as a blend of various kind of colloids such as inorganic colloids (i.e. Al/Fe oxides) and organic matter (OM; i.e. fulvic/humic acids) (Buffle and Leppard 1995; Lead et al. 1997). For all concentrates, a lower DLS laser power than the reference was observed during measurement. Knowing that the laser power is automatically reduced when the colloidal concentration is too high, this observation qualitatively confirms the concentration of the colloidal phase. The size distributions of the colloidal phases of the three concentrated samples were compared to that of the reference, which is superimposed for easier viewing (Figure 2.3-1b-d). They differed from the reference:

- The dead-end UF caused a broadening of the size distribution of colloidal particles compared to the reference (140±4 nm versus 90±3 nm), with a skewness of the distribution toward the large sizes, without modification of the smaller colloidal particles. This suggests a significant redistribution of the colloidal particles size due to agglomeration/aggregation phenomena. This could concern either the entire colloidal range with partial agglomeration/aggregation, or more specifically the largest colloidal particles.

- The centrifugal and tangential UF led to narrower dispersions than the reference one (size ranges of (80±4) and (75±3) nm respectively, systematically observed for the three replicates) and a shift of their distributions toward the largest particles. However, there was no creation of objects larger than 170 nm. The distributions remained almost Gaussian, but the smallest colloidal particle fraction originally present in the reference (i.e. particles less than about 80-90 nm) disappeared. In summary, after centrifugal or tangential UF, the size distributions not only shifted but also were compressed to sizes almost as large as those observed for the original distribution (reference). This could be explained by agglomeration/aggregation that would significantly involve the smaller colloidal particles without visibly affecting the larger ones. This phenomenon was probably quantitatively limited, which only slightly affected the Gaussian distribution. Deagglomeration of large colloidal particles should also be considered as no larger colloidal particles were detected. However, this assumption cannot be verified yet at this stage of the analysis of the results.

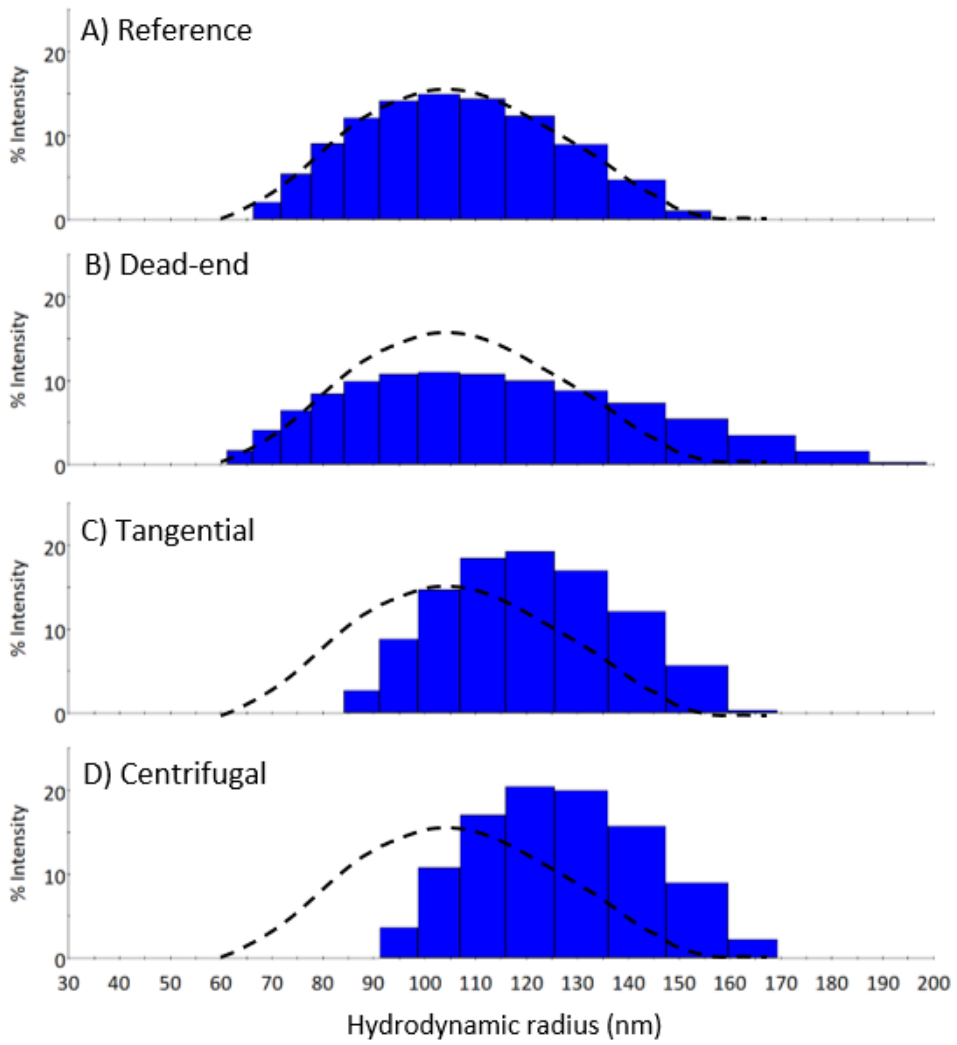

Figure 2.3-1: Size distribution of the colloidal phase of the concentrates from. A) Reference, B) Dead-end, C) Tangential, and D) Centrifugal UF. In black dotted line, for comparison: size distribution of the colloidal reference.

2.3.2 Microscopic structure of the colloidal phases

The TEM images of the colloidal phase from both the reference and the concentrates are shown in Figure 2.3-2. For the reference, three main types of components can be highlighted (see numbered black circles and images a-d in Figure 2.3-2-reference): (1) Organic matter whose structure suggests that it is mainly humic-like in a more or less network organization, which is in agreement with a previous characterization carried out on this soil (Crançon, 2001); (2) Particles from a few nanometers to a few ten of nanometers, rather spherical shaped, appearing mainly individually dispersed and which could be either inorganic (such as aluminum / iron oxides) or globular organic nanomaterial (from the condensation of humic substances) (Baalousha et al. 2005c, 2005b; Hartland et al. 2011). In addition, crystalized polygonal shaped objects of approximately 100-400 nm are also observed (image d).); (3) Assemblies of particles and humics (mixed assemblies). These assemblies also appear in a network organization, organic matter seeming to encompass

the particles. Previous studies identified these structures as inorganic particles coated by diffuse humic-acid like organic matter (Baalousha et al. 2005c). Other spheroid mixed assemblies, individually dispersed, can be seen (Figure 2.3-2, Reference: image c).).

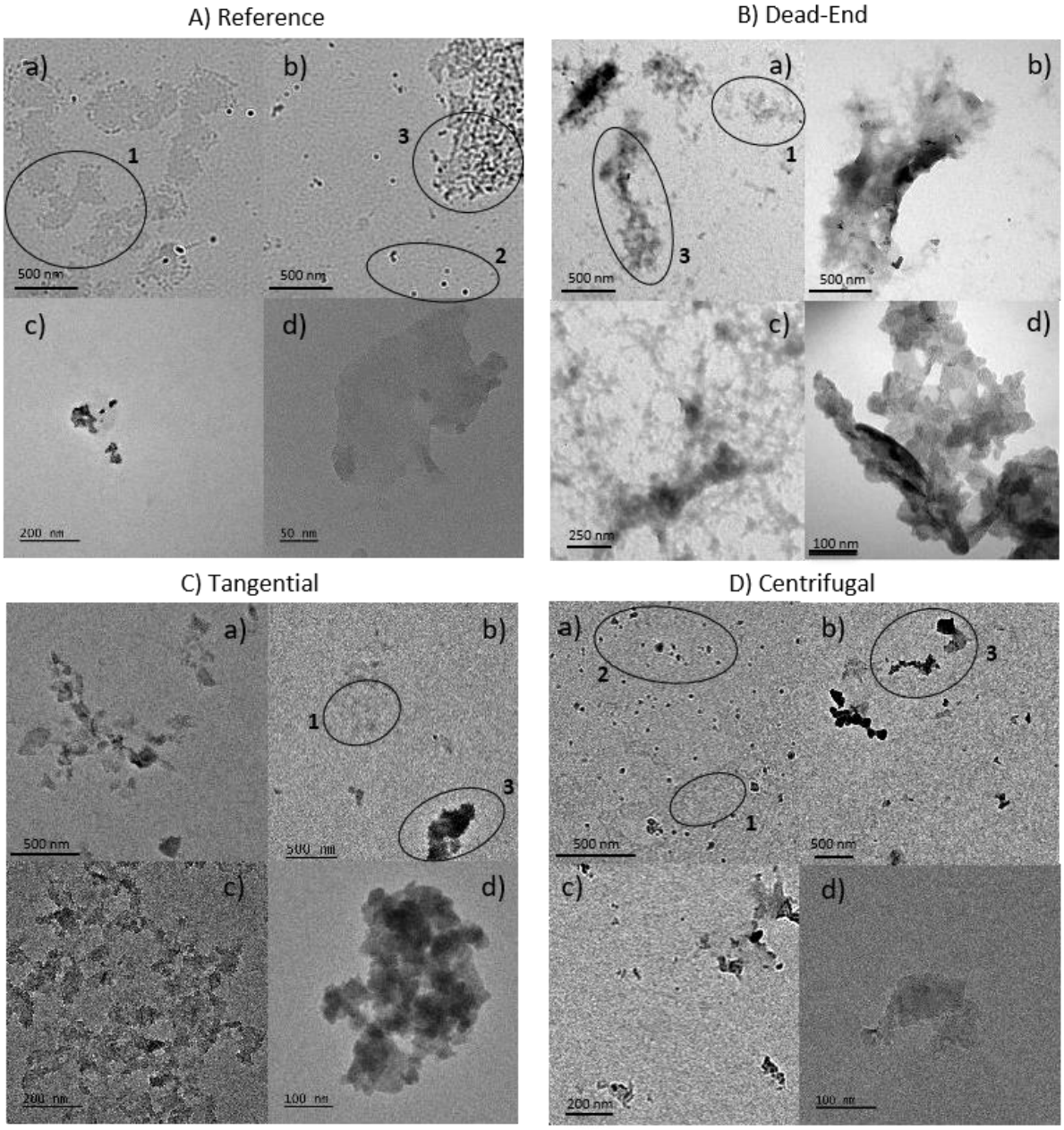

Figure 2.3-2: Microscopic structure of the colloidal phase from both the reference sample (A) and the concentrated samples (Dead-End (B), Tangential (C) and Centrifugal UF). Black circles highlight areas of interest.

For concentrates, more material is observed, which confirms the preconcentration effectiveness after the use of any of the three methods tested. However, there were some changes both in the structure and organization of the colloidal components of the concentrates compared to the reference. Indeed, while the previously identified components were still present in the three concentrates, the mixed assemblies seemed

denser and more compact, suggesting greater concentration of particles within these assemblies. After dead-end and tangential ultrafiltration especially, no more single particles can be observed. The network structures, in which particles are seen, are more expanded. In addition, aggregates appear (Figure 2.3-2, images 2d and 4d). This suggests a redistribution of the colloidal particles during both dead-end and tangential ultrafiltration, leading from an initial state of individual dispersion to that of clusters and agglomerates. In contrast, after centrifugal UF, more individually dispersed particles, and crystallized objects initially present in the reference sample can be seen (image 2d). Additionally, diffuse organic matter can be observed (image 2a).

2.3.3 Concentrate/filtrate chemical distributions

At this stage of the investigation, the analytical determination of the chemical species in the dissolved and colloidal phases of the concentrates with those of the reference sample did not appear to be relevant. Indeed, such a determination would have implied that the dissolved and colloidal phases of the reference sample were separated before analysis; and this separation step would have necessarily been a source of bias. Therefore, the chemical species (Al, Fe, U and TOC) were determined in the filtrates and concentrates obtained by the different UF methods. These species were also determined in the filters of the ultrafiltration systems in order to achieve the most complete mass balance possible. The results obtained are first presented in Figure 2.3-3. They are expressed in amounts relative to the amounts in the bulk of the reference sample in order to facilitate the comparison between the different UF methods. In addition, the absolute mass amounts found in the bulk of the reference sample and in the concentrates were reported in Figure 2.3-4 in order to (i) get an idea of their order of magnitude, (ii) evaluate behavior of uranium and associations between uranium and the major colloidal components (humic-like substances and aluminum / iron oxides mainly, as discussed above).

The recoveries are shown in Figure 2.3-3 A. The differences in recoveries do not seem significant in view of the associated uncertainties. However, elementary recoveries always exhibited the same trend, which means that the observed differences were not due to random error. Thus, Al, Fe and U recoveries were always about 100% for centrifugal and dead-end ultrafiltration. Tangential UF seems to induce elementary losses (recoveries around 85%); it is probable that the circulation of the sample to be concentrated all along the tubing favored the elemental sorption. Another cause of loss, which could be identified and therefore considered in the recovery evaluation, is that inherent to the interactions with the filter membrane. This phenomenon represented up to 16% of the mass balances for TOC, and no more than 4% for Al, Fe and U in the case of tangential UF. The result concerning the elements was expected since this method would minimize fouling of the membrane and adsorption of inorganic components on the filter surface. However, it seems difficult to conclude regarding analyte losses on filters, never appearing systematically larger for one method than for another.

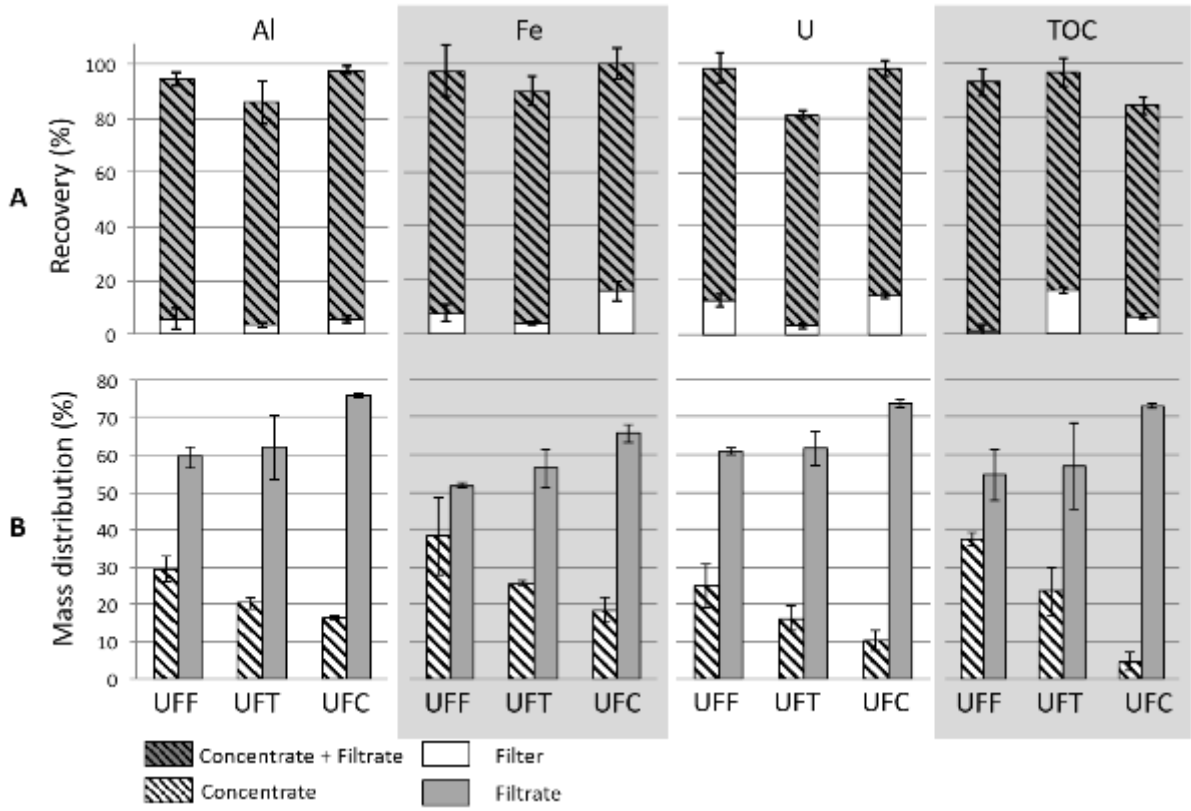

Figure 2.3-3: Mass balances for Al, Fe, U and TOC after dead-end (UFF), tangential (UFT) and centrifugal (UFC) ultrafiltration. A) Recoveries calculated from the masses in both colloidal and dissolved phases, and in the filter, compared to the bulk sample (reference) and B) Corresponding relative mass distribution between filtrate and concentrate obtained after ultrafiltration.

Concentrate / filtrate chemical distributions are presented in Figure 2.3-3 B, complementarily to Figure 2.3-4, which focuses on the absolute amounts found in concentrates. Whatever the species considered, the same trend is observed. Thus, and despite the same concentration factor, analyte masses in the concentrate increased according to centrifugal <tangential <dead-end, and analyte masses in the filtrate followed the opposite trend i.e. dead-end <tangential <centrifugal. It is interesting to note that the increase in the amount of chemical species in the concentrate may be inversely correlated with the motion of the suspension during the filtration process according to the method used. This suggests that the sorption phenomena would be favored in suspension left in static state as was previously observed during frontal filtration without stirring (Baalousha et al. 2005a). On the contrary, centrifugal ultrafiltration could minimize aggregation phenomena, and / or increase the loss of physical integrity of the most fragile colloidal assemblies. However, TEM images did not reveal any loss of integrity of the nanoparticle components. Aggregation would therefore be minimized in a filtered centrifuged suspension. Concerning TOC, mass amount is lower in the concentrates obtained by centrifugal filtration than those from the other methods. This is in agreement with the TEM images where few humic-like substances were observed in the centrifugal concentrate as in the reference (Figure 2.3-2). Given the set of TEM images of both the reference and concentrates, this suggests that the

dead-end and tangential UF methods lead to enrichment in TOC and elements of the concentrates. This is in agreement with the above discussion about mass amount increase.

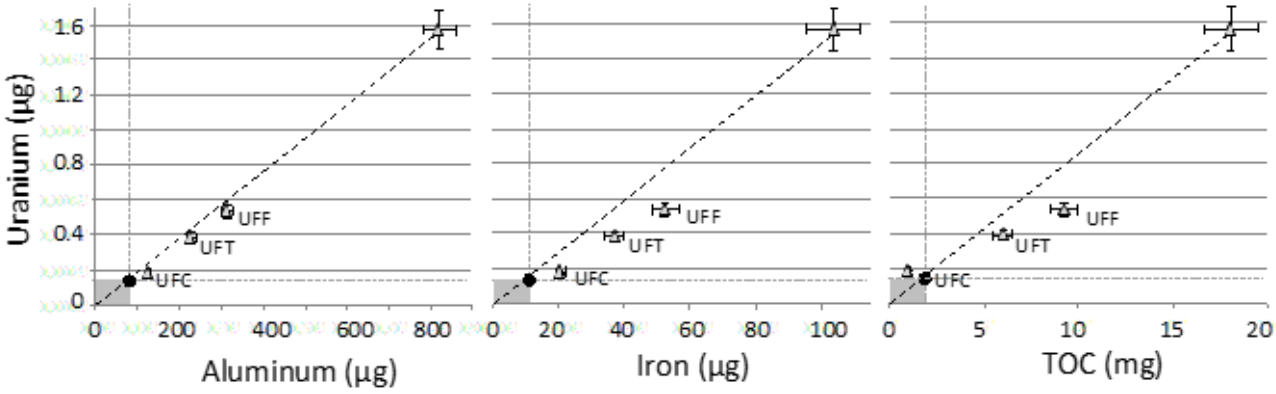

Figure 2.3-4: Uranium according to the major components in the concentrates obtained after dead-end (UFF), tangential (UFT) and centrifugal (UFC) ultrafiltration, and in the reference sample. Masses are given for 1L of reference sample.

The black dotted line formalizes a minimal theoretical preconcentration of the sample corresponding to the case where only dissolved species would be present; the black dot corresponds to a concentration factor equal to 10. It is therefore expected that couples of mass amounts (U, Al), (U, Fe) and (U, COT) are located above the black dot after effective concentration of the colloidal phase, to the right in the case of a predominant enrichment in Al, Fe or TOC with respect to U, and higher in the case of a predominant U enrichment with respect to Al, Fe or COT.

Examining the absolute mass amounts can refine all of these observations. Thus, all mass amounts of species were found to be greater than the minimum amount of preconcentration (Figure 2.3-4, black dot). Not only a concentration phenomenon of the colloidal phase is observed, but also an enrichment of this phase especially during dead-end and tangential UF. Differences exist according to the considered species. The enrichment is more important concerning iron and especially TOC: (U, Fe) and (U, TOC) being to the right from the dotted line (see Figure 2.3-4 and explanations in the legend). Thus, the mass amounts of Fe, Al and U were approximately 3 times higher after UFF than after UFC, whereas the TOC amount was multiplied by 8. All this confirms quantitatively that there is not only concentration but also enrichment in major components of the colloidal phase during ultrafiltration; the method generating the least enrichment, including uranium is the centrifugal UF. All this also suggests that the behavior of the colloidal phase including sorption phenomena depends not only on the chemical changes but also on the physical solicitations occurring during filtration.

2.3.4 Evaluation of the method convenience and comparison

In order to complete the evaluation and comparison of the methods, and regardless of their ability to preserve the colloidal phase, their practicality was also considered. In Table 2.3-1 are listed the different criteria for convenience evaluation for each of the three UF methods.

Table 2.3-1: Criteria of convenience evaluation of preconcentration methods

UF method	Filtration Time	Filtration rate	Maximum Volumes	Additional operations	Suitable for anoxic water	Suitable for field analyses
Centrifugal	≤ 15 minutes	6mL/min	100 mL maximum	Rinsing of the filter	No	Yes
Dead-End	≥ 6 hours	0.42mL/min	Up to 250 mL	Rinsing of the filter	Yes	No
Tangential	≤ 30 minutes	5mL/min	Up to several liters	Filter cartridge cleaning	Yes	Yes

The operating values indicated in the first three columns refer to conditions used in this study. They may change if the filter cut-off and/or the device model are different.

Dead-end UF is widely longer to use due to a filtration rate lower than centrifugal and tangential UF. Moreover, its very low filtration rate increases the risk of modifying the composition of the sample, in particular because of the biological activity. If large volumes have to be concentrated, tangential U appears better suited. In addition, a tangential system is space saving, light, simple and rapid to use such that it is also well suited to be used on site for field analyses. If relatively small volumes are to be filtered, and preconcentration can be done in the laboratory, centrifugal UF is also well suited.

2.4 CONCLUSIONS

The comparative evaluation of the intrinsic parameters characterizing the colloidal populations of the concentrates obtained after ultrafiltration of soil water enabled the effects of the 3 tested methods to be highlighted in morphological, structural and chemical terms. First, the preconcentration appeared to be effective for the 3 methods, with more colloidal material. However, the preconcentration led to:

(i) A change in the size distribution, which appeared to be more important for dead-end UF, especially with a significant aggregation. Given the importance of this structural parameter on the mobility of colloidal entities (which is favored by smaller size), and therefore of uranium, it is therefore important to identify the method generating the least change in size, namely the centrifugal UF.

(ii) An enrichment in both inorganic and especially organic matter of the concentrate. This enrichment led to colloidal mixed inorganic/ organic structures to the detriment of individual particles. It probably contributes to an intensified agglomeration phenomenon of the particles, which were observed embedded in very large organic clusters. This may potentially disturb the sorption equilibria on the surface of the organic matter. Given the importance of organic matter as a carrier of pollutants, and particularly uranium, any enrichment of the colloidal phase must be ideally avoided. This cannot be the case using either dead-end or tangential

UF. However, such a phenomenon was not observed after centrifugal UF, objects observed at the nanoscale appearing identical before and after UF.

From a practical point of view, centrifugal UF seems well adapted to the preconcentration of waters. Given all the results obtained, centrifugal UF appears the best preconcentration compromise in terms of preservation of the colloidal phase, with also practicality.

REFERENCES

Aosai, D., Yamamoto, Y., Mizuno, T., Ishigami, T., Matsuyama, H., 2014. Size and composition analyses of colloids in deep granitic groundwater using microfiltration/ultrafiltration while maintaining in situ hydrochemical conditions. Colloid Surf. A-Physicochem. Eng. Asp. 461, 279–286. https://doi.org/10.1016/j.colsurfa.2014.08.007

Baalousha, M., Kammer, F.V.D., Motelica-Heino, M., Le Coustumer, P., 2005a. Natural sample fractionation by FlFFF–MALLS–TEM: Sample stabilization, preparation, pre-concentration and fractionation. Journal of Chromatography A 1093, 156–166. https://doi.org/10.1016/j.chroma.2005.07.103

Baalousha, M., Kammer, F.V.D., Motelica-Heino, M., Le Coustumer, P., 2005b. 3D characterization of natural colloids by FlFFF-MALLS-TEM. Analytical and Bioanalytical Chemistry 383, 549–556. https://doi.org/10.1007/s00216-005-0006-9

Baalousha, M., Motelica-Heino, M., Galaup, S., Le Coustumer, P., 2005c. Supramolecular structure of humic acids by TEM with improved sample preparation and staining. Microscopy Research and Technique 66, 299–306. https://doi.org/10.1002/jemt.20173

Bacchin, P., Aimar, P., Field, R.W., 2006. Critical and sustainable fluxes: Theory, experiments and applications. J. Membr. Sci. 281, 42–69. https://doi.org/10.1016/j.memsci.2006.04.014

Bin, G., Cao, X., Dong, Y., Luo, Y., Ma, L.Q., 2011. Colloid Deposition and Release in Soils and Their Association With Heavy Metals. Critical Reviews in Environmental Science and Technology 41, 336–372. https://doi.org/10.1080/10643380902871464

Buffle, J., Leppard, G.G., 1995. Characterization of Aquatic Colloids and Macromolecules. 1. Structure and Behavior of Colloidal Material. Environ. Sci. Technol. 29, 2169–2175. https://doi.org/10.1021/es00009a004

Chen, V., Fane, A.G., Madaeni, S., Wenten, I.G., 1997. Particle deposition during membrane filtration of colloids: Transition between concentration polarization and cake formation. J. Membr. Sci. 125, 109–122. https://doi.org/10.1016/S0376-7388(96)00187-1

Choi, H., Zhang, K., Dionysiou, D.D., Oerther, D.B., Sorial, G.A., 2005. Effect of permeate flux and tangential flow on membrane fouling for wastewater treatment. Separation and Purification Technology 45, 68–78. https://doi.org/10.1016/j.seppur.2005.02.010

Crançon, P., 2001. Migration de l'uranium dans un podzol : le rôle des colloïdes dans la zone non saturée et la nappe ; application aux landes de Gascogne (phdthesis). Université Joseph-Fourier - Grenoble I.

Degueldre, C., Scholtis, A., Pearson, F.J., Laube, A., Gomez, P., 1999. Effect of sampling conditions on colloids and ground water chemistry. Eclogae Geol. Helv. 92, 105–114.

Faucher, S., Le Coustumer, P., Lespes, G., 2018. Nanoanalytics: history, concepts, and specificities. Environ Sci Pollut Res Int. https://doi.org/10.1007/s11356-018-1646-6

Faucher, S., Lespes, G., 2019. Nanoparticles in waters and soil. In 'FIELD FLOW FRACTIONATION: Principles and Applications.' (Eds. GUEGUEN, C., BAALOUSHA, M., WILLIAMS, K.R.). WILEY-VCH, S.l.

Gimbert, L.J., Haygarth, P.M., Beckett, R., Worsfold, P.J., 2005. Comparison of centrifugation and filtration techniques for the size fractionation of colloidal material in soil suspensions using sedimentation field-flow fractionation. Environ. Sci. Technol. 39, 1731–1735. https://doi.org/10.1021/es049230u

Hartland, A., Fairchild, I.J., Lead, J.R., Zhang, H., Baalousha, M., 2011. Size, speciation and lability of NOM–metal complexes in hyperalkaline cave dripwater. Geochimica et Cosmochimica Acta 75, 7533–7551. https://doi.org/10.1016/j.gca.2011.09.030

Iritani, E., Katagiri, N., 2016. Developments of Blocking Filtration Model in Membrane Filtration. KONA Powder Part. J. 179–202.

Knutsen, J.S., Davis, R.H., 2006. Deposition of foulant particles during tangential flow filtration. Journal of Membrane Science 271, 101–113. https://doi.org/10.1016/j.memsci.2005.06.060

Kretzschmar, R., Borkovec, M., Grolimund, D., Elimelech, M., 1999. Mobile Subsurface Colloids and Their Role in Contaminant Transport. In 'Advances in Agronomy' (Ed. Sparks, D.L.). Academic Press, pp. 121–193.

Lapworth, D.J., Stolpe, B., Williams, P.J., Gooddy, D.C., Lead, J.R., 2013. Characterization of Suboxic Groundwater Colloids Using a Multi-method Approach. Environ. Sci. Technol. 47, 2554–2561. https://doi.org/10.1021/es3045778

Lead, J.R., Davison, W., Hamilton-Taylor, J., Buffle, J., 1997. Characterizing colloidal material in natural waters. Aquatic Geochemistry 3, 213–232.

Lead, J.R., Wilkinson, K.J., 2006. Aquatic colloids and nanoparticles: Current knowledge and future trends. Environ. Chem. 3, 159–171. https://doi.org/10.1071/EN06025

Majedi, S.M., Lee, H.K., 2016. Recent advances in the separation and quantification of metallic nanoparticles and ions in the environment. Trac-Trends in Analytical Chemistry 75, 183–196. https://doi.org/10.1016/j.trac.2015.08.009

Mills, W., Liu, S., Fong, F., 1991. Literature-Review and Model (comet) for Colloid Metals Transport in Porous-Media. Ground Water 29, 199–208. https://doi.org/10.1111/j.1745-6584.1991.tb00511.x

Morrison, M.A., Benoit, G., 2001. Filtration artifacts caused by overloading membrane filters. Environ. Sci. Technol. 35, 3774–3779. https://doi.org/10.1021/es010670k

Novikov, A.P., Kalmykov, S.N., Kuzovkina, E.V., Myasoedov, B.F., Fujiwara, K., Fujiwara, A., 2009. Evolution of actinide partitioning with colloidal matter collected at PA “Mayak” site as studied by sequential extraction. J. Radioanal. Nucl. Chem. 280, 629–634. https://doi.org/10.1007/s10967-008-7397-y

Ouyang, Y., Shinde, D., Mansell, R.S., Harris, W., 1996. Colloid-enhanced transport of chemicals in subsurface environments: A review. Crit. Rev. Environ. Sci. Technol. 26, 189–204. https://doi.org/10.1080/10643389609388490

Planken, K.L., Coelfen, H., 2010. Analytical ultracentrifugation of colloids. Nanoscale 2, 1849–1869. https://doi.org/10.1039/c0nr00215a

Powell, R., Puls, R., 1993. Passive Sampling of Groundwater Monitoring Wells Without Purging - Multilevel Well Chemistry and Tracer Disappearance. J. Contam. Hydrol. 12, 51–77. https://doi.org/10.1016/0169-7722(93)90015-K

Raha, S., Pradip, Kapur, P.C., Khilar, K.C., 2009. Enhancement of Colloidal Filtration: A New Combined Approach Based on Cake and Suspension Destabilization. Ind. Eng. Chem. Res. 48, 7276–7282. https://doi.org/10.1021/ie801750w

Ryan, J.N., Elimelech, M., 1996. Colloid mobilization and transport in groundwater. Colloids and Surfaces A: Physicochemical and Engineering Aspects, A collection of papers presented at the Symposium on Colloidal and Interfacial Phenomena in Aquatic Environments 107, 1–56. https://doi.org/10.1016/0927-7757(95)03384-X

Salim, R., Cooksey, B., 1981. The Effect of Centrifugation on the Suspended Particles of River Waters. Water Res. 15, 835–839. https://doi.org/10.1016/0043-1354(81)90137-8

Shein, E.V., Devin, B.A., 2007. Current problems in the study of colloidal transport in soil. Eurasian Soil Sc. 40, 399–408. https://doi.org/10.1134/S1064229307040059

Smiles, D.E., 1999. Centrifugal filtration of particulate systems. Chem. Eng. Sci. 54, 215–224. https://doi.org/10.1016/S0009-2509(98)00229-2

Tsao, T., Chen, Y., Sheu, H., Tzou, Y., Chou, Y., Wang, M., 2013. Separation and identification of soil nanoparticles by conventional and synchrotron X-ray diffraction. Appl. Clay Sci. 85, 1–7. https://doi.org/10.1016/j.clay.2013.09.005

Vigneswaran, S., Kwon, D.-Y., 2015. Effect of ionic strength and permeate flux on membrane fouling: Analysis of forces acting on particle deposit and cake formation. KSCE J. Civ. Eng. 19, 1604–1611. https://doi.org/10.1007/s12205-014-0079-0

Wilding, A., Liu, R.X., Zhou, J.L., 2004. Validation of cross-flow ultrafiltration for sampling of colloidal particles from aquatic systems. J. Colloid Interface Sci. 280, 102–112. https://doi.org/10.1016/j.jcis.2004.07.002

Yousaf, A.M., Kim, D.W., Cho, K.H., Kim, J.O., Yong, C.S., Choi, H.-G., 2015. Effect of the preparation method on crystallinity, particle size, aqueous solubility and dissolution of different samples of the poorly water-soluble fenofibrate with HP-beta-CD. J. Incl. Phenom. Macrocycl. Chem. 81, 347–356. https://doi.org/10.1007/s10847-014-0461-z

Zirkler, D., Lang, F., Kaupenjohann, M., 2012. “Lost in filtration”-The separation of soil colloids from larger particles. Colloid Surf. A-Physicochem. Eng. Asp. 399, 35–40. https://doi.org/10.1016/j.colsurfa.2012.02.021

3) "Spatial Variations in the Molecular Composition of Dissolved Organic Matter from the Podzol soils of the Wetlands in Western France"

RESUME

Comme l'étude bibliographique du premier chapitre l'a montré, la caractérisation de la phase colloïdale est devenue un enjeu majeur dans l'étude et la gestion des mécanismes de migration de polluants au sein de l'Environnement. En fonction de la nature du milieu naturel et des conditions géochimiques existantes, la présence de polluants dans la fraction colloïdale sera favorisée ou inhibée. Dans le cas des sols, les eaux souterraines (interstitielles ou d'aquifère) sont constituées d'entités colloïdales qui ont été potentiellement générées et/ou remobilisées. Le Podzol des Landes présente une dynamique géochimique particulière avec une forte différenciation de ses horizons, principalement due à des conditions de pH très acides (Righi and Wilbert 1984). Cela entraîne la coexistence de trois compartiments géochimiques différents ayant des eaux de sol particulières (une eau de sol de subsurface acide, une eau de sol profond suboxique et une eau de nappe légèrement acide à neutre et anoxique). Le processus de différenciation du podzol est contrôlé par une migration verticale de complexes organométalliques principalement sous forme colloïdale et qui sont constitués essentiellement de substances humiques, de fer et d'aluminium. La matière organique naturelle a été identifiée comme étant le vecteur principal de U de la surface vers les horizons profonds (Crançon 2001; Crançon and Van der Lee 2003). L'efficacité et la portée de la migration de U par la MO varient selon la nature et les propriétés des phases porteuses, dépendantes elles-mêmes des conditions physico-chimiques du milieu. Dans ce podzol, la variabilité spatiale donne lieu à une variation des conditions géochimiques. Les questions qui se posent alors sont : la MO constitutive de l'eau du sol change-t-elle de nature le long du profil de sol ? Et cela peut-il avoir un impact sur la (re)mobilisation de U au sein du sol et dans l'environnement ?

La nature de la MO peut être définie à partir de sa structure moléculaire. La composition élémentaire (C, H, N, O, S), l'aromaticité, l'origine ou encore la famille moléculaire à laquelle appartiennent les différents composés organiques sont des informations qui peuvent être directement déduites de la structure de la MO. Il est possible de la caractériser via différents outils analytiques. La spectrométrie de masse haute résolution (HRMS) permet de caractériser la structure moléculaire de mélanges organiques très complexes (Hertkorn et al. 2008; Hockaday et al. 2009), et se révèle à ce titre la technique analytique la plus adaptée pour l'étude à l'échelle moléculaire de la MO naturelle de sol.

Dans ce chapitre, l'objectif est donc de déterminer la structure moléculaire de la MO constitutive de différentes eaux de sol et correspondant à différentes profondeurs :

- L'eau de sol de surface (horizon superficiel A1)
- L'eau de sol en profondeur (horizon d'accumulation Bh)
- L'eau de l'aquifère (GW)

La comparaison de ces différentes eaux devrait nous permettre d'observer une éventuelle évolution de la structure moléculaire de la MO selon sa profondeur dans le podzol pour *in fine* identifier les différents processus géochimiques qui interviennent le long du profil de sol et en déduire les impacts potentiels sur les mécanismes de complexation/adsorption de U.

Pour cela, une source d'ionisation électrospray (ESI) a été associée à un spectromètre de masse haute résolution (LTQ-Orbitrap™ XL). Les différents composés organiques déduits des spectres de masses obtenus sont dans un premier temps caractérisés par groupes en fonction de leur formule élémentaire (CHO, CHON…), puis comparés selon l'eau de sol à laquelle ils appartiennent.

L'analyse par HRMS de la MO constitutive des différentes eaux du podzol met en évidence la grande diversité de sa composition, avec la présence de plus de 3000 composés organiques identifiés (formules uniques assignées), quelle que soit l'eau de sol du podzol analysée. Ces trois eaux ont une MO présentant toutefois des similarités, étant constituée principalement de composés de type CHO et CHON, avec peu de composés soufrés. La masse molaire des composés organiques identifiés bien que globalement faible est très variable, avec un pic d'abondance autour de 200 Da. La MO des trois eaux est majoritairement constituée d'espèces organiques dérivées de la lignine, dont principalement des composés phénoliques et des acides carboxyliques, ces derniers provenant tout particulièrement de la dégradation oxydative de la lignine. Cette forte abondance en composés ligneux met bien en évidence l'origine majoritairement végétale de la MO du sol d'intérêt, et est en cohérence avec la forte acidité du site qui inhibe le développement de la faune. Les conséquences de cette acidité se retrouvent également dans la proportion de composés de type tannins que l'on retrouve dans l'horizon superficiel (A1) dont l'abondance autour de 10% témoigne d'un environnement de croissance stressant pour les végétaux.

Au-delà de leurs similarités, chaque eau du podzol possède une empreinte moléculaire particulière. Nous avons ainsi pu mettre en évidence l'évolution de la composition et de la structure de la MO constitutive des eaux en fonction de la profondeur au sein du podzol. Différents processus intervenant dans cette évolution ont pu être identifiés avec notamment :

- Un processus de réduction, déduit notamment de la diminution progressive des rapports O/C moyens des composés organiques, ainsi que de la teneur en O globale avec la profondeur. On observe également l'apparition de composés plus insaturés en profondeur qui sont, au vu de leur DBE (qui détermine le nombre d'insaturations d'une molécule organique), peu aromatiques mais possèdent plutôt des doubles liaisons (ex : acides carboxyliques).
- Un processus de dénitrification, mis en évidence par l'augmentation de la teneur en azote dans la composition moléculaire des molécules organiques ainsi que par la diminution du rapport C/N avec la profondeur. La DBE des composés riches en azote augmente le long du profil de sol, ceci est

typique de la formation de molécules organiques aromatiques et/ou insaturées et contenant de l'azote réduit.

De manière plus globale, en plus de ces précédentes observations, la composition et la structure de la MO tend à devenir plus homogène et plus simple en profondeur, avec une diminution globale des composés riches en oxygène. La présence en forte quantité de lignine, matériau particulièrement réfractaire à la dégradation, indique un état de décomposition de la MO avancé, surtout dans l'horizon superficiel. Toutes ces informations amènent à identifier un processus de diagénèse précoce de la MO, intervenant dès la première étape d'enfouissement de la MO et tout le long du profil du sol, et qui pourrait mener *in fine* à la formation de kérogène.

La MO de l'eau de l'horizon Bh se distingue par sa composition moléculaire qui comporte seulement 1% de composés organiques identiques à ceux des eaux A1 et GW. Cette différence peut être expliquée par un changement de source de MO à un moment donné, qui proviendrait pour une plus grande part d'angiospermes pour l'horizon Bh, mais qui pourrait également être le résultat de la dynamique particulière existant dans l'horizon d'accumulation où la variation régulière du niveau de la nappe donne lieu à des modifications importantes des conditions physico-chimiques.

L'évolution de la structure moléculaire de la matière organique peut avoir un impact sur sa capacité à complexer l'uranium et ainsi entraîner une variation de la mobilisation de l'uranium localement (à l'échelle de l'horizon) mais aussi sur sa migration le long du profil de sol. Pour vérifier cela, il pourrait être intéressant de comparer la structure moléculaire de la matière organique issue de ce podzol avec celle d'un autre podzol, et ainsi déterminer l'influence des caractéristiques intrinsèques du sol sur la nature de la matière organique, et sur la mobilisation et le transport colloïdal de l'uranium. L'identification d'une potentielle phase organique « type » qui serait responsable de la mobilisation et de la mobilité de l'uranium depuis le sol de surface vers l'horizon d'accumulation permettrait de prédire le devenir de l'uranium au sein de l'environnement.

3.1 INTRODUCTION

Podzols are strongly differentiated soils occurring under acidic pH conditions (Mokma et al. 2004). They tend to form under forested or heath vegetation, specifically coniferous or mixed coniferous/deciduous forest or ericaceous shrubs. The main mechanism of podzolization involves the mobilization of organic compounds from the upper horizons (organic (O) and eluvial (E)) to the illuvial horizon (B(h/s)) (Abakumov et al. 2010; Baker 1973; Sauer et al. 2007). Depending on both the age and the depth of the podzol, different processes may affect organic compounds in their structure and composition (Abakumov et al. 2010; Bonifacio et al. 2013; Lundstrom et al. 2000; Mokma et al. 2004; Sauer et al. 2007; Wright and Schnitzer 1959).

Dissolved organic matter (DOM, commonly defined as OM < 0.45 µm) consists of a complex and heterogeneous mixture of naturally occurring compounds that are involved in many important biogeochemical processes such as metal complexation (Haitzer et al. 2002), pollutant fate and transport (Schwarzenbach et al. 2002), nutrient cycling (Opsahl and Benner 1998), redox reactions and also acts as a source of energy for the microbial community (Thomas 1997). The spatial distribution of DOM reflects both its original source material as well as the degradation processes it undergoes (Wagner et al. 2015). In podzols, the production and mobilization of dissolved organic carbon (DOC, i.e. carbon < 0.45 µm constitutive of DOM) accounts for a substantial loss of carbon from the forest floor (Cronan 1985; Godde et al. 1996). The main sources of DOM in many forest soils are the canopy and the floor layers, as indicated by the relatively high DOC concentrations in seepage waters beneath the forest floor (Johnson et al. 2000; McDowell and Likens 1988). Indeed, DOM leaches into the water from plant tissues and dead organic matter, carrying an organic rich solute that is also actively decomposed by soil microbes. Dissolution and movement of organic matter through the forest soil result in the transfer of OM, metals, nutrients and pollutants through the soil to surface and ground waters (Liu and Amy 1993). Transport of organic matter, aluminum (Al) and iron (Fe) to subsoil layers is a key mechanism in podsolization (Dawson et al. 1978; Petersen 1976). Movement and retention of DOM mediated by various biogeochemical processes involved in podzolization, such as complexolysis or reprecipitation (Lundstrom et al. 2000; Petersen 1976), should alter not only the amount but also its composition.

Aquatic and soil DOM are mainly composed of humic substances (HS) which are commonly operationally defined according to the extraction procedure used to isolate them. Different fractions can thus be distinguished, such as humin (insoluble fraction), humic acids (HA, insoluble at acidic pH) and fulvic acids (FA; soluble at any pH values (Stevenson 1994). These fractions are made up of a wide variety of organic compounds differing in both composition and structure, depending on the type of substrate as well as the environmental conditions during their degradation (Aiken 1985; Steelink 2002). DOM can be processed through photoreactive processing (Spencer et al. 2009; Stubbins et al. 2010) or biological reactions (Spencer

et al. 2015). While there is a widespread concept of polydisperse polymeric constitution (Abbt-Braun et al. 2004; Ishiwatari 1992; MacCarthy et al. 1990a; Malcolm 1990), recent studies suggest that HS are composed of supramolecular assemblies of relatively low molecular weight compounds stabilized by hydrogen bonding and hydrophobic effects (Nebbioso and Piccolo 2012; Piccolo 2001) leading to a high variability of supramolecular associations, structures and properties.

The DOM composition has been studied for decades using various analytical approaches (Coble 1996; Nebbioso and Piccolo 2012). One of the simplest methods is analyzing and quantifying elemental compositions in soils (i.e. carbon, nitrogen and phosphorus) using elemental analyzers. The other approaches are measuring the amount of a specific class of compounds present in soil DOM using selective extraction methods, such as the organic solvent-based extraction for lipids and the CuO oxidation for lignins (Otto and Simpson 2006). Various spectroscopic techniques (Fourier Transform infrared (FTIR), 13C nuclear magnetic resonance (NMR), UV-Vis and excitation-emission matrix (EEM) fluorescence] have also been widely used to characterize water and soil-derived organic matter (Chen et al. 2003; Davis et al. 1999; Guo et al. 2011; Randall et al. 1997) ; however, these spectroscopic methods only provide information about the functional groups of soil DOM but not the individual components. More recently, pyrolysis-gas chromatography mass spectrometry (PyGC-MS) has been used for identifying soil organic compounds and understanding their compositional changes (Campo et al. 2011; Mehrabanian 2013; Schulten and Gleixner 1999), but even this technique is insufficient for resolving complex constituents. In this context, high-resolution mass spectrometry (HRMS) has emerged as a powerful tool for the analysis of extremely complex mixtures, such as crude oils, water and soil-derived organic substances, resulting in rapid and accurate interpretation of the elemental compositions of complex samples (Hertkorn et al. 2008; Hockaday et al. 2009; Orrego-Ruiz et al. 2016; Purcell et al. 2007; Sleighter and Hatcher 2008; Tfaily et al. 2015) and has improved our understanding of the nature and molecular structure of DOM.

Electrospray ionization (ESI) coupled with Fourier-transform mass spectrometry (FTMS) provides detailed molecular characterization of organic matter due to its high resolution and mass accuracy (Lobodin et al. 2012; Schmitt-Kopplin et al. 2012). ESI is a soft ionization method that minimizes the fragmentation of analytes, enabling intact molecules to be detected, while the high resolving power and accuracy of FTMS enables a unique chemical formula to be assigned to each peak detected. ESI is selective toward DOM molecules containing carboxylic acids and other polar functional groups. Although molecular formulae cannot be linked with specific molecular structures, as each represents many possible isomeric arrangements, they can be categorized by compound class using elemental ratios to help summarize the mass spectral composition (Šantl-Temkiv et al. 2013). The ultrahigh mass resolving power of Fourier-transform ion cyclotron resonance mass spectrometry (FT-ICRMS) has made it the tool of choice for the analysis of such complex samples as DOM. However, the Orbitrap™ mass analyzer has showed to be

particularly well suited for the investigation of very subtle biogeochemical processing of bulk DOM because featuring a < 2 ppm error using internal calibration, and due to a resolving power of > 100 000 (FHHM, 200 m/z) (Hawkes et al. 2016). This powerful analytical approach was applied in this study to investigate the molecular diversity and dynamics of dissolved organic matter isolated from the upper (A1) and the accumulation (Bh) horizons of the podzol as well as from the aquifer of a maritime pine forest in western France, using a high-resolution Orbitrap™ mass spectrometry. The final objective was to be able to evaluate the impact of the organic matter molecular structure on the mobilization dynamics of trace elements, and in particular of uranium.

3.2 METHOD

3.2.1 Study site and water samples generation and collection

The study site is located in the southwest of France, in the "Landes de Gascogne" area. The podzolic soil is characterized by a low pH (4), low nutrient availability, and high organic carbon content that can reach 55 g.kg-1 of soil (Augusto et al. 2010). The region was a vast wetland until the 19th century, when a wide forest of maritime pine (Pinus pinaster) was sown, following landscape drainage in 1850. Currently, the area is mainly occupied by pine forest (approximately 80%), with a modest proportion of croplands (approximately 15%) (Jolivet et al. 2007). Climate, hydrological functioning and geochemical system of the Landes podzol are described in previous studies (Crançon 2001; Righi and Wilbert 1984).

Three water samples from the same study site were compared. First, two leachates were fabricated by mixing soils from respectively the upper horizon (A1) and the illuvial horizon (Bh) with ultrapure water. In the former horizon (A1), complexation processes between organic and inorganic compounds (i.e. aluminum and/or iron) mainly occur. In the latter, sudden changes in the geochemical conditions lead to the precipitation of these compounds, HA first then more deeply FA. After stirring for 48 hours, the two leachates were stored in the dark under refrigeration for settling for 48 hours. The groundwater sample was directly taken from the aquifer via a mini-piezometer whom the depth is 2 meters. All samples were filtered through 0.45-µm pore size PTFE filters ahead of further preparation.

3.2.2 Sample preparation

Low TOC (total organic carbon) concentrations of the site waters entail going through a concentration step. In addition, inorganic salts should be eliminated as much as possible to avoid ionization suppression in ESI and interferences in mass spectrometry analysis. A Strata-X-AW solid phase extraction (SPE) cartridge (Phenomenex) was used, which is an anion exchange mixed phase, its hydrophobic backbone associated with di-amino ligands allowing the more targeted extraction of HS. The SPE procedure consisted in a conditioning step, where 1.5 mL of methanol were passed through the cartridge, followed by 1.5 mL of neutral pH water. Then, a 100mL aliquot of sample leachate was slowly passed (1 mL min^{-1}) through the SPE cartridge to enhance the interaction between analytes and the stationary phase. No pH adjustment was made because of the natural acidic pH of the samples. Washing is an important step of the SPE process to remove inorganic salts present in these samples as well as weakly retained materials. For this step, 1.5mL of ammonium acetate at pH 6-7 and 1.5mL of methanol were successively passed through the cartridge. After total solvent removal, by vacuum drying, the analytes were very slowly eluted using 1.5mL of methanol-containing 5% ammonium hydroxide. Aliquots were taken at each SPE step to evaluate the recovery, and concentrations of TOC were measured.

3.2.3 LTQ Orbitrap™ XL mass spectrometry analysis

Organic extracts obtained after SPE step were diluted 50/50 (v/v) with milliQ water for analysis then were infused into an ESI source with a spray voltage of 3.5 kV at a flow rate of 15 µL/min and were analyzed in negative ionization mode. Data were collected in the mass range of 100-1000 m/z and at least 50 scans were averaged together using Xcalibur software. The Orbitrap MS was externally calibrated daily using a calibration mixture specified by the manufacturer. The ESI ion source was interfaced to an LTQ-Orbitrap XL mass spectrometer (Thermo Scientific, San Jose, CA, USA). Ion optics were optimized on background ions for a best transfer at approximately m/z 500 and finally set as follow: capillary voltage: 35 V; tube lens voltage: 125 V; capillary temperature: 275 °C ; multiple 00 offset voltage: -4 V; multipole 0 Offset voltage: -4.5 V; multiple 1 offset voltage: -8.0 V; lens 0 voltage: -4.20 V; lens 1 voltage: -15 V; gate lens voltage: -35.0 V; front lens voltage :-5.25 V. The mass range acquired was m/z 50-1000. The resolving power was set to 100 000 FWHM at m/z 400 with 3 microscans and a maximum injection time of 1000 ms. Each mass spectrum was obtained from the average of 100 individual scan.

Before acquisition, the instrument was first externally calibrated as instructed by the manufacturer's manual using the manufacturer's mixture consisting of caffeine, MRFA (L-methionyl-arginyl-phenylalanyl-alanine acetate monohydrate) and ultramark 1621. During the acquisition, each individual spectrum was online recalibrated, using an internal lock mass consisting of a background ion previously identified by their isotopic distribution, mass accuracy and MS/MS analysis. Typically, phthalates such as di-2-ethylhexyl-phthalate (DEHP) at m/z 391 was used as a lock mass, and other identified background signals, such as dibutylphtalate (DBP) or polydimethylsiloxane (PDMS) were used to check the mass accuracy. All data were acquired using the Thermo Xcalibur™ software. Solvent blanks were run before and after each sample to clean up to ion source and to avoid cross-contamination and carryover from the precedent samples.

3.2.4 Data processing and elemental formula assignment

All peaks detected with a signal to noise ratio higher than 3 were processed using the Composer software (Sierra Analytics, Pasadena, CA, USA). Before processing, mass accuracy was checked by the attribution of the elemental composition of known background compound (phthalate and PDMS). The error observed for these compounds before recalibration was systematically lower than 2 ppm. The post-acquisition recalibration was then based on a 5-order polynomial equation. A set of naturally occurring compounds previously identified in lignin, natural organic matter and plants (Remucal et al. 2012) were selected to represent internal recalibrants over the mass range considered.

Annexe 2 lists these internal recalibrants together with the mass errors associated. The calibration was then validated by checking that the average error corresponding to reference masses was lower than 0.5 ppm. After background ions removal, the elemental compositions were assigned, with an error lower than 3 ppm.

The elemental compositions authorized were $C_{1\text{-}70}H_{0\text{-}140}O_{1\text{-}25}N_{0\text{-}4}S_{0\text{-}1}$ with a user-defined mass tolerance of 3 ppm and a Double Bond Equivalent (DBE) ranging from -0.5 to 25. The assignments were validated by checking the error distribution which has to be between -3 and 3 ppm, and equitably distributed around 0 ppm (Annexe 3). Data exploitation was performed using the double bond equivalent value (DBE), its ratio to the number of carbon atoms (DBE/C), and several graphical representations such as the classification by chemical families, Van Krevelen diagrams and Kendrick plots. Double Bound Equivalency (DBE) and Aromaticity Indices (AI) were computed from the elemental formulas as follows:

$$DBE_{AI} = 1 + C - O - S - \frac{1}{2}H \qquad (1)$$

$$C_{AI} = C - O - N - S \qquad (2)$$

$$AI = \frac{DBE_{AI}}{C_{AI}} = \frac{1+C-O-S-\frac{1}{2}H}{C-O-N-S} \qquad (3)$$

3.3 RESULTS AND DISCUSSION

3.3.1 Characteristics of sandy podzolic water samples from Landes, Gascony

Physical and chemical characteristics of the samples are summarized in the Table 3.3-1. We chose the use of H_2O to extract soil DOM material as H_2O extracts were recently reported to contain a greater chemical diversity of organic compounds, compared to organic solvents (such as methanol, acetonitrile, or hexane), in various types of soils (Tfaily et al. 2015).

Table 3.3-1: Physical and chemical characteristics of the samples

Samples	pH	Conductivity ($mS.cm^{-1}$)	Chemical composition		Zeta potential (mV)
			[TOC] $mg.kg^{-1}$	[TN] $mg.kg^{-1}$	
A1	3.5	0.12	166	4.3	-13.35
Bh	4.6	0.082	138	3	-13.81
GW	6.1	0.068	6.2	0.5	-19.56

3.3.2 ESI/HRMS analysis of sandy podzolic soils and aquifer samples from Landes, Gascony

Mass spectra and molecular assignments

The high resolution ESI(-) mass spectra of the upper horizon soil sample is reported in Figure 3.3-1. The broadband ESI(-) HRMS spectra display a pattern of intense ion clusters observed at odd m/z values together with less intense groups of ions at even m/z values. This pattern is attributed to deprotonated ions containing only C, H, and O. The less intense clusters of ions observed at even m/z values are attributed to the heteroatoms (i.e. nitrogen) containing compounds and/or $^{13}C_1{}^{12}C_{n-1}$ isotopologues from singly charged ions (Stenson et al. 2002). The ESI(-) HRMS spectrum has a periodicity of 14.0156 mass units, corresponding to the addition of –CH2 groups (Hertkorn et al. 2008; Reemtsma et al. 2008; Stenson et al. 2002), in agreement with previous studies of terrestrial DOM samples (Koch et al. 2007; Pracht et al. 2018). Another recurring mass spacing pattern includes 0.0364 Da (CH4 vs 16O). The ion distribution in each the mass spectrum was similar regardless of the instrument settings used (i.e. changing voltage on the ESI source or in the ion optics). ESI(-) HRMS spectra ranged from 50 to 600 Da and presented a multimodal distribution. All three ESI(-) HRMS spectra shared the same general features, with the highest intensity ions observed at m/z values < 200 Da followed by an intensity decrease with increasing m/z values (Figure 3.3-1). These spectral features are very similar to those observed from the ESI(-) HRMS analysis of Suwannee River Fulvic Acid (Remucal et al. 2012) and other natural organic matter samples (Hawkes et al. 2016).

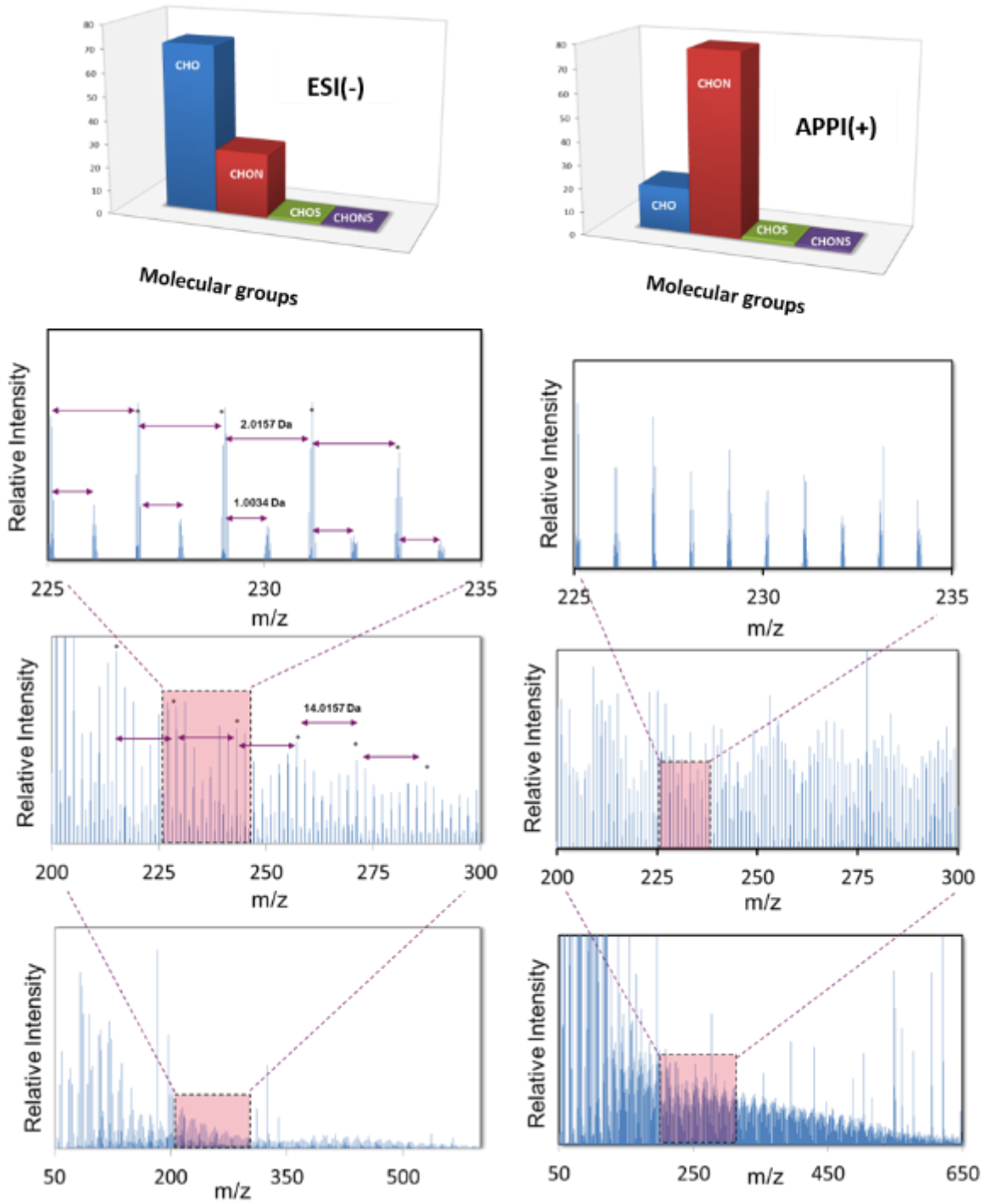

Figure 3.3-1: High resolution mass spectra of sample GW in the mass range 50-650 Da, 200-300 Da and detail on mass range 225-235 Da. Note the mass spacing commonly encountered in an HRMS spectrum of NOM. Each added ring or double bond lowers the mass by 2.01565 Da and each additional –CH2 group increases the mass by 14.011565 Da. The upper segments exhibit a series of peaks separated by multiples of 1.0034 Da (^{13}C), indicating the singly-charged state of the detected ions.

The assigned formulas were grouped into four molecular classes according to their heteroatom content: the C, H and O containing compounds subgroup (CHO), the C, H, O and N subgroup (CHON), the C, H, O and S subgroup (CHOS) and the C, H, O, N and S subgroup (CHONS). Although ESI Orbitrap™ MS is not a quantitative method when operated using direct infusion (the ionization efficiency varies widely among the compounds), all samples were treated in a similar way and normalized by the total number of detected peaks, making comparisons between samples more robust (Pracht et al. 2018).

In the three samples analyzed, very few of these latter two subgroups (CHOS and CHONS) of compounds were assigned a composition (<2%; Annexe 4). We thus decided to only focus on the CHO and CHON groups. CHO compounds represented 70,8 %, 87,4 % and 88,8 % of the assigned molecular formulas for the upper horizon (A1), illuvial horizon(Bh) and groundwater (GW) samples, respectively (Annexe 4). These patterns are frequently reported in the literature (Altieri et al. 2012; Hertkorn et al. 2008; Schmitt-Kopplin et al. 2012; Sleighter and Hatcher 2008; Wozniak et al. 2008) and are typical of terrigenous DOM such as the Suwannee River Fulvic Acid standard (SRFA), for which D'Andrilli et al. (2013) have observed similar relative abundances derived from ESI(-) HRMS analysis.

The average O/C and H/C ratios, as well as the average DBE values for the three samples, derived from ESI(-) mass spectra of all elemental compositions are listed in Table 3.3-2. O/C and H/C ratios are particularly useful to characterize the evolution of humic substances during the diagenesis process (Huc and Durand 1977; Rice and MacCarthy 1991). The average O/C ratios ranged from 0.33 to 0.45 and are consistent with O/C ratios observed for soil humic substances (Aiken 1985). These relatively low ratios (<0.5) suggest the presence of fewer O-containing functional groups and a high degree of oxidation of the DOM. The average H/C ratios were between 0.59 and 1.11, within the ranges of humic substances from soils. H/C ratio is a good indicator of the aliphaticity of an organic compound (Van Krevelen 1961). The overall average H/C ratios slightly varied and were clustered around 1.09, in accordance with observed H/C values for soil and aquatic humic substances (Aiken 1985). Average DBE values ranged from 7.20 and 12.41 and increased overall along the sequence A1 < Bh < GW which, combined with the H/C ratios mentioned above, indicate the presence of unsaturated structures.

Table 3.3-2: Soil dissolved organic matter characteristics by elemental groups

	Upper horizon A1				**Accumulation Horizon (Bh)**				**Groundwater (Gw)**		
	All	**CHO**	**CHON**		**All**	**CHO**	**CHON**		**All**	**CHO**	**CHON**
O/C	0.45 ± 0.21	0.43 ± 0.22	0.45 ± 0.21		0.38 ± 0.20	0.40 ± 0.21	0.37 ± 0.16		0.34 ± 0.19	0.33 ± 0.16	0.34 ± 0.12
H/C	1.08 ± 0.37	1.10 ± 0.39	1.08 ± 0.37		1.09 ± 0.35	1.11 ± 0.32	1.10 ± 0.42		1.09 ± 0.31	0.59 ± 0.06	0.59 ± 0.08
DBE	8.48 ± 3.41	7.20 ± 3.00	7.99 ± 3.40		8.5 ± 3.28	8.57 ± 3.08	7.44 ± 2.79		9.08 ± 3.25	10.74 ± 2.49	12.41 ± 1.66
AI	0.45 ± 0.26	0.42 ± 0.20	0.49 ± 0.32		0.44 ± 0.23	0.39 ± 0.19	0.55 ± 0.29		0.44 ± 0.22	0.43 ± 0.25	0.43 ± 0.25
OM/OC	1.78 ± 0.31	1.70 ± 0.33	1.73 ± 0.32		1.64 ± 0.29	1.62 ± 0.28	1.75 ± 0.28		1.55 ± 0.22	1.49 ± 0.21	1.66 ± 0.20

Following the protocol proposed by Grannas et al. (2006) and Hockaday et al. (2009), each molecular compound was divided into seven biomolecular classes based on a certain range of O/C and H/C values. These included lipids: H/C > 1.5, 0 ≤ O/C < 0.3; proteins: H/C > 1.5, 0.3 ≤ O/C< 0.67; aminosugars/carbohydrates (As/Ch): H/C > 1.5, O/C > 0.67; unsaturated hydrocarbons (UH): 0.7≤ H/C ≤ 1.5, O/C < 0.5; lignin-like molecules (lignins): 0.7≤ H/C ≤ 1.5, 0.1≤ O/C≤ 0.67; tannin-like molecules (tannins): 0.5 ≤ H/C ≤ 1.5, 0.67 < O/C; and condensed aromatic structures (CAS): 0.2 ≤ H/C ≤ 0.7, O/C ≤ 0.67. Figure 3.3-2 summarizes the relative abundance of the various compound classes established based on their H/C and O/C elemental ratios in the upper horizon soil (Figure 3.3-2A), the illuvial horizon soil (Figure 3.3-2B) and the groundwater sample (Figure 3.3-2C). The highest relative abundance values were assigned to lignin-like compounds in the upper horizon and the illuvial soil as well as in the groundwater. They represented 53, 79 and 73% of all compounds in each sample, respectively. The high relative abundance of lignin compounds indicate that leaching of plants debris dominates the dissolved organic matter pool released in the soil seepage waters. In fact, many molecular formulas detected where consistent with those of the G type phenolic lignin monomers, such as vanillin ($C_8H_8O_3$, DBE = 5); guaiacol ($C_7H_8O_2$, DBE = 4); 4-vinyl guaiacol ($C_9H_{10}O_2$, DBE = 5); acetoguaiacone ($C_9H_{10}O_3$, DBE = 5); ethyl guaiacol ($C_9H_{12}O_2$; DBE= 4); homovanillic acid ($C_9H_{10}O_4$, DBE= 5), isoeugenol ($C_{10}H_{12}O_2$, DBE = 5), guaiacylacetone ($C_{10}H_{12}O_3$, DBE = 5), methyl guaiacol ($C_8H_{10}O_2$, DBE = 4) eugenol ($C_{10}H_{12}O_2$, DBE = 5) as well as S-type monomers such as syringol ($C_8H_{10}O_3$, DBE = 4), syringaldehyde ($C_9H_{10}O_4$, DBE = 5), acetosyringone ($C_{10}H_{12}O_4$, DBE = 5), allylsyringol ($C_{11}H_{14}O_3$, DBE = 5) and the PP-type phenols like catechol ($C_6H_6O_2$, DBE = 4) or cresol (C_7H_8O, DBE = 4). Lignin is the second most abundant biomolecule after cellulose (Crawford 1981) and is exclusively of terrestrial/plant origin. It is an amorphous, three-dimensional polymer of substituted phenyl-propane units insoluble in its polymeric form.

Although lignin is known to be degraded at a lower rate than other plant-derived compounds such as polysaccharides and proteins (Haider 1992; Martin et al. 1980), several studies have shown the biodegradability of macromolecules such as lignin and celluloses in soils (Feng et al. 2008; Paterson and Lundquist 1985). However, the biological degradation of lignin is incomplete and results in partially oxidized fragments (most of which are phenolic acids) rather than complete mineralization products (Chen et al. 1983; McCarthy et al. 1986). These products then contribute to the soil DOM pool, percolate through and transport into the underlying soil layers (Guggenberger and Zech 1994; Kaiser et al. 2001; Kaiser and Kalbitz 2012). Besides, molecular formula reflecting carboxylic acids such as coumaric acid ($C_9H_8O_3$, DBE = 6), cinnamic acid ($C_9H_8O_2$, DBE = 6), sinapic acid ($C_{11}H_{12}O_5$, DBE = 6), ferrulic acid ($C_{10}H_{10}O_4$, DBE = 6) and caffeic acid ($C_9H_8O_4$, DBE = 6) were also detected. These results are consistent with previous findings of lignin and lignin-like compounds present in the soil solution of forested soils (Guggenberger and Zech 1994; Thevenot et al. 2010). Indeed, forests litter is an important source of soil DOM (Kalbitz et al. 2000), especially

coniferous litter, such as spruce and pine needle litter that can release lignin-derived DOM components with a high aromaticity into the soils via microbial activities (Don and Kalbitz 2005; Ide et al. 2017).

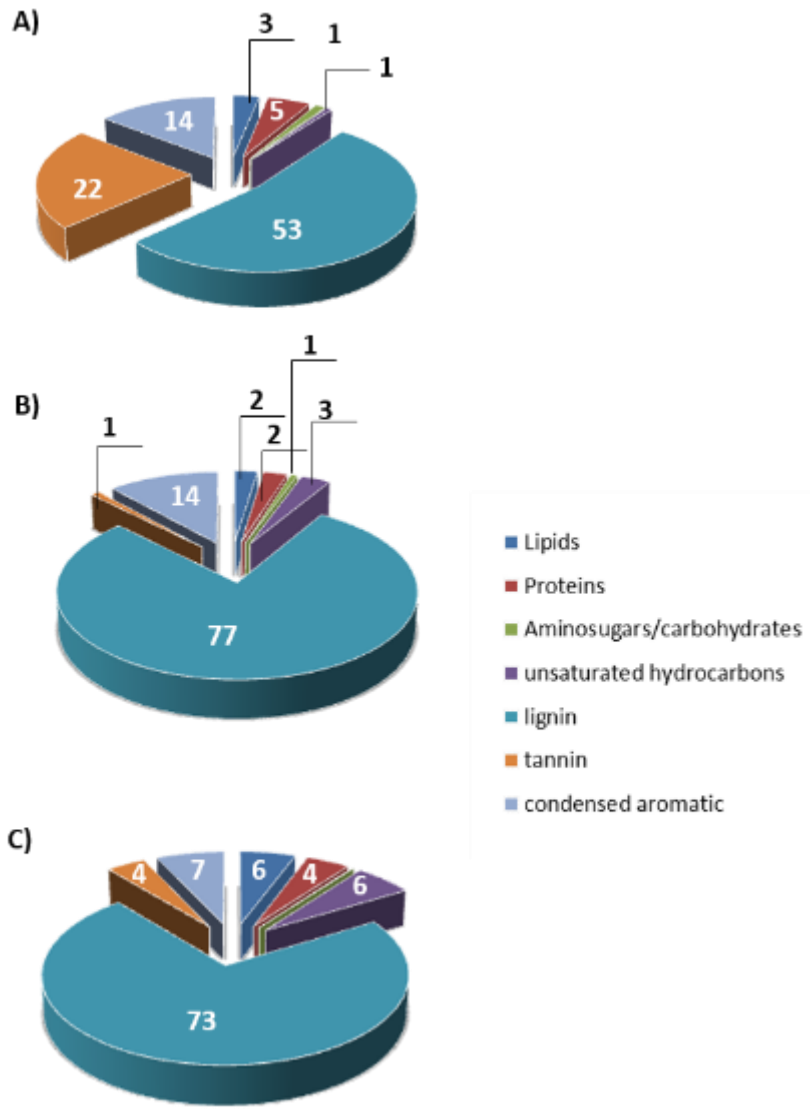

Figure 3.3-2: Relative abundance of the various compound classes established based on their H/C and O/C elemental ratios in the upper horizon soil (A), the illuvial horizon soil (B) and the groundwater sample.

Beside microbial respiration, the degradation of macromolecules such as lignin in the DOM pool may also be mediated by the presence of reactive oxygen species (ROS), such as hydroxyl radicals ($^{\bullet}OH$), singlet oxygen ($^{1}O_2$) and superoxide ($O_2^{-\bullet}$) (Waggoner et al. 2017, 2015). A recent study found that DOM exposed to $^{1}O_2$ preferentially lost molecular formulas with an O/C > 0.3, resulting in compounds associated with a higher oxygen content, while DOM exposure to $O_2^{-\bullet}$ selectively removed formulas with O/C < 0.3, generating

aliphatic formulas (H/C> 1.5). Another study pinpointed the formation of black carbon-like and alicyclic aliphatic compounds following exposure to hydroxyl radicals. Even if most ROS are produced by photochemical reactions, growing evidence suggest the presence of hydroxyradicals in systems devoid of sunlight, like soils (Aeschbacher et al. 2010; Maurer et al. 2010; Page et al. 2012). These radicals may be released by humic substances, through reactions involving O_2 and redox-active hydroquinone-type compounds (Maurer et al., 2010). Also, Fe^{2+} (naturally present in podzols) generates hydroxyl radicals through Fenton chemistry reactions (Trusiak et al. 2018; Vermilyea and Voelker 2009).

In the upper horizon soil (Figure 3.3-2A), tannin-like compounds were the second most abundant class (22%), followed by condensed aromatics (14%), proteins-like (5%) and the remaining low relative abundance compounds allocated between lipids (3%), aminosugars/carbohydrates (1%) and unsaturated hydrocarbons (1%). In contrast, the illuvial horizon soil had a much lower relative abundance of tannin-like compounds, but a higher relative abundance of lignin and condensed aromatics. The composition of the groundwater sample still displayed a high relative abundance of lignin compounds (approximately 75%) with almost equal contribution of the other molecular families considered. Ubiquitous in vascular plant tissues (leaves, roots, wood, bark, fruits and buds), tannins represent a significant portion of terrestrial biomass (Hernes and Hedges 2000). These water-soluble polyphenolic compounds usually enter the soils by leaching and litter inputs, both above- and below-ground (Kraus et al. 2003). Once they enter the soil, tannins can remain in solution, precipitate, adsorb to soil particles, complex metals, or be either biotically or abiotically transformed. Various laboratory studies have also shown that tannins can form complexes with proteins, via H-bonding and hydrophobic effects, resulting in complexes relatively resistant to decomposition (Basabara and Starkey 1966; Benoit et al. 1968; Benoit and Starkey 1968; Hagerman et al. 1998; Haslam 1993).

Condensed aromatics constitute a significant fraction of the soil DOM (Figure 3.3-2). Many studies have reported the detection of condensed aromatic compounds (dissolved black carbon) in the DOM pool isolated from both terrestrial and aquatic ecosystems (Hockaday et al. 2006; Stubbins et al. 2015; Wagner et al. 2015; Ziolkowski and Druffel 2010). Condensed aromatics usually result from the incomplete combustion of organic compounds (Goldberg 1985), and may include direct input from local combustion sources or atmospheric deposition from distant combustion sources (Spencer et al. 2015; Stubbins et al. 2012) such as industrial, automobile, agricultural, domestic wildfire, or biomass burning.

As it accounts for most of the compounds detected, further characterization of the lignin-like group is relevant. Figure 3.3-3 displays the COO-based Kendrick mass defect (KMDCOO) plot as a function of the number of oxygen atoms of the assigned formula corresponding to the lignin-like compounds (H/C = 0.7 - 1.5 ; O/C = 0.1 - 0.67, Figure 3.3-3) belonging to the CHO group. The KMDCOO converts m/z values to Kendrick mass values by multiplying the m/z value by the ratio of the nominal mass -COO group (44,00000) to the exact mass of a -COO group (43.98983) , as shown below in the equation (1). Then, KMD is

determined by subtracting the nominal Kendrick mass (KM) from KM, as shown in equation (2). Formulas with the same KMD fall on a horizontal line and differ only by –COO group (or multiple of COO groups). In this plot, data aligned vertically are more aliphatic at higher KMD value (KMDCOO values increase with the number of H and C atoms) while more aromatic compounds have lower KMDCOO values.

Kendrick Mass (COO) = exact m/z value of peak * (44.00000/43.98983) (1)

Kendrick Mass Defect (COO) = Observed nominal mass – Kendrick Mass (COO) (2)

This representation allows visualizing on similar horizontal axis lignin-like compounds differing only by their number of carboxylic groups (Yuan et al. 2017). Overall, KMDCOO values of the DOM isolated from the upper (A1) soil horizon are concentrated in the upper part of the diagram (KMDCOO > -0.25), implying that this pool of DOM is more saturated with more oxidized carbon.

The removed compounds during bioprocess were concentrated in the left part of the diagram (O < 4), and the formed compounds were scattered in the right part (O > 8), implying increased carboxyl groups in lignins/CRAM-like compounds after biodegradation. As for coagulation, a large proportion of the removed compounds were distributed in the upper right part of the diagram (O > 8 and KMD > −0.15), demonstrating that the oxidized and unsaturated lignins/CRAM-like with more carboxyl groups were preferentially removed by coagulation.

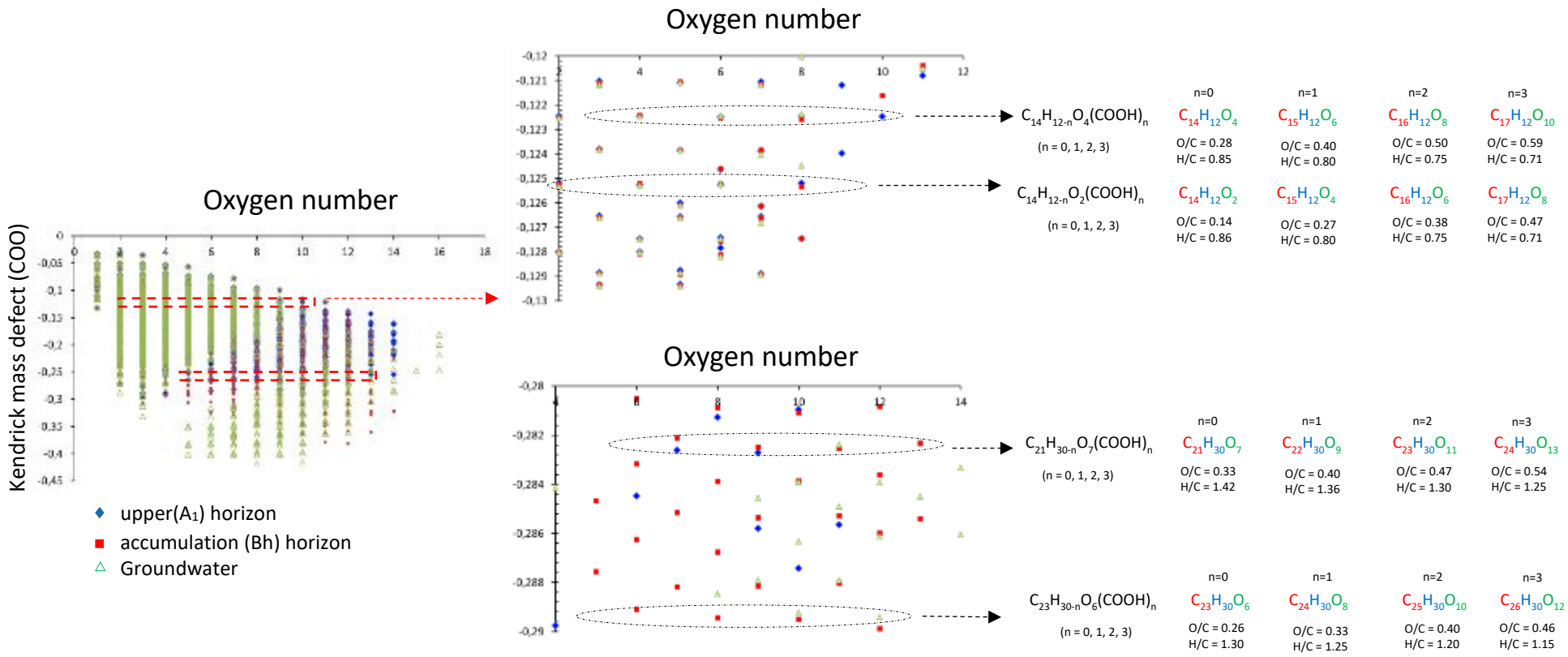

Figure 3.3-3: KMD (COO)-number of oxygen (O) in the formulas plots and its scale-expanded segments for lignin-like structures (H/C= 0.7-1.5; O/C=0.1-0.67) of CHO formulas in the DOM isolated from the upper (A1) soil horizon, accumulation (Bh) soil horizon and ground water. The assigned formulas (as $[M-H]^-$ ions) of some randomly selected points in the segments are also displayed.

Compounds containing only C, H and O

The reconstructed mass spectrum of the monoisotopic molecular formulas containing only C, H and O from the upper horizon soil sample (A1), acquired in ESI(-) after blank subtraction contains a relatively high number of isobaric anions, as shown in Figure 3.3-4a. The CHO anions detected by the Orbitrap mass analyzer cover a relatively broad mass range between 50 and 600 m/z, in agreement with the range of previously identified dissolved organic matter isolated from various types of soils (Tfaily et al. 2015; Wagner et al. 2015) such as peats, birch and spruce forest soils. Also, in contrast to Fourier Transform Ion Cyclotron Resonance (FT-ICR) mass spectrometry which usually do not consider ions below m/z 200 Da (Hertkorn et al. 2008; Stenson et al. 2003; Witt et al. 2009), the Orbitrap is able to analyze ions on the m/z 50/200 Da range. Although the relative intensity of anions produced by ESI should be considered carefully and not be regarded as quantitative, due to the strong dependence of ESI ionization mechanisms with the type of functional groups in the backbone of a molecule, the highest intensity at m/z values below 200 Da followed by a decreasing intensity with increasing m/z values. The reconstructed mass spectral inset in Figure 3.3-4a displays a zoomed view centered at m/z 259. A total of 9 isobaric CHO anions were detected within a 0.25 Da mass window. The molecular formulas of each isobaric anion within this time window are listed in Figure 3.3-4a.

The van Krevelen diagram is built from the elementary composition ratios of each assigned formula derived from the different HRMS spectra. This graphical representation allows the display of all individual elemental compositions simultaneously, providing a simple graphical tool for the demonstration of compositional differences between samples of different origins (Kew et al. 2017; Walters 2006; Wu et al. 2004). This display also allows to graphically separate the classes containing heteroatoms of interest and provides a pattern of unsaturation and alkylation for each class (Lobodin et al. 2012). The van Krevelen diagram (O/C vs. H/C) also reveals various biogeochemical relationships such as oxidation, hydration, hydrogenation, and alkylation relationships between the observed molecular formulas present in the sample (Heald et al. 2010; Kim et al. 2003; Wu et al. 2004). Oxygen-to-carbon ratios (O/C) and hydrogen-to-carbon ratios (H/C) are frequently used to describe the chemical properties of natural dissolved organic matter (Dittmar and Koch 2006; Koch and Dittmar 2006; Wu et al. 2004). Indeed, O/C is used as a proxy for the degree of oxidation of individual compounds and H/C reflects their degree of saturation. The O/C and H/C elemental ratios of individual CHO compounds analyzed by ESI(-) of the upper horizon soil A1 sample are plotted in Figure 3.3-4b. Most of the CHO compounds have O/C ratios < 1.0 and H/C ratio comprised between 0.5 and 2.0. The size of each dot in the van Krevelen plot is a function of the relative abundance of each molecular formula in the ESI(-) spectrum. The highest density and intensity of molecular formulas are in the range of 0.6 <O/C < 0.8 and 0.5 <H/C < 1.5.

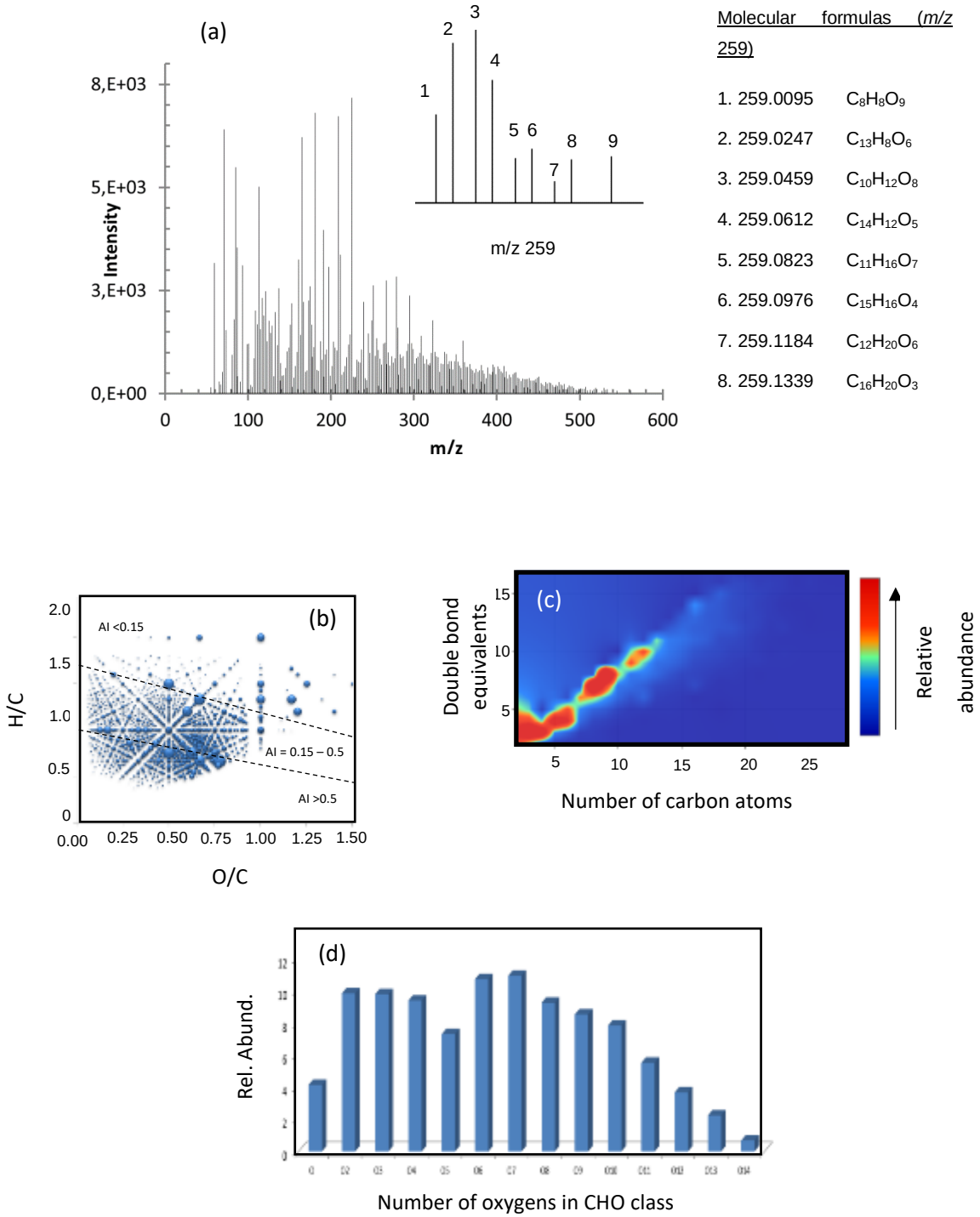

Figure 3.3-4: Reconstructed mass spectrum of the CHO compounds from the upper horizon soil A1 (a); corresponding van Krevelen diagram (b); isoabundance plot of double bond equivalents (DBE) vs. number of carbon atoms (c) and relative abundance (RA) of each subclass (d). The corresponding figures for the illuvial horizon (Bh) and the groundwater sample CHO compounds are displayed in Annexes 6 and 8.

Several compounds have an O/C>1.0, with a relatively high number of oxygen atoms (between 8 and 14), high number of double bond equivalents (between 4 and 8) and molecular weight in the range of 250-400 Da. Besides, a relatively high number (140) of CHO compounds are clustered in the lower left area of the van Krevelen diagram (O/C < 0.3, H/C < 1). This area is characteristic of aromatic compounds with high DBE values. Indeed, the average DBE value is 7.7 ± 3.0 among the 140 CHO compounds falling in this aromatic area of the van Krevelen diagram. Examples of the molecular formulas in this region include the homologous series of C12H4O3(CH2)1−11 (series containing 11 DBE) and C13H4O4(CH2)1−8 (series containing 12 DBE). Such highly aromatic and oxidized pools or organic compounds can be indicative of quinone-like moieties (Wagner et al. 2015). The average O/C ratio for the upper horizon (A1), assigned to the CHO elemental group is 0.43 (± 0.22) and the average H/C ratio is 1.10 (± 0.39) (Table 3.3-2). Overall, O/C and H/C ratios of CHO compounds in the upper horizon soil sample are within previously reported values for DOM and soil organic matter values (Aiken 1985; Ghabbour and Davies 2002).

DBE values ranging between 4 and 15 were observed among the CHO compounds, with an average DBE value of 7.20 (±3.00) (Table 3.3-2). Isoabundance plots of DBE versus carbon number for CHO class species in the upper (A1) and the accumulation (Bh) horizons soil samples are shown in Figure 3.3-4c and Annexe 6c. The color gradient from blue to red is positively correlated to the relative abundance of each molecule in each full scan MS spectrum. In both samples, most compounds in the CHO group have DBE values ≤ 10 with several hot-spots of high relative abundance DBE values at C4, C6, C9 and C12 and a clear trend of increasing DBE values with increasing carbon content (C4-C23). Average DBE values for A1 and Bh soil DOM CHO compounds are 7.20 (± 3.00) and 8.57 (± 3.08) while the DOM isolated from the groundwater sample contained an average 10.74 (± 2.49) DBE (Table 3.3-2).

The aromaticity index (AI) was also computed to include the possibility that heteroatoms can form double bonds which are not contributing to aromaticity, ring formation or condensation as described by Koch and Dittmar (2006). If the value of AI was negative, (i.e. when the number of π-bonds is lower than the number of heteroatoms), AI was defined as 0. A threshold value of AI ≥ 0.67 provides unambiguous criterion for the presence of condensed aromatic structure in the molecule. AI value comprised between 0.5 and 0.67 indicates conjugated π-system and is the criterion for the presence of aromatic cores, including combination with heteroatoms. Values of AI comprised between 0 and 0.5 are assigned to olefinic compounds and AI = 0 to aliphatic compounds. Using this metric, 60 to 75% of assigned molecular formulas was defined as aliphatic, 20 to 30% as olefinic and only less than 10% is considered as aromatic.

The oxygen content of assigned molecular formulas is another essential parameter to evaluate and may be attributed to the presence of diverse functional groups such as ether, ester, hydroxyl, peroxyl, carbonyl or carboxylic groups (Bae et al. 2011; Zhao et al. 2013). Relative abundances of each oxygen subclass for the upper horizon soil CHO compounds is displayed in Figure 3.3-4d. For this soil sample, the CHO compounds

range from O1 to O14 and a bimodal distribution with highest relative abundances observed for the O2-3 and O6-7 subclasses. Overall, low-oxygen subclasses are more abundant than high-oxygen subclasses, with a progressive decrease in relative abundance from the lowest to the highest number of oxygens in the CHO. Some of the highest relative abundance compounds observed for the O6-7 subclass include $C_9H_6O_6$ (DBE=7), $C_9H_8O_6$ (DBE = 6), $C_5H_6O_6$ (DBE = 3), $C_8H_6O_6$ (DBE = 6) as well as $C_6H_8O_7$ (DBE = 3), $C_9H_6O_7$ (DBE = 7), $C_{10}H_8O_7$ (DBE = 7), $C_{11}H_8O_7$ (DBE = 8). A few formulas display a relatively high number of oxygen atoms O12-14. These compounds have high DBE values (between 7 and 16) and display tannin-like features ($0.67 < O/C$ and $0.5 \leq H/C \leq 1.5$) as displayed in the van Krevelen diagram.

Interestingly, the CHO compounds of the illuvial horizon display a similar range from O1 to O14 but a different distribution is observed for the illuvial horizon soil (Annexe 6d). Indeed, the relative abundance peaks at the O2-3 subclass, to reach approximately 14% then decreases slowly to higher number of oxygens. Examples of the highest relative abundance compounds observed for the O2-3 subclass include $C_4H_6O_2$ (DBE=2), $C_6H_6O_2$ (DBE=4), $C_7H_8O_2$ (DBE=4) and $C_5H_6O_3$ (DBE=3), $C_6H_6O_3$ (DBE=4) and $C_5H_4O_3$ (DBE=4), with O/C and H/C features attributed to unsaturated hydrocarbons in the van Krevelen diagram. A similar trend is observed in the DOM isolated from the groundwater sample, where approximately 65% of the total relative abundance is attributed to the O1-3 subclass of CHO compounds (Annexe 8d).

Compounds containing only C, H, O and N

The reconstructed mass spectrum of the monoisotopic molecular formulas containing only C, H , O and N from the upper horizon soil sample (A), acquired in ESI(-) after blank subtraction contains a relatively high number of isobaric anions in the mass range of 75- 500 m/z, as shown in Figure 3.3-5. The reconstructed mass spectral inset in Figure 3.3-5a displays a zoomed view centered at m/z 200, with a total of 5 isobaric CHON anions within a 0.25 Da mass window. The molecular formulas of each isobaric anion within this time window are listed in Figure 3.3-5a. In general, relatively large amounts of organic nitrogen compounds were detected in each sample using ESI(-), accounting for 28% , 13% and 10% of the total relative abundance of the SOM extracted from the upper horizon, the illuvial horizon, and the groundwater samples, respectively. Hence, a higher abundance of N-containing compounds is observed at lower pH values and higher total organic carbon (TOC) and total nitrogen values (Table 3.3-1). The principal nitrogen-containing class in soil organic matter of forested soils contains amino groups (such as peptides and amino sugars) and is typically assumed to reflect the microbial activity of microheterotrophs (Kaiser et al. 2001; Knicker et al. 1997; Michalzik and Matzner 1999). Thus, the higher abundance of N-containing compounds in the upper horizon might in turn reflect a higher biological activity than in the DOM from the illuvial horizon and the groundwater samples.

The O/C and H/C elemental ratios of individual CHON compounds analyzed by ESI(-) of the upper horizon soil A sample are plotted in the van Krevelen diagram as displayed in Figure 3.3-5b. Most CHON compounds have

O/C ratios < 1.0 and H/C ratio comprised between 0.5 and 2.5. In contrast to the CHO family whose H/C ratios are mainly <1.7, many of the CHON compounds have a H/C > 1.7, characteristic of lipid-like compounds; suggesting that these compounds are both highly saturated and reduced (oxygen-poor). The molecular formulae of the homologous series C3H5NO(CH2)1-5 and/or C2H4N2O(CH2)1-8 display these characteristics. The average O/C ratio for the upper horizon (A1), assigned to the CHON elemental group is 0.45 (± 0.21) and the average H/C ratio is 1.08 (± 0.37). These values are very similar to the ones obtained for the CHO elemental group (Table 3.3-2).

Figure 3.3-5c displays the isoabundance plot of double bond equivalents (DBE) vs. number of carbon atoms in molecular formulas from the CHON class. Overall, the CHON compounds are mostly saturated, with a few exceptions. Indeed, most CHON compounds have DBE values < 10 (Figure 3.3-4c) which agrees with their H/C ratios. The number of carbon atoms range from C2 to C20 and the DBE values increase with the number of carbon atoms, up to 16 DBE (Figure 3.3-5c). Most of the hotspot CHON compounds (in terms of relative abundance) are clustered between C2-C12 and have DBE < 10. The most abundant compounds are those with C5 and relatively low values of DBE (DBE values between 2 and 6). Overall, the average DBE values are 7.99 (±3.40) for the upper horizon sample A1, 7.44 (±2.79) for the accumulation horizon Bh sample and 12.41 (±1.66) for the groundwater sample (Table 3.3-2). Only a small fraction of the CHON compounds has high DBE values from 12 to 16. Indeed, as illustrated in Figure 3.3-5c, the high-DBE CHON compounds have low relative abundances.

Upper horizon soil CHON compounds contain between 1 and 4 nitrogen atoms (Figure 3.3-5d) with ~ 64% of compounds containing one nitrogen atom (N1), followed by N2 (~22%), N3 (~8%) and N4 (~5%). To further examine the distribution of N in the molecular formulas, CHNO subclasses were further divided by the numbers of nitrogen and oxygen in the molecular formulas; they include NO1−13, N2O1−9, N3O1-7, and N4O2-9. The total relative abundance for the compounds contained within the subclasses is shown in Figure 3.3-5d.

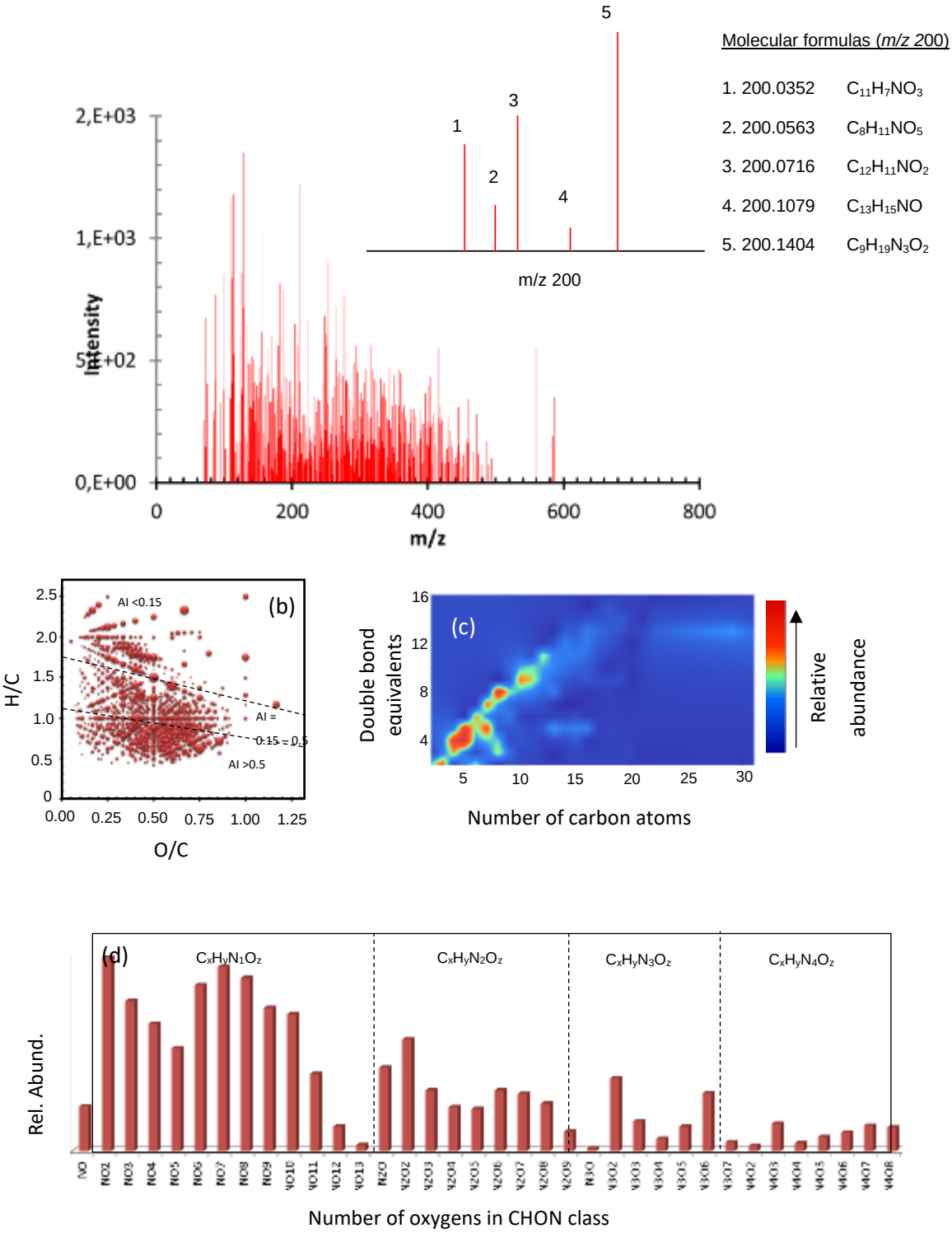

Figure 3.3-5: Reconstructed mass spectrum of the CHON compounds from the upper horizon soil A1 (a); corresponding van Krevelen diagram (b); isoabundance plot of double bond equivalents (DBE) vs. number of carbon atoms (c) and relative abundance (RA) of each subclass (d). The corresponding figures for the illuvial horizon (Bh) and the groundwater sample CHON compounds are displayed in Annexes 7 and 9.

3.3.3 Water samples comparison

From the results obtained in the previous section, the overall bulk composition of the three samples studied is largely similar. It is mainly composed of low molecular weight compounds containing mainly CHO and CHON compounds with molecular weights up to 700 Da. Sulfur containing compounds only accounted for a very small part of the total organic composition and represented less than 1% of the total elemental composition. It appears that the three water samples mostly originate from terrestrial organic matter, with a predominance of lignin-like compounds, meaning that the plant biomass contributed more to their global composition.

However, the combined study of the different compounds subgroups of OM clearly highlights that an evolution of the OM molecular composition occurs along the soil profile. Indeed, the decrease of the O/C ratios in both CHO and CHON compounds as well as the O global content simultaneous decrease suggest the existence of a reduction process. As further evidence, the tannins-like compounds abundance largely decreases with depth, dropping from approximately 10% of the total abundance in the upper horizon water to nearly 1% in GW sample. This former value is typical of these found in organic matter originated from plants growing up in stressful environments (typically in low-pH and/or poor soil) (Bussotti et al. 1998; Thoss et al. 2004), which is the present case. We can also point out an abundance shift from the high-oxygen classes to the low-oxygen classes in CHO compounds, leading us to believe that unsaturated compounds are appearing in deeper layers. Since these compounds have lower DBE and do not be aromatic-type, they're more likely to be composed of double bonds as in carboxylic acids. Lignin is here a very good indicator of the evolution of the OM along the soil profile. In effect the VSC sum decrease is a sign of lignin degradation and thus, as the lignin is a refractory material, a sign of high-rate degradation of OM. Additionally, the (Ad/Al)v ratio confirms that in the upper horizon water, there is an advanced state of lignin oxidative degradation. By focusing on the CHON compounds, it may be clearly noted that nitrogen increases in molecular composition with depth. The proportion of N1 compounds reduces for the benefit of N3 and N4 compounds along the soil profile. These latter compounds-types have higher DBE values in deeper horizons than in the superficial one. As the percentage of molecules with O/N ≥ 3 decreases with depth, and thereby the potential percentage of organonitrates, it is more likely that there are increasingly aromatic and/or unsaturated molecules with reduced nitrogen. In combination with the C/N ratio which is decreasing from approximately 10 in the upper horizon water to approximately 3 in the groundwater, it suggests the setting-up of a denitrification process in deeper layers. Overall, the molecular composition of the water organic matter has a trend to become more homogeneous and simpler with depth. In particular, the different compounds tend to concentrate in low-oxygen values. Thus, all these observations are evidences leading us to identify the OM early digenesis process occurring in our studied soil.

Although it follows the same evolution trend, the accumulation horizon water (Bh) has a very different molecular composition than the other waters. First, it presents the highest relative frequency of unique formulas with more than 99% of formulas which are only assigned in ESI or APPI modes, and less than 1% of identical formulas than A1 and GW samples. Unlike the two other waters, Bh has more assigned formulas in ESI mode than in APPI mode. It may suggest that Bh has more polar organic molecules. In its spectrum, another peak of intensity is distinguished for masses at ≈ 550Da, perhaps indicating a polymerization phenomenon due to the accumulation of organometallic complex in this horizon. Bh molecular families distribution is very heterogeneous. Even if the lignin-like compounds are predominant in its molecular composition, they account for less than 50% of the total OM. Also, lipids-like compounds only represent approximately 2% of its organic matter. In contrast, the abundance of proteins-like and unsaturated hydrocarbons is higher, which may mean that a large part of lignin has been degraded on unsaturated carbons molecules. The high DBE values and low H/C ratios confirm the presence of aromatic unsaturated carbon molecules with N and S compounds. Also, the S/V phenols ratio indicates that Bh originates more from angiosperms than A1 and GW, possibly because of a change of the plant cover over time. These molecular differences between A1/GW and Bh may come from the very complex chemical dynamic which occurs in this accumulation horizon, with especially the frequent variation of the aquifer level, involving a lot of physical and chemical modifications such as pH/Eh changes.

3.4 Conclusion

The combined use of both the ESI mode and the LTQ Orbitrap™ enables complementary data to be obtained. This hyphenated technique is necessary for a best understanding of the molecular structure of OM from ground- and surface- waters. The OM composition in waters generated from a podzolic soil is very complex with at least 3000 assigned unique formulas for each water samples. Mainly composed of CHO and CHON compounds, the waters sampled or generated from the site are overall constituted of low molecular organic compounds. Although strongly similar properties, each of the podzol water has a unique molecular fingerprint. Mainly constituted of lignin-derived compounds, such as phenolic monomers or carboxylic acids from its oxidative degradation, the plant-derived source of these organic compounds is clearly determined and correlated to the acidic conditions occurring within the podzol that inhibit the development of fauna. From this study the evolution of the organic matter with the depth within the podzol was highlighted. The numerous processes evidenced such as reduction of the compounds, degradation of the lignin, denitrification or the presence of reduced sulfur enable an early diagenesis of the organic matter occurring along the soil profile to be highlighted. The accumulation horizon water presents a very particular organic fingerprint, with a greater abundance of polar species and a likely different source of OM. Thus, it would be interesting in future investigations to compare it with the molecular composition of another podzol accumulation horizon water in order to understand more deeply the origin of these peculiarities and find out

more about the influence of the intrinsic characteristics of the soil on both the nature and the molecular structure of organic matter.

Indeed, these two parameters which have great influence on the reactivity of colloidal phases and their ability to complex trace elements such as uranium. Thus, it is essential to consider the variability of the organic matter, when the mobilization of uranium has to be characterized or for further studies about the uranium migration mechanisms within the environment.

REFERENCES

Abakumov, E., Trubetskoj, O., Demin, D., Celi, L., Cerli, C., Trubetskaya, O., 2010. Humic acid characteristics in podzol soil chronosequence. Chem. Ecol. 26, 59–66. https://doi.org/10.1080/02757540.2010.497758

Abbt-Braun, G., Lankes, U., Frimmel, F.H., 2004. Structural characterization of aquatic humic substances – The need for a multiple method approach. Aquat. Sci. 66, 151–170. https://doi.org/10.1007/s00027-004-0711-z

Aeschbacher, M., Sander, M., Schwarzenbach, R.P., 2010. Novel Electrochemical Approach to Assess the Redox Properties of Humic Substances. Environ. Sci. Technol. 44, 87–93. https://doi.org/10.1021/es902627p

Aiken, G.R., 1985. Humic Substances in Soil, Sediment, and Water: Geochemistry, Isolation, and Characterization. John Wiley and Sons.

Altieri, K.E., Hastings, M.G., Peters, A.J., Sigman, D.M., 2012. Molecular characterization of water soluble organic nitrogen in marine rainwater by ultra-high resolution electrospray ionization mass spectrometry. Atmos. Chem. Phys. 12, 3557–3571. https://doi.org/10.5194/acp-12-3557-2012

Augusto, S., Máguas, C., Matos, J., Pereira, M.J., Branquinho, C., 2010. Lichens as an integrating tool for monitoring PAH atmospheric deposition: A comparison with soil, air and pine needles. Environmental Pollution 158, 483–489. https://doi.org/10.1016/j.envpol.2009.08.016

Bae, E., Yeo, I.J., Jeong, B., Shin, Y., Shin, K.-H., Kim, S., 2011. Study of Double Bond Equivalents and the Numbers of Carbon and Oxygen Atom Distribution of Dissolved Organic Matter with Negative-Mode FT-ICR MS. Anal. Chem. 83, 4193–4199. https://doi.org/10.1021/ac200464q

Baker, W.E., 1973. The role of humic acids from Tasmanian podzolic soils in mineral degradation and metal mobilization. Geochimica et Cosmochimica Acta 37, 269–281. https://doi.org/10.1016/0016-7037(73)90134-8

Basabara, J., Starkey, R.L., 1966. Effect of plant tannins on decomposition of organic substances. Soil Science 101, 17–23.

Benoit, R.E., Starkey, R.L., 1968. Enzyme inactivation as a factor in the inhibition of decomposition of organic matter by tannins. Soil Science 105, 203–208.

Benoit, R.E., Starkey, R.L., Basabara, J., 1968. Effect of purified plant tannin on decomposition of some organic compounds and plant materials. Soil Science 105, 153–158.

Bonifacio, E., Catoni, M., Falsone, G., Said-Pullicino, D., Celi, L., 2013. Evolution of surface properties and organic matter stabilisation in podzolic B horizons as assessed by nitrogen and phosphate sorption. Biol. Fertil. Soils 49, 505–516. https://doi.org/10.1007/s00374-013-0788-4

Bussotti, F., Gravano, E., Grossoni, P., Tani, C., 1998. Occurrence of tannins in leaves of beech trees (Fagus sylvatica) along an ecological gradient, detected by histochemical and ultrastructural analyses. New Phytologist 138, 469–479. https://doi.org/10.1046/j.1469-8137.1998.00121.x

Campo, J., Nierop, K.G.J., Cammeraat, E., Andreu, V., Rubio, J.L., 2011. Application of pyrolysis-gas chromatography/mass spectrometry to study changes in the organic matter of macro- and microaggregates of a Mediterranean soil upon heating. J Chromatogr A 1218, 4817–4827. https://doi.org/10.1016/j.chroma.2011.03.038

Chen, C.-L., Chang, H.-M., Kirk, T.K., 1983. Carboxylic Acids Produced Through Oxidative Cleavage of Aromatic Rings During Degradation of Lignin in Spruce Wood by Phanerochaete Chrysosporium. Journal of Wood Chemistry and Technology 3, 35–57. https://doi.org/10.1080/02773818308085150

Chen, W., Westerhoff, P., Leenheer, J.A., Booksh, K., 2003. Fluorescence Excitation−Emission Matrix Regional Integration to Quantify Spectra for Dissolved Organic Matter. Environ. Sci. Technol. 37, 5701–5710. https://doi.org/10.1021/es034354c

Coble, P.G., 1996. Characterization of marine and terrestrial DOM in seawater using excitation emission matrix spectroscopy. Mar. Chem. 51, 325–346. https://doi.org/10.1016/0304-4203(95)00062-3

Crançon, P., 2001. Migration de l'uranium dans un podzol : le rôle des colloïdes dans la zone non saturée et la nappe ; application aux landes de Gascogne (phdthesis). Université Joseph-Fourier - Grenoble I.

Crawford, D., 1981. Microbial Conversions of Lignin to Useful Chemicals Using a Lignin-Degrading Streptomyces. Biotechnol. Bioeng. 275–291.

Cronan, C., 1985. Chemistry and Movement of Dissolved Humic Substances in 3 Forested Adirondack Watersheds. Org. Geochem. 8, 105–105. https://doi.org/10.1016/0146-6380(85)90058-0

D'Andrilli, J., Foreman, C.M., Marshall, A.G., McKnight, D.M., 2013. Characterization of IHSS Pony Lake fulvic acid dissolved organic matter by electrospray ionization Fourier transform ion cyclotron resonance mass spectrometry and fluorescence spectroscopy. Org. Geochem. 65, 19–28. https://doi.org/10.1016/j.orggeochem.2013.09.013

Davis, W.M., Erickson, C.L., Johnston, C.T., Delfino, J.J., Porter, J.E., 1999. Quantitative Fourier Transform Infrared spectroscopic investigation humic substance functional group composition. Chemosphere 38, 2913–2928. https://doi.org/10.1016/S0045-6535(98)00486-X

Dawson, H., Ugolini, F., Hrutfiord, B., Zachara, J., 1978. Role of Soluble Organics in Soil Processes of a Podzol, Central Cascades, Washington. Soil Sci. 126, 290–296. https://doi.org/10.1097/00010694-197811000-00006

Dittmar, T., Koch, B., 2006. Thermogenic organic matter dissolved in the abyssal ocean. Marine Chemistry 102, 208–217. https://doi.org/10.1016/j.marchem.2006.04.003

Don, A., Kalbitz, K., 2005. Amounts and degradability of dissolved organic carbon from foliar litter at different decomposition stages. Soil Biology and Biochemistry 37, 2171–2179.

Feng, X., Simpson, A.J., Wilson, K.P., Dudley Williams, D., Simpson, M.J., 2008. Increased cuticular carbon sequestration and lignin oxidation in response to soil warming. Nature Geoscience 1, 836–839. https://doi.org/10.1038/ngeo361

Ghabbour, E.A., Davies, G. (Eds.), 2002. Humic Substances: Structures, Models and Functions, 1 edition. ed. Royal Society of Chemistry, Cambridge.

Godde, M., David, M.B., Christ, M.J., Kaupenjohann, M., Vance, G.F., 1996. Carbon mobilization from the forest floor under red spruce in the northeastern USA. Soil Biol. Biochem. 28, 1181–1189. https://doi.org/10.1016/0038-0717(96)00130-7

Goldberg, M., 1985. Aquatic Photolysis of Oxy-Organic Compounds Adsorbed on Goethite. Abstr. Pap. Am. Chem. Soc. 189, 18-GEOC.

Grannas, A.M., Hockaday, W.C., Hatcher, P.G., Thompson, L.G., Mosley-Thompson, E., 2006. New revelations on the nature of organic matter in ice cores. Journal of Geophysical Research: Atmospheres 111. https://doi.org/10.1029/2005JD006251

Guggenberger, G., Zech, W., 1994. Composition and dynamics of dissolved carbohydrates and lignin-degradation products in two coniferous forests, N.E. Bavaria, Germany. Soil Biology and Biochemistry 26, 19–27. https://doi.org/10.1016/0038-0717(94)90191-0

Guo, X., Xi, B., Yu, H., Ma, W., He, X., 2011. The structure and origin of dissolved organic matter studied by UV-vis spectroscopy and fluorescence spectroscopy in lake in arid and semi-arid region. Water Sci. Technol. 63, 1010–1017. https://doi.org/10.2166/wst.2011.282

Hagerman, A.E., Riedl, K.M., Jones, G.A., Sovik, K.N., Ritchard, N.T., Hartzfeld, P.W., Riechel, T.L., 1998. High molecular weight plant polyphenolics (tannins) as biological antioxidants. J. Agric. Food Chem. 46, 1887–1892. https://doi.org/10.1021/jf970975b

Haider, K., 1992. Problems related to the humification processes in soils of temperate climates. In 'Soil Biochemistry, Vol 7'. Stotzky, G and J -M Bollag (Ed), New York, Usa; Basel, Switzerland, pp. 55–94.

Haitzer, M., Aiken, G.R., Ryan, J.N., 2002. Binding of Mercury(II) to Dissolved Organic Matter: The Role of the Mercury-to-DOM Concentration Ratio. Environ. Sci. Technol. 36, 3564–3570. https://doi.org/10.1021/es025699i

Haslam, E., 1993. Shikimic acid: metabolism and metabolites. Wiley, Chichester; New York.

Hawkes, J.A., Dittmar, T., Patriarca, C., Tranvik, L., Bergquist, J., 2016. Evaluation of the Orbitrap Mass Spectrometer for the Molecular Fingerprinting Analysis of Natural Dissolved Organic Matter. Anal. Chem. 88, 7698–7704. https://doi.org/10.1021/acs.analchem.6b01624

Heald, C.L., Kroll, J.H., Jimenez, J.L., Docherty, K.S., DeCarlo, P.F., Aiken, A.C., Chen, Q., Martin, S.T., Farmer, D.K., Artaxo, P., 2010. A simplified description of the evolution of organic aerosol composition in the atmosphere: VAN KREVELEN DIAGRAM OF ORGANIC AEROSOL. Geophysical Research Letters 37. https://doi.org/10.1029/2010GL042737

Hernes, P.J., Hedges, J.I., 2000. Determination of Condensed Tannin Monomers in Environmental Samples by Capillary Gas Chromatography of Acid Depolymerization Extracts. Analytical Chemistry 72, 5115–5124. https://doi.org/10.1021/ac991301y

Hertkorn, N., Frommberger, M., Witt, M., Koch, B.P., Schmitt-Kopplin, P., Perdue, E.M., 2008. Natural Organic Matter and the Event Horizon of Mass Spectrometry. Anal. Chem. 80, 8908–8919. https://doi.org/10.1021/ac800464g

Hockaday, W.C., Grannas, A.M., Kim, S., Hatcher, P.G., 2006. Direct molecular evidence for the degradation and mobility of black carbon in soils from ultrahigh-resolution mass spectral analysis of dissolved organic matter from a fire-impacted forest soil. Org. Geochem. 37, 501–510. https://doi.org/10.1016/j.orggeochem.2005.11.003

Hockaday, W.C., Purcell, J.M., Marshall, A.G., Baldock, J.A., Hatcher, P.G., 2009. Electrospray and photoionization mass spectrometry for the characterization of organic matter in natural waters: a qualitative assessment. Limnology and Oceanography: Methods 7, 81–95. https://doi.org/10.4319/lom.2009.7.81

Huc, A.Y., Durand, B.M., 1977. Occurrence and significance of humic acids in ancient sediments. Fuel 56, 73–80. https://doi.org/10.1016/0016-2361(77)90046-1

Ide, J., Ohashi, M., Takahashi, K., Sugiyama, Y., Piirainen, S., Kortelainen, P., Fujitake, N., Yamase, K., Ohte, N., Moritani, M., Hara, M., Finer, L., 2017. Spatial variations in the molecular diversity of dissolved organic matter in water moving through a boreal forest in eastern Finland. Sci Rep 7, 42102. https://doi.org/10.1038/srep42102

Ishiwatari, R., 1992. Macromolecular material (humic substance) in the water column and sediments. Marine Chemistry 39, 151–166. https://doi.org/10.1016/0304-4203(92)90099-V

Johnson, C.E., Driscoll, C.T., Siccama, T.G., Likens, G.E., 2000. Element fluxes and landscape position in a northern hardwood forest watershed ecosystem. Ecosystems 3, 159–184. https://doi.org/10.1007/s100210000017

Jolivet, C., Augusto, L., Trichet, P., Arrouays, D., 2007. Les sols du massif forestier des Landes de Gascogne : formation, histoire, propriétés et variabilité spatiale. Revue Forestière Française. https://doi.org/10.4267/2042/8480

Kaiser, K., Guggenberger, G., Haumaier, L., Zech, W., 2001. Seasonal variations in the chemical composition of dissolved organic matter in organic forest floor layer leachates of old-growth Scots pine (Pinus sylvestris L.) and European beech (Fagus sylvatica L.) stands in northeastern Bavaria, Germany. Biogeochemistry 55, 103–143. https://doi.org/10.1023/A:1010694032121

Kaiser, K., Kalbitz, K., 2012. Cycling downwards – dissolved organic matter in soils. Soil Biology and Biochemistry 52, 29–32. https://doi.org/10.1016/j.soilbio.2012.04.002

Kalbitz, K., Solinger, S., Park, J.-H., Michalzik, B., Matzner, E., 2000. Controls on the dynamics of dissolved organic matter in soils: A review. Soil Science 165, 277–304.

Kew, W., Blackburn, J.W.T., Clarke, D.J., Uhrín, D., 2017. Interactive van Krevelen diagrams – Advanced visualisation of mass spectrometry data of complex mixtures. Rapid Commun Mass Spectrom 31, 658–662. https://doi.org/10.1002/rcm.7823

Kim, S., Kramer, R.W., Hatcher, P.G., 2003. Graphical Method for Analysis of Ultrahigh-Resolution Broadband Mass Spectra of Natural Organic Matter, the Van Krevelen Diagram. Anal. Chem. 75, 5336–5344. https://doi.org/10.1021/ac034415p

Knicker, H., Ludemann, H.D., Haider, K. (Institut fur B. und physikalische B., 1997. Incorporation studies of NH4+ during incubation of organic residues by 15N-CPMAS-NMR-spectroscopy. European Journal of Soil Science (United Kingdom).

Koch, B.P., Dittmar, T., 2006. From mass to structure: an aromaticity index for high-resolution mass data of natural organic matter. Rapid Communications in Mass Spectrometry 20, 926–932. https://doi.org/10.1002/rcm.2386

Koch, B.P., Dittmar, T., Witt, M., Kattner, G., 2007. Fundamentals of Molecular Formula Assignment to Ultrahigh Resolution Mass Data of Natural Organic Matter. Anal. Chem. 79, 1758–1763. https://doi.org/10.1021/ac061949s

Kraus, T.E.C., Dahlgren, R.A., Zasoski, R.J., 2003. Tannins in nutrient dynamics of forest ecosystems - a review. Plant and Soil 256, 41–66. https://doi.org/10.1023/A:1026206511084

Liu, H., Amy, G., 1993. Modeling partitioning and transport interactions between natural organic matter and polynuclear aromatic hydrocarbons in groundwater. Environ. Sci. Technol. 27, 1553–1562. https://doi.org/10.1021/es00045a009

Lobodin, V.V., Rodgers, R.P., Marshall, A.G., 2012. Petroleomics and the analysis of complex organic mixtures with Fourier transform ion cyclotron resonance. In 'Comprehensive Environmental Mass Spectrometry (Advanced Topics in Environmental Science): 4'. ILM Publications, Glendale, AZ.

Lundstrom, U.S., van Breemen, N., Bain, D., 2000. The podzolization process. A review. Geoderma 94, 91–107. https://doi.org/10.1016/S0016-7061(99)00036-1

MacCarthy, P., Bloom, P.R., Clapp, C.E., Malcolm, R.L., 1990. Humic Substances in Soil and Crop Sciences: An Overview. Humic Substances in Soil and Crop Sciences: Selected Readings acsesspublicati, 261–271. https://doi.org/10.2136/1990.humicsubstances.c11

Malcolm, R., L., 1990. The uniqueness of humic substances in each of soil, stream and marine environments. Analytica Chimica Acta 232, 19–30. https://doi.org/10.1016/S0003-2670(00)81222-2

Martin, J.P., Haider, K., Kassim, G., 1980. Biodegradation and Stabilization after 2 Years of Specific Crop, Lignin, and Polysaccharide Carbons in Soils1. Soil Science Society of America Journal 44, 1250. https://doi.org/10.2136/sssaj1980.03615995004400060024x

Maurer, F., Christl, I., Kretzschmar, R., 2010. Reduction and Reoxidation of Humic Acid: Influence on Spectroscopic Properties and Proton Binding. Environ. Sci. Technol. 44, 5787–5792. https://doi.org/10.1021/es100594t

McCarthy, A.J., Paterson, A., Broda, P., 1986. Lignin solubilisation by Thermomonospora mesophila. Appl Microbiol Biotechnol 24, 347–352. https://doi.org/10.1007/BF00257062

McDowell, W.H., Likens, G.E., 1988. Origin, Composition, and Flux of Dissolved Organic Carbon in the Hubbard Brook Valley. Ecological Monographs 58, 177–195. https://doi.org/10.2307/2937024

Mehrabanian, M., 2013. Molecular geochemistry of soil organic matter by pyrolysis gas chromatography/mass spectrometry (GC/MS) technique: A review. Journal of Soil Science and Environmental Management 4, 11–16. https://doi.org/10.5897/JSSEM12.033

Michalzik, B., Matzner, E., 1999. Dynamics of dissolved organic nitrogen and carbon in a Central European Norway spruce ecosystem. European Journal of Soil Science 50, 579–590. https://doi.org/10.1046/j.1365-2389.1999.00267.x

Mokma, D.L., Yli-Halla, M., Lindqvist, K., 2004. Podzol formation in sandy soils of Finland. Geoderma 120, 259–272. https://doi.org/10.1016/j.geoderma.2003.09.008

Nebbioso, A., Piccolo, A., 2012. Molecular characterization of dissolved organic matter (DOM): a critical review. Anal Bioanal Chem 405, 109–124. https://doi.org/10.1007/s00216-012-6363-2

Opsahl, S., Benner, R., 1998. Photochemical reactivity of dissolved lignin in river and ocean waters. Limnol. Oceanogr. 43, 1297–1304. https://doi.org/10.4319/lo.1998.43.6.1297

Orrego-Ruiz, J.A., Gomez-Escudero, A., Rojas-Ruiz, F.A., 2016. Combination of Negative Electrospray Ionization and Positive Atmospheric Pressure Photoionization Fourier Transform Ion Cyclotron Resonance Mass Spectrometry as a Quantitative Approach of Acid Species in Crude Oils. Energy Fuels 30, 8209–8215. https://doi.org/10.1021/acs.energyfuels.6b01524

Otto, A., Simpson, M.J., 2006. Evaluation of CuO oxidation parameters for determining the source and stage of lignin degradation in soil. Biogeochemistry 80, 121–142. https://doi.org/10.1007/s10533-006-9014-x

Page, S.E., Sander, M., Arnold, W.A., McNeill, K., 2012. Hydroxyl radical formation upon oxidation of reduced humic acids by oxygen in the dark. Environ. Sci. Technol. 46, 1590–1597. https://doi.org/10.1021/es203836f

Paterson, A., Lundquist, K., 1985. Polymer biochemistry: Radical breakdown of lignin. Nature 316, 575–576. https://doi.org/10.1038/316575a0

Petersen, L., 1976. Podzols and podzolization. The Royal Veterinary and Agricultural University, Copenhagen, Denmark.

Piccolo, A., 2001. The supramolecular structure of humic substances. Soil science 166, 810–832.

Pracht, L.E., Tfaily, M.M., Ardissono, R.J., Neumann, R.B., 2018. Molecular characterization of organic matter mobilized from Bangladeshi aquifer sediment: tracking carbon compositional change during microbial utilization. Biogeosciences 15, 1733–1747. https://doi.org/10.5194/bg-15-1733-2018

Purcell, J.M., Juyal, P., Kim, D.-G., Rodgers, R.P., Hendrickson, C.L., Marshall, A.G., 2007. Sulfur speciation in petroleum: Atmospheric pressure photoionization or chemical derivatization and electrospray ionization fourier transform ion cyclotron resonance mass spectrometry. Energy Fuels 21, 2869–2874. https://doi.org/10.1021/ef700210q

Randall, E.W., Mahieu, N., Ivanova, G.I., 1997. NMR studies of soil, soil organic matter and nutrients: spectroscopy and imaging. Geoderma, NMR in Soil Science 80, 307–325. https://doi.org/10.1016/S0016-7061(97)00057-8

Reemtsma, T., These, A., Linscheid, M., Leenheer, J., Spitzy, A., 2008. Molecular and structural characterization of dissolved organic matter from the deep ocean by FTICR-MS, including hydrophilic nitrogenous organic molecules. Environ. Sci. Technol. 42, 1430–1437. https://doi.org/10.1021/es7021413

Remucal, C.K., Cory, R.M., Sander, M., McNeill, K., 2012. Low Molecular Weight Components in an Aquatic Humic Substance As Characterized by Membrane Dialysis and Orbitrap Mass Spectrometry. Environmental Science & Technology 46, 9350–9359. https://doi.org/10.1021/es302468q

Rice, J.A., MacCarthy, P., 1991. Statistical evaluation of the elemental composition of humic substances. Organic Geochemistry 17, 635–648. https://doi.org/10.1016/0146-6380(91)90006-6

Righi, D., Wilbert, J., 1984. Les sols sableux podzolisés des Landes de Gascogne (France) : répartition et caractères principaux. Science du sol 253–264.

Šantl-Temkiv, T., Finster, K., Dittmar, T., Hansen, B.M., Thyrhaug, R., Nielsen, N.W., Karlson, U.G., 2013. Hailstones: A Window into the Microbial and Chemical Inventory of a Storm Cloud. PLOS ONE 8, e53550. https://doi.org/10.1371/journal.pone.0053550

Sauer, D., Sponagel, H., Sommer, M., Giani, L., Jahn, R., Stahr, K., 2007. Review Article Podzol: Soil of the Year 2007 A review on its genesis, occurrence, and functions. J. Plant Nutr. Soil Sci. 170, 581–597. https://doi.org/10.1002/jpln.200700135

Schmitt-Kopplin, P., Harir, M., Tziotis, D., Zelimir, G., Hertkorn, N., 2012. Ultrahigh resolution Fourier transform ion cyclotron (FTICR) mass spectrometry for the analysis of natural organic matter from various environmental systems. In 'Comprehensive Environmental Mass Spectrometry'. ILM Publications, pp. 443–460.

Schulten, H.-R., Gleixner, G., 1999. Analytical pyrolysis of humic substances and dissolved organic matter in aquatic systems: structure and origin. Water Research 33, 2489–2498. https://doi.org/10.1016/S0043-1354(98)00493-X

Schwarzenbach, R.P., Gschwend, P.M., Imboden, D.M., 2002. Environmental Organic Chemistry, 2 edition.ed. Wiley-Interscience, New York.

Sleighter, R.L., Hatcher, P.G., 2008. Molecular characterization of dissolved organic matter (DOM) along a river to ocean transect of the lower Chesapeake Bay by ultrahigh resolution electrospray ionization Fourier transform ion cyclotron resonance mass spectrometry. Mar. Chem. 110, 140–152. https://doi.org/10.1016/j.marchem.2008.04.008

Spencer, R.G.M., Mann, P.J., Dittmar, T., Eglinton, T.I., McIntyre, C., Holmes, R.M., Zimov, N., Stubbins, A., 2015. Detecting the signature of permafrost thaw in Arctic rivers: SIGNATURE OF PERMAFROST THAW IN RIVERS. Geophysical Research Letters 42, 2830–2835. https://doi.org/10.1002/2015GL063498

Spencer, R.G.M., Stubbins, A., Hernes, P.J., Baker, A., Mopper, K., Aufdenkampe, A.K., Dyda, R.Y., Mwamba, V.L., Mangangu, A.M., Wabakanghanzi, J.N., Six, J., 2009. Photochemical degradation of dissolved organic matter and dissolved lignin phenols from the Congo River. Journal of Geophysical Research: Biogeosciences 114. https://doi.org/10.1029/2009JG000968

Steelink, C., 2002. Peer Reviewed: Investigating Humic Acids in Soils. Anal. Chem. 74, 326 A-333 A. https://doi.org/10.1021/ac022040m

Stenson, A.C., Landing, W.M., Marshall, A.G., Cooper, W.T., 2002. Ionization and fragmentation of humic substances in electrospray ionization Fourier transform-ion cyclotron resonance mass spectrometry. Anal. Chem. 74, 4397–4409. https://doi.org/10.1021/ac020019f

Stenson, A.C., Marshall, A.G., Cooper, W.T., 2003. Exact Masses and Chemical Formulas of Individual Suwannee River Fulvic Acids from Ultrahigh Resolution Electrospray Ionization Fourier Transform Ion Cyclotron Resonance Mass Spectra. Anal. Chem. 75, 1275–1284. https://doi.org/10.1021/ac026106p

Stevenson, F.J., 1994. Humus chemistry: genesis, composition, reactions. John Wiley & Sons, New York.

Stubbins, A., Hood, E., Raymond, P.A., Aiken, G.R., Sleighter, R.L., Hernes, P.J., Butman, D., Hatcher, P.G., Striegl, R.G., Schuster, P.F., Abdulla, H.A.N., Vermilyea, A.W., Scott, D.T., Spencer, R.G.M., 2012. Anthropogenic aerosols as a source of ancient dissolved organic matter in glaciers. Nature Geoscience 5, 198201. https://doi.org/10.1038/ngeo1403

Stubbins, A., Spencer, R.G.M., Chen, H., Hatcher, P.G., Mopper, K., Hernes, P.J., Mwamba, V.L., Mangangu, A.M., Wabakanghanzi, J.N., Six, J., 2010. Illuminated darkness: Molecular signatures of Congo River dissolved organic matter and its photochemical alteration as revealed by ultrahigh precision mass spectrometry. Limnology and Oceanography 55, 1467–1477. https://doi.org/10.4319/lo.2010.55.4.1467

Stubbins, A., Spencer, R.G.M., Mann, P.J., Holmes, R.M., McClelland, J.W., Niggemann, J., Dittmar, T., 2015. Utilizing colored dissolved organic matter to derive dissolved black carbon export by arctic rivers. Front. Earth Sci. 3. https://doi.org/10.3389/feart.2015.00063

Tfaily, M.M., Chu, R.K., Tolić, N., Roscioli, K.M., Anderton, C.R., Paša-Tolić, L., Robinson, E.W., Hess, N.J., 2015. Advanced solvent based methods for molecular characterization of soil organic matter by high-resolution mass spectrometry. Anal. Chem. 87, 5206–5215. https://doi.org/10.1021/acs.analchem.5b00116

Thevenot, M., Dignac, M.-F., Rumpel, C., 2010. Fate of lignins in soils: A review. Soil Biology and Biochemistry 42, 1200–1211. https://doi.org/10.1016/j.soilbio.2010.03.017

Thomas, J.D., 1997. The role of dissolved organic matter, particularly free amino acids and humic substances, in freshwater ecosystems. Freshwater Biology 38, 1–36. https://doi.org/10.1046/j.1365-2427.1997.00206.x

Thoss, V., Shevtsova, A., Nilsson, M.C., 2004. Environmental manipulation treatment effects on the reactivity of water-soluble phenolics in a subalpine tundra ecosystem. Plant Soil 259, 355–365. https://doi.org/10.1023/B:PLSO.0000020984.17403.82

Trusiak, A., Treibergs, L.A., Kling, G.W., Cory, R.M., 2018. The role of iron and reactive oxygen species in the production of CO2 in arctic soil waters. Geochimica et Cosmochimica Acta 224, 80–95. https://doi.org/10.1016/j.gca.2017.12.022

Van Krevelen, D.W., 1961. Graphical-statistical method for the study of structure and reaction processes of coal. Fuel 29, 269–283.

Vermilyea, A.W., Voelker, B.M., 2009. Photo-Fenton Reaction at Near Neutral pH. Environ. Sci. Technol. 43, 6927–6933. https://doi.org/10.1021/es900721x

Waggoner, D.C., Chen, H., Willoughby, A.S., Hatcher, P.G., 2015. Formation of black carbon-like and alicyclic aliphatic compounds by hydroxyl radical initiated degradation of lignin. Org. Geochem. 82, 69–76. https://doi.org/10.1016/j.orggeochem.2015.02.007

Waggoner, D.C., Wozniak, A.S., Cory, R.M., Hatcher, P.G., 2017. The role of reactive oxygen species in the degradation of lignin derived dissolved organic matter. Geochim. Cosmochim. Acta 208, 171–184. https://doi.org/10.1016/j.gca.2017.03.036

Wagner, S., Cawley, K.M., Rosario-Ortiz, F.L., Jaffé, R., 2015. In-stream sources and links between particulate and dissolved black carbon following a wildfire. Biogeochemistry 124, 145–161. https://doi.org/10.1007/s10533-015-0088-1

Walters, C.C., 2006. The Origin of Petroleum. In 'Practical Advances in Petroleum Processing' (Eds. Hsu, C.S., Robinson, P.R.). Springer New York, New York, NY, pp. 79–101. https://doi.org/10.1007/978-0-387-25789-1_2

Witt, M., Fuchser, J., Koch, B.P., 2009. Fragmentation Studies of Fulvic Acids Using Collision Induced Dissociation Fourier Transform Ion Cyclotron Resonance Mass Spectrometry. Anal. Chem. 81, 2688–2694. https://doi.org/10.1021/ac802624s

Wozniak, A.S., Bauer, J.E., Sleighter, R.L., Dickhut, R.M., Hatcher, P.G., 2008. Technical Note: Molecular characterization of aerosol-derived water soluble organic carbon using ultrahigh resolution electrospray ionization Fourier transform ion cyclotron resonance mass spectrometry. Atmospheric Chemistry and Physics 8, 5099–5111. https://doi.org/10.5194/acp-8-5099-2008

Wright, J., Schnitzer, M., 1959. Oxygen-Containing Functional Groups in the Organic Matter of a Podzol Soil. Nature 184, 1462–1462. https://doi.org/10.1038/1841462a0

Wu, Z., Rodgers, R.P., Marshall, A.G., 2004. Two- and three-dimensional van krevelen diagrams: a graphical analysis complementary to the kendrick mass plot for sorting elemental compositions of complex organic mixtures based on ultrahigh-resolution broadband fourier transform ion cyclotron resonance mass measurements. Anal. Chem. 76, 2511–2516. https://doi.org/10.1021/ac0355449

Yuan, Z., He, C., Shi, Q., Xu, C., Li, Z., Wang, C., Zhao, H., Ni, J., 2017. Molecular Insights into the Transformation of Dissolved Organic Matter in Landfill Leachate Concentrate during Biodegradation and Coagulation Processes Using ESI FT-ICR MS. Environ. Sci. Technol. 51, 8110–8118. https://doi.org/10.1021/acs.est.7b02194

Zhao, Y., Hallar, A.G., Mazzoleni, L.R., 2013. Atmospheric organic matter in clouds: exact masses and molecular formula identification using ultrahigh-resolution FT-ICR mass spectrometry. Atmos. Chem. Phys. 13, 12343–12362. https://doi.org/10.5194/acp-13-12343-2013

Ziolkowski, L.A., Druffel, E.R.M., 2010. Aged black carbon identified in marine dissolved organic carbon. Geophysical Research Letters 37. https://doi.org/10.1029/2010GL043963

4) "DYNAMICS OF URANIUM MOBILIZATION FROM SOIL BY NATURAL HUMIC COLLOIDS"

RESUME

A la suite du précédent chapitre, qui considère la variabilité de la composition et des propriétés de la MO au sein du sol podzolisé des Landes de Gascogne, nous avons voulu étudier l'impact de cette variabilité sur l'association entre entités colloïdales et uranium, à l'échelle d'un horizon du sol (horizon superficiel), et évaluer le conséquences de cette association sur la mobilisation de l'uranium depuis les matériaux du sol vers le milieu aqueux.

Dans cette partie, la mobilisation de l'uranium à partir du sol sableux dans les conditions acides du podzol (pH 4) est objet de nos investigations. Cette mobilisation a été étudiée à partir de lixiviations réalisées en réacteur fermé (batch). Ces travaux visaient à caractériser la dynamique de la mobilisation de l'uranium du sol vers la phase aqueuse, afin d'en évaluer les conséquences environnementales. Pour cela, les lixiviations ont été étudiées pour des durées variant de 5 minutes à 29 heures. Les caractérisations des cinétiques de lixiviation de l'uranium, de l'association de l'uranium avec des entités colloïdales du sol, et des propriétés physicochimiques des colloïdes ont été réalisées à l'aide d'une approche multi-technique, notamment via l'utilisation complémentaire du fractionnement par couplage flux-force asymétrique (A4F) avec la spectrométrie de masse à plasma à couplage inductif (ICPMS), la diffusion de la lumière multi-angles (MALS) ainsi qu'avec les spectroscopies de fluorescence et d'absorption UV.

Moins de 0,1% de la masse initiale d'uranium contenue dans le sol a été libérée après 5 heures de lixiviation. Cette fraction atteint 2% après 29 heures de lixiviation. La mobilisation de l'uranium résultant du lessivage du sol s'avère ainsi être assez rapide mais limitée. Ceci confirme la faible réversibilité de l'adsorption de l'uranium à la surface des matériaux du sol. La concentration maximale en uranium dans le lixiviat, estimée à partir d'un modèle cinétique, est proche de 2 $\mu g.L^{-1}$. Le comportement de l'uranium au cours de la lixiviation du sol est fortement influencé par la répartition des ligands organiques entre les phases solide et liquide. L'uranium lixivié se trouve être principalement distribué dans la fraction dissoute (≈73%). Dans la fraction colloïdale, l'uranium est associé à des entités colloïdales dont les tailles correspondent à des rayons de giration allant d'environ 20 à 170 nm et possédant une aromaticité significative. Ceci suggère que la migration de l'uranium dans le sous-sol est principalement contrôlée par la lixiviation d'entités colloïdales de petite taille contenant des substances fulviques et humiques de faibles masses moléculaires. Ces entités colloïdales sont lessivées en permanence. Cependant, elles s'avèrent susceptibles de changer de nature et de taille au cours du temps de lixiviation, en fonction de la mobilisation de composés de masses moléculaires plus élevées lorsque le temps de lessivage augmente, et/ou d'une agglomération des composés de petite taille dans le lixiviat.

Les dynamiques de mobilisation du carbone organique, du Fe et de Al colloïdaux depuis le sol semble suivre le même schéma de dynamique de mobilisation, car les ordres des cinétiques de mobilisation pour U, Fe et

Al dans les fractions totales et dissoutes sont globalement similaires. Les vitesses de mobilisation apparentes relatives depuis le sol sont les suivantes: U> Fe> Al. La mobilisation du carbone organique total (COT) total et colloïdal depuis le sol vers les fractions lors de la lixiviation présente un comportement différent des autres espèces suivies. Cela suggère qu'un mécanisme unique ne pourrait pas expliquer la mobilisation globale de l'U, du carbone organique, de l'Al et du Fe provenant du sol, car différents comportements peuvent être observés entre les fractions dissoutes et colloïdales. La modélisation cinétique indique que des processus de sorption réversibles contrôlent principalement le taux de mobilisation de l'U du sol, plutôt qu'un transport non réactif de l'uranium à partir des gisements initiaux.

D'un point de vue environnemental, la lixiviation en continue de l'uranium adsorbé sur les matériaux du sol sous-jacents aux dépôts initiaux peut constituer une source de pollution secondaire. Le lessivage des sols par infiltration des précipitations devrait devenir le principal contributeur aux concentrations d'uranium observées dans les eaux souterraines et les eaux de surface en aval de la zone de dépôt.

4.1 INTRODUCTION

Uranium is a natural trace element present in the environment and can be introduced by human activities, including agriculture, uranium mining, nuclear industry or military applications (Ragnarsdottir and Charlet, 2000; Ribera et al., 1996). High-density uranium alloys are used in ammunition and weapon fabrication (Hamilton, 2001; Handley-Sidhu et al., 2010). These activities have left a legacy of uranium waste in terrestrial environments, so uranium concentration in soils above levels classically found in subsurface environment can be observed in former battlefields (Hamilton, 2001; Sansone et al., 2001b; UNEP, 2001) or weapons testing sites (Oliver et al., 2007).

Corrosion of fragmented solid uranium phases following rainfall leaching in oxic or suboxic subsurface environments produces highly soluble U(VI) compounds (Cachoir et al., 1996; McBride and Spiers, 2001; McEachern and Taylor, 1998), which are available for migration through soil toward the surface of the shallow aquifer (Handley-Sidhu et al., 2010; Ragnarsdottir and Charlet, 2000; Schimmack et al., 2007). In sandy and moderately organic soils, solid uranium phases undergo a continuous kinetically-controlled oxidative dissolution, with dissolution rates close ranging from roughly 0.1 to 2 g cm^{-2} yr^{-1} (Lind et al., 2009; Schimmack et al., 2007; Toque et al., 2014), and apparent solubility estimated about 2 - 20 mg L^{-1} (De Windt et al., 2003; Handley-Sidhu et al., 2009). Key factors influencing the mobility, dispersal, bioavailability and environmental fate of uranium are its speciation and its partitioning amongst the various components of soil (Choppin, 2006; Di Lella et al., 2005; Ragnarsdottir and Charlet, 2000; Ribera et al., 1996). Complexation with oxyanions can significantly influence speciation of both U(IV) and U(VI) (Grenthe et al., 1992; Guillaumont et al., 2003; Maher et al., 2013; Moulin and Moulin, 2001), and controls the availability of uranium for sorption reactions (Choppin, 2006; Maher et al., 2013; Ragnarsdottir and Charlet, 2000). Under stable chemical conditions, and for pH between roughly 5 and 8, soluble U(VI) species are strongly immobilized in subsurface materials by sorption or coprecipitation mechanisms (Abdelouas et al., 1998; Brown et al., 1998; Camus et al., 1999; Del Nero et al., 1999; Dhoum and Evans, 1997; Gabriel et al., 1998; Maher et al., 2013; Welch and Lico, 1998). This immobilization appears not definitive, since sorption reactions are partially reversible (Braithwaite et al., 1997; Crançon et al., 2010; Gabriel et al., 1998; Ho and Miller, 1985a; Ho and Miller, 1985b; Zheng and Wan, 2005).

The high stability of U(VI)–humate complexes dominates uranium speciation in natural waters (Choppin, 2006; Crançon and van der Lee, 2003; Lenhart et al., 2000; Moulin and Moulin, 1995; Zeh et al., 1997). Thus, humic substances influence greatly the fate of uranium in subsurface environment (Maher et al., 2013; Moulin and Moulin, 1995; Moulin and Moulin, 2001; Ragnarsdottir and Charlet, 2000; Reiller, 2010; Reiller and Buckau, 2012). The pH range of U(VI) adsorption onto mineral surfaces in organic soils is then shifted towards lower pH values (pH < 5) (Benes et al., 1998; Labonne-Wall et al., 1997; Lenhart and Honeyman, 1999; Murphy et al., 1992; Murphy et al., 1999). In acidic soil such as in podzols, humic aggregates are

responsible for strong immobilization of uranium in soil (Crançon et al., 2010; Crançon and van der Lee, 2003; Wei et al., 2007). A reduced mobility of uranium in soils and groundwater is mainly observed when the system is at thermodynamic equilibrium, or under steady-state flow (Barnett et al., 2000). Association of uranium with large Fe/Al/organic colloids with low mobility was also considered to be a precursor to the removal of U from soil porewater to the solid phase (Graham et al., 2011). The stability of soil aggregates is however highly sensitive to soil moisture, and velocity and chemistry of the water phase (Kaiser and Zech, 1999; Kretzschmar and Sticher, 1997; Murphy et al., 1994; Reemtsma et al., 1999). As a result, perturbations of soil water hydrodynamics and chemistry caused by successive rainfall events may lead to either an increase in colloids retention or a remobilization of water-dispersible colloids in the mobile phase (Bottcher et al., 1997; Marshall et al., 2000; McDowell-Boyer, 1992; Seta and Karathanasis, 1997; Sinke et al., 1998).

On the other hand, soluble and colloidal humic substances compete as strong ligands with adsorption sites for the coordination of U(VI) (Artinger et al., 2002; Benes et al., 1998; Crançon and van der Lee, 2003; Guillaumont et al., 2003; Ho and Miller, 1985b; Lenhart and Honeyman, 1999; Moulin and Moulin, 1995; Murphy et al., 1992; Zeh et al., 1997) and U(IV) (Wang et al., 2013). Uranium migration is enhanced due to colloidal transport may be responsible for a potential long-range migration of uranium in the subsurface (Artinger et al. 2002; Buckau et al. 2000; Crançon et al. 2010; David L. Finnegan and Joseph L. Thompson 2001; Franke et al. 2000; Graham et al. 2008; Kersting et al. 1999b; Mibus et al. 2007; Montavon et al. 2000; Ragnarsdottir and Charlet 2000; Zeh et al. 1997). A significant proportion of uranium in surface water (Andersson et al., 2001) or groundwater (Franke et al., 2000; Zeh et al., 1997) is transported as suspended nano-objects such as colloidal particles or macromolecular assemblies (Hargindeguy et al., 2018; Ragnarsdottir and Charlet, 2000). Colloids are found to be associated with uranium (Claveranne-Lamolere et al., 2011; Crançon et al., 2010; Graham et al., 2008; Lesher et al., 2013), and are involved in the vertical migration of U(VI) through the soil followed by lateral transport in groundwater (Crançon et al., 2010; Hargindeguy et al., 2018; Harguindeguy et al., 2014). Extremely varied values of the percent of uranium mobilized by colloidal entities are reported in literature, from <1% to almost 100% (Bednar et al., 2007; Ranville et al., 2007), while colloidal uranium accounted for 10 to 30% of uranium in surface water (Harguindeguy et al., 2014) and 70 to 90% in groundwater (Crançon et al., 2010). This can be attributed to the nature of colloids involved, and the wild variability of their structure, reactivity and physicochemical properties in natural environments (Reiller, 2015).

The role of nano-objects in uranium migration is thus site-specific. Soils are often strongly differentiated in a multiple-layers scheme such as in podzols. Hence, various combinations of nanomineral phases, colloidal organic compounds and inorganic colloidal particles, such as clays or Al and Fe colloidal oxyhydroxydes, can be present in the aqueous phase after their release from native minerals following complexolysis and eluviation processes (Giesler et al., 2000; Lundström, 1993; Lundström et al., 2000b; Riise et al., 2000).

Thus, the partitioning of uranium amongst these different phases shall be fully characterized to be understood. From a macroscopic point of view, this partitioning has been widely studied in soils (Barnett et al., 2000; Del Nero et al., 1999; Echevarria et al., 2001; Radenkovic et al., 2008; Roh et al., 2000; Waite et al., 2000), notably by common approaches using selective or sequential extractions, where soils are subjected to a range of chemical extractants in order to solubilize any pollutant of interest from increasingly resistant soil fractions. Common sequential extraction procedures are based on the Tessier diagram (Tessier et al., 1979), or from NIST (Schultz et al., 1998) or Community Bureau of Reference (BCR) (Ure et al., 1993) schemes.

Lesser attention was paid to the partitioning amongst nanoscopic colloidal fractions. Colloidal phases can exhibit various compositions and dimensionalities. The size distribution and continuum, shape, and chemical composition of colloidal nano-objects, as well as their polydispersity and supramolecular structure, must be taken into consideration, since their mobility depends on them (Faucher et al., 2018; Fillela, 2007; Piccolo, 2001; Reiller, 2015; Reiller et al., 2006; Small, 1974). Fractionation and characterization of colloid properties can be conducted by integrated approaches using for example capillary electrophoresis (Claveranne-Lamolere et al., 2011; d'Orlyé and Reiller, 2011; Dabek-Zlotorzynska et al., 1998; Fetsch and Havel, 1998), or sequential approaches using ultrafiltration (Buffle et al., 1992; d'Orlyé and Reiller, 2011; Graham et al., 2011; Zeh et al., 1997). A methodology was designed to provide consistent information on the origin and nature of colloids by determining the variations and distributions in size, shape, carbon content, and elemental chemical composition of colloidal particles carrying uranium (Gigault et al., 2012; Hargindeguy et al., 2018). This methodology was defined such that multidimensional information could be obtained in the size continuum of colloids, in order to minimize the bias inherent to filtrations methods (Lead and Wilkinson, 2006; Riise et al., 1994). Due to its high resolution and its capability to fractionate in the size range of interest with a minimum of interaction with the analytical system, asymmetric flow field-flow fractionation (AF4) has proven to be an ideal technique for the separation and characterization of natural colloids (Dubascoux et al., 2008; El Hadri et al., 2014; Faucher et al., 2018; Lespes et al., 2015). The detectors of choice to be coupled to the AF4, with respect to the objective of determining uranium distribution amongst the colloidal phases, are (i) multi-angle laser light scattering (MALS) to obtain size and shape information, (ii) ultraviolet-visible spectrometry (UV) to provide indications on organic carbon content, and (iii) atomic mass spectrometry (ICPMS) to monitor the trace elements of interest (Hargindeguy et al., 2018). Considering these characterization methods, uranium is shown to be mobilized in soil porewater essentially in truly dissolved fraction, or in association with mobile small and medium organic colloidal entities (3 kDa – 200 nm) (Graham et al., 2008; Graham et al., 2011; Hargindeguy et al., 2018). In contrast, uranium association with larger Al/Fe/organic colloids is likely to favors the immobilization of uranium in soil materials (Graham et al., 2011).

The fate of uranium in soil and subsurface environment is consequently driven by a delicate balance of uranium association between immobile and mobile phases. Thus, the migration of uranium in any polluted

site's environment can be mainly controlled by the mobilization of sorbed uranium from soil, rather than from the dissolution of initial uranium in primary deposits. Consequently, the dynamic of uranium mobilization from soil shall be considered in any environmental assessment as a secondary, but primordial, source of pollution. The present paper investigates the mobilization of uranium from a sandy podzol, a strongly differentiated soils occurring in cool humid climates, under acidic pH conditions. The main mechanism of podzolization involves the dissolution of native mineral from parent material, the mobilization of colloidal organic acids from the upper horizons (organic (O) and eluvial (E)), and their immobilization in deeper illuvial horizon (B(h/s)) (Lundström et al., 2000a; Riise et al., 1994). Transport of Al and Fe through the soil profile as organic complexes has, therefore been generally accepted as the dominant mechanism of eluviation (Lundström et al., 2000a). Because of this particular role of colloidal ligands in podzolization process, assessment of uranium migration in this particular subsurface context needs a careful characterization of the different colloidal phases involved, and the extent of the uranium association with these colloidal phases.

As an operational proof of concept, this methodology was used for a site application. Field observations and laboratory experiments as shown evidences for both a strong retention of uranium in the podzolic soil, and an enhanced migration of uranium in association with humic colloids in deep soil horizons and groundwater, after several years of surface pollution by dispersed uranium deposits (Crançon et al., 2010; Crançon and van der Lee, 2003; Hargindeguy et al., 2018). Uranium is both of natural and anthropogenic origin, making this site ideal for understanding uranium migration processes (Crançon et al., 2010; Crançon and van der Lee, 2003; Hargindeguy et al., 2018; Harguindeguy et al., 2014).

The environmental expectations of this work were to acquire knowledge about the dynamics of uranium mobilization from soil, then in the aquatic environment. The investigation approach was based on the characterization of uranium lixiviation kinetics and uranium association with soil colloids, together with the characterization of the physicochemical properties of leached colloids by a multi-technique approach as described above.

4.2 MATERIALS AND METHODS

4.2.1 Field context and characterization

The site that was studied is located in the wetlands of Landes Gascony (France), and is described in detail in previous works, as well as the location of soil and water samples (Crançon et al., 2010; Crançon and van der Lee, 2003; Hargindeguy et al., 2018; Harguindeguy et al., 2014). Briefly, pyrotechnic experiments in the context of military activities using depleted uranium have led to deposits of metal fragments on the surface of a podzolic soil with low microbial activity, situated on poorly mineralized Pleistocene to Holocene fluvio-

eolian sands. These deposits were then continuously exposed to weathering and undergo a continuous kinetically-controlled oxidative dissolution.

The studied soil area overlies a surficial, shallow and anoxic sandy aquifer, leading to typical to hydromorphic podzols with a high acidity (pH ~ 4.0) and typical redox potentials E_H ranging from 50 to 350 mV. The vertical migration of labile organometallic complexes leads to a marked differentiation of the soil's profile into three main horizons. The main chemical and mineralogical properties of the soil and aquifer, as well as the location of soil and groundwater samples, together with analysis methodologies, can be found elsewhere (Crançon et al., 2010; Crançon and van der Lee, 2003; Hargindeguy et al., 2018; Harguindeguy et al., 2014).

4.2.2 Leaching experiments

The leaching method designed for the monitoring of uranium and colloids mobilization from soil with time consists in a static batch experiment, in which the leaching conditions are controlled. Leaching experiments were conducted by mixing with a rotary shaker of the initial soil from eluvial horizon (E), dried and sieved at 2 mm, and de-ionized water (18.2 $M\Omega.cm^{-1}$) from a Milli-Q Elix 3 system (Millipore System, Bedford, MA, USA), with a liquid/solid mass ratio set to 5 (adapted from (Claveranne-Lamolere et al., 2011)). Leaching was carried out with different contact durations distributed regularly on a log scale (5 min, 15 min, 45 min, 300 min (5h) and 1740 min (29h), referred as leaching time thereafter). After these periods, mixtures were kept at 4.0±0.5°C and sheltered from the light for 48 hours after in order to settle the largest suspended particles down. The supernatants were then recovered and filtered preliminarily at 0.45 µm using regenerated cellulose filters (Millipore, Bedford, MA, USA), since 80% of the uranium was previously found in finer fractions (Harguindeguy et al. 2014). Then separation of colloidal (> 10 kDa) and dissolved (< 10 kDa) fractions from bulk total leachate is conducted using centrifugal ultrafiltration with 10 kDa cutoff (Centricons®). All experiments were triplicated.

4.2.3 Leaching kinetics

To study the effect of the kinetic behavior of the uranium mobilization process, the temporal evolution of uranium (and other elements) concentration in leachate during soil lixiviation was examined. Leaching kinetics models were fitted using the experimental data.

Zero-order model

Chemical reactions where reaction velocity is independent of reactants concentrations can follow zero-order kinetics (or pseudo-zero-order when considering initial step of reactions). Equation given below (Pogliani, 2008) is adapted for leaching experiments:

$$[\boldsymbol{c}(t)] = [\boldsymbol{c}_0] + \boldsymbol{k_z t} \qquad \textit{Eq. 1}$$

Where [c(t)] is the evolution of element or compound of interest concentration in the leachate,

[c_0] is the initial element concentration in the lixiviation solution,

k_z is the zero-order apparent reaction rate (mg L^{-1} hr^{-1}), and *t* (hr) is the time.

Pseudo-first-order: Lagergren model

A pseudo-first-order kinetic equation for leaching reaction was previously adapted from the modeling of sorption reaction (Lagergren and Svenska, 1898; Srivastava et al., 2009). It is given as follows in a modified form compared to the original model:

$$\frac{d\,c(t)}{d\,t} = k_{lag} \times \left(c_{max} - c(t)\right) \qquad \textit{Eq. 2}$$

Where c_{max}, and *c(t)* (mg L^{-1}) are the concentration of element at steady-state and at time *t* (hr) respectively, $k_{lag.}$ (hr^{-1}) is the apparent pseudo-first order rate constant, and *t* (hr) is the time.

In this context, a pseudo-first order Lagergren model should assume that the rate of element leaching with time is directly proportional to the difference between the maximum concentration in leachate at steady-state, and the concentration of element leached at a given time t, $\left(c_{max} - c(t)\right)$. The solution for the differential equation (Eq.2) leads to this linear form:

$$\ln\left(c_{max} - c(t)\right) = \ln(c_{max}) - k_{lag} \times t \qquad \textit{Eq. 3}$$

The values of the apparent pseudo-first-order rate constant (k_{lag}) for element leaching from soil, and theoretical maximum concentration in solution ($c_{max,cal}$) were determined from the plot of $\ln\left(c_{max} - c(t)\right)$ vs *t*.

Pseudo-second-order: Blanchard model

On the same way, a pseudo-second-order leaching kinetic can be adapted from sorption reactions modeling, and is given as follows in a modified form compared to the original model (Blanchard et al., 1984; Ho, 2006):

$$\frac{\mathrm{d}\,c(t)}{\mathrm{d}\,t} = k_{bla} \times \left(c_{max} - c(t)\right)^2 \qquad \textit{Eq. 4}$$

Where c_{max}, and *c(t)* (mg L^{-1}) are the concentration of element at steady-state and at time *t* (hr) respectively, k_{bla} (L mg^{-1} hr^{-1}) is the apparent pseudo-second-order rate constant, and *t* (min) is the time.

In this context, a pseudo-second order model should assume that the element leaching is a pseudo-chemical reaction process: the driving force is the difference between the maximum concentration of element in solution at steady-state, and the concentration of element lixiviated at any time, $\left(c_{max} - c(t)\right)$, and the overall leaching rate is proportional to the square of the driving force.

Integrating Eq.4 considering *c(t=0)=0*, the following linear equation is obtained:

$$\frac{t}{c(t)} = \frac{1}{k_{bla} \times {c_{max}}^2} + \frac{t}{c_{max}} \qquad \textit{Eq. 5}$$

The values of the apparent pseudo-second-order rate constant (k_{bla}) for element leaching from soil and theoretical steady-state concentration in solution ($c_{max,cal}$) were determined from the plot of $\frac{t}{c(t)}$ vs t.

4.2.4 Chemical analysis

Atomic Mass Spectrometry

Elemental concentrations of Al, Fe and U were determined in bulk leachate sample, as well as in colloidal and dissolved fractions, by atomic mass spectrometry (ICP-MS). An Agilent 7900ce model (Agilent Technology, Tokyo, Japan) equipped with a concentric nebulizer (MicroMist), an ultra-high matrix introduction (UHMI) spray chamber model cooled to 2°C and a Collision Reaction Cell (CRC) in hydrogen mode (operating conditions in Table 4.2-1) was used. Prior to the analyses, a 5% nitric acid solution containing two internal standards (Yttrium and Bismuth) was added to compensate any instrumental sensitivity variation. The acidified samples were then introduced into the ICP mass spectrometer. A range of separate standards of known concentrations of Al, Fe and U were used for external calibration. ^{27}Al, ^{57}Fe and ^{238}U were the isotopes monitored. Detection limits (DL) were 0.012, 0.24 and 0.26 µg L^{-1} for U, Fe and Al respectively. Quantification limits (QL) were 0.036, 0.76 and 0.78 µg L^{-1} for U, Fe and Al respectively.

Table 4.2-1. ICP-MS Operating conditions

Nebulizer	MicroMist
Sampler and skimmer cones	Ni
Carrier gas flow rate	0.90 L min^{-1}
Makeup/Dilution gas flow rate	0.20 L min^{-1}
Collision cell gas flow rate (H_2)	6 mL min^{-1}
Dwell time	0.1 s
Isotopes	^{27}Al, ^{57}Fe, ^{238}U
Tuning solutions	1 µg L^{-1} Li, Y, Tl , Ce in 2wt% HNO3

Total Organic Carbon (TOC)

Total organic carbon content was measured using a Shimadzu TOC-V CSN analyzer which was calibrated with solutions of sodium hydrogen carbonate and potassium hydrogen phthalate for the inorganic and total carbon measurements respectively (Nacalai Tesque, Kyoto, Japan). The organic carbon was calculated as the difference between total and inorganic carbon measures. Detection and quantification limits were 0.04 and 0.12µg (TOC) respectively.

4.2.5 Characterization of the colloidal phases

X-ray diffraction

X-ray diffraction was conducted on separated unfiltered and dried colloidal suspension from soil leaching using a Bruker - D8 Advance A25 diffractometer, with a Cu-kα X-ray source (λ_{em} = 1.54 Å) (Bruker Co., USA).

Microscopic characterization

The microscopic structure and composition of the colloidal fraction of soil leachates was determined by both scanning electron microscopy (SEM) and transmission electron microscopy (TEM).

SEM analyses were conducted using a Hirox SH-5000M device (Hirox Co., Japan) equipped with a Bruker Quantax energy dispersive X-ray spectroscopic analyzer (EDS) (Bruker Co., USA). X-EDS elemental quantification was realized by considering either PbZAF or PhiRhoZ methods. Observations were carried out on both soil sample and colloidal suspension from leaching experiment. In the latter case, a drop of the soil colloids suspension was deposited onto a TEM copper grid then dried at room temperature.

TEM analyses were conducted using a Tecnai G2 Spirit TWIN device (FEI, ThermoFisher). The samples were prepared as described by Baalousha et al. (Baalousha et al., 2005) : a drop of the soil solution was deposited onto a TEM grid covered by a copper membrane and after drying on filter paper, the grids were rinsed with milliQ water. Potential changes in size and/or shape of the colloidal species generated throughout the leaching process could be determined as well as their amount identified by TEM analysis. The leaching times considered were chosen so that both short and long leaching durations were characterized (15 minutes and 29 hours respectively).

Asymmetric Flow-Field Flow Fractionation

Separation of colloidal entities was conducted using Asymmetric Flow-Field Flow Fractionation (A4F) system “Eclipse2” (Wyatt Technology, Dernbach, Germany). A general presentation of this device can be found elsewhere (Hargindeguy et al., 2018). Flows were controlled using an Agilent 1100 series isocratic pump equipped with a micro vacuum degasser. Injections were made using an autosampler (Agilent Technologies 1100 series). Details of A4F operating conditions are given in Table 4.2-2.

The mobile phase for AF4 analyses was prepared by dissolving ammonium nitrate (NH_4NO_3, 99.5%) in de-ionized water. Polystyrene nanospheres (PS) ranging from 20 to 400 nm in hydrodynamic diameter (9–155 nm in gyration radius) from Duke Scientific Corp (Microgenics Corporation, Fremont, CA, USA) were used as standard spheres in the size calibration process.

Table 4.2-2. A4F Operating conditions

Channel	26.5 cm long and 0.6 to 2.1 cm wide
Spacer	350µm
Membrane	Polyethersulfonate (PES) 10 kDa
Mobile Phase	NH_4NO_3 10^{-5} mol.L^{-1}
Focus flow rate	2 mL min^{-1}
Elution rate	0.7 mL min^{-1}
Cross flow rate	2 mL min^{-1}
Injection flow rate	0.2 mL min^{-1}

Multi-angle light scattering and gyration radius determination

A multi-angle light scattering (MALS) detector (DAWN DSP-F, Wyatt Technology, Santa Barbara, USA) was also associated to the AF4 system to evaluate the colloidal size, expressed as the gyration radius (r_G). Because MALS is sensitive to both size and concentration of colloids, differences in MALS signals (typically in the peak intensity) in two different fractionated samples with similar gyration radii can be attributed to differences in concentration, as explained elsewhere (Gigault et al., 2012). MALS signals were later used with this approach. Data from MALS detector were collected and analyzed using Astra 6.1.1.17 software (Wyatt technology). Changes in radius of gyration over leaching time were filtered and processed as indicated by Harguindeguy et al. (2018).

Ultra-violet organic carbon monitoring

A variable wavelength UV-Diode Array Detector (UV-DAD, Agilent Technology, 1260 series from Agilent, Tokyo, Japan) was coupled to the AF4 channel for online detection of organic carbon. Data from UV detector were collected and analyzed using Astra 6.1.1.17 software (Wyatt technology). UV detector is mainly sensitive, with possible various responses, to the different chromophore functional groups of the organic matter present in the samples. Additionally, it can also respond to inorganic particles because it is sensitive to the turbidity of the sample; however, this response is expected to be much less important than that corresponding to the presence of chromophore organic groups (Lewis and Sjöstrom, 2010).

Functional analysis: UV-Vis and Fluorescence Spectroscopy

Functional analyses are largely applied in the characterization of the dissolved organic matter. They enable the typical functional groups of the DOM to be identified as indications of its nature. Fluorescence 3-dimensional spectra were obtained using a spectrofluorometer FL920 (Edinburgh Instruments, UK) with a high-pressure Xenon lamp 450W as excitation source and a double monochromator in emission and excitation with a 0.05 nm resolution. The detection was done with a sensitive photomultiplier in the red

cooled by Peltier effect. The acquisition was performed by counting the photons arriving on the emission photomultiplier, with a dark current of about 15 shots. The soil colloids suspension was analyzed with the following parameters: excitation wavelength range of 300-500 nm with step of 10 nm, emission wavelength range of 400-650 nm with step of 0.5 nm, and a dwell time of 0.2s.

A UV-Vis spectrophotometer (Libra S12, Biochrom Libra Instruments) with a 1 cm optical path-length quartz cell was used for the acquisition of absorbance spectrum for each leaching duration. A blank measure was carried out prior any sample analysis and was automatically subtracted to the sample measures. For each sample, optical parameters were determined as follows:

- Specific UV Absorbance (SUVA) at the specific wavelength 254 and 280 nm. It was calculated as the absorption at the fixed wavelengths (254 and 280 nm) normalized by the TOC concentration corresponding to each leaching time (Eq 6). This value is a relevant indicator of the aromaticity of the dissolved organic matter. As reported by Swietlik and Silorska (2006), $SUVA_{254}$ values lower than 3 $L.mgC^{-1}.m^{-1}$ are typical of water with hydrophilic and low molecular-weight organic matter whereas values above 4 $L.mgC^{-1}.m^{-1}$ are typically found for waters with high hydrophobic, aromatic and high molecular-weight organic matter.

$$SUVA_{254} = \frac{a254}{[TOC]} \qquad \textit{Eq. 6}$$

With a254 the absorption at 254 nm (in cm^{-1}) and [TOC] the total organic carbon concentration (in $mg.L^{-1}$)

- E2/E3 ratio corresponding to the ratio of absorptions at 250nm and 365nm indicates changes in the relative size of dissolved organic matter (DOM) molecules. A decreasing E2/E3 ratio stands for an increase in the DOM molecular size, due to the stronger light absorption by high molecular weight DOM at longer wavelengths (Helms et al. 2008).

4.3 RESULTS AND DISCUSSION

4.3.1 Field and laboratory preliminary observations

Soil interstitial water from E horizon is acidic and strongly buffered (mean pH = 4.0 ±0.2) and contains about 0.6 wt% of organic matter and 1 wt% of clay materials. Its uranium total concentration in the geochemical background is lower than 1 mg kg^{-1} in most of the horizons, except Bh accumulation horizon where uranium concentration ranges from 1.6 to 4.1 mg kg^{-1} due to the presence of amorphous Fe-hydroxides (Crançon et al., 2010; Harguindeguy et al., 2014). The extent of the subsurface anthropogenic uranium deposit is spatially limited. In the soils from the deposition area, the bulk total U concentration is susceptible to local variation because of the nugget effect related to the scattering of fragments, whom diameter ranges from 0.5 mm to

more than 5 cm. Uranium is mainly found lying in the top 20 cm of soil (E horizon), with typical uranium concentration in soil material in deposits area locally ranging from 10 up to 10^5 mg kg^{-1}. Soil uranium content decreases sharply with depth by more than five orders of magnitude in less than one meter deep. Up to 95 mass % of dissolved uranium infiltrated with incoming meteoric water may adsorb onto soil materials, with more than 60 mass % in the first centimeters of soil (Crançon et al., 2010). These observations were confirmed in laboratory by experimental sorption isotherms, retention coefficient values determination (*Kd*) and mass balance calculations (Crançon et al., 2010; Crançon and van der Lee, 2003). *Kd* values for uranium in bulk E horizon materials was very high (750 L kg^{-1}). Uranium was preferentially adsorbed onto the fine < 50 µm soil particles (Kd = 2200 L kg^{-1}): the lower the granulometric fraction, the higher the organic content, and the higher the uranium retention coefficient (Crançon and van der Lee, 2003). The vertical migration of uranium in soil was thus strongly limited by sorption onto soil materials, as observed in similar studies concerning uranium migration in soils (Oliver et al., 2007; Sansone et al., 2001a). Uranium dissolved from surface deposits is then likely to be majorly immobilized in surficial soil horizons.

Nevertheless, U(VI) concentrations observed in groundwater and surface water showed evidences for uranium mobilization from soil surficial horizons (Crançon et al., 2010; Hargindeguy et al., 2018; Harguindeguy et al., 2014). The total-uranium concentrations measured in the shallow aquifer are heterogeneous. Highest uranium concentration observed in groundwater does not exceed 150 µg L^{-1}. The concentration of uranium in groundwater decreases rapidly with increasing distance from the deposits areas, so the longitudinal extend of the uranium plume along a flow line in the shallow aquifer does not exceed 1 km north-eastward, suggesting a limited enhanced mobility from soils. In surface waters, total aqueous concentrations for uranium are generally lower than in groundwater, increase when drains cross the U-deposition area, and then decrease downstream.

Colloid-bound uranium dominates the distribution of uranium. In the surface waters, the percentage of colloidal uranium is generally lower (between 10% and 32%) than in groundwater (between 68% and 90%). These results are in agreement with observations from the soil leaching experiments, where about 80–90% of uranium in leachates was present in the colloidal fraction (Harguindeguy et al., 2014). Uranium was found to be mainly associated to small-size Fe/Al/organic colloids: while gyration radius distributions for bulk natural colloids in surface water ranged from about 5, and roughly 200nm, colloidal uranium was found at 75% with gyration radii less than 60–70 nm (Hargindeguy et al., 2018). Moreover, changes observed in colloidal structures and compositions suggest that a colloidal redistribution would have occurred during drainage of soil and surficial aquifer groundwater underneath the deposit area, in possible relation with contrasts in both pH and redox conditions fond respectively in soil, aquifer and surface flows, especially with regards to the oxidation of Fe(II) in Fe(III) compounds.

4.3.2 U, Fe, Al and organic carbon leaching experiments

Following the initial contact time, pH reached rapidly a stable value in leachate (pH = 4.0 ± 0.1), while specific conductivity increases linearly with time (data not shown, see Annexe 10). These observations suggest that:

- Soil leachate pH is strongly buffered by organic acids,
- Mineralization of the leaching solution is progressive, due to a kinetic control of soil leaching.

Leaching of U from soil

Evolution of uranium concentration in leachate with time in total, dissolved (< 10 kDa) and colloidal (> 10 kDa) fractions are given in Figure 4.3-1, together with corresponding fittings of pseudo-second-order kinetic curves.

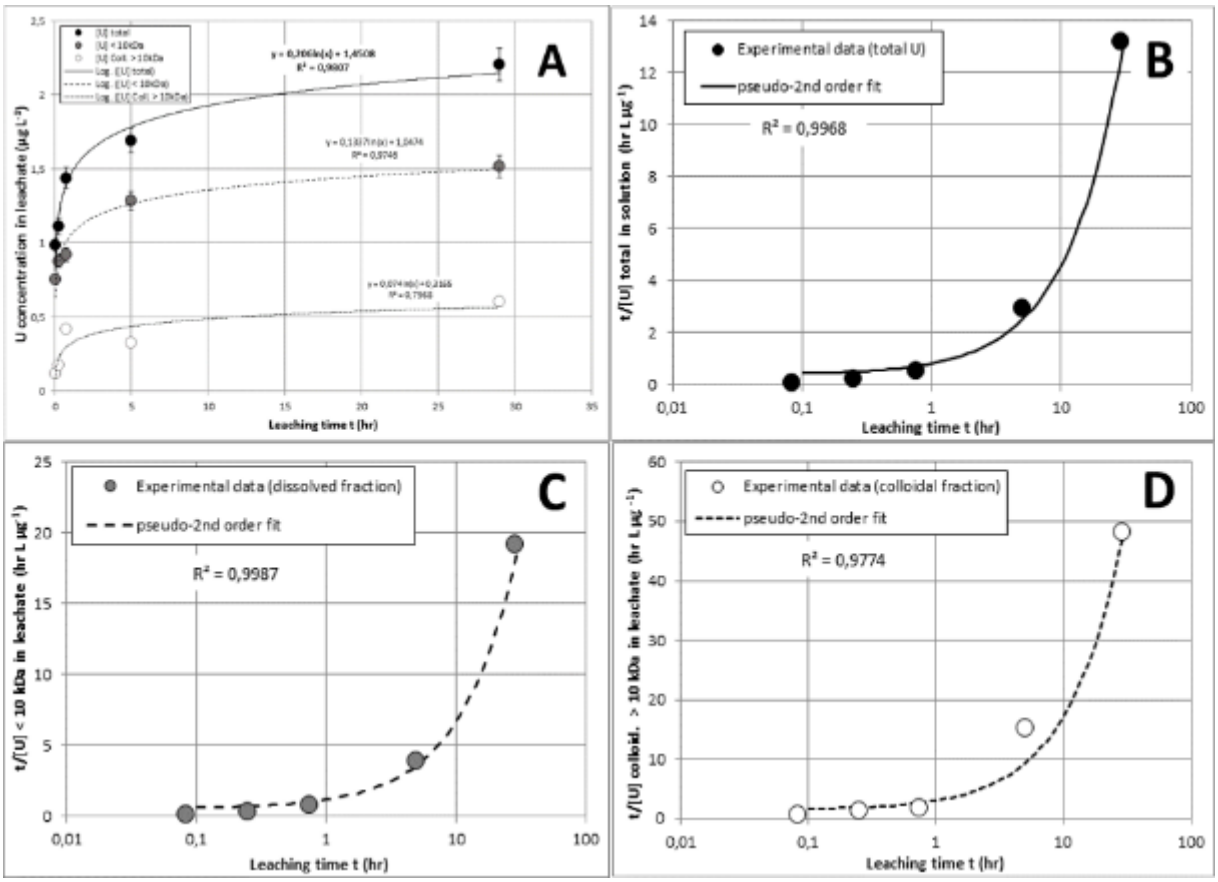

Figure 4.3-1: Evolutions of U concentration in leachate as a function of leaching time in total fraction (black circles), dissolved fraction < 10 kDa (grey circles) and colloidal fraction > 10 kDa (white circles) (graph A). Graphs B, C and D exhibit the fitting of kinetic order for total U, dissolved U (< 10 kDa) and colloidal U (> 10 kDa) in leachate respectively.

In total, dissolved and colloidal fractions, the concentration of U in leachate increased continuously, but non-linearly, with leaching time. Uranium concentration in leachate increased with time, from initial contact t_0 to t_0+29 h, toward a theoretical maximal concentration at steady-state following an asymptotic, pseudo-

logarithmic scheme. These observations indicate that the processes involved in uranium leaching were quite rapid, and typically more than 90% of the maximum uranium concentration in leachate occurred within the first 24 hours of the experiment. The transient state took about 15 to 20 hours.

Kinetic studies are crucial for gaining inside on the physical chemistry of the uranium leaching processes. The experimental dataset from batch leaching experiments were used in a modeling exercise where three kinetic models were tested: zero-order model, as well as pseudo-1st and -2nd order models adapted from Lagergren and Blanchard models respectively as explained above (Blanchard et al., 1984; Lagergren and Svenska, 1898). The most suitable kinetic model is the one which leads to the highest regression coefficient and the lowest root mean square error values: the results showed that for both uranium in total, dissolved and colloidal fractions, the pseudo-second order adapted from Blanchard model was better than the other models Table 4.3-1).

Table 4.3-1: Synthesis of parameter estimation for U, Fe, Al and organic leaching kinetics on the basis of leaching experiments data with k app the apparent reaction rate and C_{eq} app the apparent equilibrium concentration of species.

Element, fraction	Type of evolution	Order	Model	R^2	C_{eq} app.	Unit	k app.	Unit
U tot.	pseudo-Logarithmic	2	Blanchard	0.99678	2.375	µg L^{-1}	0.45	L µg^{-1} hr^{-1}
U <10kDa	pseudo-Logarithmic	2	Blanchard	0.99865	1.64	µg L^{-1}	0.65	L µg^{-1} hr^{-1}
U coll. >10kDa	pseudo-Logarithmic	2	Blanchard	0.97744	0.638	µg L^{-1}	1.61	L µg^{-1} hr^{-1}
TOC tot.	Linear	2	Blanchard	0.98342	300	mg L^{-1}	0.033	L mg^{-1} hr^{-1}
TOC <10kDa	Linear	2	Blanchard	0.98662	218	mg L^{-1}	0.0048	L mg^{-1} hr^{-1}
TOC coll. >10kDa	Linear	1	Lagergren	0.98949	126	mg L^{-1}	0.118	hr^{-1}
Fe tot.	pseudo-Logarithmic	2	Blanchard	0.99257	162	µg L^{-1}	0.0065	L µg^{-1} hr^{-1}
Fe <10kDa	pseudo-Logarithmic	2	Blanchard	0.99364	68	µg L^{-1}	0.016	L µg^{-1} hr^{-1}
Fe coll. >10kDa	Linear	1	Lagergren	0.99571	80	µg L^{-1}	0.102	hr^{-1}
Al tot.	pseudo-Logarithmic	2	Blanchard	0.99347	1500	µg L^{-1}	7.0E-04	L µg^{-1} hr^{-1}
Al <10kDa	pseudo-Logarithmic	2	Blanchard	0.99537	1000	µg L^{-1}	0.0011	L µg^{-1} hr^{-1}
Al coll >10kDa	Linear	1	Lagergren	0.98836	490	µg L^{-1}	0.099	hr^{-1}

This model successfully explains the evolution of uranium concentration in leachate. Uranium concentration in leachate tended to reach a maximum value, corresponding to pseudo-equilibrium or steady-state, determined from model fitting of the $\frac{t}{c(t)}$ vs t plot (Table 4.3-1).

At steady-state, maximum uranium concentrations in leachate reached 2.4, 1.6 and 0.64 µg L^{-1} for total, dissolved (< 10kDa) and colloidal (> 10kDa) fractions, respectively. These values were found to be slightly lower than the ones observed for the leaching of the same soil sample, using comparable methodology but

with a liquid/solid ratio equal to 10 (Harguindeguy et al., 2014). This is not surprising since higher liquid/soli ratios lead to higher leaching efficiency, thus higher concentrations of elements in leachate, as ever observed in comparable conditions (Hargindeguy et al., 2018). Leached uranium was found to be mainly distributed in the dissolved fraction (73 ± 6 %) rather than in the colloidal one (21 ± 7 %). The distribution of uranium between the colloidal and dissolved fractions was found not to evolve significantly with the leaching time.

The apparent contradiction with results obtained on the same sample in former works under comparable leaching conditions, where 80% of lixiviated uranium was found in the colloidal fraction (Hargindeguy et al., 2018), may lay in the differences in the methodology used for treatment of the leachates before ICP-MS analysis. In the present work, the leachate was let to settle for 2 days. No centrifugal step was used to remove the supernatant from the soil sample, whereas in former studies, supernatant was centrifuged at 4500 rpm for 30 min to remove larger particles. Such latter conditions, aggregation or shearing of colloidal particles may occur, leading to structural modifications of the colloidal phase (Planken and Coelfen, 2010; Salim and Cooksey, 1981). Hence, small colloids may aggregate in larger entities, thus biasing the apparent distribution of uranium between the colloidal and the dissolved fractions by overestimating association of uranium with larger entities (Maria et al., in prep).

Table 4.3-2. Calculation of mobilization efficiency for U, Al, Fe and Total Organic Carbon during soil leaching experiment from mass balance calculations.

TOTAL fraction											
Element	Initial mass in soil sample (mg)	Evolution of mass in leachate (total fraction) with leaching time (mg)					Mobilization efficiency (%)				
		0.08 hr	0.25 hr	0.75 hr	5 hr	29 hr	0.08 hr	0.25 hr	0.75 hr	5 hr	29 hr
U	0.00313	0.00002	0.00003	0.00004	0.00004	0.00006	0.08	0.09	1.1	1.4	1.8
Al	26.45	0.0155	0.0179	0.0206	0.0252	0.0363	0.06	0.07	0.08	0.10	0.14
Fe	12.95	0.0013	0.0015	0.0021	0.0025	0.0038	0.01	0.01	0.02	0.02	0.03
TOC	28.5	3.3	3.5	3.2	4.3	7.3	11.6	12.3	11.2	14.9	25.6

Moreover, the evolution of uranium concentration in leachate over time was comparable, whether in total, or dissolved and colloidal fractions. Mobilization of uranium from soil during leaching exhibited apparent pseudo-2nd order rates equal to 0.45 ; 0.65 and 1.6 L μg^{-1} hr^{-1} for total, dissolved and colloidal U fractions, respectively. These values are relatively close one to each other, thus mechanisms controlling U leaching from soil are not expected to be significantly different for total, dissolved and colloidal fractions.

From the batch leaching experiments conducted on surface soil, the total uranium mass initially present in the soil and leached increased with time from about 0.8% (for $t_{leaching}$ = 5 min) to about 2% (for $t_{leaching}$ = 29 hr)

for total fraction (Table 4.3-2). These results are significantly lower (but consistent), with ones obtained in a previous study on the same soil sample in comparable conditions, but with higher liquid/solid ratio (about 9%) (Harguindeguy et al., 2014).

The leaching efficiency or uranium from soil appeared to be quite limited, despite uranium was expected to be easily mobilized.

Leaching of Fe and Al from soil

The evolution of Fe and Al concentrations in leachate with time in total, dissolved (< 10 kDa) and colloidal (> 10 kDa) fractions are given respectively in Figure 4.3-2 and Figure 4.3-3, together with corresponding fittings of kinetic curves.

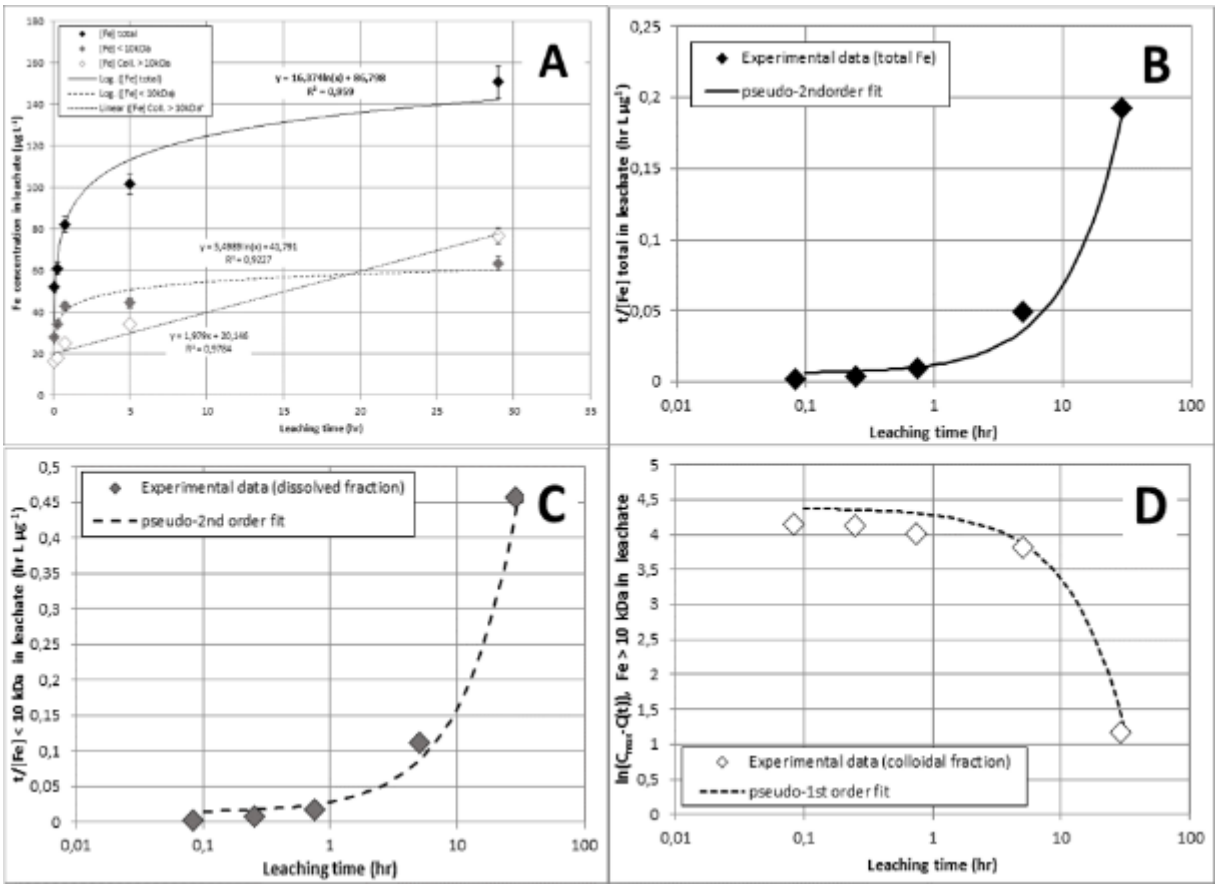

Figure 4.3-2. Evolutions of Fe concentration in leachate as a function of leaching time in total fraction (black circles), dissolved fraction < 10 kDa (grey circles) and colloidal fraction > 10 kDa (white circles) (graph A). Graph B, C and D exhibits the fitting of kinetic order for total Fe, dissolved Fe (< 10 kDa) and colloidal Fe (> 10 kDa) in leachate respectively.

Fe and Al exhibited very similar behavior regarding leaching dynamics and distribution in dissolved and colloidal fractions, suggesting their fates to be correlated during soil leaching. In total, dissolved and colloidal fractions, the concentrations of Fe and Al in leachate increased continuously, but non-linearly, with leaching

time. Fe and Al concentration in total and dissolved fractions increased in leachate with time, from initial contact t_0 to t_0+29 h, toward a theoretical maximal concentration at steady-state following an asymptotic, pseudo-logarithmic scheme. The asymptotic tendency is less clear in the colloidal fraction, where > 10 kDa Fe and Al concentrations increased regularly with leaching time following a pseudo-linear scheme.

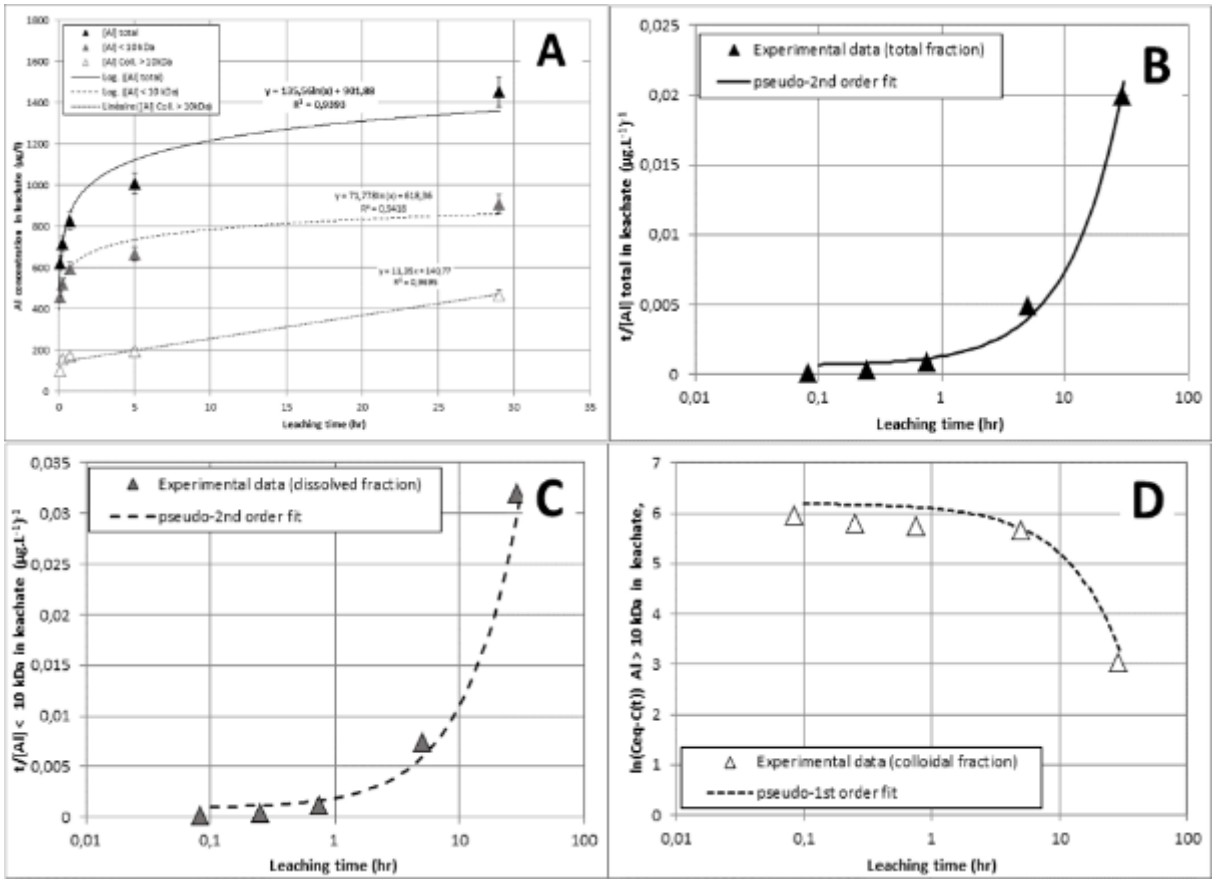

Figure 4.3-3. Evolutions of Al concentration in leachate as a function of leaching time in total fraction (black circles), dissolved fraction < 10 kDa (grey circles) and colloidal fraction > 10 kDa (white circles) (graph A). Graph B, C and D exhibits the fitting of kinetic order for total Al, dissolved Al (< 10 kDa) and colloidal Al (> 10 kDa) in leachate respectively.

These observations indicate that the processes involved in Fe and Al leaching were quite rapid. Typically, more than 90% of the maximum Fe and Al concentrations in leachate occurred within the first 24 hours of the experiment. The transient state took about 15 to 20 hours.

The most suitable kinetic model leading to the highest regression coefficient and the lowest root mean square error values is a pseudo-second order adapted from Blanchard model for Fe and Al total and dissolved fraction (Table 4.3-1). For both Fe and Al colloidal fractions, a pseudo-first order model adapted from Lagergren model appears more suitable. This suggests that mechanisms controlling Al and Fe leaching from soil were not fully identical for dissolved and colloidal fractions. Total Al and Fe leaching dynamics followed whom of the most abundant respective fractions: in both cases, the < 10 kDa dissolved fraction.

Pseudo-2nd and -1st order models successfully explain the evolution of Fe and Al concentrations in leachate for total, dissolved and colloidal fractions, respectively. These concentrations tended to reach maximum values corresponding to pseudo-equilibrium or steady-state, determined from model fitting of the $\frac{t}{c(t)}$ vs t plot, or the $ln(c_{max} - c(t))$ vs t plot, respectively for pseudo-2nd and -1st order models (Figure 4.3-2 and Figure 4.3-3). At steady-state, maximum Fe concentrations in leachate reached 162, 68 and 80 µg L^{-1} for total, dissolved (< 10kDa) and colloidal (> 10kDa) fractions, respectively. Corresponding maximum concentration values for Al are respectively 1500, 1000 and 490 µg L^{-1}.

Leached Fe and Al were found to be mainly distributed in the dissolved fraction (respectively 50 ± 6 % for Fe, and 70 ± 5 % for Al) rather than in the colloidal one (respectively 35 ± 9 % for Fe, and 22 ± 6 % for Al). These distributions of Al and Fe between the colloidal and dissolved fractions were found to evolve slightly but significantly with leaching time: the higher the leaching time, the higher the concentration of Fe and Al in the colloidal fraction.

Mobilization of Fe and Al from soil during leaching experiment exhibited:

- Apparent pseudo-2nd order kinetics for total and dissolved fraction, with rates equal to 0.0065 and 0.0155 ; 0.0007 and 0.0011 L μg^{-1} hr^{-1} respectively for Fe and Al in total and dissolved fractions,
- Apparent pseudo-1st order kinetics for colloidal fraction, with rates close to 0.1 hr^{-1} for both Fe and Al.

Kinetics orders were identical for Fe and Al in total and dissolved fractions, suggesting that mechanisms controlling Fe and Al leaching from soil were correlated or identical. Dynamics of colloidal Fe and Al fractions mobilization from soil appeared to be different, since these fractions followed pseudo-1st order kinetics. Apparent kinetic rates were quite identical for Fe and Al in colloidal fractions, suggesting that mechanisms controlling colloidal Fe and Al leaching from soil were correlated or identical.

From the batch leaching experiments conducted on surface soil, the total Fe and Al mass initially present in the soil and released in the leachate increase regularly with time from about 0.01% (for $t_{leaching}$ = 5 min) to about 0.03% (for $t_{leaching}$ = 29 hr) for Fe in total fraction, and from about 0.06% (for $t_{leaching}$ = 5 min) to about 0.14% (for $t_{leaching}$ = 29 hr) for Al in total fraction (Table 4.3-2). Thus, mobilization of Fe and Al appeared to be quite limited during batch leaching experiment.

Leaching of TOC from soil

Evolution of total organic carbon (TOC) concentrations in leachate with time in total, dissolved (< 10 kDa) and colloidal (> 10 kDa) fractions are given in Figure 4.3-4, together with corresponding fittings of kinetic curves. In total, dissolved and colloidal fractions, the concentration of TOC in leachate increased continuously and pseudo-linearly with leaching time.

Hence, an asymptotical transient state characterized by a maximal concentration at steady-state can hardly be determined.

Nevertheless, the most suitable kinetic models leading to the highest regression coefficient and the lowest root mean square error values are: 1/ a pseudo-second order adapted from Blanchard model for total TOC and TOC in dissolved fraction, and 2/ a pseudo-first order model adapted from Lagergren model for colloidal TOC fraction. Mobilization of TOC from soil during leaching experiment exhibits:

- Apparent pseudo-2nd order kinetics for total and dissolved fraction, with rates equal to 0.033 and 0.0048 L µg^{-1} hr^{-1} respectively,
- Apparent pseudo-1st order kinetics for TOC colloidal fraction, with rates close to 0.18 hr^{-1}.

But in these cases, theoretical pseudo-equilibrium or steady-state TOC concentrations determined from model fitting of the $\frac{t}{c(t)}$ vs t plot, or the $ln\left(c_{max} - c(t)\right)$ vs t plot respectively for pseudo-2nd and -1st order models shall be taken with care (Figure 4.3-4, Table 4.3-1).

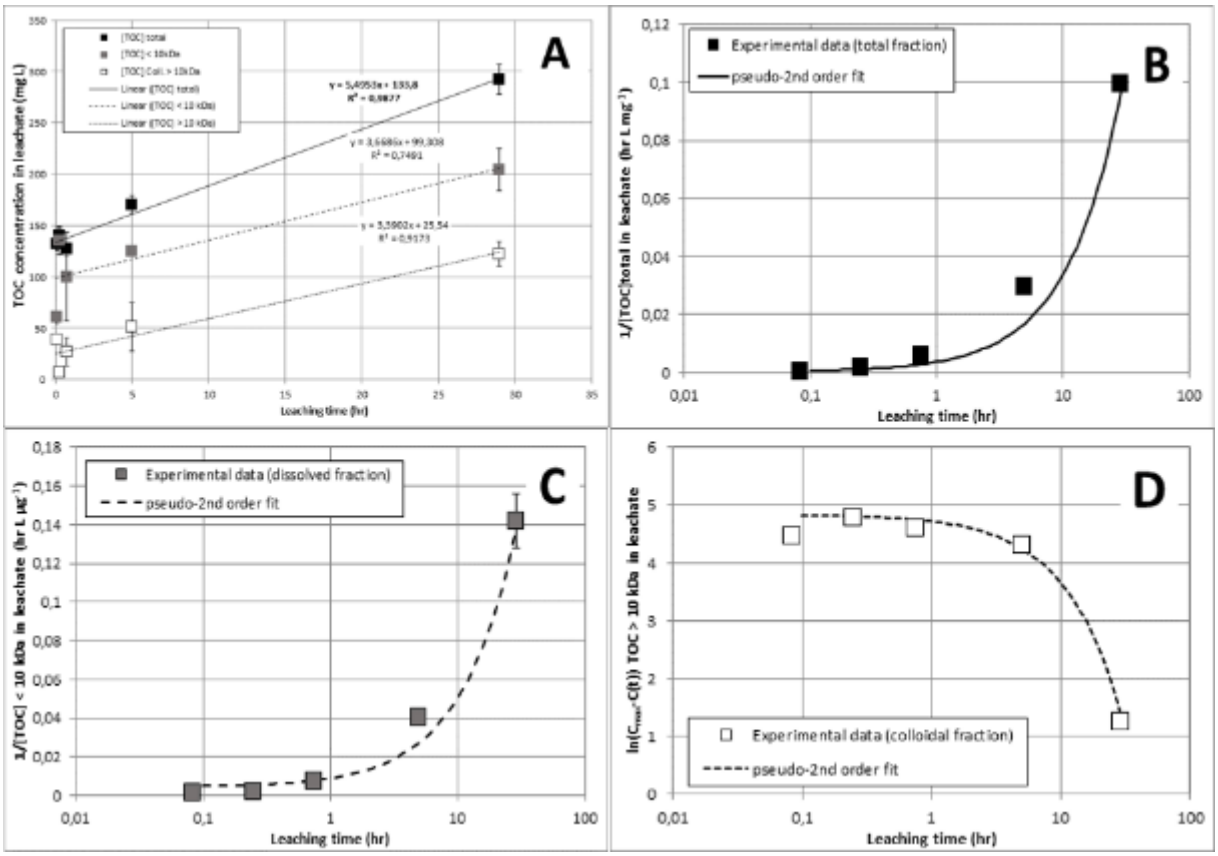

Figure 4.3-4. Evolutions of Total Organic Carbon (TOC) concentration in leachate as a function of leaching time in total fraction (black circles), dissolved fraction < 10 kDa (grey circles) and colloidal fraction > 10 kDa (white circles) (graph A). Graph B, C and D exhibits the fitting of kinetic order for total TOC, dissolved TOC (< 10 kDa) and colloidal TOC (> 10 kDa) in leachate respectively.

Typically, more than 10 % of the TOC mass initially present in the soil sample was leached within the first 5 minutes of the experiment, and about 25 % mass was released after 29 hr of leaching. These observations indicate that the processes involved in TOC leaching were quite rapid, with important mobilization of soil TOC during the leaching experiment. Leached TOC was found to be mainly distributed in the dissolved fraction (73 ± 18 %) rather than in the colloidal one (respectively 22 ± 6 %). This distribution was found not to evolve significantly with leaching time.

TOC in total and dissolved fractions exhibit singular behaviors regarding leaching dynamics of U, Al and Fe in corresponding fractions. Meanwhile, TOC in colloidal fraction exhibit similar kinetic order and rate than Al and Fe, suggesting their fates to be correlated during soil leaching.

Correlations between U, Fe, Al and organic carbon during leaching

Correlation and linear regression coefficient matrices can be calculated comparing evolution of pH, specific conductivity, and U, Fe, Al and TOC concentrations in leachate for total, dissolved and colloidal fractions (see Annexe 11).

Correlation coefficients calculated between these variables throughout leaching experiment are generally high (>0,90), but may be probably overestimated sometime by the weak number of sampling dates during the leaching experiment: particularly when a single data point stands for a high concentration observed at t = 29 hr. Meanwhile, some significant correlations arise between U, Fe, Al and TOC during the soil leaching in total, dissolved and colloidal fractions (Figure 4.3-5). These correlations show that the distribution and fate of U, Fe, Al and TOC during the soil leaching in total, dissolved and colloidal fractions were similar during the leaching process. Thus, the mobilization process of U, Fe, Al and TOC from soil was likely to be globally the same for all these elements.

Consequently, uranium linked to TOC, Fe and Al-rich colloids could be promoted for mobilization from soil and, for colloidal transport throughout the soil. Relative concentrations of colloidal uranium, aluminum, iron and organic carbon (and corresponding concentration ratios, U/Al, U/Fe and U/TOC, data not shown) remained similar in total, dissolved and colloidal fractions, and were not varying significantly with leaching time. This suggests that colloids brought and/or from soil leaching showed no significant changes in their physicochemical characteristics throughout the leaching experiment.

Mobilization kinetic orders were globally identical for U, Fe and Al in total and dissolved fractions suggesting that mechanisms controlling U, Fe and Al leaching from soil are not rather different. Apparent mobilization pseudo-second order rates were found to be consistent between total and dissolved fractions but differ with element. Relative apparent mobilization velocities from soil were found to be U > Fe > Al.

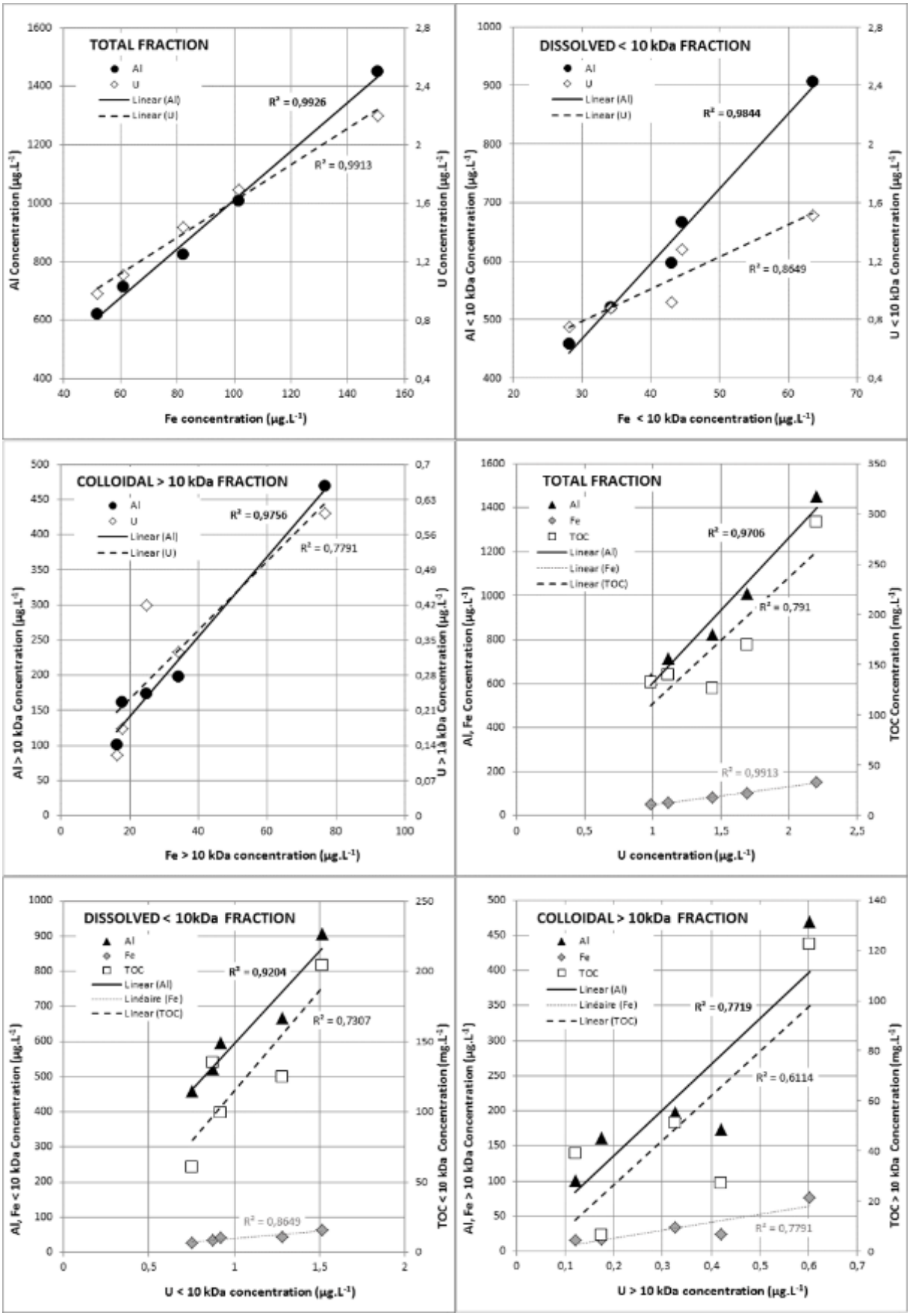

Figure 4.3-5. Illustrations for some correlations between Al, Fe, U and TOC concentrations in soil leachate, in total, dissolved and colloidal fractions.

TOC mobilization from soil during leaching exhibited pseudo-linear behavior in total, dissolved and colloidal fractions, in apparent inconsistence with U, Fe and Al mobilization behaviors. This may come either from a difference in the mobilization mechanism, or from a scale effect introduced by the large difference in concentrations values observed in leachate for TOC (~ 100 mg L^{-1}) compared to U, Fe and Al ones (~ 1 – 1000 µg L^{-1}).

Dynamics of colloidal TOC, Fe and Al fractions mobilization from soil appeared to follow the same mobilization dynamics scheme, since these fractions all followed pseudo-1st order kinetics. Apparent kinetic rates were quite identical for TOC, Fe and Al in colloidal fractions, suggesting that mechanisms controlling colloidal organic carbon, Fe and Al leaching from soil were correlated or identical, and directly driven by the difference between the equilibrium capacity of the leaching solution and the amount of element leached at a given time.

This suggests a unique mechanism could not address the global mobilization of U, organic carbon, Al and Fe from soil, since different behaviors can be observed between dissolved and colloidal fractions.

4.3.3 Properties of the natural colloidal phases in soil leachates

As uranium mobilization from soil appears to be promoted by soil organic colloids, a special attention was paid to characterize the physicochemical properties of organic colloids by a multi-method approach.

X-Ray diffraction analysis

X-ray diffraction spectra conducted on separated unfiltered and dried colloidal suspension from soil leaching is given in Figure 4.3-6.

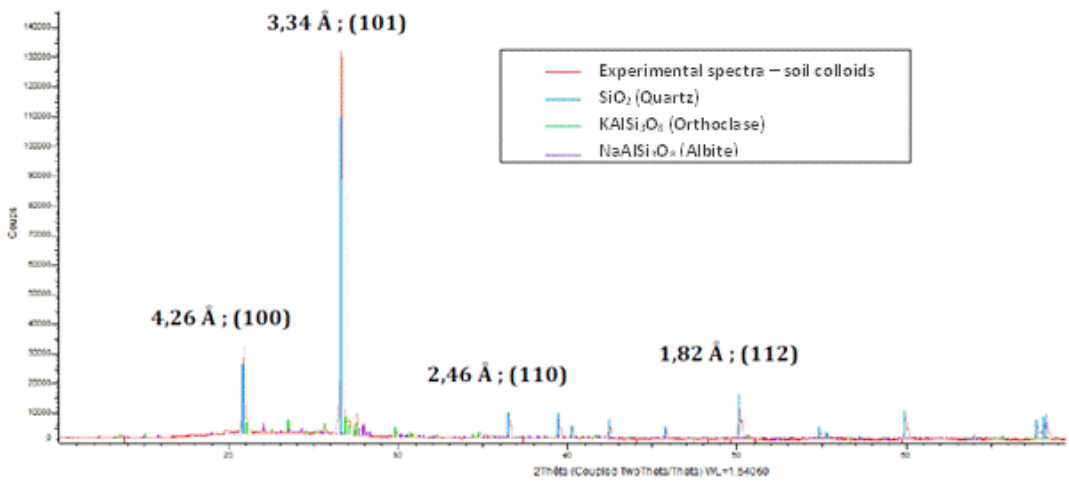

Figure 4.3-6. X-Ray diffraction spectra of unfiltered colloid suspension from soil leaching.

X-Ray diffraction analysis shows that colloidal entities to be partially composed of crystallized mineral compounds, such as micro- and nanocrystals of detrital quartz (SiO_2) majorly, and in a lesser extent orthoclase ($KAlSi_3O_8$) and albite ($NaAlSi_3O_8$).

SEM observations

Some SEM imagery data are reported in Figure 4.3-7. The colloid deposit in the Cu grid looks like a cracked skin 10x100 µm in size (Figure 4.3-7, A).

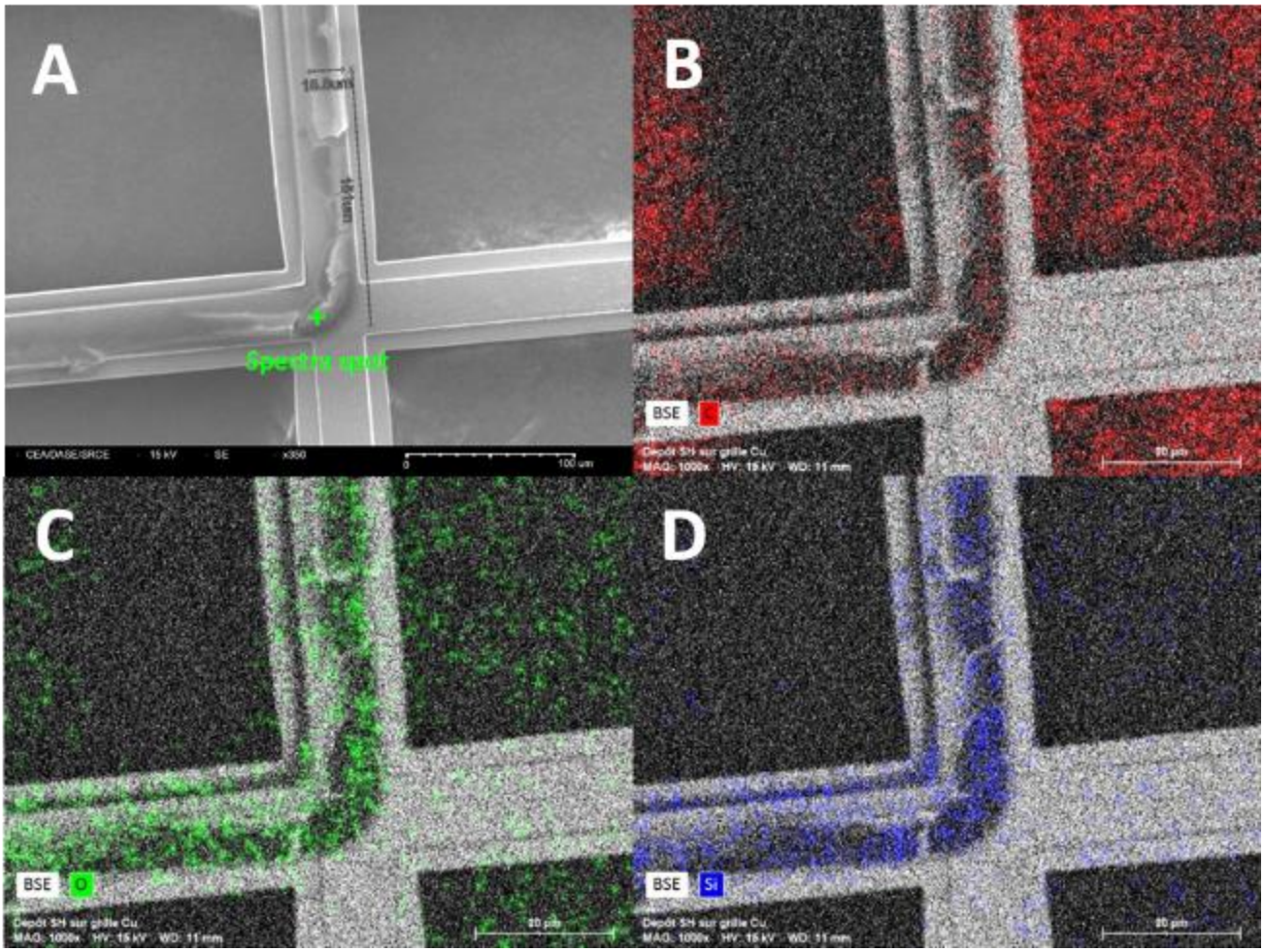

Figure 4.3-7. SEM observation of a deposit of soil organic colloids on a TEM copper grid: A/ Secondary electrons image of the colloids deposit, with indication of the localization of the spot energy dispersive spectroscopy (EDS) ; B, C, D/ superposed backscattered electrons images and EDS analysis for respectively C, O and Si distributions on the colloids deposit.

Table 4.3-3: SEM-EDS analysis results showing the bulk composition of soil organic colloids

Element	Mass. %	Atom. %	std-dev (2-sigma) %
C	44.39	52.95	4.81
O	48.58	43.51	5.24
Al	1.71	0.91	0.79
Si	5.06	2.58	0.42
Total	99.7	100.0	

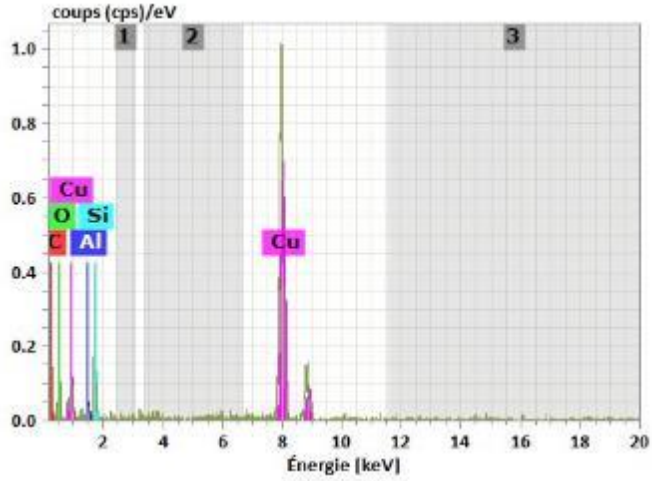

Figure 4.3-8: EDS spectra for spot analysis of the soil organic colloids deposit on the copper TEM grid .

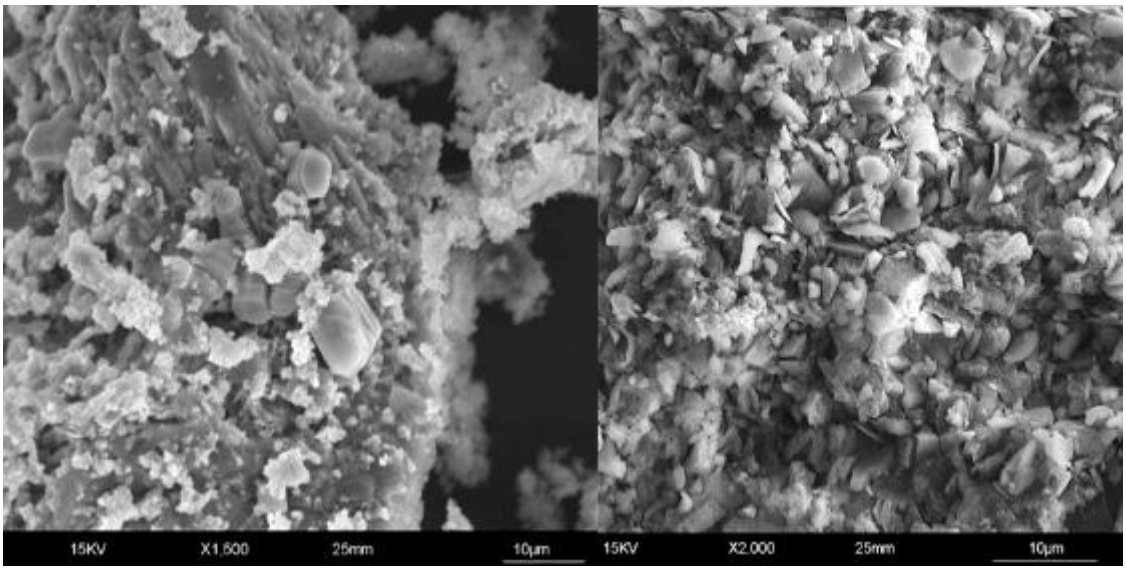

Figure 4.3-9. SEM secondary electron images showing the presence of silicate microcrystals in soil aggregates from bulk surface soil sample.

Natural colloids in soil leachate are mainly composed of C (52 at.%), O (43 at.%), Si (3 at.%) and Al (1 at.%). Si and Al distribution can be directly related to the presence of inherited nano-crystals of detrital minerals such as quartz and tectosilicates composing soil parent material (see Figure 4.3-6).

These silicate minerals were found to compose aggregates (Figure 4.3-9) together with humic substances (Crançon and van der Lee, 2003).

Oxygen was thus distributed between the structure of these silicate minerals, and oxygen incorporated in the structure of organic supramolecular entities, in association with carbon. Accounting for about 6 at. % of oxygen in the structure of the silicate minerals, the mean O/C atomic ratio of the organic constituents of the colloidal phase should be about 0.7.

Colloid size, structure and morphology

Structural properties of the colloidal phase were determined from TEM observations as well as coupling between A4F and MALS. The dimensional and structural evolution of the colloidal materials in unfiltered soil leachates as a function of leaching time is shown in Figure 4.3-10.

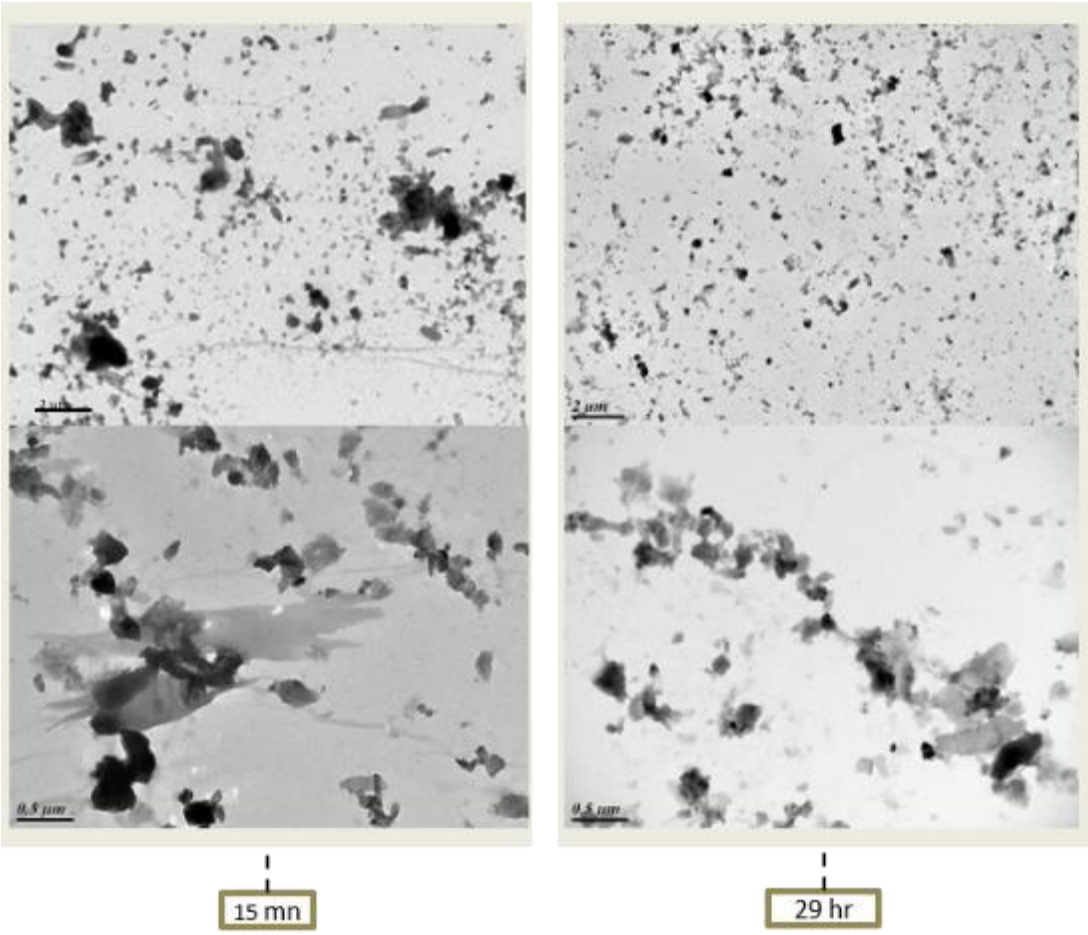

Figure 4.3-10: Dimensional and structural evolution of the colloidal phase from TEM observations as a function of the soil leaching times in the unfiltered leachates

The monitoring of mean and median gyration radii of the colloidal phases over leaching time is given in Figure 4.3-11. The size distribution of the colloidal phase in leachate, and its evolution as a function of soil leaching time, are given in Figure 4.3-12.

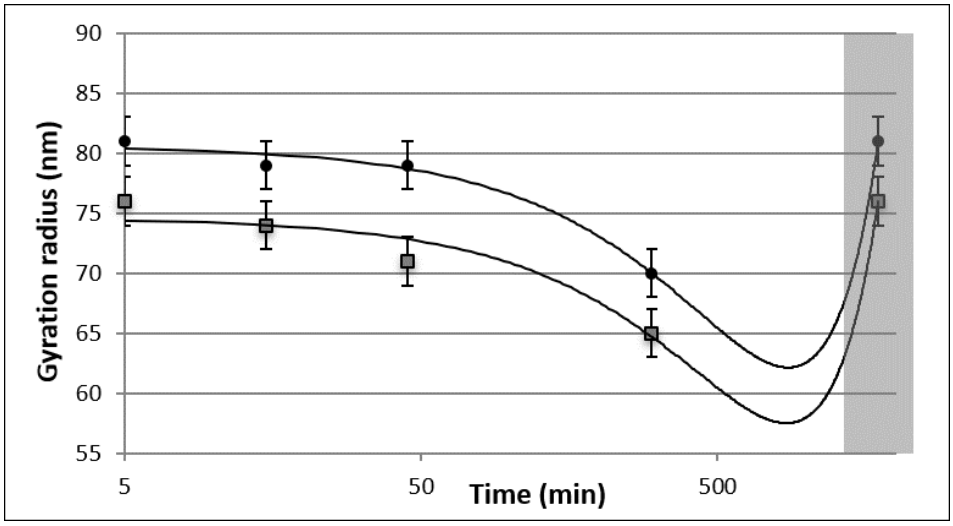

Figure 4.3-11. Dimensional evolution of the colloidal phase, as a function of the soil leaching times. Black circles and opened squares exhibit respectively the mean and median gyration radii evolution as a function of leaching time, as determined from MALS analysis.

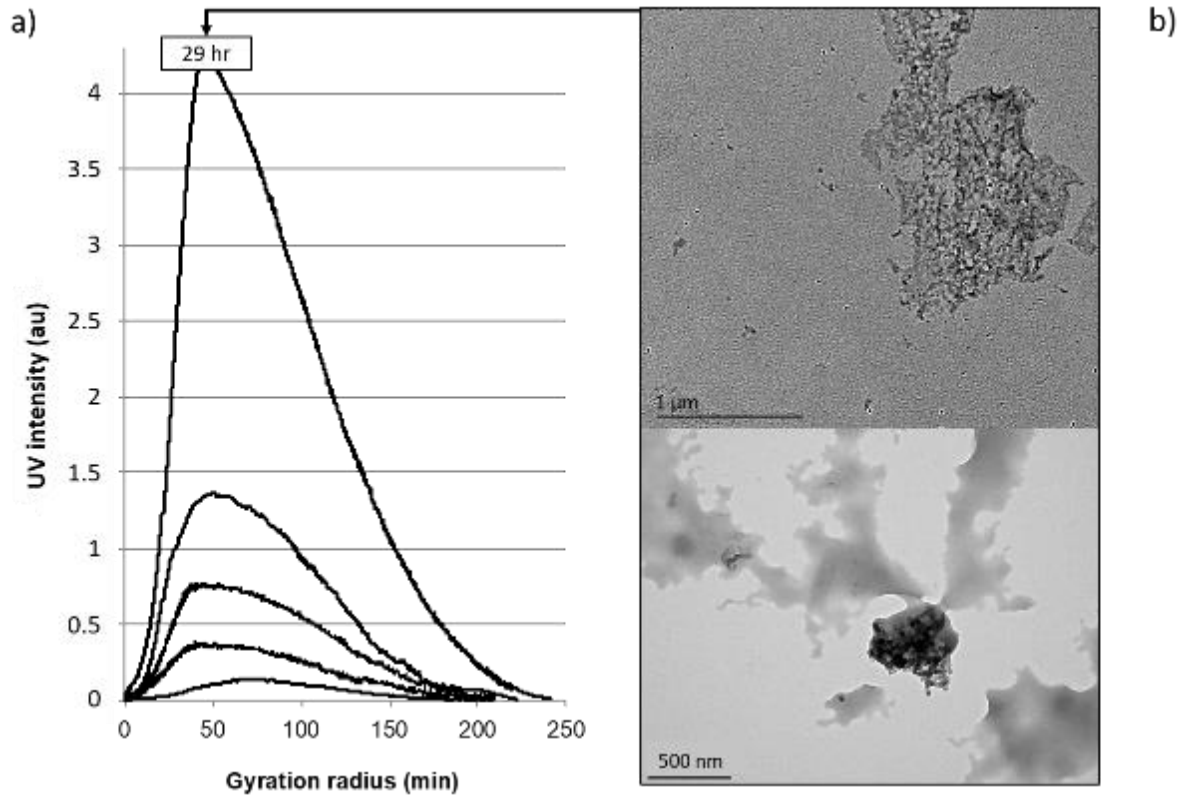

Figure 4.3-12. a) Evolution of size distribution of the colloidal phase in the soil leachate with increasing leaching time from AF4-MALS analysis. b) TEM images of structure and morphology of the colloids for 29 hr leaching time.

It can be seen that size distributions of colloids are asymmetric, and their shape did not exhibit significant change over leaching time between 15 and 50 minutes. The colloid size distribution covers a continuum from a few nanometers to almost 250 nanometers in gyration radius. The mean and median gyration radii (Rg) of soil organic colloids were about 80 nm, showing the size of colloids to be quite small. This observation suggests that:

(i) an important part of organic matter was present in the <10kDa fraction, consistently with results obtained from mass-balance calculations on TOC, showing that leached TOC was found to be mainly distributed in the < 10 kDa fraction (73 ± 18 %),

(ii) the larger particles were predominantly inorganic materials, aggregated and more or less coated by organic matter.

TEM observations show that colloidal phase was constituted by aggregation of various organic and mineral components. These nano-objects were found to exhibit sub-angular and/or rounded morphologies, with sizes ranging of a few nanometers to several hundreds of nanometers. After 29 hours of leaching (Figure 4.3-11 and Figure 4.3-12b), associations between diffuse organic matter and denser spherical particles into aggregates of a few hundred nanometers apparent radius could be observed. This aggregation of colloids and particles is not directly highlighted by any significant increase in mean and/or median radii as a function of leaching time. At the same time as the concentration of particles increased, their size tended to become uniform. Thus, the largest particles disappeared, probably due to mechanical abrasion.

From AF4-MALS analysis, an apparent shift of the gyration radius continuum toward higher values when leaching time increased can be pointed out from Figure 4.3-12a. This can be explained by an agglomeration of medium colloids (Rg > 100 nm) into aggregates larger than few hundred nanometers.

Colloidal organic matter properties from UV fluorescence and absorption spectroscopy

The UV fluorescence excitation-emission matrix (EEM) of soil leachate obtained after 1740 min (29h) of leaching time is presented in Figure 4.3-13. A maximum fluorescence emission is observable for a maximum excitation wavelength around 340 nm. This fluorescence was found to have a maximum emission wavelength around 440 nm. This area, named “peak C”, was widely identified as being associated with the presence of humic-type material (Coble, 1996). The slightly shift of peak C towards longer emission wavelengths as the excitation wavelength increases is typical of multiple compounds-humic substances from natural waters (Aiken, 2014). The fluorescence intensity of this peak is correlated with the higher concentrations of Dissolved Organic Carbon (DOC, i.e. organic carbon <0.45 µm) in leachate. Exact position of fluorescence peaks in EEM made it possible to identify the nature of the OM in the soil leachate (wavelengths Em / Ex = 440/340) as from interstitial freshwater (Aiken, 2014; Coble, 1996).

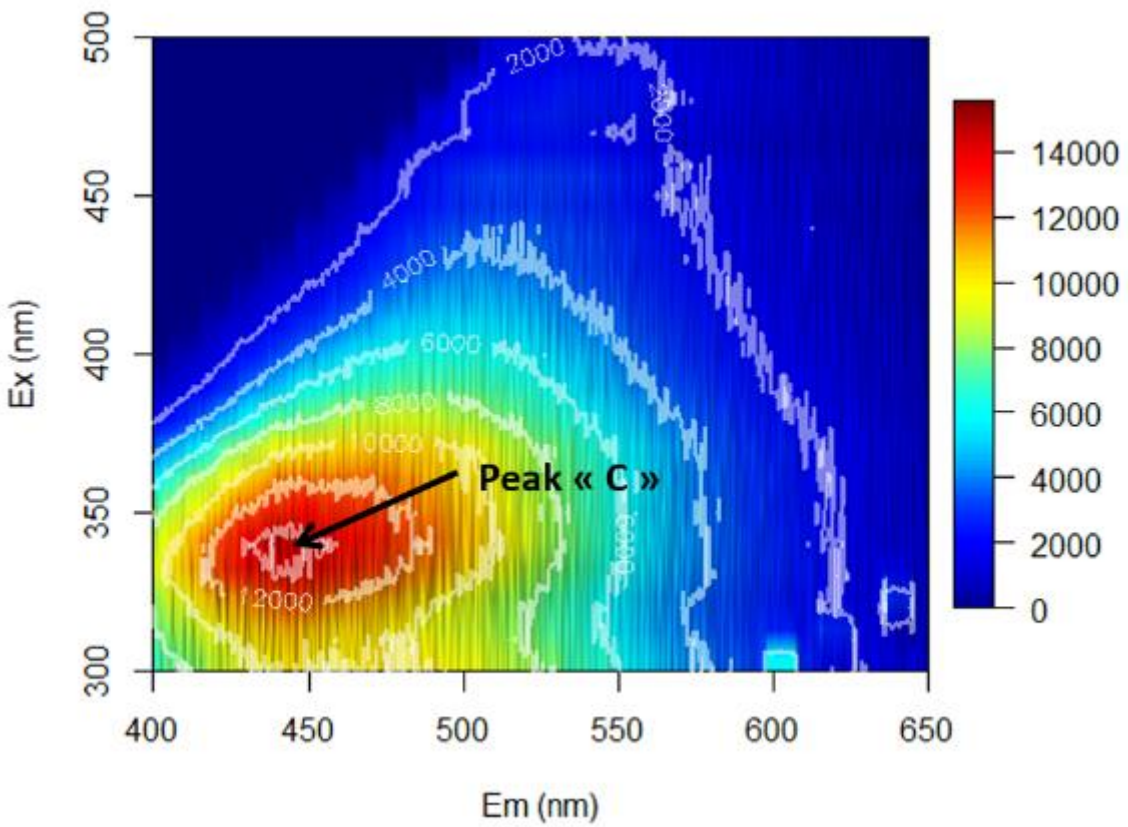

Figure 4.3-13. UV fluorescence excitation-emission matrix (EEM) of soil leachate obtained after 1740 min (29h) of leaching time, showing the presence of humic substances in the colloidal phase.

A secondary fluorescence peak can be observed for the wavelengths Ex = 480 / Em = 540, but its intensity is relatively low compared to that of the peak C. This peak of lower energy was defined as typical of terrestrial humic substances (derived from lignin) (Matthews et al., 1996). It was demonstrated that the peak "C" is particularly visible for samples containing aromatic-rich organic matter such as fulvic acids, whereas the peak of lower energy shows a greater intensity of absorption for soil humic acids (Chen et al., 2003).

The fluorescence index (FI), is an optical parameter calculated from excitation-emission matrix as the ratio of the fluorescence intensities at 470 and 520 nm at an excitation wavelength of 370 nm. Values of FI are related to the nature of the organic matter, and are representative of the aromaticity and the origin of the OM (McKnight et al. 2001). FI values calculated FI for the soil leachate after 1740 minutes of leaching (29h) was 1.17 ± 0.01. This value approaches those observed for terrestrial fulvic acid (SRFA) standards (Cory et al., 2010) and excludes a microbial origin, which is consistent with the acidic conditions and low microbial activity of podzolized soils.

For soil leachate, the organic matter would be consequently mainly composed of fulvic-like compounds, very aromatic, with a low proportion of less mobilizable humic-like organic compounds, consistently with OM predominantly observed in podzolized soils (Kononova and Alexandrova, 1973).

The UV absorption spectra of soil leachates are given in Figure 4.3-14 for various leaching times.

Humic substances are known to have significant absorption capacity in the UV range, mainly due to the high concentration of aromatic groups of which they are constituted (Schnitzer and Khan, 1972; Traina et al., 1990). The UV absorbance spectra recorded for soil leachates exhibited a decrease of their intensity with increasing wavelength (Figure 4.3-14). A shoulder of absorbance spectrum was observed around 260 nm. This absorption zone is known to be representative of energetic transitions related to the presence of C = C aromatic groups (Traina et al., 1990).

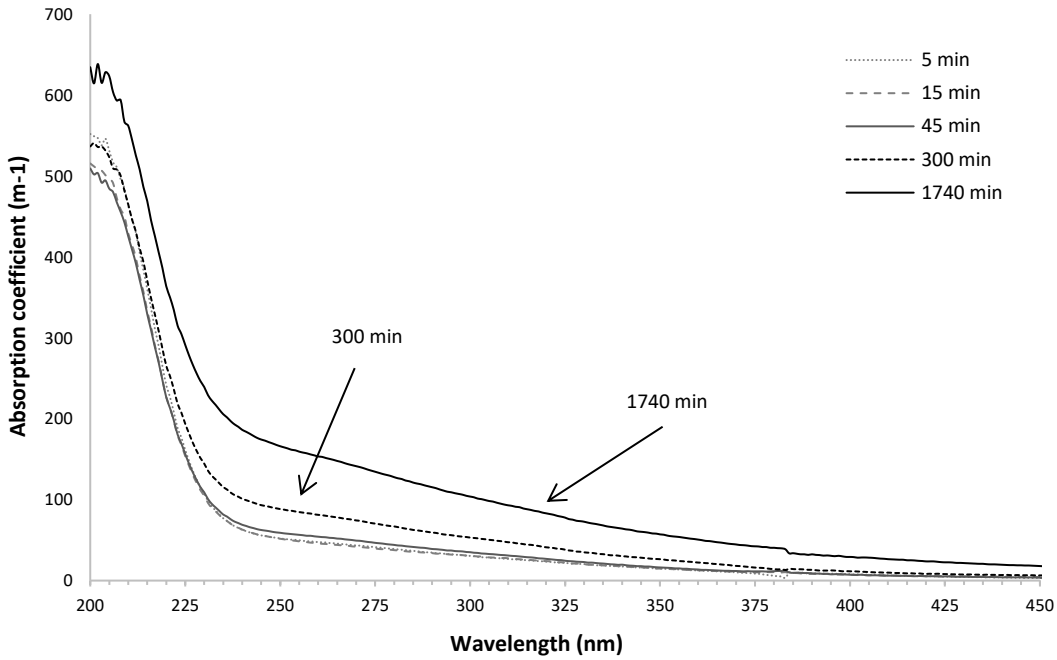

Figure 4.3-14. Absorption spectra of soil leachate at various leaching time.

For wavelengths below 250 nm, the high UV absorption of soil leachates may be due to the presence of C = C groups but also carbonyl (C = O) groups (Chen et al., 2002). When a strong absorption of OM in the visible wavelengths is observed, it may be due to the condensation of aromatic nuclei as well as the presence of organic molecules of high molecular weight (Schnitzer and Khan, 1972). In soil leachates, absorption observed for wavelengths above 350 nm are very low, as observed for mobilizable compounds of natural organic matter, suggesting that colloidal organic matter consist in small organic molecules, with poorly condensed aromatic cycles (Chen et al., 2002).

$SUVA_{254}$ is a parameter related to the concentration of aromatic chromophores (Weishaar et al., 2003). The $SUVA_{254}$ values obtained for the soil leachates range from 0.1 to 0.4 L mgC^{-1} m^{-1}. These values are lower than ones commonly observed for OM in surface water ($SUVA_{254}$ between 1 and 6 L mgC^{-1} m^{-1}). The low degradation status of organic matter in podzolized soils may justify these low $SUVA_{254}$ values. E2 / E3 ratios,

which are correlated with the molecular size of the OM, were found to have values ranging between 5 and 10 in soil leachates. These values were relatively high, suggesting the presence of very small organic molecules in the organic phases of soil leachates (Guo and Chorover, 2003). The evolutions of $SUVA_{254}$ values and of the E2/E3 ratio in soil leachate with leaching time are reported Figure 4.3-15. $SUVA_{254}$ increased regularly with leaching time, showing an increase in OM aromaticity. The E2/E3 ratio did not exhibit significant evolution during leaching, suggesting no significant evolution of OM molecular weight during soil leaching.

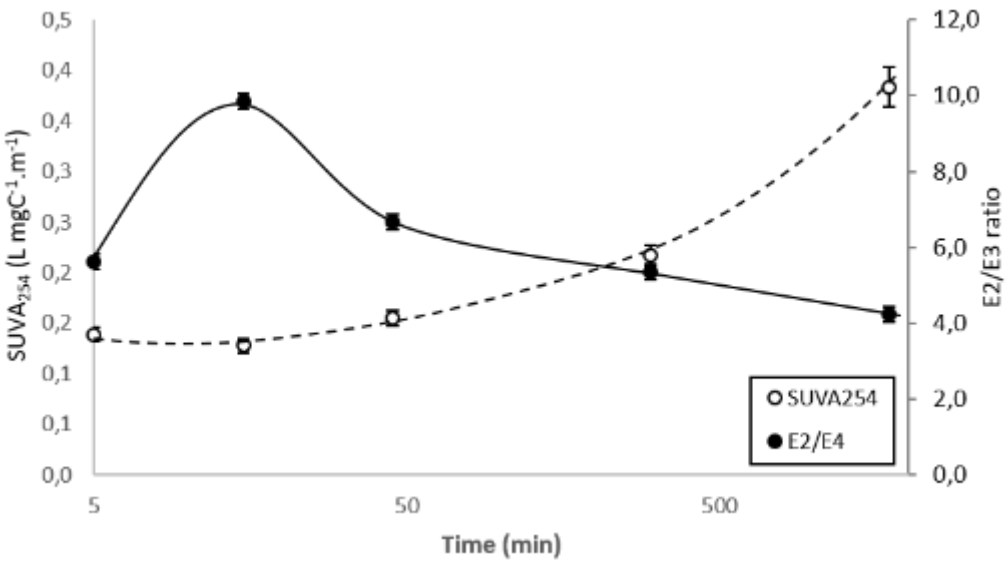

Figure 4.3-15. Evolution of the optical parameters SUV254 and E2/E4 in soil leachate with leaching time.

Typical fractograms of the colloidal phase (> 10 kDa) in soil leachate are presented in Figure 4.3-16 for five leaching times (5, 15, 45, 300 and 1740 minutes). The elution time from A4F-MALS is assigned to a gyration radius. The fractograms enable the "void peak" to be visualized. This peak is due to very diffusive entities, which size is lower than a few nanometers, and which are not lost during the focus step in A4F because of the pore size and/or membrane-analyte electrical repulsion. These fractograms observed for different leaching times are, overall, very close to those determined on the same soil sample in previous works (Hargindeguy et al., 2018).

The presence of carbonyl and aromatic groups (resp. C = O and C = C) in high concentration in the void peak is consistent with probable membrane/analyte repulsions. These groups appeared in a lesser abundance in the colloidal phase, especially in larger colloidal sizes.

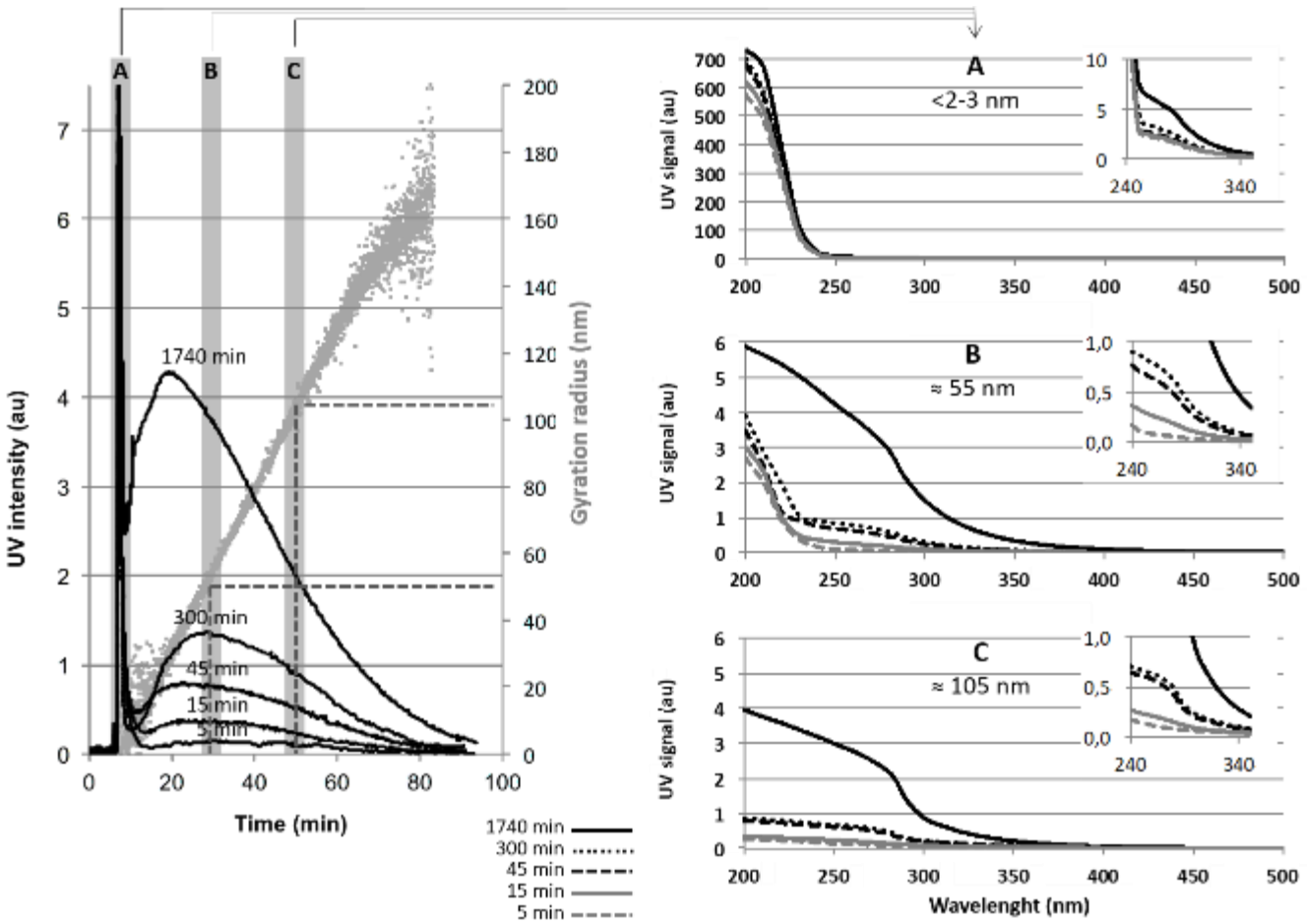

Figure 4.3-16. Typical fractograms of colloids from soil leachate, with gyration radius variation and UV spectra at different elution times and so corresponding to different gyration radius: A/ void peak (< 2-3 nm), B/ 30 min (≈ 55 nm) and C/ 50 min (≈ 110 nm) of elution. (*gyration radius variation corresponding 300 min leaching, the variation for the other durations being quasi-similar).*

UV absorption spectrum associated to respectively < 2-3 nm, ~55 nm and ~105 nm R_g colloidal fractions are presented next to the fractograms for selected leaching times (5, 15, 45, 300 and 1740 minutes). The shoulder at the absorbance band around 260 nm is characteristic for the presence of labile aromatic organic compounds (McKnight et al., 2001). This shoulder appeared to be more visible as the leaching time increased, correlatively to the increase in the UV peak total area, which is representative of the total concentration of colloids in leachate. Intermediate sized colloids (i.e. ≈ 55 nm) could consist of more labile organic compounds such as carbohydrates(Chen et al., 2002).

These observations suggest:

- the predominance of organic matter materials over the 2 – 200 nm range of colloid size, and particularly in larger colloids fractions (R_g > 50 nm) when leaching time increased, as shown by the progressive increasing of UV absorbance intensity at 260 nm (Figure 4.3-16),

- the increasing of OM content and aromaticity in larger colloids with increasing leaching time, suggesting an agglomeration of small-sized organic macromolecules during leaching experiment,
- the relative stability (in terms of structure and composition) of diffusive entities in the void peak (i.e. small organic colloids < 2-3 nm) over leaching time.

In summary, soil leachates were found to be mainly constituted by small-sized organic colloidal entities containing fulvic and humic substances of small molecular weight with significant aromaticity. OM colloids were leached continuously but changed in nature over leaching time. Indeed, at the beginning of the leaching process were mobilized low-molecular weight compounds (easily mobilizable) following by either (i) the mobilization of higher molecular weight compounds with increasing leaching time, or (ii) an agglomeration phenomenon of the small-sized compounds.

4.4 CONCLUSION

Uranium mobilization from a polluted soil was studied from batch leaching experiments. Although uranium speciation and mobility in natural environments are usually site-specific, a number of processes of general interest were observed.

Under moderately acidic conditions (pH ~4), about 2% of the initial mass of uranium was leached from soil after 29 hours of leaching. Mobilization of uranium from soil leaching was quite rapid but limited, confirming the low reversibility of uranium adsorption onto soil materials. This observation is consistent with previous studies conducted using the same soil (Crançon et al., 2010). The behavior or uranium in soil was strongly influenced by its speciation, particularly in relation with the distribution organic ligands between the solid, the colloidal and the dissolved phases, in association with Al and Fe complexolysis and eluviation processes. Leached uranium was found to be mainly distributed in the dissolved fraction. In the colloidal fraction, U is likely to be associated to small and medium-sized colloids with gyration radius ranging from about 20 to 170 nm. Maximum uranium leaching capacities estimated from kinetic modeling of leaching experiments are consistent with uranium concentrations observed in site groundwater and stream water downstream uranium deposits (Crançon et al., 2010). This suggests that uranium migration in subsurface is mainly controlled by leaching of medium- and small-sized (R_g < ~ 100 nm) organic colloidal entities. Similar observations were made for the uranium association with mobilizable organic complexes that enhance uranium mobility in soils from United Kingdom (Graham et al., 2011) or Southern Serbia (Radenkovic et al., 2008). These results highlight the importance of the small-sized supramolecular entities in the mobilization of uranium.

Soil leachate contained small-sized organic colloidal entities of low molecular weight containing fulvic and humic substances with significant aromaticity, released in soil porewater as a consequence of partial

decomposition of solid phase organic matter. Organic colloids were leached continuously but were likely to change in nature and size over leaching time. Indeed, at the beginning of the leaching process were mobilized low-molecular weight compounds (very labile) following by either (i) the mobilization of higher molecular weight compounds when leaching time increase, or (ii) an agglomeration phenomenon of the small-sized compounds in the leachate.

Mobilization kinetics orders were globally similar for U, Fe and Al in total and dissolved fractions, with relative apparent mobilization velocities from soil as follows: U > Fe > Al. TOC mobilization from soil in total and dissolved during leaching exhibits a singular behavior.

Dynamics of colloidal TOC, Fe and Al fractions mobilization from soil appeared to follow the same mobilization dynamics scheme. Apparent kinetic rates were quite identical for organic carbon, Fe and Al in colloidal fractions, suggesting that mechanisms controlling mobilization of these elements from soil by colloidal entities are correlated or identical.

This suggests a unique mechanism could not address the global mobilization of U, organic carbon, Al and Fe from soil, since different behaviors can be observed between dissolved and colloidal fractions. Nevertheless, kinetic modeling indicates that reversible sorption processes is mostly the rate-controlling step for the mobilization of U from soil, rather than a non-reactive transport of uranium from initial deposits, consistently with former observations (Harguindeguy et al., 2014).

Consequently, from an environmental point of view, the continuous leaching of uranium adsorbed on soil materials underlying deposits may act as a secondary source of pollution. Soil leaching by rainfall infiltration should become the major contributor to the uranium concentrations observed in groundwater and stream waters downstream of the deposit area.

REFERENCES

Abdelouas, A., Lutze, W., Nuttall, E., 1998. Chemical reactions of uranium in ground water at a mill tailings site. Journal of Contaminant Hydrology, 34: 343-361.

Aiken, G., 2014. Fluorescence and Dissolved Organic Matter, In: 'Aquatic Organic Matter Fluorescence' 'Cambridge Environmental Chemistry Series'. Cambridge University Press, pp. 35-74.

Andersson, S., Porcelli, D., Gustafsson, Ö., Ingri, J., Wasserburg, G.J., 2001. The importance of colloids for the behaviour of uranium isotopes in the low-salinity zone of a stable estuary. Geochimica et Cosmochimica Acta, 65(1): 13-25.

Artinger, R. et al., 2002. Humic colloid-borne migration of uranium in sand columns. Journal of Contaminant Hydrology, 58(1-2): 1-12.

Baalousha, M., Motelica-Heino, M., Galaup, S., Le Coustumer, P., 2005. Supramolecular structure of humic acids by TEM with improved sample preparation and staining. Microscopy Research and Technique, 66: 299-309.

Barnett, M.O., Jardine, P.M., Brooks, S.C., Selim, H.M., 2000. Adsorption and transport of uranium (VI) in subsurface media. Soil Sci. Soc. Am. J., 64: 908-917.

Bednar, A.J. et al., 2007. Effects of organic matter on the distribution of uranium in soil and plant matrices. Chemosphere, 70: 237-247.

Benes, P., Kratzer, K., Vlckova, S., Sebestova, E., 1998. Adsorption of uranium on clay and the effect of humic substances. Radiochimica Acta, 82(367-373).

Blanchard, G., Maunaye, M., Martin, G., 1984. Removal of heavy metals from waters by means of natural zeolites. Water Res., 18: 1501-1507.

Bottcher, J., Strebel, O., Lauer, S., 1997. Spatial variability of groundwater solute concentrations at the water table level under a pine stand on sandy soil with deep ground water. Zeitschrift fur Pflanzenernahrung und Bodenkunde, 160(1): 62-72.

Braithwaite, A., Livens, F.R., Richardson, S., Howe, M.T., 1997. Kinetically controlled release of uranium from soils. European Journal of Soil Science, 48: 661-673.

Brown, P.L., Guerin, M., Hankin, S.I., Lowson, R.T., 1998. Uranium and other contaminant migration in groundwater at a tropical Australian uranium mine. Journal of Contaminant Hydrology, 35(295-303).

Buckau, G. et al., 2000. Origin and mobility of humic colloids in the Gorleben aquifer system. Applied Geochemistry, 15: 171-179.

Buffle, J., Perret, D., Newman, M., 1992. The use of filtration and ultrafiltration for size fractionation of aquatic particle, colloids and macromolecules. In: Buffle, J., Van Leuwen, H.P. (Eds.), Environmental Particles. Lewis, pp. 171-230.

Cachoir, C., Gallien, J.P., Trocellier, P., 1996. Chemical durability of uranium dioxide stored in geologic medium : Uranium remobilisation. Annales de Chimie-Science des Matériaux, 21(8): 567-592.

Camus, H. et al., 1999. Long-term contaminant migration and impacts from uranium mill tailings. Journal of Environmental Radioactivity, 42: 289-304.

Chen, J., Gu, B., LeBoeuf, E.J., Pan, H., Dai, S., 2002. Spectroscopic characterization of the structural and functional properties of natural organic matter fractions. Chemosphere, 48: 59-68.

Chen, J., LeBoeuf, E.J., Dai, S., Gu, B., 2003. Fluorescence spectroscopic studies of natural organic matter fractions. Chemosphere, 50: 639-647.

Choppin, G.R., 2006. Actinide speciation in aquatic systems. Marine Chemistry, 99(83-92).

Claveranne-Lamolere, C. et al., 2011. Investigation of uranium-colloid interactions in soil by dual field-flow fractionation/capillary electrophoresis hyphenated with inductively coupled plasma-mass spectrometry. Talanta, 85: 2504-2510.

Coble, P.G., 1996. Characterization of marine and terrestrial DOM in seawater using excitation emission matrix spectroscopy. Mar. Chem., 51: 325-346.

Cory, R.M., Miller, M.P., McKnight, D.M., Guerard, J.J., Miller, P.L., 2010. Effect of instrument-specific response on the analysis of fulvic acid fluorescence spectra. Limnology and Oceanography: Methods 8: 67-78.

Crançon, P., Pili, E., Charlet, L., 2010. Uranium facilitated transport by water-dispersible colloids in field and soil columns. Science of the Total Environment, 408: 2118-2128.

Crançon, P., van der Lee, J., 2003. Speciation and mobility of uranium(VI) in humic-containing soils. Radiochim. Acta, 91: 673-679.

d'Orlyé, F., Reiller, P., 2011. Contribution of capillary electrophoresis to an integrated vision of humic substances size and charge characterizations. Journal of colloid and interface science, 368: 231-240.

Dabek-Zlotorzynska, E., Lai, E.P.C., Timerbaev, A.R., 1998. Capillary electrophoresis: the state-of-the-art in metal speciation studies. Analytica Chimica Acta, 359: 1-26.

De Windt, L., Burnol, A., Montarnal, P., van der Lee, J., 2003. Intercomparison of reactive transport models applied to UO2 oxidative dissolution and uranium migration. Journal of Contaminant Hydrology, 61: 303-312.

Del Nero, M., Salah, S., Miura, T., Clément, A., Gauthier-Lafaye, F., 1999. Sorption/desorption processes of uranium in clayey samples of the Bangombé natural reactor zone, Gabon. Radiochimica Acta, 87: 135-149.

Dhoum, R.T., Evans, G.J., 1997. Evaluation of uranium and arsenic retention by soil from a low level radioactive waste management site using sequential extraction. Applied Geochemistry, 13(4): 415-420.

Di Lella, L.A., Nannoni, F., Protano, G., Riccobono, F., 2005. Uranium contents and 235U/238U atom ratios in soil and earthworms in western Kosovo after the 1999 war. Science of the Total Environment, 337: 109-118.

Dubascoux, S., Le Hécho, I., Potin-Gautier, M., Lespes, G., 2008. On-line and off-line quantification of trace elements associated to colloids by As-Fl-FFF and ICP-MS. Talanta, 77(1): 60-65.

Echevarria, G., Sheppard, M.I., Morel, J.L., 2001. Effect of pH on the sorption of uranium in soils. Journal of Environmental Radioactivity, 53: 257-264.

El Hadri, H., Gigault, J., Chéry, P., Potin-Gautier, M., Lespes, G., 2014. Optimisation of flow field-flow fractionation for the characterization of natural colloids. Anal Bioanal Chem, 406(6): 1639-1649.

Faucher, S., Le Coustumer, P., Lespes, G., 2018. Nanoanalytics: history, concepts, and specificities. Environ. Sci. Pollut. Res.: 1-15.

Fetsch, D., Havel, J., 1998. Capillary zone electrophoresis for the separation and characterization of humic substances. Journal of Chromatography, A, 802: 189-202.

Fillela, M., 2007. Colloidal properties of submicron particles in natural waters, In: Environmental colloids and particles. Wiley, Hoboken, pp. 17-93.

Franke, K., Rössler, D., Gottschalch, U., Kupsch, H., 2000. Mobilization and retardation of uranium DOC species at three mines piles in Schlema/Alberoda, Saxony, Germany. Isotopes Environ. Health Stud., 36: 223-239.

Gabriel, U., Gaudet, J.P., Spadini, L., Charlet, L., 1998. Reactive transport of uranyl in a goethite column : an experimental and modelling study. Chemical Geology, 151(1-4): 107-128.

Giesler, R. et al., 2000. Distribution and mobilization of Al, Fe and Si in three podzolic soil profiles in relation to the humus layer. Geoderma, 94: 249-263.

Gigault, J., Grassl, B., Lespes, G., 2012. Size characterization of the associations between carbon nanotubes and humic acids in aqueous media by asymmetrical flow field-flow fractionation combined with multiangle light scattering. Chemosphere, 86: 177-182.

Graham, M.C., Oliver, I.W., MacKenzie, A.B., Ellam, R.M., Farmer, J.G., 2008. An integrated colloid fractionation approach applied to the characterisation of porewater uranium-humic interactions at a depleted uranium contaminated site. Science of the Total Environment, 404: 207-217.

Graham, M.C., Oliver, I.W., MacKenzie, A.B., Ellam, R.M., Farmer, J.G., 2011. Mechanisms controlling lateral and vertical porewater migration of depleted uranium (DU) at two UK weapons testing sites. Science of the Total Environment, 409: 1854-1866.

Grenthe, I. et al., 1992. Chemical Thermodynamics of Uranium. North Holland, Amsterdam, 711 pp.

Guillaumont, R. et al., 2003. Update on the chemical thermodynamics of uranium, neptunium, americium, and technetium. Elsevier, Amsterdam, OECD Nuclear Energy Agency, 919 pp.

Guo, M., Chorover, J., 2003. Transport and fractionation of dissolved organic matter in soil columns. Soil Science, 168: 108-118.

Hamilton, E.I., 2001. Depleted uranium (DU): a holistic consideration of DU and related matters. Science of the Total Environment, 281(1-3): 5-21.

Handley-Sidhu, S. et al., 2009. Corrosion and transport of depleted uranium in sand-rich environments. Chemosphere, 77: 1434-1439.

Handley-Sidhu, S., Keith-Roach, M.J., Lloyd, J.R., Vaughan, D.J., 2010. A review of the environmental corrosion, fate and bioavailability of munition grade depleted uranium. Science of the Total Environment, 408: 5690-5700.

Hargindeguy, S., Crançon, P., Potin-Gautier, M., Pointurier, F., Lespes, G., 2018. Colloidal mobilization from soil and transport of uranium in (sub)-surface waters. Environmental Science and Pollution Research, In Press: 1-11.

Harguindeguy, S., Crançon, P., Pointurier, F., Potin-Gautier, M., Lespes, G., 2014. Isotopic investigation of the colloidal mobility of depleted uranium in a podzolic soil. Chemosphere, 103: 343-348.

Ho, C.H., Miller, N.H., 1985a. Adsorption of Uranyl species from bicarbonate solutions onto hematite particles. Journal of Colloids and Interface Science, 110(1): 165-171.

Ho, C.H., Miller, N.H., 1985b. Effect of humic acid on uranium uptake by hematite particles. J. Colloid Interface Science, 110(2): 165-171.

Ho, Y., 2006. Review of second-order models for adsorption systems. J. Hazard. Mater., 136: 681-689.

Kaiser, K., Zech, W., 1999. Release of natural organic matter sorbed to oxides and a subsoil. Soil Science Society of America Journal, 63(5): 1157-1166.

Kersting, A.B. et al., 1997. Laboratory and Field Studies Related to Radionuclide Migration at the Nevada Test Site. LA-13419-PR, Los Alamos National Laboratory, Los Alamos, New Mexico.

Kononova, M.M., Alexandrova, I.V., 1973. Formation of humic acids during plant residue humification and their nature. Geoderma, 9: 157-164.

Kretzschmar, R., Sticher, H., 1997. Transport of humic-coated iron oxide colloids in a sandy soil : influence of Ca2+ and trace metals. Environmental Science & Technology, 31(12): 3497-3504.

Labonne-Wall, N., Moulin, V., Villarem, J.P., 1997. Retention properties of humic substances onto amorphous silica : consequences for the sorption of cations. Radiochimica Acta, 79: 37-49.

Lagergren, S., Svenska, B.K., 1898. About the theory of so-called adsorption of soluble substances. Veternskapsakad Handl., 24: 1-39.

Lead, J.R., Wilkinson, K.J., 2006. Aquatic colloids and nanoparticles: Current knowledge and future trends. Environ. Chem., 3: 213-232.

Lenhart, J.J., Cabaniss, S.E., MacCarthy, P., Honeyman, B.D., 2000. Uranium (VI) complexation with citric, humic and fulvic acids. Radiochim. Acta, 88: 345-353.

Lenhart, J.J., Honeyman, B.D., 1999. Uranium(VI) sorption to hematite in the presence of humic acid. Geochimica et Cosmochimica Acta, 63(19/20): 2891-2901.

Lesher, E.K., Honeyman, B., Ranville, B., 2013. Detection and characterisation of uranium-humic complexes during 1-D transport studies. Geochim. Cosmochim. Acta, 109: 127-142.

Lespes, G., Gigault, J., Battu, S., 2015. Field flow fractionation, In: Analytical separation science. Wiley-VCH, Weinheim, pp. 1143-1176.

Lewis, J., Sjöstrom, J., 2010. Optimizing the experimental design of soil columns in saturated and unsaturated transport experiments. J.Contam. Hydrol., 115: 1-13.

Lind, O.C. et al., 2009. Solid state speciation and potential bioavailability of depleted uranium particles from Kosovo and Kuwait. Journal of Environmental Radioactivity, 100: 301-307.

Lundström, U.S., 1993. The role of organic acids in the soil solution chemistry of a podzolized soil. Journal of Soil Science, 44: 121-133.

Lundström, U.S., Van Breemen, N., Bain, D., 2000a. The podzolisation process, a review. Geoderma, 94(2-4): 91-107.

Lundström, U.S. et al., 2000b. Advances inunderstanding the podzolization process rsulting from a multidisciplinary study of three coniferous forest soils in the Nordic Countries. Geoderma, 94: 335-353.

Maher, K., Bargar, J.R., Brown, G.E., 2013. Environmental speciation of actinides. Inorganic Chemistry, 52: 3510-3532.

Marshall, J.D., Shimada, B.W., Jaffe, P.R., 2000. Effect of temporal variability in infiltration on contaminant transport in the unsaturated zone. Journal of Contaminant Hydrology, 46: 151-161.

Matthews, B.J.H., Jones, A.C., Theodorou, N.K., Tudhope, A.W., 1996. Excitation-emission-matrix fluorescence spectroscopy applied to humic acid bands in coral reefs. Marine Chemistry, 55: 317-332.

McBride, M.B., Spiers, G., 2001. Trace element content of selected fertilizers and dairy manures as determined by ICP-MS. Communications in Soil Science and Plant Analysis, 32(1-2): 139-156.

McDowell-Boyer, L., 1992. Chemical mobilization of micron-sized particles in saturated porous media under steady flow conditions. Environ. Sci. Technol., 26: 586-593.

McEachern, R.J., Taylor, P., 1998. A review of the oxidation of uranium dioxide at temperatures below 400 degrees Celsius. Journal of Nuclear Materials, 254(2-3): 87-121.

McKnight, D.M. et al., 2001. Spectrofluorometric characterization of dissolved organic matter for indication of precursor organic material and aromaticity. Limnology and Oceanography: Methods 46: 38-48.

Mibus, J., Sachs, S., Pfingsten, W., Nebelung, C., Bernhard, G., 2007. Migration of uranium(IV)/(VI) in the presence of humic acids in quartz sand: A laboratory column study. Journal of Contaminant Hydrology, 89: 199-217.

Montavon, G. et al., 2000. Complexation studies of UO22+ with humic acid at low metal ion concentrations by indirect speciation methods. Radiochim. Acta, 88: 17-24.

Moulin, V., Moulin, C., 1995. Fate of actinides in the presence of humic substances under conditions relevant to nuclear waste disposal. Applied Geochemistry, 10: 573-580.

Moulin, V., Moulin, C., 2001. Radionuclide speciation in the environment : a review. Radiochim. Acta, 89: 773-778.

Murphy, E.M., Zachara, J.M., Smith, S.C., Phillips, J.L., 1992. The sorption of humic acids to mineral surfaces and their role in contaminant binding. The Science of the Total Environment, 117/118: 413-423.

Murphy, E.M., Zachara, J.M., Smith, S.C., Phillips, J.L., Wlestma, T.W., 1994. Interaction of hydrophobic organic compounds with mineral-bound humic substances. Environ. Sci. Technol., 28(7): 1291-1299.

Murphy, R., Lenhart, J.J., Honeyman, B.D., 1999. The sorption of thorium(IV) and uranium(VI) to hematite in the presence of natural organic matter. Colloids and surfaces A: Physicochemical and Engineering Aspects, 157: 47-62.

Oliver, I.W., Graham, M.C., MacKenzie, A.B., Ellam, R.M., Farmer, J.C., 2007. Assessing depleted uranium(DU) contamination of soil, plants and earthworms at UK weapons testing sites. Journal of Environmental Monitoring, 9(7): 740-748.

Piccolo, A., 2001. The supramolecular structure of humic substances. Soil science, 166: 810-832.

Planken, K.L., Coelfen, H., 2010. Analytical ultracentrifugation of colloids. Nanoscale, 2: 1849-1869.

Pogliani, L., 2008. Pseudo-zero-order reactions. Reaction Kinetics and Catalysis Letters, 93(2): 187-191.

Radenkovic, M.B., Cupac, S.A., Joksic, J.D., Todorovic, D.J., 2008. Depleted uranium mobility and fractionation in contaminated soil (Southern Serbia). Env. Sci. Pollut. Res., 15: 61-67.

Ragnarsdottir, K.V., Charlet, L., 2000. Uranium behaviour in natural environments, Environmental Mineralogy. (Eds. Cotter-Howells J., Batchelder M.,Valsami-Jones E.) - Mineral. Soc. of Great Britain and Ireland, London, pp. 333-377.

Ranville, J.F., Hendry, M.J., Reszat, T.N., Xie, Q., Honeyman, B.D., 2007. Quantifying uranium complexation by groundwater dissolved organic carbon using asymmetrical flow field-flow fractionation. Journal of Contaminant Hydrology, 91: 233-246.

Reemtsma, T., Bredow, A., Gehring, M., 1999. The nature and kinetics of organic matter release from soil by salt solutions. European Journal of Soil Science, 50(1): 53-64.

Reiller, P., 2010. Bilan prospectif sur l'influence de la complexation par la matière organique sur l'effet accélérant ou retard du transport des radionucléides : cas de la rétentiond es substances humiques. CEA-R-6255, Commissariat à l'Energie Atomique.

Reiller, P., 2015. Structure-reactivity relationships in the interactions between humic substances, pollutants from the nuclear cycle, and mineral surfaces. CEA-R-6407, Commissariat à l'Energie Atomique.

Reiller, P., Amekraz, B., Moulin, C., 2006. Sorption of Aldrich Humic Acid onto Hematite : Insights into fractionation phenomena by electrospray ionisation with quadrupole time-of-flight mass spectrometry. Environ. Sci. Technol., 40: 2235-2241.

Reiller, P., Buckau, G., 2012. Impacts of humic substances on the geochemical behaviour of radionuclides, In: Radionuclide Behaviour in the Natural Environment: Science, Implications and Lessons for the Nuclear Industry, pp. 103-160.

Ribera, D., Labrot, F., Tisnerat, G., Narbonne, J.F., 1996. Uranium in the environment: occurence, transfer and biological effects. Reviews of Environmental Contamination and Toxicology, 16: 53-89.

Riise, G., Salbu, B., Vogt, R.D., Ranneklev, S.B., Mykkelbost, T.C., 1994. Mobility of humic substances, major and minor elements in lake Skjervatjern and its catchment area. Environ. Int., 20: 287-298.

Riise, G., Van Hees, P., Lundstrom, U., Strand, L.T., 2000. Mobility of different size fractions of organic carbon, Al, Fe, Mn and Si in podzol. Geoderma, 94(2-4): 237-247.

Roh, Y., Lee, S.R., Choi, S.K., Elless, M.P., Lee, S.Y., 2000. Physicochemical and Mineralogical Characterization of Uranium-Contaminated Soils. Soil and Sediments Contamination, 9(5): 463-486.

Salim, R., Cooksey, B., 1981. The Effect of Centrifugation on the Suspended Particles of River Waters. Water Res., 15: 835-839.

Sansone, U. et al., 2001a. Radioecological survey at selected sites hit by depleted uranium ammunitions during the 1999 Kosovo conflict. Science of the Total Environment, 281(1-3): 23-35.

Sansone, U. et al., 2001b. Levels of depleted uranium in Kosovo soils. Radiation Protection Dosimetry, 97(4): 317-320.

Schimmack, W., Gerstmann, U., Schultz, W., Geipel, G., 2007. Long-term corrosion and leaching of depleted uranium (DU) in soil. Radiat. Environ. Biophys., 46: 221-227.

Schnitzer, M., Khan, S.U., 1972. Humic substances in the environment. Books in soils and the environment. Marcel Dekker, New York.

Schultz, M.K., Burnett, W.C., Inn, K.G.W., 1998. Evaluation of a sequential extraction method for determining actinide fractionation in soils and sediments. Environ. Radioact., 40: 155-174.

Schurtenberg, P., Newman, M.E., 1993. Characterization of biological and environmental particles using static and dynamic light scattering, Environmental Particles, In: Environmental Particles. IUPAC Environmental Analytical and Physical Chemistry Series, Lewis, Boca Raton, pp. 37-115.

Seta, A.K., Karathanasis, A.D., 1997. Stability and transportability of water-dispersible soil colloids. Soil Science Society of America Journal, 61(2): 604-611.

Sinke, A.J.C., Dury, A.J.C., Zobrist, J., 1998. Effects of a fluctuating water table : column study on redox dynamics and fate of some organic pollutants. Journal of Contaminant Hydrology, 33(1-2): 231-246.

Small, H., 1974. Hydrodynamic chromatography. A technique for size analysis of colloidal particles. J. Col. Int. Sci., 48(147-161).

Srivastava, V.C., Swamy, M.M., Mall, I.D., Prasad, B., Mishra, I.M., 2009. Adsorptive removal of phenol by bagasse fly ash and activated carbon: Equilibrium, kinetics and thermodynamics. Colloids Surf. Physicochem. Eng. Asp., 272: 89-104.

Tessier, A., Campbell, P.G.C., Bisson, M., 1979. Sequential extraction procedure for the speciation of trace metals. Anal. Chem., 51: 844-851.

Toque, C., Milodowski, A.E., Baker, A.C., 2014. The corrosion of depleted uranium in terrestrial and marine environments. Journal of Environmental Radioactivity, 128: 97-105.

Traina, S.J., Novak, J., Smeck, N.E., 1990. An Ultraviolet Absorbance Method of Estimating the Percent Aromatic Carbon Content of Humic Acids. Journal of Environmental Quality 19: 151-153.

UNEP, 2001. Depleted uranium in Kosovo, post-conflict environmental assessment, United Nations Environment Program, Switzerland.

Ure, A.M., Quevauviller, P., Muntau, H., Griepink, B., 1993. Speciation of heavymetals in soils and sediments - an account of the improvement and harmonization of extraction techniques undertaken under the auspices of the BCR of the Commission-of-the-European-Communities. Int. J. Environ. Anal. Chem. Geol., 51: 135-151.

Waite, T.D., Davis, J.A., Fenton, B.R., Payne, T.E., 2000. Approaches to modelling uranium(VI) adsorption on natural mineral assemblages. Radiochim. Acta, 88: 687-693.

Wang, Y. et al., 2013. Mobile uranium(IV)-bearing colloids in a mining-impacted wetland. Nature communications, 4:2942: 1-9.

Wei, M. et al., 2007. Interaction between uranium and humic acid (1): Adsorption behaviors of U(VI) in soil humic acids. Nuclear Science and Techniques, 18(5): 287-293.

Weishaar, J.L. et al., 2003. Evaluation of Specific Ultraviolet Absorbance as an Indicator of the Chemical Composition and Reactivity of Dissolved Organic Carbon. Environ. Sci. Technol., 37: 4702-4708.

Welch, A.H., Lico, M.S., 1998. Factors controlling As and U in shallow ground waters, southern Carson Desert, Nevada. Applied Geochemistry, 13(4): 521-539.

Zeh, P., Czerwinski, K.R., Kim, J.I., 1997. Speciation of uranium in Gorleben groundwaters. Radiochimica Acta, 76: 37-44.

Zheng, Z.P., Wan, J.M., 2005. Release of contaminant U(VI) from soils. Radiochim. Acta, 93(4): 211-217.

5) CONCLUSION ET PERSPECTIVES

Ce travail de thèse a été consacré à la caractérisation des phases porteuses, plus particulièrement organiques, de l'uranium permettant sa remobilisation dans une eau de sol au sein d'un site d'intérêt présentant un sol particulier : le podzol des Landes de Gascogne.

Parce que les eaux naturelles, notamment les eaux souterraines, peuvent être très faiblement concentrées en entités colloïdales qui s'avèrent pourtant être un vecteur de contamination significatif, une étape de préconcentration doit parfois être appliquée en amont de l'analyse proprement dite. Cependant, cette étape est susceptible de générer une modification de la phase colloïdale, et par là même d'induire des biais dans l'étude des associations colloïdes-uranium. C'est pourquoi, l'une des premières étapes de cette étude a été d'évaluer et comparer différentes méthodes de séparation membranaire utilisées pour concentrer la phase colloïdale.

La matière organique a été identifiée comme un fort complexant des radionucléides et jouant un rôle déterminant dans le transport colloïdal de l'uranium sur de longues distances. Faisant suite à de précédentes études sur la migration de l'uranium au sein de ce même site d'intérêt, nous avons choisi dans le présent travail de nous intéresser à la caractérisation de la structure moléculaire de la matière organique constitutive de différentes eaux de sol afin de déterminer s'il existe une évolution spatiale des composés organiques le long du profil de sol (c'est-à-dire avec la profondeur). Cette évolution spatiale correspond également à une évolution temporelle, que nous avons voulu caractériser de manière plus approfondie au sein de l'horizon superficiel, via un suivi temporel de la remobilisation des espèces colloïdales et dissoutes depuis la phase solide vers la phase aqueuse en se focalisant plus particulièrement sur l'uranium, le carbone organique, le fer et l'aluminium.

5.1 PRINCIPAUX RESULTATS

En conséquence et via la mise en place de différentes stratégies d'expérimentations et de caractérisation, ce travail de recherche a permis de répondre à différentes questions :

- Quel est l'impact de l'utilisation d'une méthode de préconcentration sur la phase colloïdale d'une eau de sol, en termes de morphologie et de structure ? Et quelles sont ses conséquences pour l'étude de la phase colloïdale d'une eau de sol ?

- Quelles sont les structures moléculaires de la matière organique constitutive des eaux du sol ? Y-a-t-il une évolution le long du profil de sol ?

- Quelle est la dynamique de mobilisation colloïdale de l'uranium depuis le sol vers la phase aqueuse ? Quelles sont les caractéristiques morphologiques et structurelles de la phase colloïdale au cours du temps ? Y-a-t-il une évolution temporelle dans la distribution de l'uranium et des composants majeurs entre compartiments colloïdal et dissous ?

La comparaison de différentes méthodes de séparation membranaire pour la préconcentration de la phase colloïdale de l'eau de sol a mis en évidence que, quelle que soit la méthode utilisée, une préconcentration engendre une modification des paramètres intrinsèques des entités colloïdales :

- La distribution en taille de ces entités : celle-ci se trouve décalée vers des tailles plus grandes et l'ampleur de ce décalage diffère selon la méthode utilisée. Ainsi il est plus important pour la méthode frontale, plus limité pour l'ultrafiltration tangentielle et centrifuge. Les conséquences potentielles peuvent être un biais dans l'appréhension de la réactivité de ces phases vis-à-vis des autres espèces et aussi de la mobilité de certains éléments, dont l'uranium. La formation d'agrégats lors de cette étape peut également mener à mal apprécier les mécanismes de complexation/adsorption ayant lieu à la surface des entités colloïdales mais aussi la stabilité de la phase colloïdale dans l'eau de sol.

- La distribution des espèces entre les phases colloïdale et dissoute : celle-ci semble moins impactée, en particulier après ultrafiltration centrifuge. Des taux de recouvrement proches de 100% ont en effet été obtenus, excepté pour l'ultrafiltration tangentielle qui a tendance à favoriser l'adsorption de matière sur les parois de son système de filtration. En revanche, un enrichissement des espèces chimiques suivies est observé dans le concentrat par sorption des formes dissoutes, et ce, quelle que soit la méthode de préconcentration utilisée. Cet enrichissement est particulièrement significatif pour la matière organique, et après ultrafiltration frontale et tangentielle.

In fine, l'ultrafiltration centrifuge est la méthode qui paraît être le meilleur compromis entre une efficacité de préconcentration et la conservation de l'intégrité physico-chimique de la phase colloïdale.

La double caractérisation fonctionnelle et moléculaire de la matière organique présente dans l'eau du sol a permis d'appréhender que :

- Elle contient majoritairement des composés de type CHO et CHON et peu de composés soufrés.

- Elle est constituée de molécules organiques de type acides fulviques et humiques dont la taille apparaît être inférieure à 1 kDa. Elle est d'origine terrestre et garde dans sa structure la trace des conditions physico-chimiques de croissance des plantes dont elle est dérivée (c'est-à-dire un pH très acide). En particulier, l'aromaticité qui paraît faible au regard des valeurs obtenues dans d'autres études mais qui est liée à la très faible dégradation microbienne de

la matière organique. La nature même du sol d'intérêt a donc un fort impact sur la nature et la structure de la matière organique, et en conséquence sur la mobilisation de l'uranium.

- Ces petites molécules organiques sont mobilisées très rapidement et de manière continue lors d'une lixiviation mais tendent ensuite à s'agglomérer au cours de la lixiviation, formant alors des assemblages colloïdaux mixtes, enrobant des particules inorganiques. Dans ce cas, que l'uranium soit complexé à la matière organique et/ou à des particules colloïdales inorganiques n'aurait pas d'incidence sur sa mobilité. La formation de larges assemblages mixtes pourrait en revanche favoriser son transport par effet stérique.

- La composition moléculaire est cependant variable. Une évolution de la nature et de la structure moléculaire de la matière organique a en effet été mise en évidence le long du profil de sol, c'est-à-dire avec la profondeur. Cela a permis d'identifier différents processus géochimiques ayant lieu au sein du podzol et pouvant avoir un impact sur la mobilisation et le transport de l'uranium. En particulier, nous avons observé une dégradation oxydative de la matière organique en subsurface, des processus de réduction et de dénitrification avec la profondeur, donnant lieu à l'apparition de composés organiques pauvres en oxygène mais enrichis en azote réduit. L'horizon d'accumulation présente à ce titre une composition moléculaire particulière avec notamment une plus forte abondance en composés polaires. Cela peut être le résultat des conditions géochimiques particulières qui existent au sein de cet horizon et qui varient énormément selon le niveau de l'aquifère.

- L'évolution de la matière organique est également observée à l'échelle de l'horizon superficiel. Sa nature et sa taille sont en effet susceptibles de varier au cours du temps. On voit ainsi apparaître différents chromophores durant son processus de remobilisation dans l'eau de sol. De la même manière, au début de la lixiviation sont générées des phases colloïdales labiles et de petites tailles qui voient ensuite leur taille augmenter en conséquence d'un phénomène d'agglomération et/ou de la mobilisation de plus gros composés colloïdaux.

- La nature particulière du podzol ainsi que le battement régulier de la nappe superficielle ont un impact important sur la nature de la MO. On voit en effet beaucoup plus de composés organiques contenant de l'azote dans les horizons plus profonds, où ont lieu des processus de dénitrification.

L'étude de la mobilisation des éléments et espèces d'intérêt (c'est-à-dire U, COT, Fe, Al) dans l'eau de sol confirme la libération et/ou la formation d'entités colloïdales au cours du processus de lixiviation. Elle met néanmoins en évidence des mécanismes de mobilisation qui diffèrent selon l'élément :

- L'uranium est rapidement mobilisé mais de manière limitée. Après 29h de lixiviation, seul 2% de l'uranium du sol se retrouvent dans la phase aqueuse. Cela confirme la faible réversibilité de l'adsorption de U sur la matrice du sol. L'uranium lixivié est présent majoritairement dans la fraction inférieure à 10kDa ; dans la fraction colloïdale il est associé à des entités dont les rayons sont compris entre 20 et 170 nm.
- Les ordres de cinétique de mobilisation de l'uranium, du fer et de l'aluminium en total et dans la phase dissoute sont similaires. En revanche, le COT dans la suspension en total et dans la phase dissoute présente une mobilisation différente. Les éléments sous forme dissoute ne seraient donc pas influencés par la mobilisation de la matière organique dissoute.
- En revanche, le COT, l'aluminium et le fer colloïdaux suivent une même dynamique de mobilisation, avec des constantes de cinétiques similaires. Les mécanismes qui contrôlent leur mobilisation sont donc liés entre eux, voire identiques.
- Il résulte de ces observations qu'il n'existe pas un mécanisme unique de mobilisation de l'uranium, de la matière organique, du fer et de l'aluminium car ces éléments et espèces chimiques présentent des comportements différents selon leur nature colloïdale ou dissoute.

Les résultats de ce travail confirment que la matière organique joue un rôle prédominant dans la remobilisation de l'uranium depuis le sol mais n'a cependant pas un contrôle total de ce processus. De plus, le processus de sorption réversible de l'uranium, même s'il est limité, a été identifié comme déterminant dans la mobilisation de l'uranium, plutôt qu'un transport non-réactif des gisements initiaux.

Identifier le(s) processus responsables de la mobilisation de la phase colloïdale paraît donc être une question secondaire puisque les différentes espèces (U et composants majeurs) ne suivent pas les mêmes dynamiques de mobilisation et se retrouvent pourtant associées au sein de la phase aqueuse. Il serait en revanche intéressant d'étudier plus en détail les processus qui permettent aux complexes colloïdaux de rester stables dans les eaux souterraines, c'est-à-dire de ne pas être immobilisés, et d'estimer la pérennité de ces complexes dans le milieu jusqu'à l'aquifère où ils sont susceptibles de migrer plus facilement.

5.2 PERSPECTIVES

Certains aspects de la mobilisation colloïdale n'ont pas été pris en compte dans cette étude et pourraient l'être afin de contribuer à mieux définir l'ensemble des processus intervenant.

En particulier une étude cinétique beaucoup plus fine de ces processus permettrait de préciser les relations d'interdépendance des éléments et de la matière organique entre eux. Pour cela, un pas de temps plus petit et régulier (par exemple 5h au-delà d'1h) permettrait une plus grande précision et donc une meilleure fiabilité des ajustements cinétiques. La caractérisation moléculaire de la matière organique via l'analyse HRMS pour chacun de ces points de cinétique pourrait apporter également plus d'informations quant à l'évolution temporelle de la matière organique à l'échelle de l'horizon étudié. Il est également important de noter que dans le présent travail la phase colloïdale a été considérée de manière opérationnelle comme étant celle dans le continuum de tailles comprises entre 10kDa et 0,45µm. Or, les résultats obtenus dans ce travail de recherche qui ont permis à la fois d'identifier des espèces organiques dont la taille sont de l'ordre du kDa et de montrer que la majeure partie de l'uranium se trouve dans la fraction inférieure à 10 kDa. Il serait donc intéressant de « réajuster » l'échelle d'investigation pour caractériser de manière plus ciblée la « phase à l'interphase entre le dissous et le colloïdal » et son comportement de mobilisation pour appréhender *in fine* le transport colloïdal de l'uranium de manière plus fine.

Dans cette même optique, la comparaison de la structure moléculaire de la matière organique issue de ce podzol avec un autre podzol pourrait être intéressante pour déterminer l'influence des caractéristiques intrinsèques du sol sur la nature de la matière organique, et sur la mobilisation et le transport colloïdal de l'uranium. Il serait ainsi intéressant de comparer dans un premier temps la matière organique des horizons supérieurs de différents podzols pour identifier une éventuelle phase organique « type » qui serait responsable de la mobilisation et de la mobilité de l'uranium depuis le sol de surface vers l'horizon d'accumulation. Ceci permettrait de répondre à la question suivante : la matière organique impliquée dans la mobilisation de l'uranium est-elle identique à celle responsable de sa migration verticale le long du profil de sol et jusque dans l'aquifère ? En effet, si la matière organique change spatialement, comme on a pu le constater dans le présent travail de recherche, c'est que sa structure moléculaire n'a pas d'impact direct sur son association avec l'uranium. On peut alors supposer que des composés organiques (ou sites d'adsorption comme COO-) communs à toute matière organique de sol seraient responsables à la fois de la mobilisation et de la migration de l'uranium dans l'environnement.

Si la remobilisation de l'uranium et donc potentiellement son transport dépendent de la concentration et de la nature de la matière organique, alors il paraît primordial de considérer conjointement la variabilité temporelle et spatiale de la matière organique dès lors que l'on veut étudier la migration colloïdale de l'uranium.

Enfin, pour pouvoir poursuivre dans l'étude du transport colloïdal de l'uranium dans les sols et eaux souterraines, il est également important de faire le lien entre la mobilisation de l'uranium et sa mobilité au sein du milieu. Comme cette dernière dépend de la stabilité des complexes colloïdaux dans la phase aqueuse, étudier les facteurs influençant cette stabilité permettrait de compléter nos connaissances sur les conditions de migration de l'uranium et ainsi de mieux prévoir sa dispersion au sein de l'environnement. Obtenir de telles informations pourrait être possible en faisant varier les conditions de lixiviation lors d'un suivi cinétique ou bien en étudiant la mobilisation de l'uranium depuis des sols différents, avec une échelle d'investigation physico-chimique permettant d'appréhender les ligands entre dissous et colloïdal.

ANNEXES

Annexe 1 : Tableau récapitulatif des données de préconcentration

		Masse totale (g)		Al (µg)				Fe (µg)				U (µg)				COT (µg)			
		n°1	n°2	n°1	n°2	**Mean**	**SD**	n°1	n°2	**Mean**	**SD**	n°1	n°2	**Mean**	**SD**	n°1	n°2	**Mean**	**SD**
UFF	TOTAL	155,86	152,12	134,17	134,23	**135,9**	**2,4**	17,35	17,09	**17,4**	**0,1**	0,2736	0,2661	**0,2731**	**0,001**	3361,9	2835,5	**3098**	**372**
	Concentrat	28,44	20,68	42,75	36,25	**46,3**	**5,0**	7,86	5,26	**7,5**	**0,4**	0,0789	0,0549	**0,0772**	**0,002**	1293,6	1020,6	**1157**	**193**
	Filtrat	124,39	126,39	82,48	76,90	**79,1**	**4,8**	8,91	8,91	**8,8**	**0,1**	0,1662	0,1629	**0,1632**	**0,004**	1670,7	1682,4	**1676**	**8**
	Filtre	0,33	0,29	4,17	11,50	**8,8**	**6,5**	0,93	1,08	**1,1**	**0,2**	0,030	0,0378	**0,0371**	**0,010**	30	38	**34**	**6**
	TOTAL (%)	***100***	***100***	***100***	***100***	***100***	***0***	***100***	***100***	***100***	***0***	***100***	***100***	***100***	***0***	***100***	***100***	***100***	***0***
	Concentrat (%)	***18***	***14***	***32***	***27***	***29***	***3***	***45***	***31***	***38***	***10***	***29***	***21***	***25***	***6***	***38***	***36***	***37***	***2***
	Filtrat (%)	***80***	***83***	***61***	***57***	***59***	***3***	***51***	***52***	***52***	***1***	***61***	***61***	***61***	***0***	***50***	***59***	***55***	***7***
	Filtre (%)	***0***	***0***	***3***	***9***	***6***	***4***	***5***	***6***	***6***	***1***	***11***	***14***	***13***	***2***	***1***	***1***	***1***	***0***
	TOTAL Conc+Filtr	***98***	***97***	***93***	***84***	***89***	***6***	***97***	***83***	***90***	***10***	***90***	***82***	***86***	***5***	***88***	***95***	***92***	***5***
	RECOVERY (%)	***98***	***97***	***96***	***93***	***95***	***3***	***102***	***89***	***96***	***9***	***101***	***96***	***98***	***3***	***89***	***97***	***93***	***5***
UFT	TOTAL	152,64	151,89	131,40	134,03	**133,0**	**2,3**	16,99	17,07	**17,1**	**0,1**	0,2679	0,2657	**0,2674**	**0,001**	3292	2831	**3061**	**326**
	Concentrat	18,99	21,79	25,35	28,67	**25,2**	**0,3**	4,40	4,30	**4,1**	**0,5**	*0,042*	0,0491	**0,0424**	**0,001**	672	739	**706**	**48**
	Filtrat	127,74	118,31	89,72	74,92	**85,3**	**6,2**	10,18	8,98	**9,9**	**0,3**	0,1742	0,1552	**0,1709**	**0,005**	2047	1482	**1764**	**400**
	Filtre	5,93	4,92	5,58	3,82	**5,1**	**0,7**	0,80	0,60	**0,8**	**0,1**	0,0091	0,0084	**0,010**	**0,001**	480	500	**490**	**14**
	TOTAL (%)	***100***	***100***	***100***	***100***	***100***	***0***	***100***	***100***	***100***	***0***	***100***	***100***	***100***	***0***	***100***	***100***	***100***	***0***
	Concentrat (%)	***12***	***14***	***19***	***21***	***20***	***1***	***26***	***25***	***26***	***1***	***16***	***18***	***17***	***2***	***20***	***26***	***23***	***4***
	Filtrat (%)	***84***	***78***	***68***	***56***	***62***	***9***	***60***	***53***	***56***	***5***	***65***	***58***	***62***	***5***	***62***	***52***	***57***	***7***
	Filtre (%)	***4***	***3***	***4***	***3***	***4***	***1***	***5***	***4***	***4***	***1***	***3***	***3***	***3***	***0***	***15***	***18***	***16***	***2***
	TOTAL Conc+Filtr	***96***	***92***	***88***	***77***	***82***	***7***	***86***	***78***	***82***	***6***	***81***	***77***	***79***	***3***	***83***	***78***	***81***	***3***
	RECOVERY (%)	***100***	***95***	***92***	***80***	***86***	***8***	***91***	***81***	***86***	***7***	***84***	***80***	***82***	***3***	***97***	***96***	***97***	***1***
UFC	TOTAL	90,50	88,95	77,91	78,49	**78,9**	**1,4**	10,07	9,99	**10,1**	**0,1**	0,1589	0,1556	**0,1586**	**0,0004**	1952	1658	**1805**	**208**
	Concentrat	5,35	7,80	11,51	14,43	**10,7**	**1,1**	1,85	2,31	**1,7**	**0,2**	0,0173	0,0191	**0,0152**	**0,003**	95	118	**106**	**16**
	Filtrat	82,44	81,03	59,36	59,18	**59,8**	**0,6**	6,61	6,90	**6,8**	**0,3**	0,1137	0,1146	**0,1151**	**0,002**	1415	1219	**1317**	**139**
	Filtre	0,28	0,28	4,47	4,20	**4,4**	**0,1**	1,62	1,14	**1,4**	**0,3**	0,0227	0,0228	**0,0230**	**0,0003**	117	119	**118**	**1**
	TOTAL (%)	***100***	***100***	***100***	***100***	***100***	***0***	***100***	***100***	***100***	***0***	***100***	***100***	***100***	***0***	***100***	***100***	***100***	***0***
	Concentrat (%)	***6***	***9***	***15***	***18***	***17***	***3***	***18***	***23***	***21***	***3***	***11***	***12***	***12***	***1***	***5***	***7***	***6***	***2***
	Filtrat (%)	***91***	***91***	***76***	***75***	***76***	***1***	***66***	***69***	***67***	***2***	***72***	***74***	***73***	***1***	***73***	***74***	***73***	***1***
	Filtre (%)	***0***	***0***	***6***	***5***	***6***	***0***	***16***	***11***	***14***	***3***	***14***	***15***	***14***	***0***	***6***	***7***	***7***	***1***
	TOTAL Conc+Filtr	***97***	***100***	***91***	***94***	***92***	***2***	***84***	***92***	***88***	***6***	***82***	***86***	***84***	***2,5***	***77***	***81***	***79***	***2***
	RECOVERY (%)	***97***	***100***	***97***	***99***	***98***	***2***	***100***	***104***	***102***	***2***	***97***	***101***	***99***	***2,7***	***83***	***88***	***86***	***3***

Annexe 2: Compounds previously identified in lignin, natural organic matter and plants with unique chemical structures identified that correspond to unique molecular formulas identified in the sample (list of identified recalibrants).

Identity	Theor. m/z	m/z	Recal. m/z	Error (mDa)	Error (ppm)
Fumaric	115.00368	115.00386	115.00368	0	0
Levulinic	115.04007	115.04021	115.04003	0.035	0.308
Benzoic	121.0295	121.02969	121.02952	-0.015	-0.12
Hydroxyhexanoic	129.05572	129.05591	129.05574	-0.026	-0.203
Malic	133.01425	133.01445	133.01429	-0.04	-0.304
Hydroxybenzoic	137.02442	137.02459	137.02443	-0.013	-0.097
Coumalic	139.00368	139.00383	139.00367	0.009	0.066
Cinnamic	147.04515	147.0453	147.04515	0	0
Umbelliferone	161.02442	161.02451	161.02439	0.027	0.169
p-Coumaric	163.04007	163.04015	163.04003	0.033	0.201
Vanillic	167.03498	167.03508	167.03497	0.009	0.052
Esculetin	177.01933	177.01942	177.01933	0	0
Syringaldehyde	181.05063	181.05067	181.05059	0.045	0.247
Coumarin-3-carboxylic	189.01933	189.01939	189.01932	0.016	0.085
Scopoletin	191.03498	191.03504	191.03497	0.014	0.075
Quinic	191.05611	191.05612	191.05605	0.064	0.333
Acetosyringone	195.06628	195.06637	195.0663	-0.019	-0.097
Syringic	197.04555	197.04558	197.04551	0.034	0.174
Sinapic	223.0612	223.06124	223.0612	0	0
p-Hydroxy	243.06628	243.06627	243.06626	0.02	0.082
Dehydrovanillin-p-hy	271.0612	271.06115	271.0612	0	0
Vanillovanillone	273.07685	273.07672	273.07677	0.077	0.282
Vanillil	301.07176	301.07167	301.07176	0	0
Vanillosyringone	303.08741	303.08722	303.08732	0.094	0.311
Gallocatechol	305.06668	305.06649	305.06659	0.082	0.27

Identity	Theor. m/z	m/z	Recal. m/z	Error (mDa)	Error (ppm)
Dehydrovanillinvanillic	331.11871	331.1185	331.11871	0	0
Dehydrovanillin	345.06159	345.06139	345.06168	-0.091	-0.264
5-Syringoacetovanillone	345.09798	345.09783	345.09812	-0.146	-0.423
5-Syringovanillic	347.07724	347.07706	347.07736	-0.123	-0.354
autre1	353.0514	353.05126	353.05159	-0.19	-0.537
Chlorogenic	353.08781	353.08757	353.0879	-0.094	-0.267
autre2	357.098	357.09773	357.09807	-0.066	-0.186
autre3	359.1136	359.1133	359.11364	-0.035	-0.098
Syringil	361.09289	361.09256	361.09289	0	0
2-Syringlyacetosyringone	361.12928	361.129	361.12933	-0.054	-0.151
2-Syringlysyringic	363.10854	363.10825	363.10857	-0.031	-0.085
autre5	365.1606	365.16026	365.16057	0.032	0.087
autre6	367.1762	367.17611	367.1764	-0.201	-0.547
autre7	381.0827	381.0824	381.08251	0.186	0.489
autre8	395.0983	395.09832	395.0983	0	0
autre9	401.0878	401.08766	401.08764	0.163	0.407
autre10	407.1347	407.13458	407.13458	0.122	0.301
autre11	409.114	409.114	409.11401	-0.008	-0.02
autre15	415.1034	415.10342	415.10347	-0.066	-0.159
autre16	417.1191	417.11889	417.11895	0.15	0.361
autre17	421.0776	421.07757	421.07766	-0.055	-0.132
autre19	431.062	431.06187	431.062	0	0
autre20	433.0776	433.07746	433.07759	0.006	0.014
autre22	435.1296	435.12922	435.12936	0.242	0.557
autre23	439.1609	439.16082	439.16096	-0.065	-0.147
autre25	465.1038	465.10368	465.1038	0	0
autre26	477.1766	477.17708	477.17711	-0.506	-1.06
autre28	493.1715	493.17164	493.17164	-0.14	-0.284

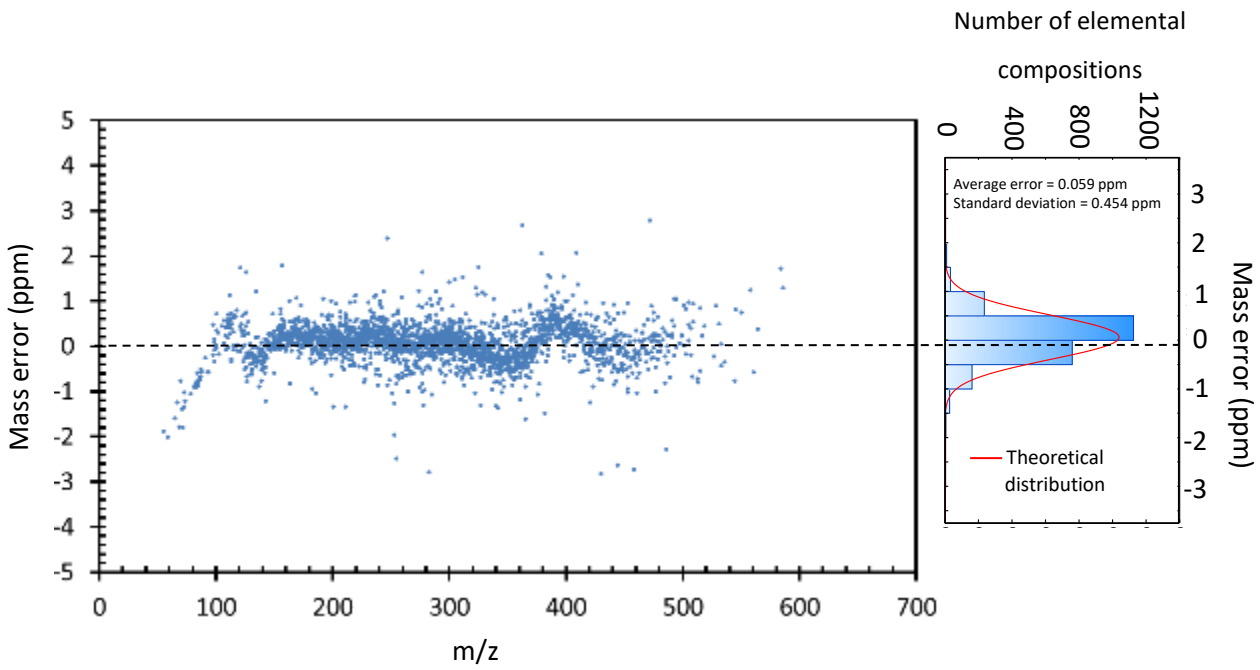

Annexe 3: Error distribution and Shapiro-Wilk tests for the analysis of the upper horizon soil A

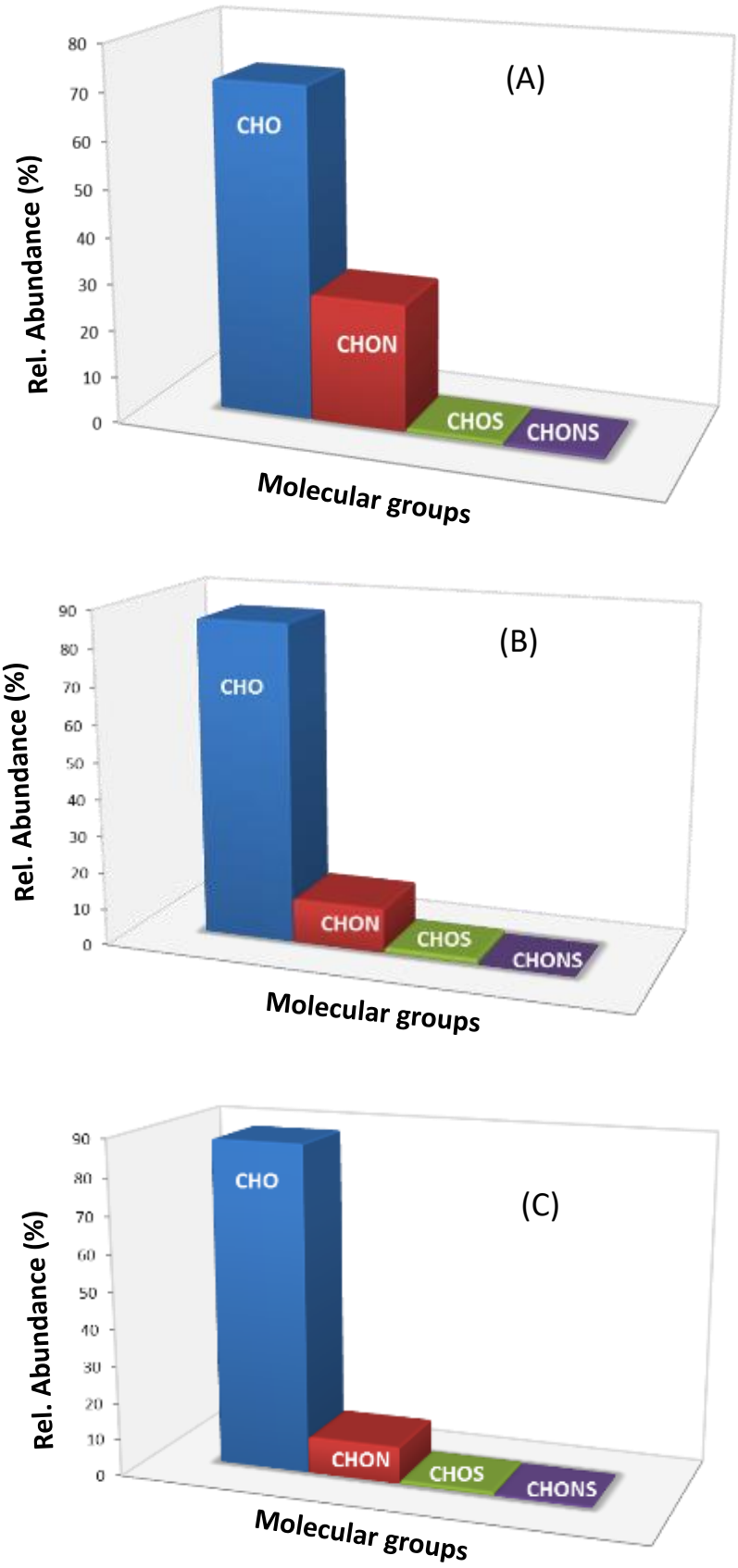

Annexe 4: Bar charts representing the relative abundance of each molecular group assigned (CHO, CHON, CHOS and CHONS) for the upper soil horizon (A), the illuvial horizon soil (B) and the groundwater sample (C).

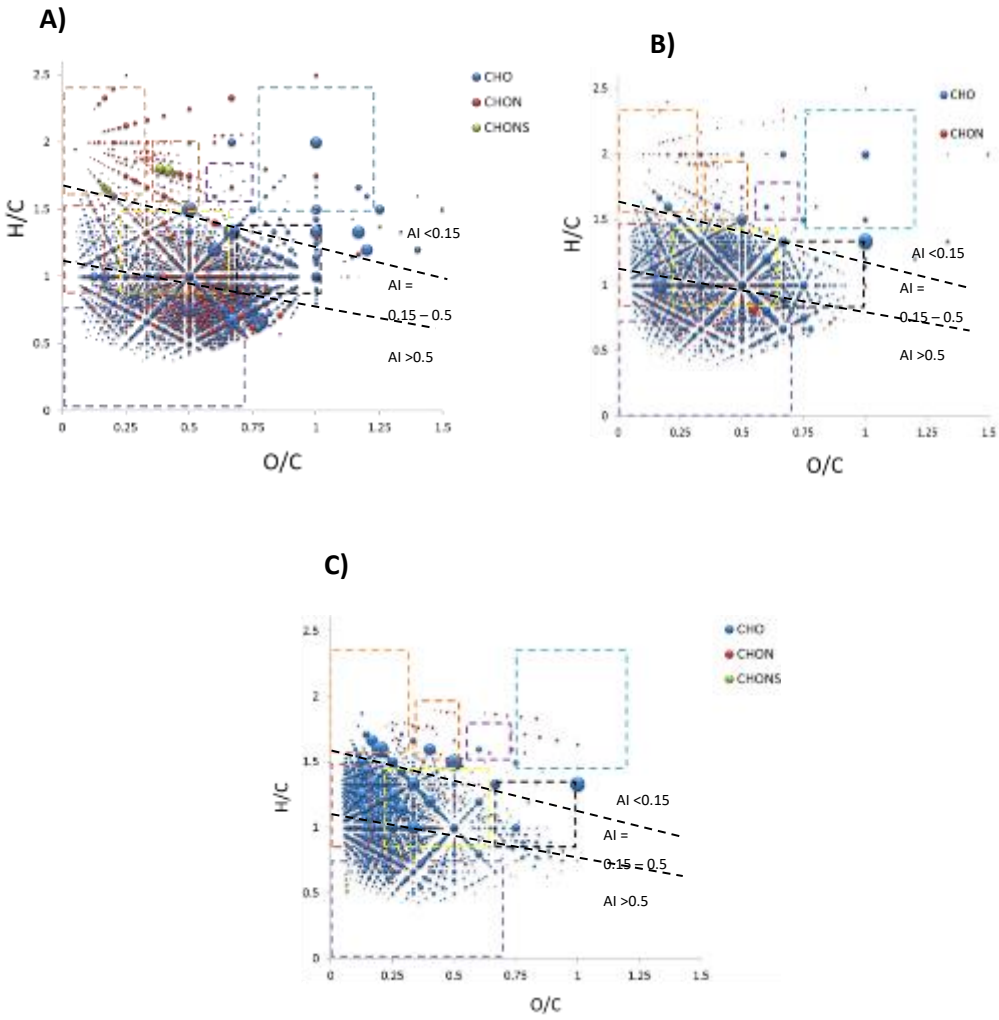

Annexe 5: Van Krevelen diagram of SOM compounds from the upper horizon soil (A), the illuvial horizon soil (B) and the groundwater sample, analyzed in ESI(-) (A-C).

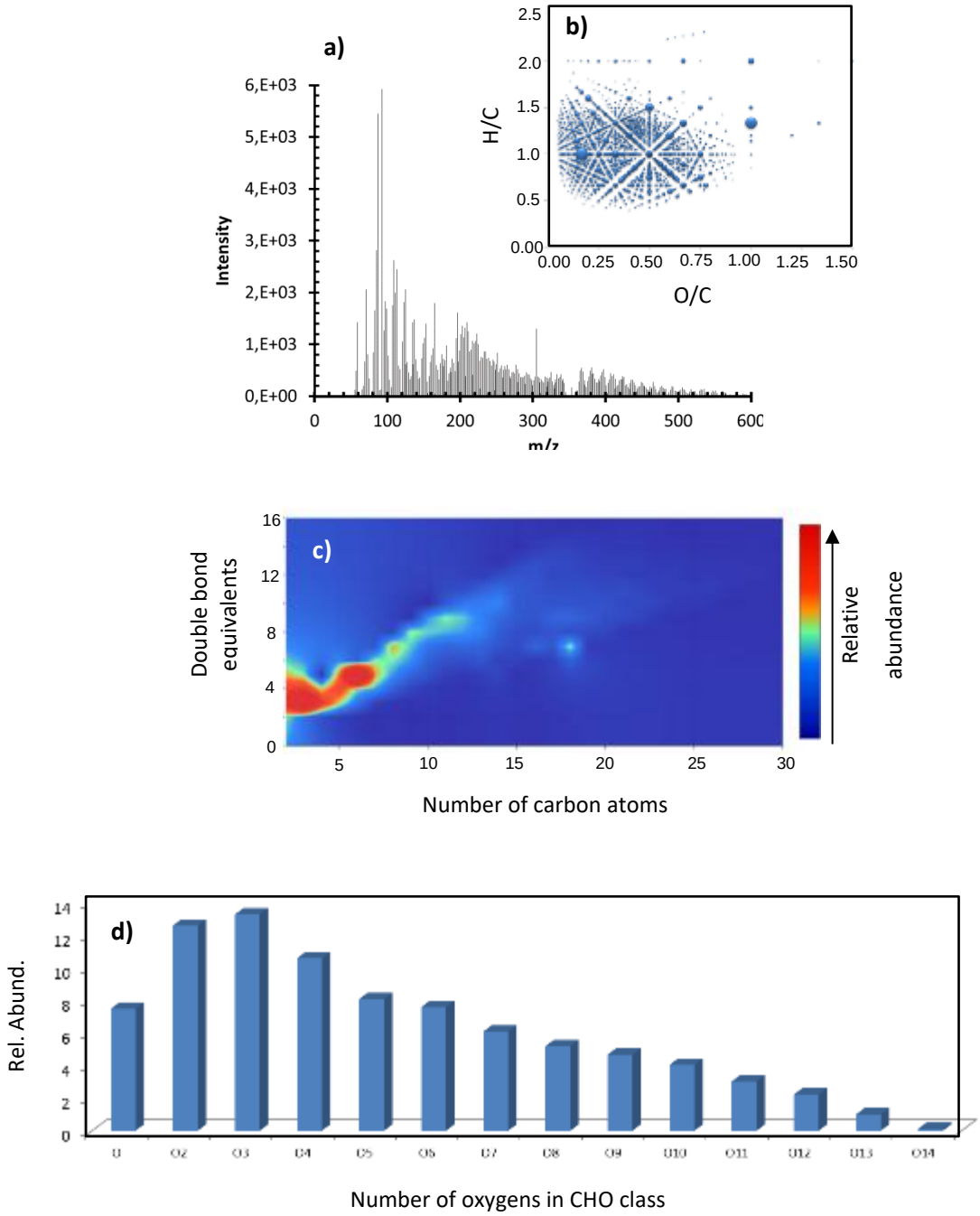

Annexe 6: Van Krevelen diagram of CHO compounds analyzed by ESI(-) from the illuvial horizon (a). Isoabundance plot of double bond equivalents (DBE) vs. number of carbon atoms in molecular formulas from the CHO class (b). Relative abundance (RA) of each subclass for illuvial horizon soil Bh CHO compounds (c).

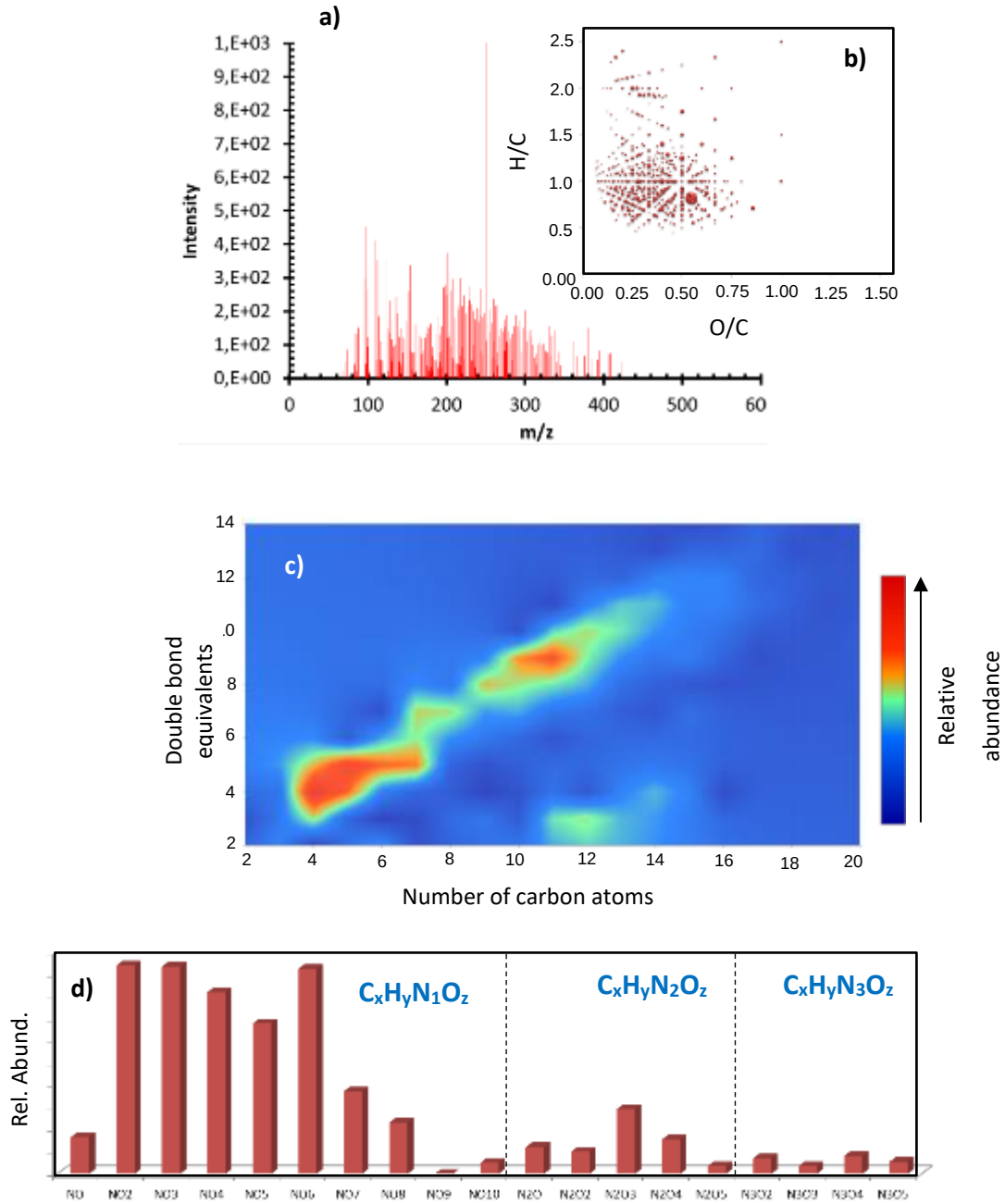

Annexe 7: Van Krevelen diagram of CHON compounds analyzed by ESI(-) from the illuvial horizon (a). Isoabundance plot of double bond equivalents (DBE) vs. number of carbon atoms in molecular formulas from the CHON class (b). Relative abundance (RA) of each subclass for illuvial horizon soil Bh CHON compounds (c).

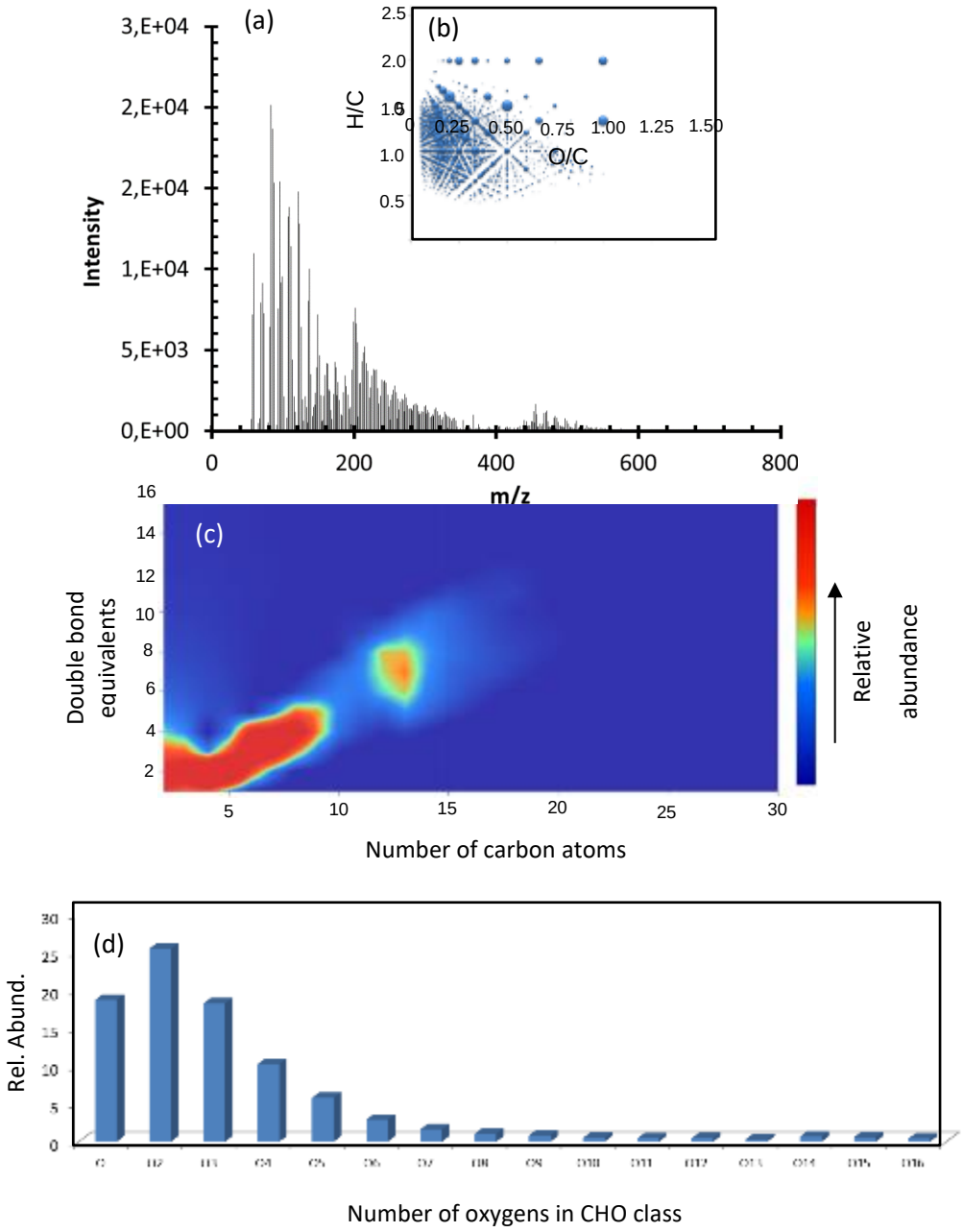

Annexe 8: Van Krevelen diagram of CHO compounds analyzed by ESI(-) from the underground water (a). Isoabundance plot of double bond equivalents (DBE) vs. number of carbon atoms in molecular formulas from the CHO class (b). Relative abundance (RA) of each subclass for the underground water CHO compounds (c).

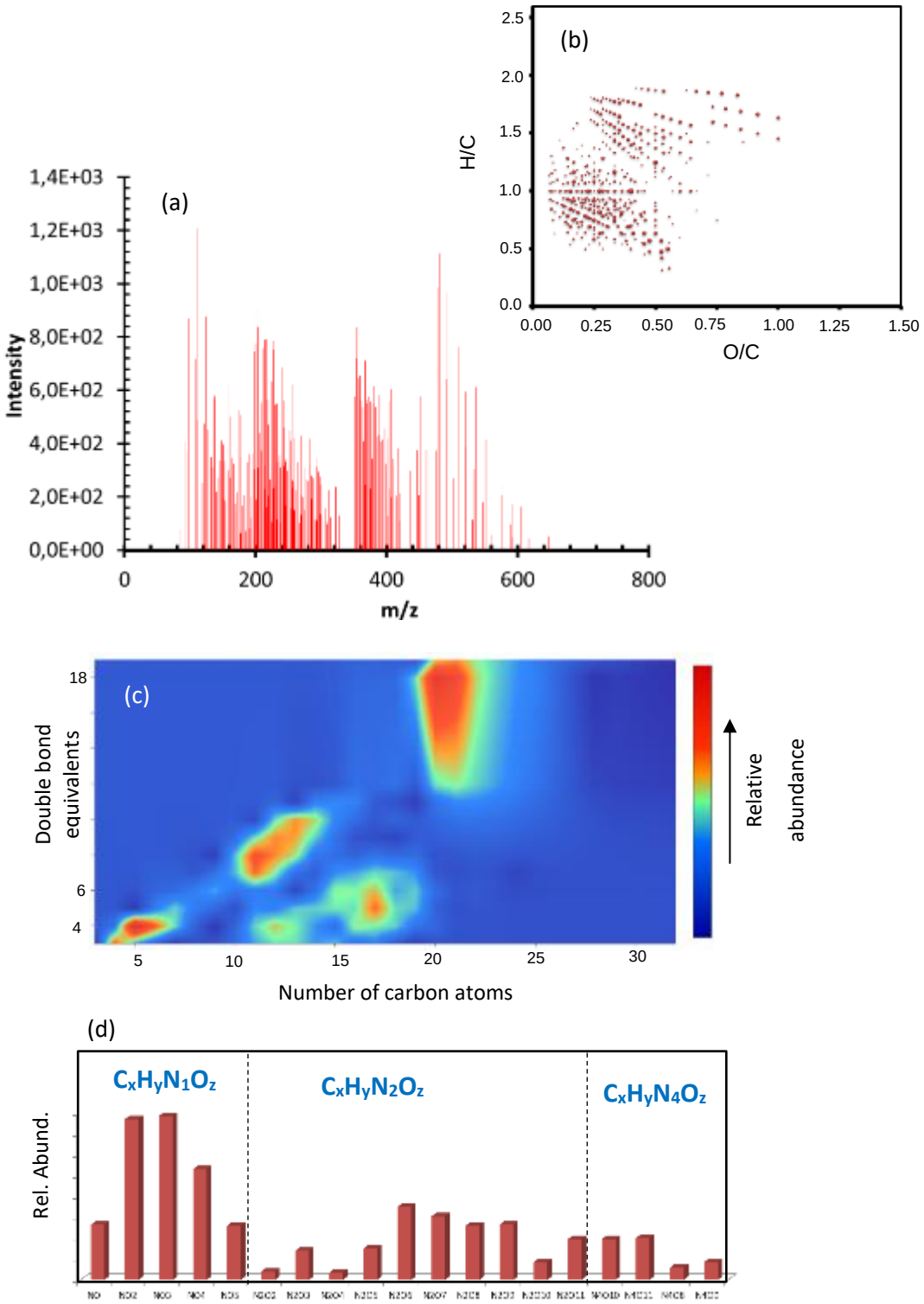

Annexe 9: Van Krevelen diagram of CHON compounds analyzed by ESI(-) from the underground water (a). Isoabundance plot of double bond equivalents (DBE) vs. number of carbon atoms in molecular formulas from the CHON class (b). Relative abundance (RA) of each subclass for the underground water CHON compounds (c).

Annexe 10 : Evolution of soil leachate properties with leaching time

		Ti	T0	T1	T2	T3	T3bis	T4	Ti	T0	T1	T2	T3	T3bis	T4	
	time (h)	**0**	**0,08**	**0,25**	**0,75**	**5**	**24**	**29**	**0**	**0,08**	**0,25**	**0,75**	**5**	**24**	**29**	
	parameters	**value**	**value**	**value**	**value**	**value**	**value**	**value**	*st-dev*	*st-dev*	*st-dev*	*st-dev*	*st-dev*	*st-dev*	*st-dev*	
	pH	6,3		3,90	4,08	4,00		4,07	*0,3*		*0,01*	*0,03*	*0,01*		*0,04*	
	Conductivité µS.cm-1	21,15		69,30	71,0	70,30		74,60	*1,06*		*0,02*	*0,1*	*0,04*		*0,03*	
ICPMS µg.L-1	**[U]_G1**		0,98	1,11	1,44	1,69		2,20		*0,16*	*0,14*	*0,08*	*0,08*		*0,18*	
	[U]_G1 <10kDa		0,75	0,88	0,92	1,28		1,51		*0,08*	*0,09*	*0,09*	*0,13*		*0,15*	
	[U]_G1 coll.		0,12	0,17	0,42	0,33		0,60		*0,01*	*0,02*	*0,04*	*0,03*		*0,06*	
	[Fe]_G1		52,0	61,0	82,2	101,6		150,5		*10,9*	*13,1*	*12,3*	*19,8*		*14,9*	
	[Fe]_G1 <10kDa		28,2	34,2	43,0	44,5		63,5		*2,8*	*3,4*	*4,3*	*4,5*		*6,4*	
	[Fe]_G1 coll.		16,3	17,8	25,0	34,3		76,8		*1,6*	*1,8*	*2,5*	*3,4*		*7,7*	
	[Al]_G1		622	716	824	1007		1451		*93*	*69*	*48*	*127*		*111*	
	[Al]_G1 <10kDa		459	521	597	667		907		*46*	*52*	*60*	*67*		*91*	
	[Al]_G1 Colloidal (> 10kDa)		101	161	173	198		469		*10*	*16*	*17*	*20*		*47*	
TOC mg.L-1	**[TOC]_G1**		132	141	127	170		292		*28*	*2*	*30*	*18*		*49*	
	[TOC]_G1 < 10kDa		61	135	100	125		204		*6*	*14*	*43*	*3*		*20*	
	[TOC]_G1 coll. > 10kDa		39,0	6,7	27,1	51,4		122,5		*3,9*	*0,7*	*13,7*	*23,6*		*12,2*	
Absorbance (a.u.)	a_{210}		2,021	1,888	1,862	2,035		2,477								
	a_{230}		0,476	0,48	0,488	0,6		1,075								
	a_{250}		0,235	0,249	0,271	0,4		0,757								
	a_{254}		0,227	0,238	0,3	0,4		0,735								
	a_{280}		0,178	0,188	0,206	0,307		0,591								
	a_{350}		0,073	0,089	0,085	0,131		0,284								
	a_{365}		0,058	0,076	0,069	0,105		0,242								
	a_{440}		0,025	0,045	0,032	0,046		0,121								
	a_{465}		0,021	0,039	0,028	0,040		0,105								
	a_{665}		0,01	0,026	0,015	0,018		0,04								
Absorption Coefficient (m-1) Decadal	**210**		200,1	183,2	182,9	199,8		239,4								
	230		45,6	42,4	45,5	60,7		99,2								
	250		21,5	19,3	23,8	36,3		67,4								
	254		20,7	18,2	22,9	35,0		65,2								
	280		15,8	13,2	17,3	27,0		50,8								
	350		5,3	3,3	5,2	9,4		20,1								
	365		3,8	2,0	3,6	6,8		15,9								
	440		0,5	-1,1	-0,1	0,9		3,8								
	465		0,1	-1,7	-0,5	0,3		2,2								
	665		-1,0	-3,0	-1,8	-1,9		-4,3								
Absorption Coefficient (m-1) Neperian	**210**		463,5	429,2	425,5	464,9		562,2								
	230		107,7	104,9	109,0	144,6		239,3								
	250		52,2	51,7	59,1	88,4		166,0								
	254		50,3	49,2	57,0	85,4		161,0								
	280		39,0	37,7	44,1	67,0		127,8								
	350		14,9	14,9	16,2	26,4		57,1								
	365		11,4	11,9	12,6	20,5		47,4								
	440		3,8	4,7	4,0	6,9		19,6								
	465		2,9	3,3	3,1	5,5		15,9								
	665		0,3	0,3	0,1	0,4		0,9								
SUVA L mgC-1 m-1 (Decadal)	**$SUVA_{254}$**		0,16	0,13	0,18	0,21		0,22		*0,03*	*0,00*	*0,04*	*0,02*		*0,04*	
	$SUVA_{280}$		0,12	0,09	0,14	0,16		0,17		*0,03*	*0,00*	*0,03*	*0,02*		*0,03*	
E2/E3 Decadal	250/365		5,6	9,8	6,7	5,4		4,2		*0,3*	*0,5*	*0,3*	*0,3*		*0,2*	
MALS	Rg Median (nm)		76	74	71	65		76		*2*	*2*	*2*	*2*		*2*	
	Rg Mean (nm)		81	79	79	70		81		*2*	*2*	*2*	*2*		*2*	
	S(MALS)		756	898	1650	1820		1901		*34*	*41*	*78*	*81*		*93*	
UV	Rg Median (nm)		79	74	75	73		77		*2*	*2*	*2*	*2*		*2*	
	Rg Mean (nm)		82	80	81	79		85		*2*	*2*	*2*	*2*		*2*	
	S(UV)		792	2299	4850	8388		24990		*40*	*138*	*264*	*257*		*1100*	
UV (void peak)	254		2,853	2,425	2,625	3,645		6,743								Height of UV peak in fractogram
	260		2,650	2,275	2,451	3,378		6,252								
	270		2,391	2,032	2,199	3,000		5,552								
	280		2,007	1,704	1,847	2,609		4,826								
	300		1,117	0,958	1,032	1,340		2,478								
	S(280)		**0,456**	**0,388**	**0,420**	**0,580**		**1,073**								
UV à tR=30 min	254		0,089	0,282	0,660	0,817		4,085								
	260		0,078	0,256	0,611	0,773		3,850								
	270		0,064	0,219	0,548	0,693		3,450								
	280		0,050	0,175	0,462	0,594		2,943								
	300		0,028	0,096	0,238	0,307		1,496								
	S(280)		**0,012**	**0,041**	**0,105**	**0,133**		**0,662**								
UV à tR=50 min	254		0,129	0,224	0,599	0,653		2,908								
	260		0,115	0,211	0,568	0,632		2,793								
	270		0,095	0,178	0,515	0,580		2,538								
	280		0,079	0,146	0,420	0,492		2,207								
	300		0,058	0,087	0,199	0,228		0,877								
	S(280)		**0,018**	**0,034**	**0,097**	**0,111**		**0,489**								

Annexe 11: Correlation and linear regression coefficient matrixes for pH, specific conductivity, and U, Fe, Al, organic carbon in total, dissolved and colloidal fraction in leachate during leaching experiment.

Correlation matrix	pH	Sp. Conductivity µS.cm^{-1}	total [U] (µg.L^{-1})	[U] <10kDa (µg.L^{-1})	[U] colloidal > 10 kDa (µg.L^{-1})	total [Fe] (µg.L^{-1})	[Fe] <10kDa (µg.L^{-1})	[Fe] colloidal > 10 kDa (µg.L^{-1})	total [Al] (µg.L^{-1})	[Al] <10kDa (µg.L^{-1})	[Al] colloidal (> 10kDa) (µg.L^{-1})	total [TOC] (mg.L^{-1})	[TOC] < 10kDa (mg.L^{-1})	[TOC] colloidal > 10kDa (mg.L^{-1})
pH		0,72	0,70	0,49	0,89	0,66	0,72	0,58	0,60	0,64	0,52	0,42	0,18	0,62
Sp. Conductivity µS.cm^{-1}	0,72		0,92	0,80	0,96	0,94	0,98	0,96	0,94	0,96	0,96	0,91	0,81	0,95
total [U] (µg.L^{-1})	0,70	0,92		0,97	0,93	1,00	0,98	0,95	0,99	0,99	0,92	0,89	0,84	0,87
[U] < 10kDa (µg.L^{-1})	0,49	0,80	0,97		0,83	0,97	0,93	0,92	0,97	0,96	0,89	0,90	0,85	0,85
[U] colloidal > 10 kDa (µg.L^{-1})	0,89	0,96	0,93	0,83		0,93	0,97	0,88	0,90	0,93	0,88	0,78	0,76	0,78
total [Fe] (µg.L^{-1})	0,66	0,94	1,00	0,97	0,93		0,99	0,97	1,00	1,00	0,95	0,93	0,86	0,91
[Fe] <10kDa (µg.L^{-1})	0,72	0,98	0,98	0,93	0,97	0,99		0,96	0,98	0,99	0,96	0,90	0,88	0,86
[Fe] colloidal > 10 kDa (µg.L^{-1})	0,58	0,96	0,95	0,92	0,88	0,97	0,96		0,99	0,98	0,99	0,98	0,87	0,96
total [Al] (µg.L^{-1})	0,60	0,94	0,99	0,97	0,90	1,00	0,98	0,99		1,00	0,97	0,95	0,89	0,92
[Al] < 10kDa (µg.L^{-1})	0,64	0,96	0,99	0,96	0,93	1,00	0,99	0,98	1,00		0,97	0,94	0,89	0,90
[Al] colloidal > 10kDa (µg.L^{-1})	0,52	0,96	0,92	0,89	0,88	0,95	0,96	0,99	0,97	0,97		0,98	0,92	0,91
total [TOC] (mg.L^{-1})	0,42	0,91	0,89	0,90	0,78	0,93	0,90	0,98	0,95	0,94	0,98		0,88	0,95
[TOC] < 10kDa (mg.L^{-1})	0,18	0,81	0,84	0,85	0,76	0,86	0,88	0,87	0,89	0,89	0,92	0,88		0,71
[TOC] colloidal > 10kDa (mg.L^{-1})	0,62	0,95	0,87	0,85	0,78	0,91	0,86	0,96	0,92	0,90	0,91	0,95	0,71	

Linear regression coefficient R^2 matrix	pH	Sp. Conductivity µS.cm^{-1}	total [U] (µg.L^{-1})	[U] <10kDa (µg.L^{-1})	[U] colloidal > 10 kDa (µg.L^{-1})	total [Fe] (µg.L^{-1})	[Fe] <10kDa (µg.L^{-1})	[Fe] colloidal > 10 kDa (µg.L^{-1})	total [Al] (µg.L^{-1})	[Al] <10kDa (µg.L^{-1})	[Al] colloidal (> 10kDa) (µg.L^{-1})	total [TOC] (mg.L^{-1})	[TOC] < 10kDa (mg.L^{-1})	[TOC] colloidal > 10kDa (mg.L^{-1})
pH		0,52	0,49	0,24	0,80	0,44	0,52	0,34	0,36	0,41	0,27	0,18	0,03	0,39
Sp. Conductivity µS.cm^{-1}	0,52		0,84	0,65	0,91	0,88	0,96	0,93	0,88	0,92	0,93	0,83	0,65	0,90
total [U] (µg.L^{-1})	0,49	0,84		0,94	0,87	0,99	0,97	0,90	0,97	0,98	0,85	0,79	0,70	0,76
[U] <10kDa (µg.L^{-1})	0,24	0,65	0,94		0,68	0,94	0,86	0,85	0,94	0,92	0,79	0,80	0,73	0,73
[U] colloidal > 10 kDa (µg.L^{-1})	0,80	0,91	0,87	0,68		0,86	0,93	0,78	0,82	0,87	0,77	0,61	0,58	0,61
total [Fe] (µg.L^{-1})	0,44	0,88	0,99	0,94	0,86		0,98	0,95	0,99	0,99	0,91	0,86	0,74	0,82
[Fe] <10kDa (µg.L^{-1})	0,52	0,96	0,97	0,86	0,93	0,98		0,92	0,96	0,98	0,91	0,81	0,77	0,74
[Fe] colloidal > 10 kDa (µg.L^{-1})	0,34	0,93	0,90	0,85	0,78	0,95	0,92		0,97	0,96	0,98	0,96	0,76	0,91
total [Al] (µg.L^{-1})	0,36	0,88	0,97	0,94	0,82	0,99	0,96	0,97		1,00	0,94	0,91	0,79	0,84
[Al] <10kDa (µg.L^{-1})	0,41	0,92	0,98	0,92	0,87	0,99	0,98	0,96	1,00		0,94	0,88	0,79	0,81
[Al] colloidal > 10kDa (µg.L^{-1})	0,27	0,93	0,85	0,79	0,77	0,91	0,91	0,98	0,94	0,94		0,95	0,85	0,82
total [TOC] (mg.L^{-1})	0,18	0,83	0,79	0,80	0,61	0,86	0,81	0,96	0,91	0,88	0,95		0,78	0,90
[TOC] < 10kDa (mg.L^{-1})	0,03	0,65	0,70	0,73	0,58	0,74	0,77	0,76	0,79	0,79	0,85	0,78		0,50
[TOC] colloidal > 10kDa (mg.L^{-1})	0,39	0,90	0,76	0,73	0,61	0,82	0,74	0,91	0,84	0,81	0,82	0,90	0,50	